CR-168180
PWA-5719-34

BROAD SPECIFICATION FUELS COMBUSTION TECHNOLOGY PROGRAM
PHASE I

FINAL REPORT

by

R. P. Lohmann and R. A. Jeroszko

Engineering Division
Pratt & Whitney Aircraft Group
United Technologies Corporation

Prepared for

NATIONAL AERONAUTICS AND SPACE ADMINISTRATION
Lewis Research Center
Under
Contract NAS3-22392

(NASA-CR-168180) BROAD SPECIFICATION FUELS TECHNOLOGY PROGRAM, PHASE 1 Final Report (Pratt and Whitney Aircraft Group) 210 p HC A10/MF A01 CSCL 21B

N83-30551

Unclas
G3/25 28419

UNITED TECHNOLOGIES
PRATT&WHITNEY
AIRCRAFT

400 Main Street
East Hartford, Connecticut 06108

In reply please refer to:
RPL:JK KBA1C (0559N)
Ref. No. PWA-5719-34

July 29 1983

To: National Aeronautics and Space Administration
Lewis Research Center
21000 Brookpark Road
Cleveland, Ohio 44135

Attention: L. Schopen
Contracting Officer

Subject: Broad Specification Fuels Combustion Technology Program - Phase I Final Report

References:
(1) NASA Contract NAS3-22392
(2) NASA Lewis Letter 2513, J. S. Fear to R. P. Lohmann, dated 3 June 1983

Gentlemen:

We submit herewith the Contractor Final Report (CR-168180) for the subject program in compliance with the reporting requirements of the Reference (1) contract. NASA approval for final submittal of this report, contingent on incorporation of the revisions and corrections specified by NASA, was received via the Reference (2) letter. Additional distribution of this report is being made in accordance with the distribution list supplied by NASA.

Sincerely yours,

UNITED TECHNOLOGIES CORPORATION
Pratt & Whitney Aircraft Group
Engineering Division

R. P. Lohmann
Program Manager

1. REPORT NO.	2. GOVERNMENT AGENCY	3. RECIPIENT'S CATALOG NO.
NASA CR-168180		

4. TITLE AND SUBTITLE	5. REPORT DATE / 6. PERFORMING ORG. CODE
Broad Specification Fuels Technology Program Phase I	5. REPORT DATE: 11 October 1982 6. PERFORMING ORG. CODE:
7. AUTHOR(S): R. P. Lohmann and R. A. Jeroszko	8. PERFORMING ORG. REPT. NO.: PWA-5719-34
9. PERFORMING ORG. NAME AND ADDRESS: United Technologies Corporation Pratt & Whitney Aircraft Group Commercial Engineering	10. WORK UNIT NO.: 11. CONTRACT OR GRANT NO.: NAS3-22392
12. SPONSORING AGENCY NAME AND ADDRESS: National Aeronautics and Space Administration 21000 Brookpark Road Cleveland, Ohio 44135	13. TYPE REPT./PERIOD COVERED: Contractor Final Report 14. SPONSORING AGENCY CODE:

15. SUPPLEMENTARY NOTES

16. ABSTRACT

An experimental evaluation was conducted to assess the impact of the use of broadened properties fuels on combustor design concepts. Emphasis was placed on establishing the viability of design modifications to current combustor concepts and the use of advanced technology concepts to facilitate operation on Experimental Referee Broad Specification (ERBS) fuel while meeting exhaust emissions and performance specifications and maintaining acceptable durability. Three different combustor concepts, representative of progressively more aggressive technology levels, were evaluated. When operated on ERBS rather than Jet A fuel, a single stage combustor typical of that in the most recent versions of the JT9D-7 engine was found to produce excess carbon monoxide emissions at idle and elevated liner temperatures at high power levels that were projected to reduced liner life by 13 percent. The introduction of improved component technology, such as refined fuel injectors and advanced liner cooling concepts were shown to have the potential of enhancing the fuel flexibility of the single stage combustor. Both of the advanced combustor concepts, a staged and a variable geometry combustor, were found to be more adaptable to the use of broadened properties fuels due to the additional flexibility of operation. Idle emissions, ignition and smoke output goals were generally attainable with these concepts and some reduction in NO_x emissions relative to single stage combustors was demonstrated. The lean combustion achieved at high power in these advanced concepts leads to reduced heat load on the liner and was shown in the variable geometry combustor to offset the increases in liner temperature associated with a Jet A to ERBS transition.

17. KEY WORDS (SUGGESTED BY AUTHOR(S))	18. DISTRIBUTION STATEMENT
Combustion, Fuels, Combustor Design	

19. SECURITY CLASS (THIS REPT)	20. SECURITY CLASS (THIS PAGE)	21. NO. PGS	22. PRICE *
Unclassified	Unclassified		

* For sale by the National Technical Information Service, Springfield, VA 22161

FOREWORD

This report presents the results of an experimental evaluation conducted to assess the potential of combustor design modifications and the use of advanced technology concepts to facilitate operation on broadened properties fuels. The program was conducted as Phase I of the Broad Specification Fuels Combustion Technology Program under Contract NAS3-22392.

The NASA Project Manager for this contract was Mr. James S. Fear of the Aerothermodynamics and Fuels Division, Lewis Research Center, Cleveland, Ohio, and the Pratt and Whitney Aircraft Program Manager was Dr. Robert P. Lohmann. The principal investigators were Dr. Lohmann and Mr. Ronald A. Jeroszko.

TABLE OF CONTENTS

TABLE OF CONTENTS (Cont'd)

TABLE OF CONTENTS (Cont'd)

LIST OF ILLUSTRATIONS

LIST OF ILLUSTRATIONS (Cont'd)

LIST OF ILLUSTRATIONS (Cont'd)

LIST OF ILLUSTRATIONS (Cont'd)

LIST OF ILLUSTRATIONS (Cont'd)

LIST OF TABLES

LIST OF TABLES (Cont'd)

SECTION 1.0

SUMMARY

This report presents the results of Phase I of the Broad Specification Fuels Combustion Technology program. The objective of the overall program is to identify and evolve the combustor technology required to accommodate the use of broadened properties fuels in current and future high bypass ratio engines for Conventional Takeoff and Landing (CTOL) aircraft. The specific objective of the Phase I program was to establish the viability of design modifications to current combustor concepts and to introduce advanced technology concepts to facilitate operation on broadened properties fuels while meeting exhaust emissions and performance specifications and maintaining acceptable durability characteristics.

The target broadened properties fuel for this program was Experimental Referee Broad Specification fuel, hereafter referred to by the acronym ERBS. This fuel had a hydrogen content of 12.93 percent as opposed to a nominal level of about 13.7 percent in Jet A. The program goals had been stipulated for a combustor operating on ERBS fuel and included durability and operational characteristics, such as stability and ignition, consistent with the reference JT9D-7F engine combustor when it was operated on Jet A fuel. Further goals included aggressive levels of control of the combustor exit temperature distribution, section pressure loss and combustion efficiency as well as compliance with the proposed 1981 and 1984 Environmental Protection Agency standards for emissions and smoke output.

The Phase I program was structured around the experimental evaluation of three combustor concepts; a single stage combustor, a staged Vorbix combustor, and a variable geometry combustor. The selection of these concepts established the overall direction of the effort and was specifically intended to cover a wide range of combustor technology.

After the JT9D-7F engine was selected as the reference engine for the program, the production combustor used in that engine was selected as the initial configuration of the single stage combustor concept. This allowed program results to be related to in-service engine experience. Subsequent configurations of the single stage combustor were variations of a more advanced combustor that is used in the more recent models of the JT9D engine series.

Staged combustors, with two distinct combustion zones serviced by independent fuel systems, offer opportunities for improved stoichiometry control. A second generation version of the staged Vorbix combustor is being evolved under the National Aeronautics and Space Administration/Pratt & Whitney Aircraft Energy Efficient Engine Program and this staged combustor was selected as the second concept in the Phase I program. Finally, a variable geometry combustor, in which movable gaspath components are used to shift the airflow distribution within the combustor to achieve optimum stoichiometry, was selected as the third and most advanced combustor concept.

To accomplish the objectives of the program, a total of sixteen configurations of these three basic combustor concepts were tested in rigs that incorporated a sector of the appropriate full size annular combustor. The tests were conducted in a facility capable of providing nonvitiated air at pressures, temperatures and airflow rates consistent with the full takeoff power level of the engine. The final configuration of each concept was evaluated for combustion stability and ignition capability in an al'itude test facility. The fuel for the majority of these tests was ERBS but se'.cted critical configurations were also evaluated with Jet A and blended fuels of lower hydrogen content.

The evaluation of the baseline configurations of the single stage combustor concept indicated that the advanced combustor was capable of achieving nearly all of the appropriate program goals while operating on Jet A fuel. Only the combustor exit temperature pattern factor exceeded the program goal of 0.25 but the observed levels were consistent with experience with this combustor. When this combustor was operated on ERBS fuel, two major deficiencies were observed. The increased radiant heat load led to higher liner temperatures and a projected 13.5 percent loss of liner life. In addition, use of this fuel led to increases in the carbon monoxide emissions at idle that were sufficient to exceed the program goal for this constituent.

Subsequent variations to the single stage combustor concept explored different means for overcoming these deficiencies and enhancing their ability to operate on broadened properties fuels. Changing the stoichiometry and residence time history in the combustor by revising airflow distribution produced changes in emissions, smoke and performance characteristics which were consistent with experience. Unfortunately, the key factors in a Jet A to ERBS transition -- idle emissions and liner heat load -- require opposing changes in primary zone stoichiometry. For this reason, it appears that changing current design practice to alter primary zone stoichiometry in single stage combustors is not an attractive generic approach to accommodating broadened properties fuels. However, this approach may be of value in accommodating unique combinations of combustors and fuels.

More fundamental improvements in combustor performance were achieved by introducing advanced technology design concepts. The use of modified fuel injectors in the single stage combustor led to significant improvements in high power performance including a reduction in peak liner temperatures, lower pattern factor and reduced smoke and NO_x output. More advanced liner cooling concepts also offer the potential for significant improvements in combustor performance. Advanced liners offset the increased heat load produced by broad property fuels without requiring increases in liner cooling airflow which would compromise performance and emissions characteristics.

Evaluation of the advanced Vorbix combustor demonstrated that the operational flexibility of the staged combustor concept could be advantageous in accommodating the use of broadened properties fuels. While this concept was weighed against more stringen' emissions goals based on the proposed Environmental Protection Agency standards for engines certified after 1934, the sensitivity of the emissions output to fuel composition was less than encountered with the single stage concept. The program goal for carbon monoxide emissions was achieved with both Jet A and ERES fuel. Unburned hydrocarbon emissions were low with both fuels but the levels were marginal relative to the program goal. Although NO_x emissions were not reduced enough to satisfy the proposed standards, output was substantially below the level which could be achieved with a conventional single stage combustor in the high pressure ratio Energy Efficient Engine. In fact, the levels attained with the staged Vorbix combustor were the lowest in the program.

Changes in fuel composition produced several divergent effects on liner metal temperatures in the staged Vorbix combustor. Some of the data indicate that the increments in liner temperature associated with broad property fuels are considerably smaller than the temperature changes encountered in louver cooled single stage combustors. It is not clear whether these findings should be attributed to locally leaner combustion achieved with staging or a reduction in sensitivity to fuel composition due to the internal convective cooling of the advanced technology liner structure incorporated in this combustor. However, the remaining data indicate that liner temperatures in the main stage are extremely sensitive to fuel composition. It appears that significant variations in the dispersion of fuel toward the inner liner altered the convective heat loads on these surfaces. The mechanisms causing these temperature excursions must be identified and desensitized before this particular type of staged combustor could be considered viable for extensive operation with broadened properties fuels.

The synthesis of the characteristics of fully modulated variable geometry combustors from the evaluation of appropriate fixed geometry configurations indicates that this concept has considerable potential for accommodating the use of broadened properties fuels. The ability to enrich the primary combustion zone by restricting its airloading at low power levels was found to improve the ignition and stability margins relative to a fixed geometry single stage combustor. In this operating mode the idle emissions levels were sufficiently low with ERBS fuel to achieve the program goals of carbon monoxide and unburned hydrocarbon emissions less than the proposed EPA standards for engines certified after 1984. Furthermore, by increasing the primary zone air loading to the maximum possible at high power levels to reduce the bulk equivalence ratio to about 0.60 at takeoff, the heat load on the liners was reduced. The associated increments in liner metal temperature were more than adequate to offset those associated with a Jet A to ERBS transition. However, the NO_x emissions characteristics were substantially higher than anticipated and were traced to incomplete mixing in the conventional swirl stabilized primary combustion zone. This result could be indicative of the need for more complex combustor designs if a greater degree of mixture homogeneity is required for control of NO_x emissions.

At the conclusion of the Phase I program, it was evident that the advanced technology design approaches and combustor concepts evaluated could be exploited to enhance combustor performance and durability while operating with broadened properties fuels. Use of the advanced staged and variable geometry combustors offer the greatest opportunity but these approaches also require significant revisions even at the conceptual level to adapt them to engine operational requirements. These aspects will be addressed in Phase II of the program.

SECTION 2.0

TECHNICAL BACKGROUND

2.1 INTRODUCTION

Over the past decade, escalating fuel costs have severely impacted the economics of both commercial and military aircraft operations. The problem has been compounded by a reduction in the quantity of high quality petroleum crude available to produce aviation fuels to current specifications. One method of alleviating fuel cost and availability concerns is to modify these specifications to allow the use of lower quality fuels. Another alternative is to accelerate production of synthetic fuels from shale or coal-derived feed stocks to reduce our dependence on uncertain foreign sources and stabilize fuel prices. However, either of these approaches could lead to variations in the chemical composition and physical properties of the fuel which would have adverse impacts on the operation and maintainability of aircraft engines. Intelligent selection of fuels for the aircraft of the future will require careful cost/benefit analysis which recognizes not only fuel cost and availability but also the impact of increased engine maintenance costs and the expense of developing technology to accommodate the new fuels.

As early as 1974, the National Aeronautics and Space Administration (NASA) recognized this impending situation in the aircraft industry and initiated programs to evaluate the effects of changes in fuel composition on the performance, emissions and overall design and operation of gas turbine combustors. This effort included both in-house investigations and contracted studies such as the Alternate Fuels Addendums to the Experimental Clean Combustor Program (References 1 and 2). This initial evaluation indicated that relaxing the fuel specification to permit higher aromatic contents or lower hydrogen/carbon ratios in the fuel would have significant impacts on gas turbine combustion systems.

At the time it seemed most appropriate to coordinate the efforts to evolve fuel-related combustor technology by concentrating on the implications of a single fixed broadened properties fuel. The Jet Aircraft Hydrocarbon Fuels Technology Workshop, convened at NASA-Lewis Research Center in June 1977, provided the basis for identifying this particular fuel (Reference 3). The attendees, including representatives of the petroleum industry, engine and airframe manufacturers, airlines, the military, and NASA, reviewed the experience to date and arrived at a tentative specification for Experimental Referee Broad Specification Fuel, hereafter referred to by the acronym ERBS.

Under Contract NAS3-20802 (Reference 4), Pratt & Whitney Aircraft conducted a design study to assess the impact of the use of ERBS specification fuel on combustors for current and advanced gas turbine engines for commercial aircraft. This design study identified specific areas where new technology must be developed and substantiated to produce combustion systems capable of operating on ERBS specification fuel without compromising the environmental acceptability, performance, durability or reliability of the combustor. The Broad Specification Fuels Combustion Technology Program is directed at this specific objective.

2.2 ERBS FUEL COMPOSITION

In Table 1 the specification for ERBS fuel as defined in Reference 3 is compared to the specification for Jet A, the fuel currently used for the majority of commercial aircraft operations in the United States. Specifications of this type stipulate only allowable limits on the composition of the fuel. The method of defining these limits differs, most notably in the means of limiting the fractions of aromatics and complex aromatics. The Jet A specification stipulates specific limits on the concentration of these constituents while the ERBS specification uses the hydrogen content of the fuel as the controlling parameter. Hydrogen content provides a characterization of the hydrocarbon composition of the fuel: since the aromatic compounds have a high ratio of carbon to hydrogen atoms, increasing the aromatic content reduces the hydrogen content. The hydrogen content stipulated in the ERBS specification would permit the aromatic content to be in the range of 30 to 35 percent. (The actual ERBS fuel used in this program was procured to a more rigorous specification than Table 1 to provide control of hydrocarbon composition. Details on the composition of this fuel are provided in Section 5.1).

Table 1

Comparison of Specifications for Jet A and ERBS Fuel

	ASTM D 1655 Jet A	ERBS
Aromatic Content - % vol	20 max	Report
Hydrogen Content - % wt	--	12.8 $\pm$0.2
Sulphur Mercaptan - % wt	0.003 max	0.003
Sulphur Total - % wt	0.3 max	0.3 max
Nitrogen Total - % wt	--	Report
Naphthalene Content - % vol	3.0 max	Report
Hydrocarbon Compositional Analysis	--	Report
Distillation Temperature - °K (°F)		
Initial Boil Point	--	Report
10 Percent	477 (400) max	477 (400) max
50 Percent	505 (450) max	Report
90 Percent	--	534 (500) min
Final Boil Point	561 (550) max	Report
Residue - % vol	1.5 max	Report
Loss - % vol	1.5 max	Report
Flashpoint - °K (°F)	316 (110) min	316 (110) min
API Gravity	--	Report
Freezing Point - °K (°F)	233 (-40) max	244 (-20) max
Maximum Viscosity - cs	8 @ 253°K (-4°F)	12 @ 249°K (-10°F)
Specific Gravity	0.7753 to 0.8299	Report
Heat of Combustion - MJ/kg (BTU/lb)	42.8 (18,400) min	Report
Thermal Stability:		
JFTOT Breakpoint		
Temperature - K° (°F)	533 (500) min	511 (460) min
Method	Visual Code 3	TDR = 13.
	ΔP = 12	ΔP = 25

The lower hydrogen content of ERBS fuel is also reflected in the distillation temperature distribution where the high end of the distillation range occurs at higher temperature levels. The decrease in hydrogen content also necessitates an increase in freezing point relative to Jet A -- a factor that affects both fuel storage and pumpability during ground operations and on long duration high altitude flights. The proximity of the fuel temperature to the freezing point has a strong influence on viscosity and deteriorated fuel atomization could compromise cold engine starting. Consequently, the ERBS specification also includes a limit on low temperature fuel viscosity. The differences in the maximum allowable breakpoint temperature imply that the thermal stability of ERBS fuel will be poorer than that of Jet A.

These changes in the chemical composition and physical properties of the fuel are expected to have significant impacts on the design and operation of combustors for aircraft gas turbine engines. These impacts are characteristic of all reduced hydrogen content broadened property fuels and include:

- Increased flame luminosity resulting in higher radiant heat transfer to the combustor liner which will shorten liner life.
- Increased carbon monoxide and unburned hydrocarbon emissions output at low power levels because of poorer fuel atomization and more complex fuel chemistry.
- Increased smoke production and NO_x emissions because of the more complex fuel chemistry.
- More difficult cold starting and altitude relight because of increased fuel viscosity and in the case of some fuels, reduced volatility. These factors could also impair combustion stability.
- Greater propensity toward carbon deposition on liners, and fuel injector plugging and streaking because of the reduced thermal stability of the fuel.

Under the Broad Specification Fuels Combustion Technology Program the magnitude of these concerns with use of ERBS fuel rather than Jet A are investigated. The technology required to resolve these problems with minimal impact on the acceptability of the engine is also identified and demonstrated.

2.3 PROGRAM OBJECTIVES AND STRUCTURE

The overall objective of the Broad Specification Fuels Combustion Technology Program is to identify, develop and ultimately demonstrate the technology required to use broadened properties fuels in current and future high bypass ratio engines for commercial aircraft. Combustor design concepts will be established which minimize the impact of Experimental Referee Broad Specification (ERBS) fuel on the emissions, performance, durability and operating characteristics of these engines. The data accumulated under this program will provide valuable input to the cost/benefit analysis of broadened properties fuels.

A three phase program was originally formulated to meet these objectives. These phases consisted of:

Phase I - Combustor Concept Screening

Phase I, which is the subject of this report, consisted of combustor rig testing to evaluate various approaches to enhancing the performance, emissions, durability and operating characteristics of different combustor concepts operating on broadened properties fuels.

Phase II - Combustor Optimization Tests

This phase which is currently under way consists of additional combustor rig tests, conducted on the best combustor concepts identified during Phase I, to identify the optimum combustor system, based on performance, emissions and durability. The interaction of the combustor with other engine components is also being addressed.

Phase III - Engine Verification Testing

This phase, which has been deleted from the program would have involved evaluation of the best combustor concept from the Phase II rig testing in a complete high bypass ratio turbofan engine. Both transient and steady state testing would have been conducted to assess the overall acceptability of the combustor design in an actual engine environment.

The Phase I program was structured around the experimental evaluation of three combustor concepts; a single stage combustor, a staged Vorbix combustor, and a variable geometry combustor. The selection of these concepts established the overall direction of the effort and was specifically intended to cover a wide range of combustor technology.

After the JT9D-7 was selected as the reference engine for the program, the single stage combustor currently used in this engine was selected as the first combustor concept. This selection allowed some of the less complex technological advances, such as fuel injectors with improved atomization and enhanced liner cooling approaches, to be evaluated as a means of accommodating broadened properties fuels. The selection also allowed program results to be compared to in-service engine experience.

In selecting the two remaining concepts, it was recognized that a substantial body of combustion technology has evolved over the past decade in programs aimed at reducing aircraft engine emissions and improving fuel consumption. It was logical to consider the combustor concepts developed in these programs as approaches to minimizing the sensitivity of the combustion system to fuel composition. Of particular interest are the staged combustors developed under the emissions reduction programs. The principal feature of these burners is the use of two distinct combustion zones, each serviced by an independent fuel injection system. By operating the combustor on only one zone at low power levels and both zones at high power, the combustor may be optimized at two operating conditions, rather than a single condition. Use of a rich mixture strength in the low power stage produces low carbon monoxide and unburned hydrocarbon emissions at idle. When the two stages are used in combination, a low equivalence ratio can be maintained at high power to minimize NO_x and smoke output. This type of stoichiometry control appears useful in circumventing some of the problems associated with broadened properties fuel. For example, rich primary zone stoichiometry at low power could offset potential deterioration in ignition capability while lean combustion at high power levels could reduce the radiant heat load on the burner liners. For this reason a staged combustor was selected as the second concept to be evaluated in the Phase I program. The Vorbix staged combustor concept was developed under the NASA/Pratt & Whitney Aircraft Experimental Clean Combustor Program (References 5, 6, and 7). More recently, a second generation or improved version of this concept was designed and developed under the NASA/Pratt & Whitney Aircraft Energy Efficient Engine Program (References 8 and 9). This advanced combustor was selected as the staged combustor concept for the Phase I program.

More recent studies (References 10 and 11) have indicated that variable geometry combustors, in which airflow distribution is shifted with operating condition to achieve optimum stoichiometry at all power levels, offer significant advantages in meeting performance and emissions requirements. As in the staged combustor concept, the enhanced control of stoichiometry could be used to advantage in accommodating broadened properties fuels. Consequently, the variable geometry combustor was selected as the third and most advanced combustor concept for the Phase I program.

To accomplish the objectives of the program, these three combustor concepts were tested in rigs which incorporated a sector of the appropriate full size annular combustor. The tests were conducted in a facility where nonvitiated air was provided at pressures, temperatures and airflow rates consistent with the full takeoff power level of the engine.

Since a major objective of the program was to assess the ability of the three combustors to operate with broadened properties fuels, the initial test of each combustor concept consisted of a comprehensive evaluation of its sensitivity to fuel composition. Four different test fuels were used for these initial tests: Jet A, Experimental Referee Broad Specification (ERBS) fuel and two additional blended fuels. The latter were produced by blending stock with a high aromatic content and ERBS to produce fuels with nominal hydrogen contents of 12.3 and 11.8 percent (compared to 12.8 and 13.7 percent for ERBS and Jet A, respectively). The Jet A fuel then provided a baseline which reflected current experience while the blended fuels provided variation in fuel composition which extended beyond the target ERBS specification.

Following the initial assessment of the sensitivity of each combustor concept to fuel composition, several different single stage and variable geometry combustor configurations were tested to evaluate alternate design approaches to accommodating broadened properties fuels. Variations to the single stage combustor concept included modified fuel injectors, advanced liner cooling approaches, and revisions to primary zone stoichiometry/residence time. Perturbations to the variable geometry combustor concept were aimed primarily at exploring the mode and extent of airflow schedule variation required. The tests conducted on the intermediate configurations were generally narrower in scope than the tests conducted on the original configuration and were restricted to only ERBS and Jet A fuel.

At the end of the Phase I program, the final, or "best" configuration for each combustor concept was assembled by incorporating the most effective features and approaches identified during the preceding rig tests. These final configurations were then tested to demonstrate the advances in technology which had been accomplished during Phase I. All four types of fuel were used in these demonstration tests.

2.4 PROGRAM GOALS

The objective of the Broad Specification Fuel Combustion Technology Program is to identify and evolve the technology required to operate current and advanced commercial aircraft engines on broadened properties fuels with minimal impact on the performance, emissions, durability and operating characteristics of the engines. To provide guidelines for this program, goals were established for both combustor performance and emissions.

2.4.1 Performance Goals

The following performance goals were established for combustors operating on Experimental Referee Broad Specification fuel:

- Combustion efficiency of 99 percent, as defined by emissions measurements, at all operating conditions.
- Combustor section total pressure loss of no more than 6 percent at sea level takeoff with a preference for the lower section loss of the current JT9D engine.
- Combustor exit temperature pattern factor of 0.25.
- Combustor exit average radial temperature profile consistent with turbine design requirements.
- Liner metal temperatures comparable to those currently obtained with Jet A fuel to maintain liner life.
- Altitude relight and cold starting capability consistent with engine specifications.

These goals were considered to be long range objectives for the entire program and were not given equal emphasis in Phase I. In particular, combustor exit temperature pattern factor and radial profile goals were deemphasized in order to concentrate Phase I effort on the other performance and emissions goals. These goals could be addressed during the latter parts of the Phase II program when effort would be restricted to only one combustor concept.

2.4.2 Emissions Goals

The emissions goals for the program are those advanced by the Environmental Protection Agency for Class T-2 aircraft engines with thrust levels in excess of 90 kilonewtons (Reference 12) at the time the program was formulated. Using the pressure ratio of the JT9D-7F engine cycle, these goals are listed in Table 2 in terms of the Environmental Protection Agency parameter, which is defined by weighting the emissions indices over the landing and takeoff cycle of Reference 12. Although the Environment Protection Agency did not include a limitation on NO_x emissions for engines manufactured prior to January 1, 1984 a goal has been established for this parameter to provide for the possibility that the combustion system developed might also be used in engines manufactured after that date.

Table 2

Emissions Goals for Combustors in the JT9D-7F Engine

	Engines Manufactured after January 1, 1981*	Engines Manufactured after January 1, 1984	Engines Certified after January 1, 1984
EPA Parameter (kg/kN)			
Carbon Monoxide	36.1	36.1	25.0
Unburned Hydrocarbon	6.7	6.7	3.3
Oxides of Nitrogen	33.0	33.0	33.0
Maximum SAE Smoke Number	19.2	19.2	19.2

*Compliance date since extended to January 1, 1983

In establishing appropriate goals from these proposed standards it was evident that combustor concepts or technology evolved from this program would be incorporated primarily in engines manufactured after January 1, 1984 and would consequently be subject to the constraint on emissions of oxides of nitrogen. Further, the advanced technology staged Vorbix and variable geometry combustor concepts would require diffuser/burner cases and fuel supply/control systems which are substantially different from those currently used in the JT9D-7 engine. As a result, incorporation of either of these combustor concepts would most likely be restricted to newer engine models that would be certified in the post 1984 time period when the more stringent carbon monoxide and unburned hydrocarbon emissions standards would also be applicable.

SECTION 3.0

REFERENCE ENGINE AND COMBUSTOR

The Pratt & Whitney Aircraft JT9D-7F was selected as the reference engine for this program. The JT9D-7F is part of a large family of JT9D engines which have seen extensive service in current wide body aircraft and are expected to be used well into the 21st century. At 50,000 pounds of thrust, the JT9D-7F is considered a representative high technology engine for wide body commercial aircraft.

This section contains a brief description of the engine and detailed information on the mechanical design, performance, and emissions characteristics of the combustor.

3.1 REFERENCE ENGINE SELECTION

The JT9D-7F has been selected as the reference engine for the Broad Specification Fuels Combustor Technology Program. The JT9D engine family, designed and developed by Pratt & Whitney Aircraft, powers a number of wide body commercial aircraft including the Boeing 747 and the McDonnell Douglas DC-10-40. More recent JT9D engine models are also used in the Airbus Industries A-300 and A-310 and the Boeing 767. Since the economic life of these aircraft exceeds 20 years, the JT9D engine family is expected to continue in active service in the commercial wide body aircraft well into the twenty-first century.

There are a number of JT9D engine models that incorporate cycle variations unique to the thrust and mission requirements of the particular aircraft in which they are used. The models in the JT9D-7 series, which include the -7A, -7F, -7J, -7R, and -20, are designed to an essentially common gas path. The combustors in these models are mechanically interchangeable, differing primarily in liner air schedules used to accommodate different cooling flow levels. Different thrust ratings are achieved primarily by varying pressure ratio and turbine inlet temperature in the otherwise common engine core.

There are also a limited number of JT9D engine models at the high end of the thrust range, including the JT9D-7Q and JT9D-59/70. The design of these models varies substantially from the basic JT9D-7 series, featuring larger diameter fans, increased low compressor stages and a high capacity turbine to achieve higher takeoff thrust ratings. The combustor sections of these engines, while similar to those of the JT9D-7 series, are not interchangeable primarily because of differences in turbine elevations.

The pressure ratio and turbine inlet temperature of the JT9D-7F place it in the middle of the JT9D family of engines, minimizing the degree to which program results have to be extended to match the operating conditions of other models. This was a major factor in the selection of the JT9D-7F as the reference engine.

3.2 REFERENCE ENGINE DESCRIPTION

The JT9D-7F engine is an advanced, dual-spool, axial-flow turbofan with a high overall compression ratio and a high bypass ratio. The mechanical configuration is shown in Figure 1. The engine consists of five major modules: fan and low-pressure compressor, high-pressure compressor, combustor, high-pressure turbine, and low-pressure turbine. The low-pressure spool consists of a single-stage fan and a three-stage low-pressure compressor driven by a four-stage low-pressure turbine. The high-pressure spool consists of an eleven-stage high-pressure compressor driven by a two-stage high-pressure turbine. The accessory gearbox is driven through a towershaft located between the low and high-pressure compressors.

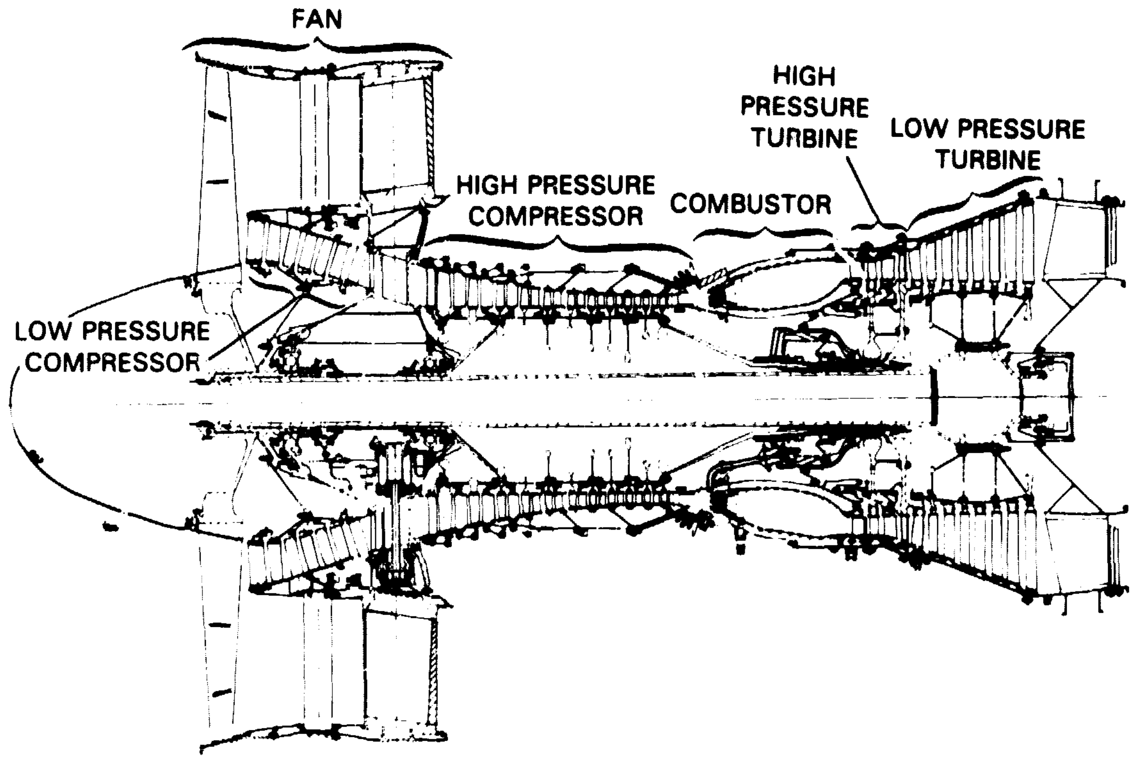

Figure 1 Cross Section of the JT9D-7 Reference Engine

3.3 REFERENCE COMBUSTOR DESCRIPTION

The mechanical design of the reference JT9D combustor is shown in Figure 2. Figure 3 is a cutaway of the combustor liner and diffuser case while Figure 4 shows additional detail of the construction of the front end of the combustor. The combustor is an annular design with an overall length of 604 mm (23.78 in) between the trailing edge of the compressor exit guide vane and the leading edge of the turbine inlet guide vane. The burning length between the fuel nozzle face and the turbine inlet guide vane leading edge is 0.45 m (17.7 in). The diffuser section incorporates an inner ramp and outer trip followed by a dump section. A burner hood provides a positive pressure feed to the combustor front end. The hood is indented locally in ten places downstream of each diffuser case strut. A film-cooled louver construction is used for the combustor liners. The liner assembly features inner and outer slipjoints to facilitate assembly as well as to allow for liner thermal expansion. The fuel system features direct liquid fuel injection using twenty duplex/pressure atomizing fuel nozzles. The nozzle portion of the fuel injector is enclosed in twenty short-cone swirler modules as shown in Figure 3-4. The cones provide primary zone flame stabilization. Optional take-off thrust augmentation is provided by water injection through the fuel nozzle heatshields. Further details on the geometry and operating characteristics of this combustor are provided in Section 4.1.1.

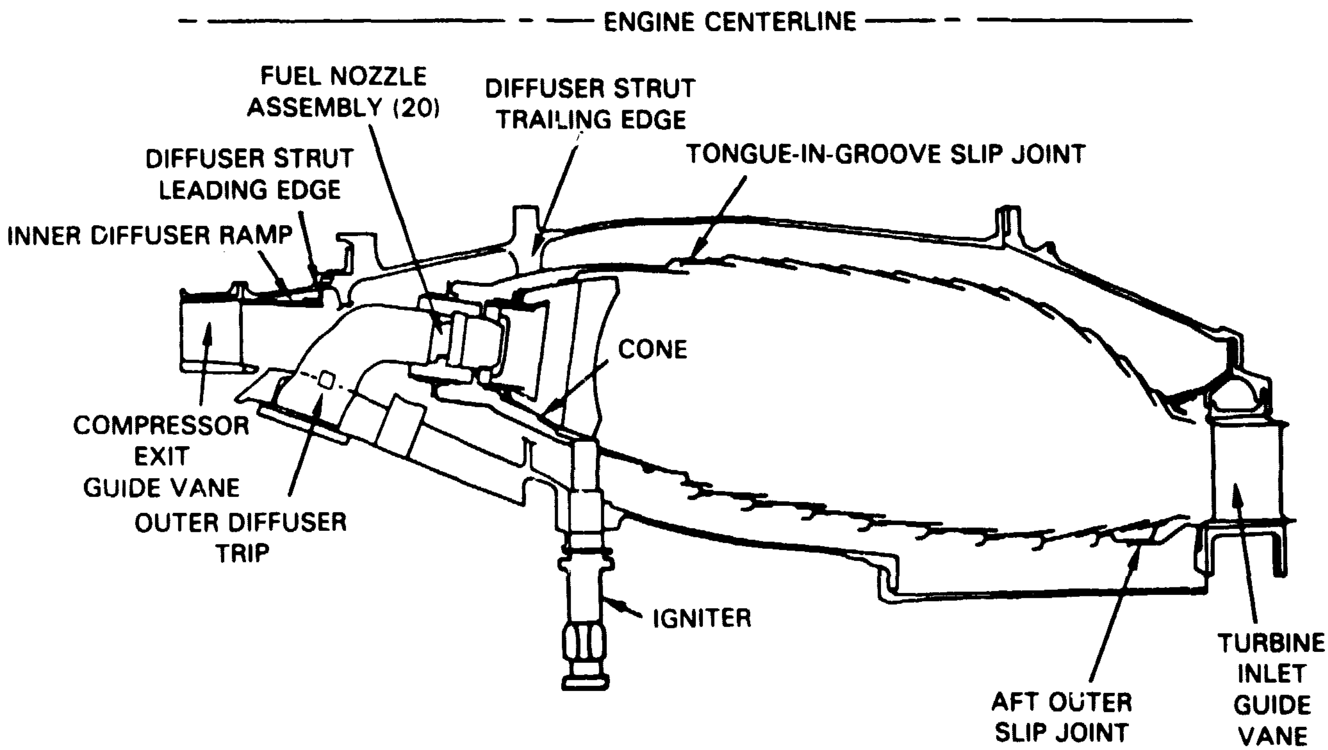

Figure 2 Cross Section of the JT9D-7 Reference Combustor

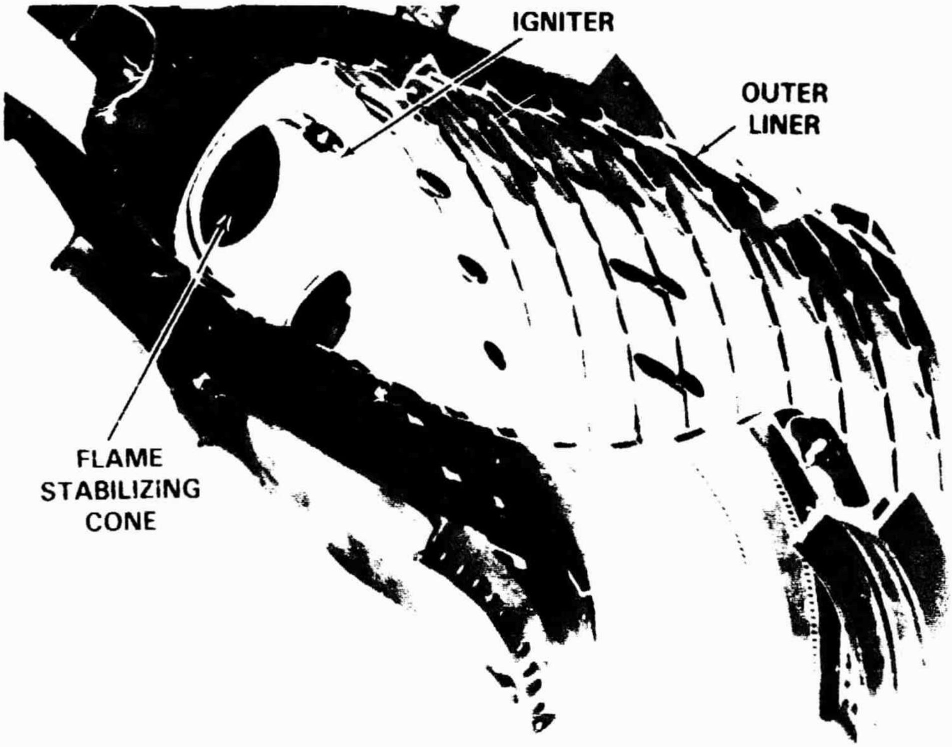

Figure 3 JT9D-7 Combustor Section Cutaway

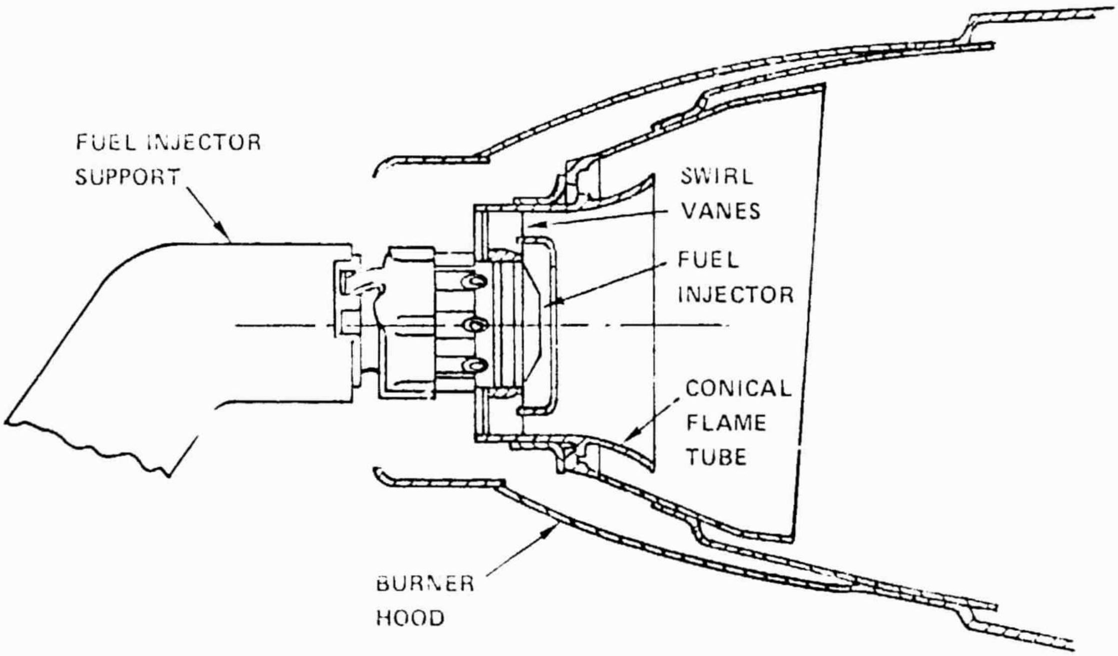

Figure 4 Front End of the JT9D-7 Combustor

3.4 REFERENCE COMBUSTOR PERFORMANCE

Table 3 lists the critical operating parameters for the JT9D-7F combustor at the four sea level static conditions of the Environmental Protection Agency landing and takeoff cycle and the maximum cruise aerodynamic design point of the engine. The idle condition is the minimum set point at which thrust is 6.37 percent of takeoff thrust. Other critical design parameters for the combustor at the sea level takeoff condition are:

Compressor Exit Axial Mach Number	0.26
Combustor Reference Velocity - m/sec (ft/sec)	25 (82)
Combustor Section Total Pressure Loss (%)	5.4
Combustor Exit Temperature Pattern Factor	0.42

Table 3

JT9D-7F Engine Combustor Operating Parameters

Operating Condition	Inlet Total Pressure MPa (psia)	Inlet Total Temperature °K (°F)	Combustor Airflow kg/sec (lb/sec)	Combustor Fuel/Air Ratio
Ground Idle (6.37% Thrust)	0.369 (53.6)	447 (345)	20.79 (45.75)	0.0109
Approach (30% Thrust)	0.896 (129.9)	582 (588)	42.14 (92.70)	0.0156
Climbout (85% Thrust)	1.972 (286.0)	735 (864)	80.48 (177.05)	0.0226
Sea Level Takeoff (100% Thrust)	2.257 (327.4)	767 (921)	89.18 (196.20)	0.0248
Max Cruise (10,668m/35,000 ft, M - 0.9)	0.946 (137.2)	700 (800)	38.93 (85.65)	0.0231

In addition to meeting the pattern factor requirement, the circumferentially averaged radial profile of the combustor exit temperature distribution must also be consistent with the design gas temperature distribution of the high pressure turbine blades. Figure 5 shows the required radial temperature profile.

Figure 6 shows the design flight envelope of the JT9D-7 engine. The engine must be capable of self starting with the combustor driven only by a windmilling fan and compressor over a substantial fraction of the flight envelope. Table 4 lists the combustor operating conditions at the lettered points on the upper boundary of the relight envelope as defined from the windmilling performance characteristics of the JT9D-7 compressor. As shown in the figure, flight testing of the JT9D-7 engine demonstrates that ignition has been accomplished over a wide range of conditions including conditions more severe than the required envelope.

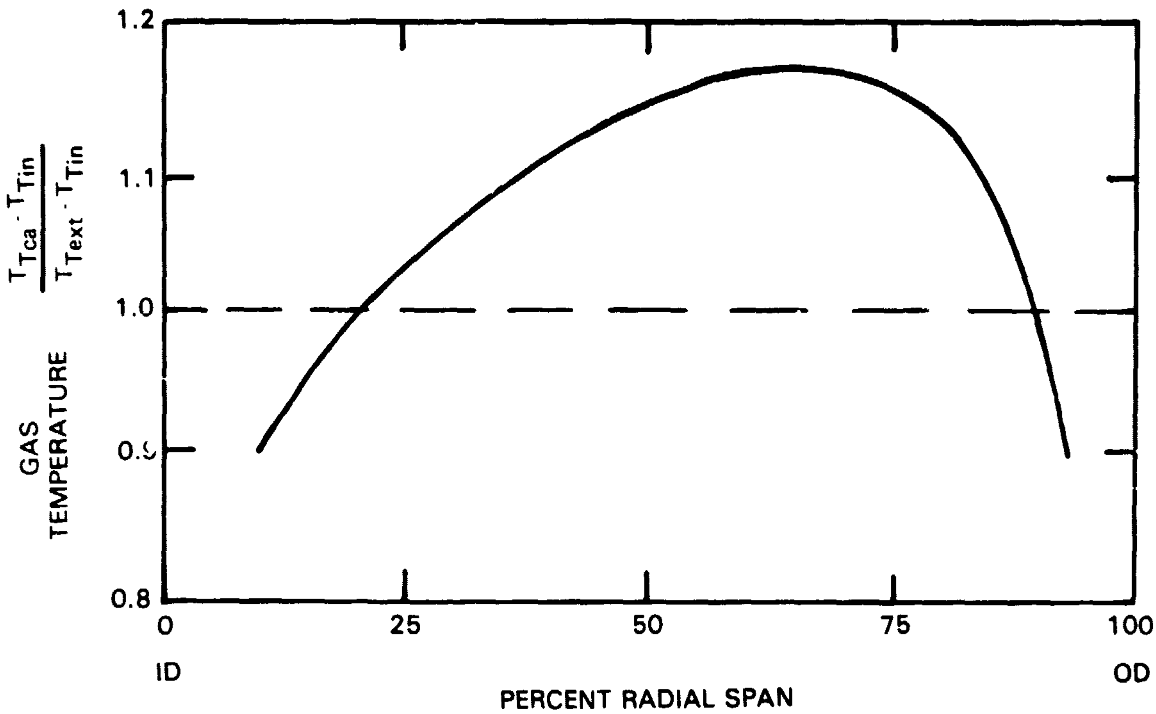

Figure 5 JT9D Combustor Exit Average Radial Temperature Profile

Table 4

Combustor Inlet Conditions at Altitude Pelight

Point of Figure 5:	A	B	C	D
Flight Mach Number	0.67	0.74	0.82	0.92
Altitude - meters (feet)	9150 (30,000)	9150 (30,000)	10,688 (35,000)	10,688 (35,000)
Combustor Inlet Total Pressure - MPa (psia)	0.038 (5.52)	0.041 (5.96)	0.036 (5.30)	0.044 (6.38)
Combustor Inlet Total Temperature - °K (°F)	256 (0)	261 (11)	258 (5)	270 (27)
Engine Airflow kg/sec (lb/sec)	3.48 (7.66)	4.15 (9.14)	4.04 (8.89)	5.32 (11.70)
*Fuel Flow - kg/hr (lb/hr)	289 (635)	289 (635)	289 (635)	289 (635)

*Minimum fuel flow of JT9D engine control schedule

ORIGINAL PAGE IS
OF POOR QUALITY

The JT9D engine specification also requires ground start capability at an ambient temperature of 219°K (-65°F) or the temperature at which the fuel viscosity is 12 centistokes. With Jet A fuel this occurs at an ambient temperature of about 239°K (-30°F). When the engine is cranked at this temperature the engine airflow is approximately 6.8 kg/sec (15.0 lb/sec), the combustor inlet total pressure is about 0.11 MPa (15.85 psia) and the air temperature rise in the compressor is essentially negligible. The fuel flow used for cranking start is 362 kg/hr (796 lb/hr).

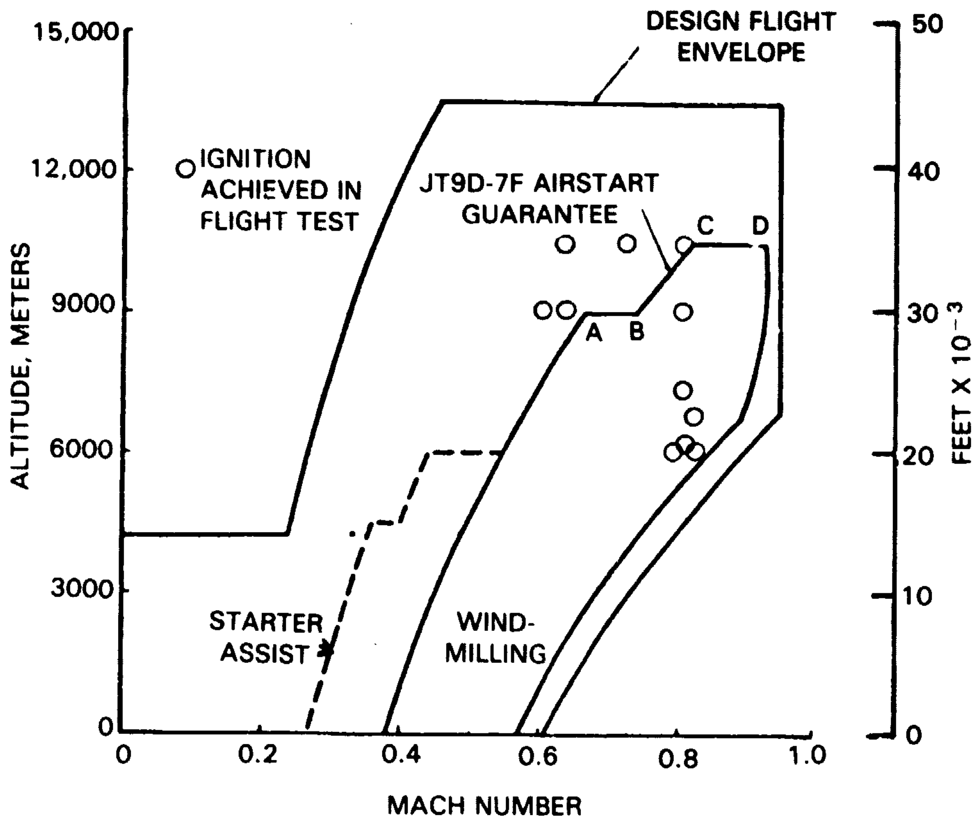

Figure 6 JT9D-7 Airstart Envelope and Demonstrated Ignition Capability from Flight Testing

3.5 REFERENCE COMBUSTOR EMISSIONS CHARACTERISTICS

Since the JT9D engine and combustion system were designed before current standards for gaseous pollutants had been issued, the combustor was not specifically intended to provide low emissions. However, the combustor does incorporate smoke reduction features and produces no visible smoke at any operating condition.

Exhaust emissions are periodically monitored during JT9D production acceptance tests. Typical results for the idle, 30 percent, 85 percent, and 100 percent sea level static thrust power settings are shown in Table 5. These power settings correspond to the simulated ground idle, approach, climbout, and takeoff conditions specified by the Environmental Protection Agency (EPA) to establish aircraft engine emission standards. The data presented in Table 5 represent average emission levels for JT9D-7F production engines incorporating the current combustor configuration. This combustor has been installed in production engines shipped since November 1975. The data have been corrected to standard day temperature and pressure and to an ambient humidity level of 6.3g H_2O/kg dry air. Jet A fuel was used for the tests. The corresponding values of the Environmental Protection Agency Parameter (EPAP) are also presented in Table 5. This parameter combines emission rates at the idle, approach, climb, and takeoff operating modes, integrated over a specific landing/takeoff cycle (Reference 12).

Table 5

Emission Characteristics of the JT9D-7F Combustor

	Emissions Index gm/kg			
	Carbon Monoxide	Total Unburned Hydrocarbons	Oxides of Nitrogen	SAE Smoke Number
Ground Idle	60.0	29.0	3.1	--
Approach (30% Thrust)	2.9	0.5	7.8	--
Climbout (85% Thrust)	0.4	0.3	34.4	--
Sea Level Takeoff (100% Thrust)	0.4	0.3	46.0	4
Max Cruise (M = 0.9, 10668 m/35,000 ft)	0.8	0.6	24.2	--
EPA Parameter - gm/kN	101	48	69	

Notes: Data for oxides of nitrogen presented as nitrogen dioxide equivalent.

Ground idle data is without compressor air bleed at minimum idle set point and approximately 6.37% of rated takeoff thrust.

Cruise emissions estimated on the basis of data obtained from sea level operating line.

SECTION 4.0

COMBUSTOR CONCEPTS AND TEST CONFIGURATIONS

The Phase I program was structured around the experimental evaluation of three combustor concepts which were selected to encompass a wide range of combustor technology. These concepts consisted of, in order of increasing complexity and potential:

- o A single stage combustor representative of the state of the art in current engines.
- o The staged Vorbix combustor developed under recent emissions abatement programs.
- o A variable geometry combustor in which the airflow to individual zones may be modulated to provide optimum stoichiometry.

A description of the baseline configuration of each of these combustor concepts is provided in this section. The modifications that were incorporated in subsequent configurations of each combustor are also identified and the motivation for the revisions is established.

4.1 SINGLE STAGE COMBUSTOR CONCEPT

After the JT9D-7 engine had been selected as the reference engine for the program, the combustor in this engine became the reference single stage combustor concept. The initial configuration was identical to the production combustor used in the JT9D-7F engine and was designated Configuration SS-1. Six additional single stage combustor configurations, Configurations SS-2 through SS-7, were also evaluated. All of these were based on an alternate JT9D combustor construction designated the "Advanced Bulkhead" combustor. This construction evolved from the basic JT9D-7 production combustor and is the Bill of Material burner in more recent engine models such as the JT9D-7R4.

4.1.1 Configuration SS-1; Production JT9D-7F Combustor

The mechanical arrangement of the JT9D-7 combustor has been discussed in Section 3.3 and illustrated in Figures 2 through 4. The basic mechanical configuration shown therein is common to several JT9D-7 engine models. Components for specific models such as the JT9D-7F differ primarily in liner air schedules to accommodate different cooling flow levels. Figure 7 shows the actual test combustor liner for Configuration SS-1. The test rig is constructed from a sector of an engine diffuser case and the test combustor liners are a 72 degree sector cut from a full annular production JT9D-7F combustor liner. The only modification to these liners is the installation of flanges for attachment to the rig endwalls. This assures accurate reproduction of engine combustor geometry and airflow schedule.

Figure 7 Current Production JT9D-7 Combustor Liner Sector

Figure 8 shows the airflow distribution in Configuration SS-1 as deduced from pressure measurements in the test rig. The corresponding airflow aperture sizes in the liners of this and all of the other test combustor configurations are listed in Appendix A of this report. As shown in the figure, nearly half of the combustor airflow is used for cooling with a substantial fraction of the airflow used on the flame stabilization cones in the front end of the burner. Primary zone airloading in this combustor is about 35 percent of the total combustor airflow. It consists of the air admitted through the fuel injector-swirler aperture, the combustion air jets in the first louvers of the inner and outer liner, and a fraction of the cone cooling air. This loading produces an equivalence ratio in the primary zone of about unity at takeoff and 0.5 at idle operating conditions. This stoichiometry is consistent with the historical observation of low smoke output from the JT9D-7F engine and would also indicate that substantial reduction in idle carbon monoxide and unburned hydrocarbon emissions could be achieved by enriching the primary combustion zone, i.e., by reducing the airloading.

The fuel injector in the JT9D-7 production combustor is a duplex pressure atomizing injector with concentric primary and secondary orifices producing hollow cone spray patterns. Figure 9 shows the flow schedule of the injector. The fuel supply system includes a pressurizing valve to control the primary/secondary fuel flow split. At low fuel flow rates all fuel is discharged through the primary system, but when the pressure drop across the fuel injector exceeds 1.03 MPa (150 psi) the pressurizing valve opens to admit flow to the secondary system. As fuel supply pressure is increased further the valve scheduling admits progressively more fuel flow into the secondary system. As shown in the figure, the fuel flow split between the primary and secondary system is about 50-50 at the nominal JT9D-7F idle condition. At higher fuel flow conditions the fraction of the total fuel passing through the primary system is substantially less; about 15 percent at cruise and about 6.5 percent at takeoff.

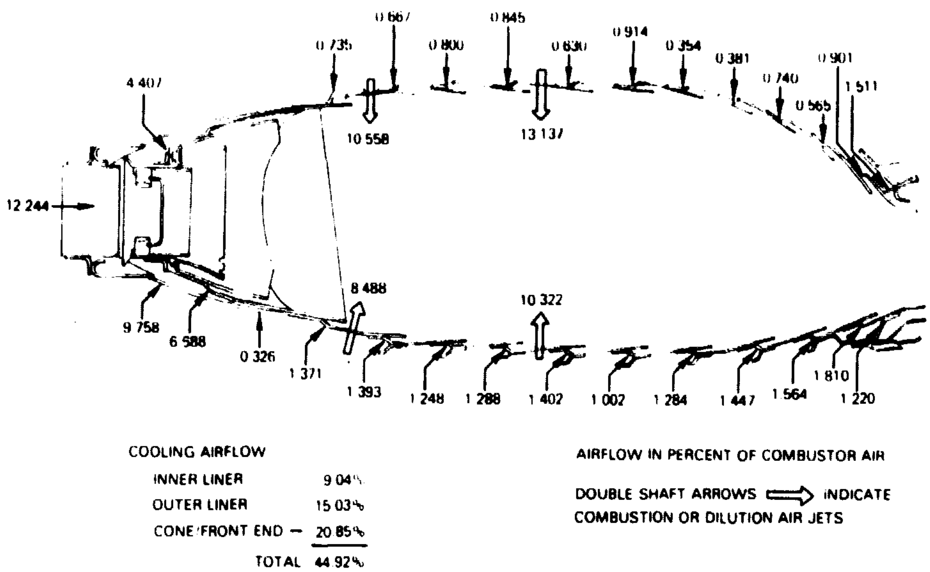

Figure 8 Airflow Distribution in Configuration SS-1

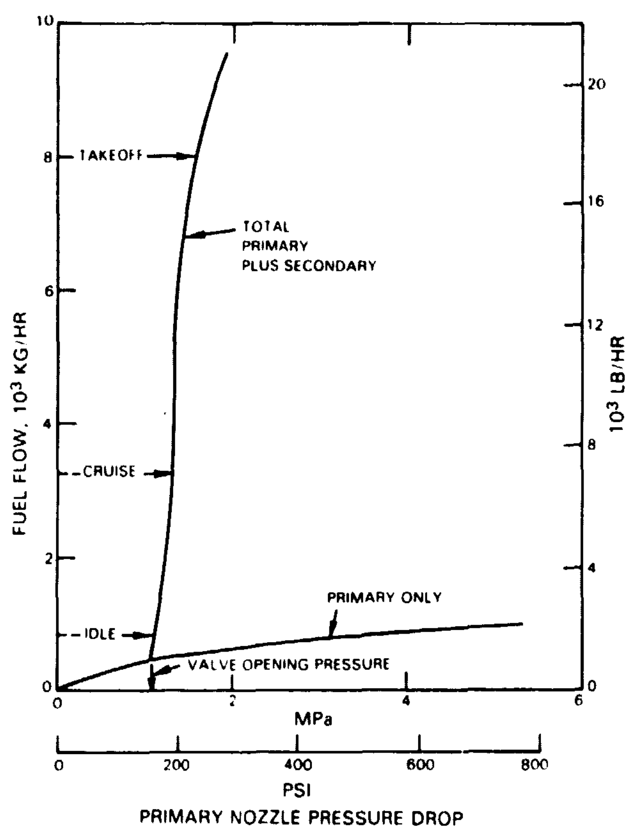

Figure 9 JT9D-7 Fuel Flow Schedule

4.1.2 Configuration SS-2; Advanced Bulkhead Combustor

The advanced bulkhead combustor was originally designed to provide a retrofit combustor for the JT9D-7 series of engine models that would be capable of satisfying the proposed Environmental Protection Agency standards for carbon monoxide, unburned hydrocarbon and smoke emissions from engines manufactured after January 1, 1981 (Table 2). From the onset the design was constrained by the requirements for compatability with the other engine components, including the diffuser case and fuel supply system, as well as a desire for maximum parts commonality with the current production combustor. As the development of this combustor progressed it became evident that it would achieve these emissions goals while satisfying the operational requirements of in-service components and offering advantages in durability relative to the production combustor. After the current production combustor had been selected as the reference single stage combustor for this program it was logical to select the advanced bulkhead combustor as the first perturbation of the single stage concept and it was adopted as Configuration SS-2.

Figure 10 shows a cross section of the advanced bulkhead combustor. It differs mechanically from the current production combustor in two particular aspects: the construction of the front end and the type of fuel injector. Following its namesake, the front end of the combustor has been revised to incorporate a bulkhead rather than multiple cone type construction. This configuration considerably simplifies burner construction and makes more effective use of cooling air in the primary combustion zone because of the smaller surface area of the annular bulkhead. The bulkhead construction also removes cooled walls from the immediate proximity of the reaction zones which minimizes the interaction of the cooling air on these surfaces with critical carbon monoxide and unburned hydrocarbon consuming reactions.

In the advanced bulkhead combustor, the duplex pressure atomizing fuel injector of the current production combustor has been replaced with a duplex injector with an aerated secondary fuel system. Figure 11 shows a cross section of this fuel injector. It incorporates highly swirling airflow radially inside and outside the prefilming surface to atomize the secondary fuel. For compatability with the existing JT9D-7 fuel system the primary/secondary flow schedules and splits as well as pressure drops are identical with those of the baseline injector shown in Figure 9. The aerated secondary fuel system was incorporated in the advanced bulkhead combustor because it was recognized that the combustor might have to operate at richer primary zone equivalence ratios than the current production combustor in order to reduce idle carbon monoxide and unburned hydrocarbon emissions. These richer equivalence ratios could lead to excessive smoke formation at high power levels. Use of the aerated injector leans the critical smoke formation region near the injector face and reduces the fuel droplet size at high power - both of which are conducive to reduced smoke formation. Fuel injector atomization evaluations conducted under the present program (reported in Appendix B) confirmed the superior atomization characteristics of this fuel injector relative to the duplex pressure atomizing injector.

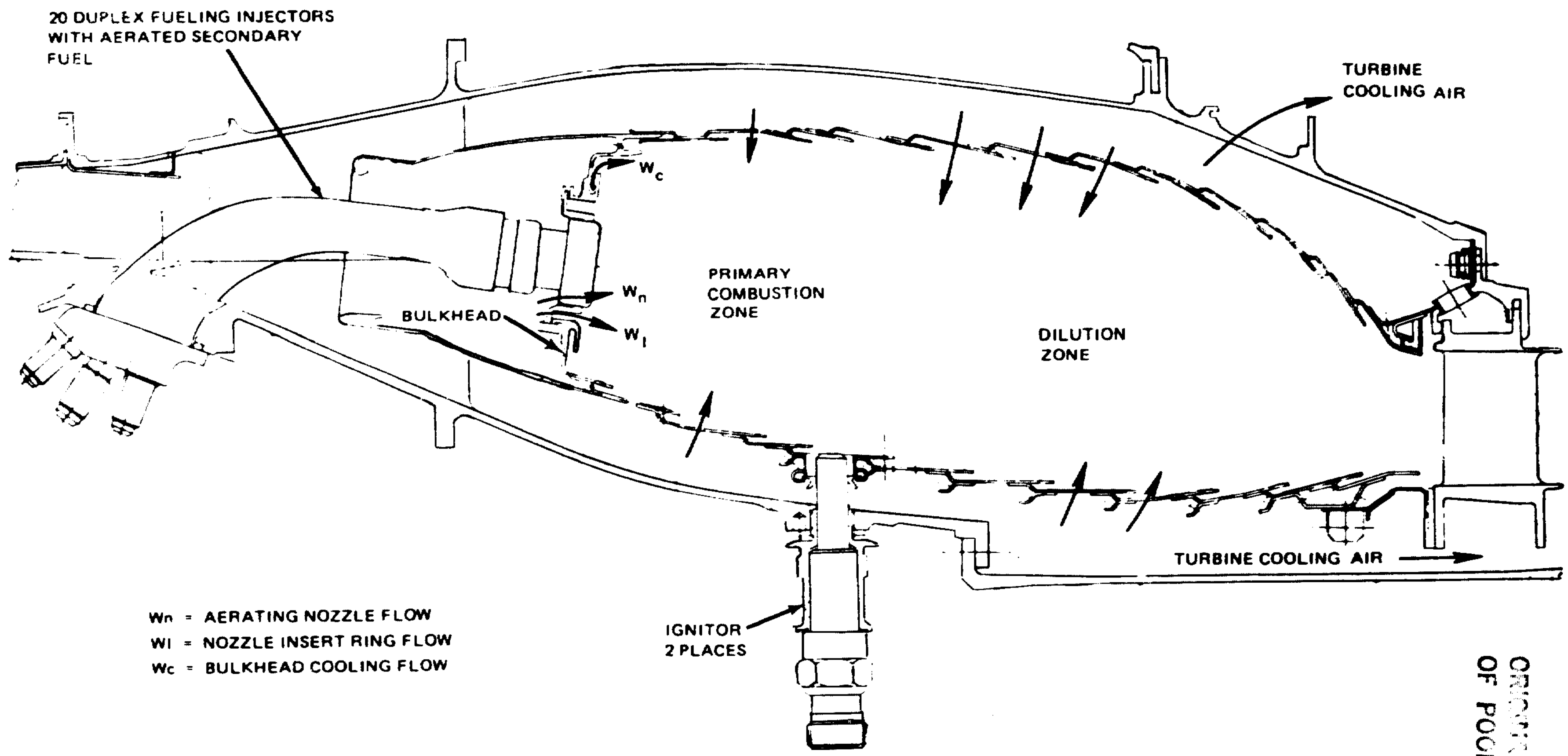

Figure 10 JT9D-7 Advanced Bulkhead Combustor

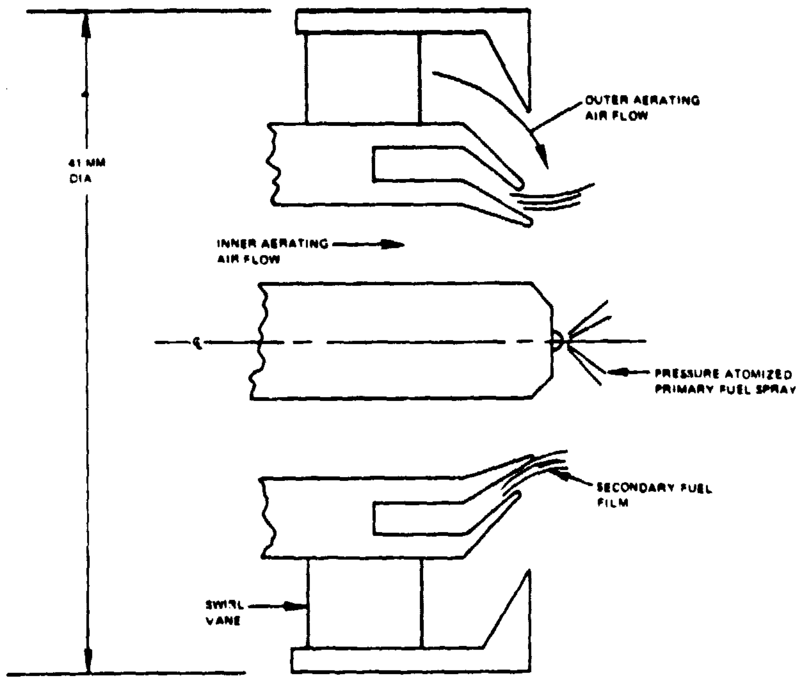

Figure 11 Schematic Cross Section of Experimental Duplex Aerating Injector Used in the Advanced Bulkhead Combustor Concept

While the circumferential fuel injector density is identical, use of the bulkhead construction shifted the point of fuel injection downstream relative to the current production combustor. Long injector supports had to be used to retain the injector mount position on the diffuser case. The configuration of the hood enclosing the front end of the combustor was also modified to accommodate installation of the larger aerating injectors and to enhance the airflow feed to the front end of the combustor.

The louver cooled liner of the advanced bulkhead combustor is essentially identical to the liner in the production combustor over the downstream two thirds of its length; the only variation is in the sizes of the cooling air and dilution air jet orifices and the locations of the latter.

Figures 12 and 13 show the advanced bulkhead combustor sector that was used during the experimental evaluation. The above cited modifications to the combustor hood relative to the current production combustor are evident on comparison with Figure 7.

Figure 12 JT9D Bulkhead Combustor Sector

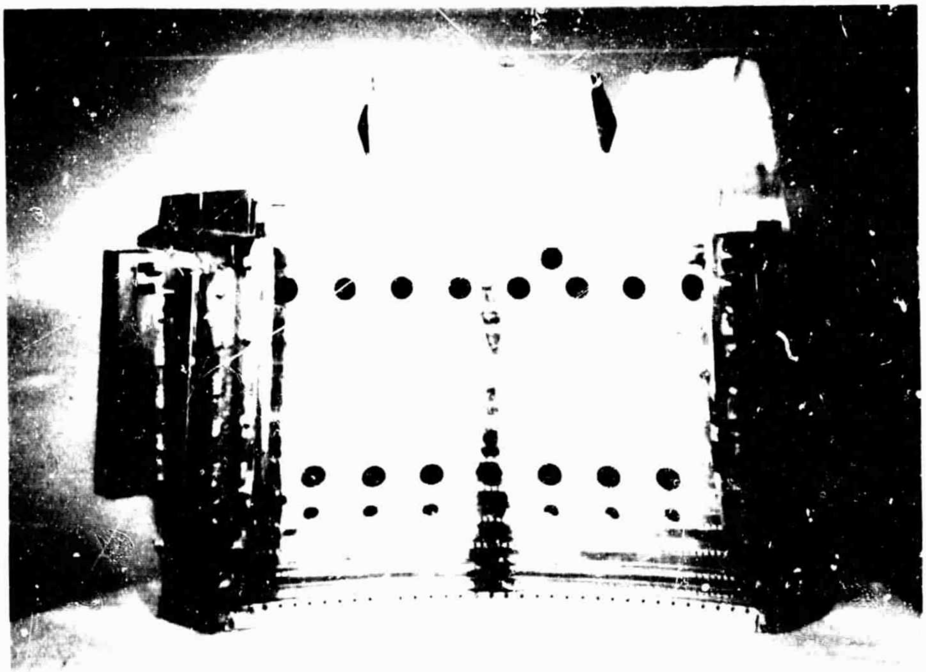

Figure 13 Inner Liner Side of JT9D Bulkhead Combustor Sector

Figure 14 shows the airflow distribution observed in Configuration SS-2. The liner aperture sizing schedule for this configuration duplicates the optimum established in the engine development program. The primary zone stoichiometry had evolved through a tradeoff of low power carbon monoxide emissions, high power smoke output and operational considerations. Primary zone airloadings are derived from the injector and insert airflows and the flows through the combustion air holes in the second louver panel of the inner and outer liner and total 29.74 percent of combustor airflow. This produces primary zone bulk equivalence ratios of about 0.5 at idle and 1.0 at takeoff. These are comparable to the equivalence ratios in the current production combustor and suggest that the idle emissions reduction accomplished with the bulkhead combustor may be attributable to avoiding reaction quenching with cooling air rather than richer stoichiometry. However, there is some evidence that the combustion air jets entering the bulkhead combustor act only to stabilize the location of a primary reaction zone formed by the injector and insert airflow but do not become intimately mixed with these streams. On this premise the actual primary reaction zone is considerably richer than the bulk equivalence ratio would indicate and stoichiometry may also be a significant factor in the improved low power emissions characteristics. Further evidence of this locally rich combustion will be found in the discussion of other test configurations.

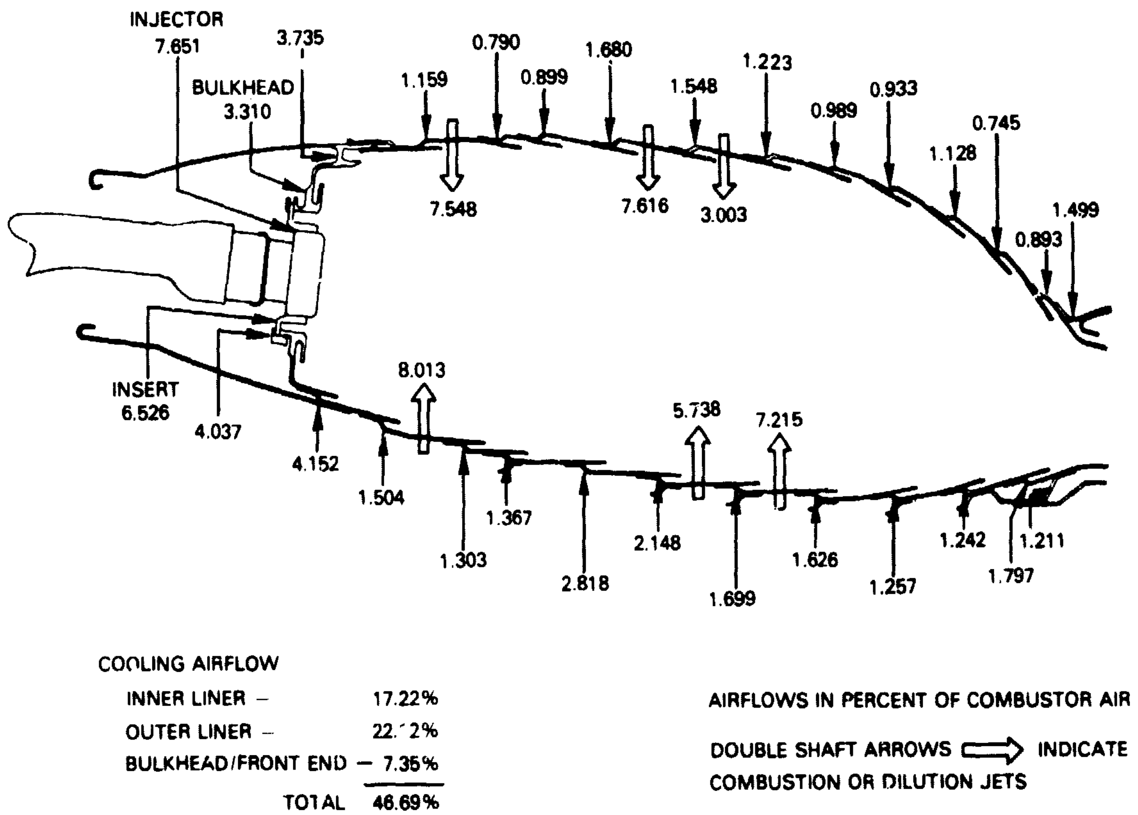

Figure 14 Airflow Distribution in Configuration SS-2

The data of Figures 8 and 14 indicate that the total cooling airflow requirements of the advanced bulkhead combustor and the current production combustor are comparable. However, the quantity of air used to cool the bulkhead and injector insert in the bulkhead type combustor is less than half that used to cool the front end of the production combustor. The deleted front end cooling air is diverted to the louvers in the liners of the advanced bulkhead combustor to enhance the durability of these components. With comparable primary zone airloading and liner cooling air requirements, both combustors have about the same 23 percent of combustor airflow available for use in the dilution zone to control the combustor exit temperature distribution.

4.1.3 Additional Modifications to the Single Stage Combustor Concept

The assessment of the sensitivity of the current production JT9D-7 combustor to fuel composition, derived from the evaluation of Configuration SS-1, established a baseline for the remainder of the program. Subsequent testing of Configuration SS-2 extended this baseline to an improved single stage combustor consistent with the most recent models in the JT9D engine series. The remaining configurations of the single stage combustor concept, Configurations SS-3 through SS-7, were defined to investigate the effect of design perturbations to the advanced bulkhead combustor and to identify those modifications that would reduce the sensitivity of the combustor to fuel composition. Table 6 lists the seven single stage combustor configurations evaluated. Configurations SS-1 and SS-2 establish the baseline. The remaining configurations are used to determine the effects of changes to (1) fuel injectors, (2) primary zone stoichiometry and residence time, and (3) liner cooling approach. These configurations are described further in the remainder of this section.

Fuel Injector Modifications

Variations in fuel properties, primarily viscosity but to a lesser extent surface tension and specific gravity, are known to affect the atomization characteristics and spray patterns produced by fuel injectors. Figure 15 shows the variation in Sauter Mean Diameter of the spray from the duplex pressure atomizing primary/aerating secondary system fuel injector used in Configuration SS-2. These data are reproduced from Appendix B of this report which includes the results of a series of spray characterization tests conducted on the fuel injectors used during this program. The data shown demonstrate a trend toward increasing droplet size with the shift from Jet A to Experimental Referee Broad Specification Fuel and continuing increases as fuel viscosity is increased further. Since deterioration of fuel atomization could adversely impact several combustor performance parameters, including ignition capability, emissions at lower power and smoke formation, a modified fuel injector was evaluated in Configuration SS-4. This injector was a modified version of the basic duplex pressure atomizing primary/aerating secondary fuel injector shown in Figure 11 and incorporated revisions designed to enhance the atomization of a more viscous broadened properties fuel. These included redesign of the swirl vanes in the outer aerating air passage and the entry to the inner aerating air passage to increase the swirl angle of the air. The contours of a passage feeding wash air over the face of the primary fuel nozzle face were also revised to enhance fuel atomization with this system. Airflow calibrations of the injectors indicated that the net effect of these modifications was to reduce the airflow capacity of the injector by about four percent while the swirl strength of the discharging airflow was increased about ten percent.

Table 6

Single Stage Combustor Test Configurations

Configuration Number	Combustor Type	Fuel Injector[1]	Primary Zone Equivalence Ratio Idle/Takeoff	Primary Zone Length - cm (in)[2]	Comments
SS-1	Production	Pressure Atomized	0.48/1.09	21.3 (8.4)	Baseline relevant to engine experience.
SS-2	Bulkhead	Aerated	0.44/0.98	13.7 (5.4)	New baseline with improved combustor construction.
SS-3	Bulkhead	Aerated	0.44/0.98	21.2 (8.3)	Effect of increase in primary zone residence time relative to Configuration SS-2.
SS-4	Bulkhead	Modified Aerated	0.44/0.98	13.7 (5.4)	Effect of modified fuel injector relative to Configuration SS-2.
SS-5	Bulkhead	Aerated	0.94/2.13	17.5 (6.9)	Richer — Effect of primary zone equivalence ratio relative to Configuration SS-2.
SS-6	Bulkhead	Aerated	0.34/0.77	17.5 (6.9)	Moderately Leaner — Effect of primary zone equivalence ratio relative to Configuration SS-2.
SS-7	Bulkhead with Finwall®	Modified Aerated	0.41/0.92	13.7 (5.4)	Best features of above configurations in combination with improved primary zone cooling approach.

1 - Refers to secondary fuel system mode.
2 - From fuel injector face to leading edge of first dilution air hole in liner.

ORIGINAL PAGE IS OF POOR QUALITY

Before incorporating this injector in the high pressure combustor rig for Configuration SS-4, bench tests were conducted to assess its atomization characteristics relative to the baseline injector used in Configuration SS-2. The results of these investigations are also presented in Appendix B. These data revealed that the objective of enhancing atomization by revising the aerating passages of the secondary system had been accomplished. When the injector was operated on the secondary fuel system, Sauter Mean Diameters of the spray averaged 25 percent less than the baseline injector operating at comparable conditions. Improvements of this magnitude would be expected to offset the adverse effect of changes in fuel viscosity identified in Figure 15. The revisions to the airflow in the primary fuel injection system did not appear to produce any significant improvement in atomization characteristics.

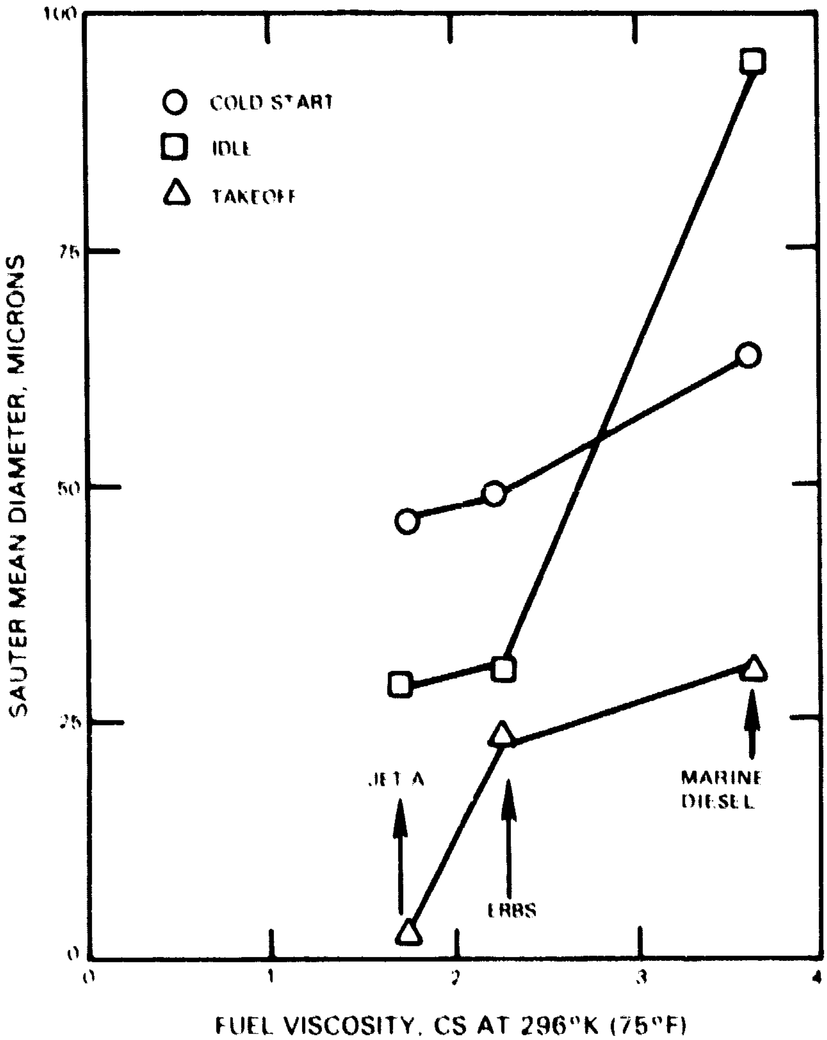

Figure 15 Atomization Characteristics of Duplex Aerating Secondary Fuel Injector Used in Configuration SS-2

Airflow Schedule Revisions

Primary zone stoichiometry is known to be a fundamental combustor design parameter affecting combustion stability, emissions, particulate formation and liner heat loading. Optimum stoichiometry is generally established by a trade between these operating parameters. The introduction of broadened property fuels can alter combustor operation and necessitate reoptimization to achieve the best overall combustor performance. Consequently, perturbations to the residence time and the equivalence ratio in the primary zone of the single stage combustor were investigated to provide the basis for such a reoptimization of the advanced bulkhead combustor with ERBS fuel.

Three combustor configurations, Configurations SS-3, SS-5 and SS-6 were involved in this sequence of perturbations. Figure 16 shows the airflow distribution in these configurations relative to the baseline bulkhead type combustor configuration (SS-2) while Table 6 indicates the bulk primary zone stoichiometry of these configurations. Details on the aperture sizes in the liners are provided in Appendix A.

In Configuration SS-3 the residence time in the primary zone was extended relative to the baseline by moving the dilution air jet orifices downstream on the liner. Increasing the length of the reaction zone prior to quenching with dilution air jets could provide more time for oxidation of carbon monoxide or particulates but could also allow more oxides of nitrogen to be formed.

Configurations SS-5 and SS-6 were used to evaluate richer and leaner primary zone equivalence ratios. In Configuration SS-5 the primary combustion air jet orifices in the second louver panel of the inner and outer liner were plugged and the air diverted to additional holes in the dilution zone of the combustor. This increased the bulk primary zone equivalence ratio at idle to nearly unity, a change which would be expected to minimize carbon monoxide and unburned hydrocarbon emissions at this condition. The reduced primary zone airloading could also be conducive to easier ignition and enhanced stability if either of these parameters were compromised by the use of broadened properties fuels. While not pursued in this phase of the program, proper use of the additional dilution air made available by reducing the primary zone loading could enhance control of the combustor exit temperature distribution. However, the higher primary zone equivalence ratios could also increase particulate formation and heat load on the combustor liner at high power.

In Configuration SS-6, the primary zone equivalence ratios were reduced by increasing the airloading on the primary zone. This was accomplished by enlarging the combustion air jet orifices on the second louver panel and making a compensating reduction in the area of the dilution air orifices in order to maintain essentially the same combustor section total pressure drop as the baseline configuration. This excursion was expected to relieve some of the additional liner heat load caused by the use of a lower hydrogen content fuel. However, the extent of the shift in primary zone airloading incorporated in Configuration SS-6 was limited to minimize adverse impacts on low power combustion stability and emissions.

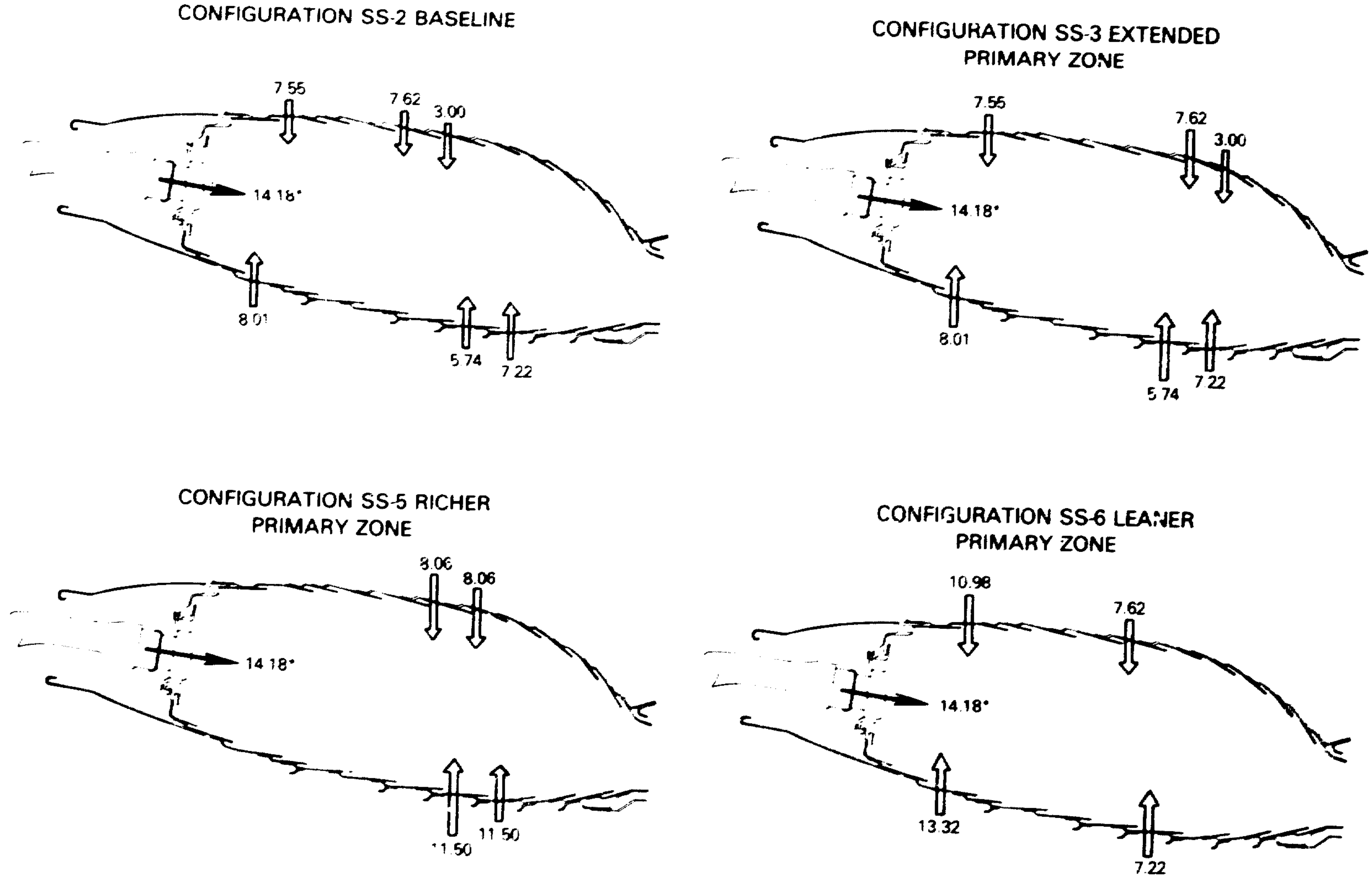

FLOWS IN PERCENT OF COMBUSTOR AIRFLOW

* COMBINED INJECTOR AND INSERT FLOW
COOLING AIR FLOWS OF ALL CONFIGURATIONS ESSENTIALLY IDENTICAL TO CONFIGURA... SS-2 ON FIGURE 4-8

Figure 16 Airflow Distribution in Single Stage Combustor Configurations

Improved Liner Cooling Approach

A major concern with the use of broadened properties fuels is the potential increase in radiant heat load on the combustor liner and the attendant increase in metal temperatures and reduction in liner life. Higher heat loads can be countered by increasing the quantity of cooling air and thus maintaining metal temperatures at current levels, but this appproach can have adverse effects on combustor operation. Higher coolant levels in the primary combustion zone can quench reactions that would otherwise consume carbon monoxide and unburned hydrocarbons and therefore lead to increased levels of these pollutants. The increased cooling air also must be diverted from another function - most likely dilution of the combustion gases - which could impede maintenance of the design combustor exit temperature distribution. To avoid these compromises while still maintaining liner life it would be advantageous to replace the conventional film cooled louvers in the combustor with a construction incorporating a more effective cooling concept. This approach was pursued in Configuration SS-7 by incorporating Finwall® panels in place of the louvers enclosing the primary zone of the advanced bulkhead combustors. As shown in Figure 17, Finwall® is a double walled liner construction with a multitude of parallel axially directed internal cooling air passages. Because of the characteristically small dimensions of the passages, there is a high rate of heat transfer to the cooling air which is subsequently discharged to film cool the gas side of the downstream panel. Combustion or dilution air jets are directed through the Finwall® panels without compromising local cooling by installing grommets around the holes. The grommet serves as a manifold to collect the cooling air flow from the interrupted passages and redistribute it into the passages downstream of the hole.

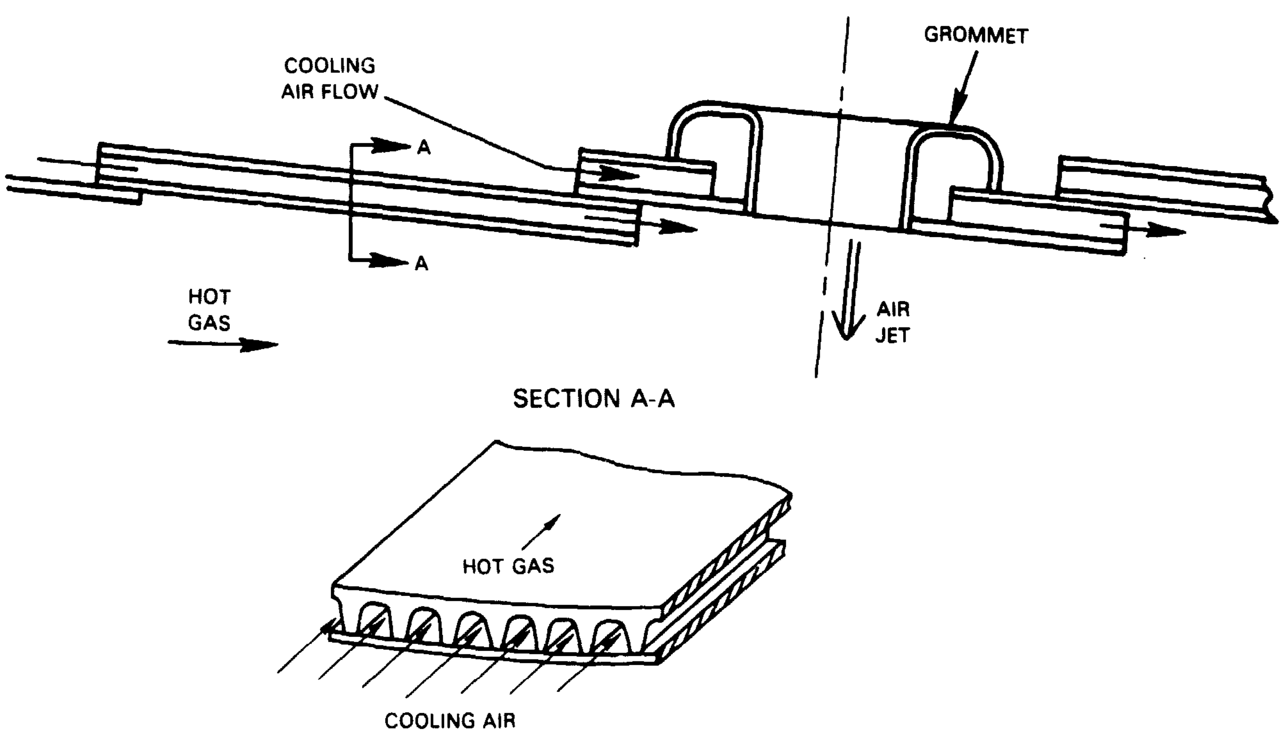

Figure 4-11 Finwall® Liner Configuration

Figures 18 and 19 show the sector of the advanced bulkhead combustor with the Finwall® panels installed in the liner. On the inner liner three louvers have been replaced with two panels of Finwall®, while four louvers of the outer liner have been replaced with three Finwall® panels. The design of this configuration was based on the requirement that the maximum combustion gas side metal temperature on the Finwall® panels at sea level takeoff with ERBS fuel would be no higher than that encountered in the louver liner with Jet A fuel. Thermal analysis indicated that this requirement could be met while the net cooling air flow to five Finwall® panels was 27.5 percent less than the cooling air flow in the seven louver panels they replaced.

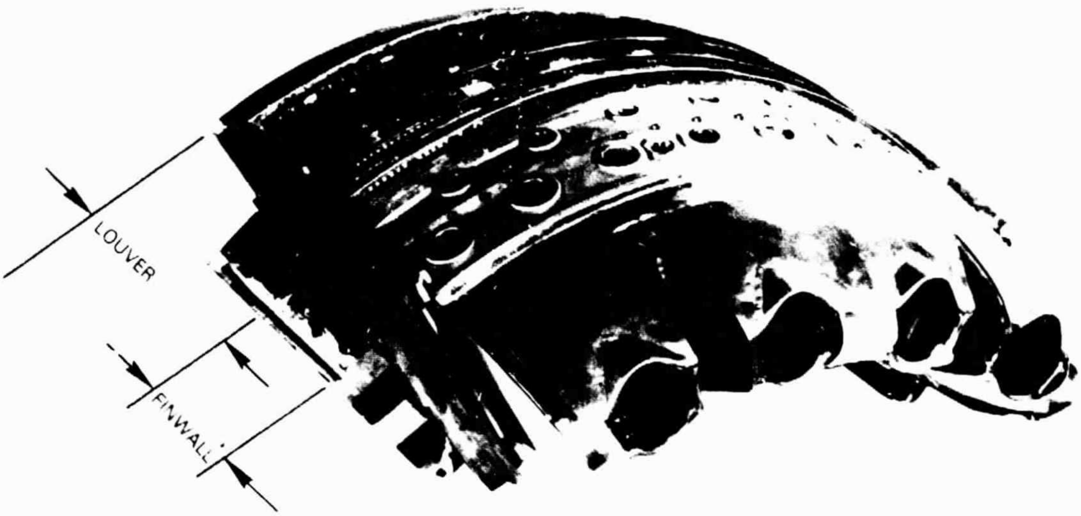

Figure 18 Outer Liner Side of JT9D-7 Bulkhead Combustor with Finwall® Liner Panels

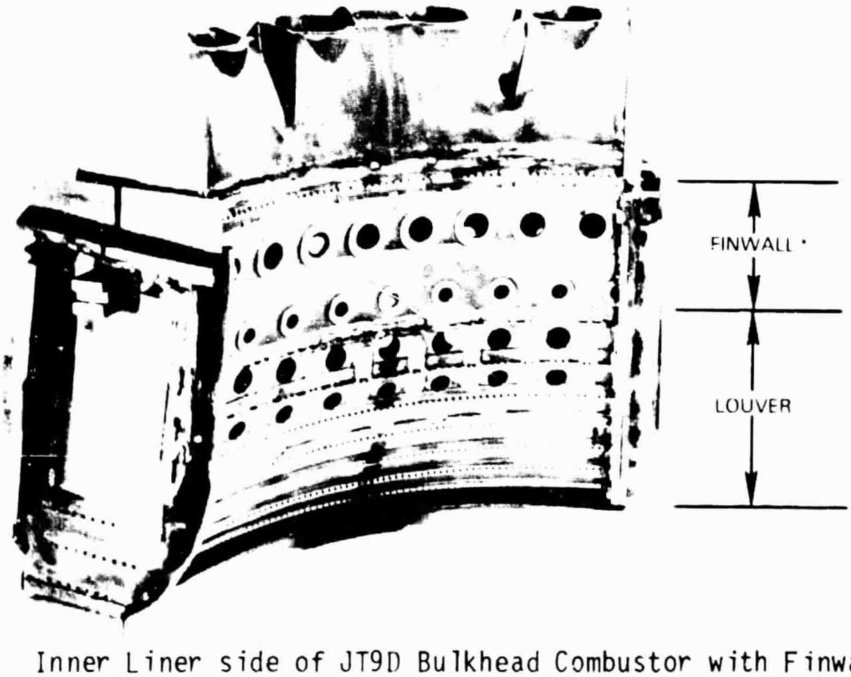

Figure 4-13 Inner Liner side of JT9D Bulkhead Combustor with Finwall® Liner Panels

Figure 20 shows the airflow distribution in Configuration SS-7 and reflects this reduction in primary zone cooling air. Relative to the baseline bulkhead combustor of Configuration SS-2, the diverted liner cooling air, which amounted to about 3 percent of the combustor airflow, was redistributed among the primary zone combustion air and dilution zone orifices in the liner. The cooling flow to the remaining louvers of the liner, and the front end airflow to the fuel injector, insert and bulkhead cooling system were essentially identical to those of Configuration SS-2 (shown on Figure 14). Since this configuration was intended to represent the final or best configuration of the single stage combustor concept the modified pressure atomized primary/aerated secondary fuel injector from Configuration SS-4 was used because this injector was found to offer advantages over the baseline injector.

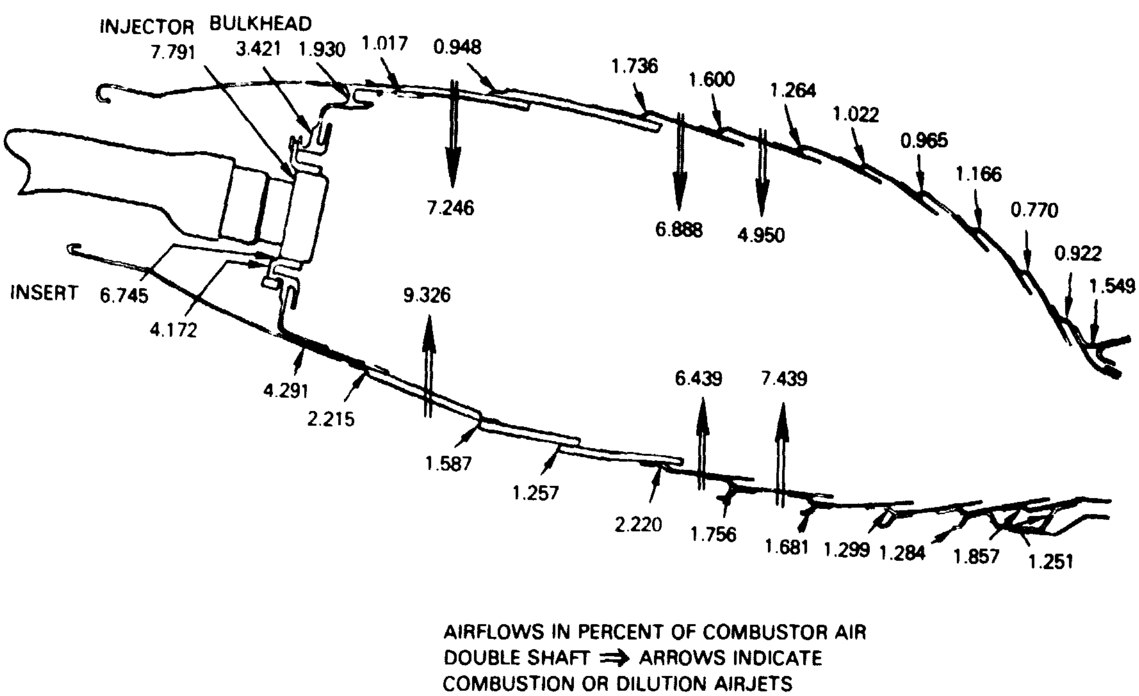

Figure 20 Airflow Distribution in Configuration SS-7

The photographs of the burner sector for the bulkhead combustor with Finwall® panels (Figures 18 and 19) show larger and more numerous primary combustion air holes than required to admit the primary zone airflow indicated on Figure 20. This occurs because this burner sector was also used to assess configurations of the variable geometry combustor concept in which high primary zone airloadings were employed (c.f. Section 4.3). Grommeted holes were made in the Finwall® liners for these maximum airloading configurations and plugs or washers were installed on the grommets to eliminate or restrict flow to the level required in the other configurations, including Configuration SS-7.

4.2 STAGED COMBUSTOR CONCEPT

A staged combustor was selected as the second concept for evaluation in the Phase I program. The principal feature of these burners is the use of two distinct combustion zones, each serviced by an independent fuel injection system. By operating the combustor on only one zone at low power levels and both zones at high power the combustor may be optimized at two operating conditions, rather than a single condition. This type of stoichiometry control would be required if emissions of oxides of nitrogen were severely restricted in the airport vicinity. It also appears to be useful in circumventing some of the problems associated with the use of broadened properties fuels. The Vorbix staged combustor concept had been evolved under the NASA/Pratt & Whitney Experimental Clean Combustor Program (References 5, 6, and 7). More recently, a second generation or improved version of this concept was developed under the NASA/Pratt & Whitney Energy Efficient Engine Program (Reference 8); this advanced version was selected as the staged combustor concept for the Phase I program.

4.2.1 Staged Combustor Description

Figure 21 shows a cross section of the staged Vorbix combustor as it is configured in the Energy Efficient Engine. The combustor includes two distinct burning zones -- a pilot zone and a main combustion zone. The pilot zone operates at all flight conditions and is designed to minimize emissions at idle and provide adequate stability and ignition characteristics. The main zone is operative at conditions above idle. In this zone, lean combustion occurs to minimize emissions of smoke and oxides of nitrogen at high power. The combined operation of these zones provides emissions control throughout the entire flight spectrum.

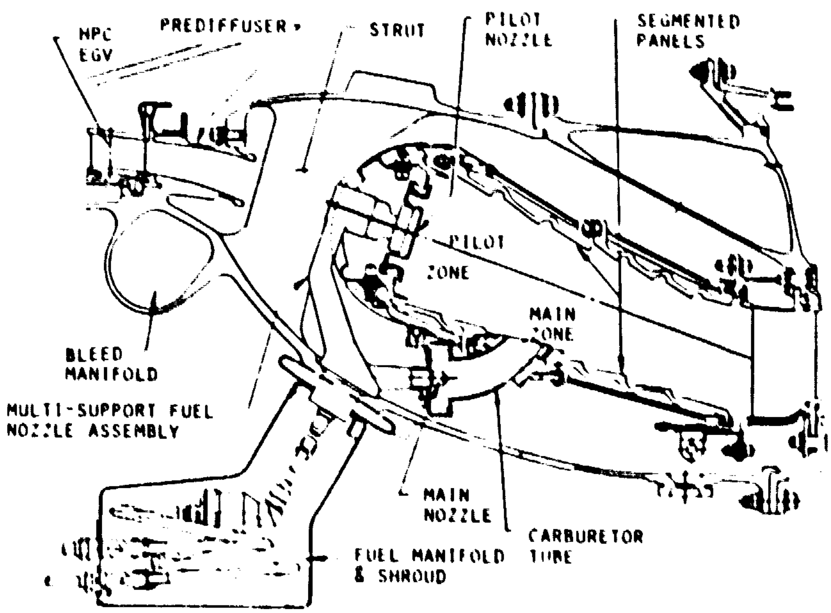

Figure 21 Cross Section of Staged Vorbix Combustor from the Energy Efficient Engine

This advanced Vorbix combustor includes a number of significant improvements over the first generation combustor evolved under the NASA/Pratt & Whitney Experimental Clean Combustor Program. The spatial heat release rate of the pilot zone is considerably lower. This results in lower reference velocities and higher residence times, which is conducive to lower carbon monoxide and unburned hydrocarbon emissions. Another characteristic is the increase in dome height. This provides a larger recirculation zone for better relight and starting and enhances the capability to reduce emissions at idle.

Aerated fuel injectors are used in the pilot zone rather than the pressure atomizing nozzles used in the Experimental Clean Combustor design. The aerated injector provides adequate fuel spray characteristics at idle where the fuel flow and pressure drop are low.

The combustor main zone design retains the oxides of nitrogen reduction features demonstrated in the Experimental Clean Combustor Program and incorporates modifications to improve liner durability, reduce high power smoke and simplify the configuration. These enhancements provide a more viable combustor for a commercial engine.

The most notable difference between the two designs is the method by which fuel is injected into the main zone. In the first generation Vorbix staged combustor, fuel was injected directly into the main zone through pressure atomizing injectors and mixed with swirling airstreams issued from swirlers in the inner and outer liner walls. The advanced Vorbix combustor concept features a compact carburetor tube arrangement, shown in Figure 22, that premixes the fuel and air prior to combustion. Fuel is supplied to each of the forty-eight carburetor tubes by a simplex pressure atomizing fuel nozzle. A fraction of the fuel is vaporized while the remaining fuel is centrifuged out to the walls of the tube via air introduced through a radial inflow swirler. The fuel film formed at the exit plane of the tube is sheared into droplets by the swirling core and secondary jets. This accomplishes three tasks: (1) some premixing of fuel and air occurs to eliminate rich burning zones in the combustor and to reduce smoke emissions; (2) the combination of swirler and fuel injector results in a reduced blockage flow area in the outer shroud passage; (3) the fuel is conveyed into the burning zone by the carburetor tube swirling air resulting in better fuel penetration and dispersion.

The liner in the staged combustor in the Energy Efficient Engine is unique in that it employs Counter Parallel Flow Finwall® cooling in conjunction with a segmented construction (see Figure 23). This cooling concept offers distinct advantages over more conventional internally cooled constructions in that the cooling air is introduced through apertures in the outer wall at the center of the panels and flows both forward and aft in the internal channels before being discharged into the combustor gaspath. Because the juncture region between panels is contacted only by cooling air that has been heated in its passage through the panels, temperature gradients in the metal in these regions are minimized. This feature offsets the fundamental difficulty encountered with previous internally cooled liner concepts in which the unidirectional cooling air flow caused significant thermal gradients at the panel junctures that were simultaneously subjected to "cold" inlet cooling air and heated air discharging from the upstream panel.

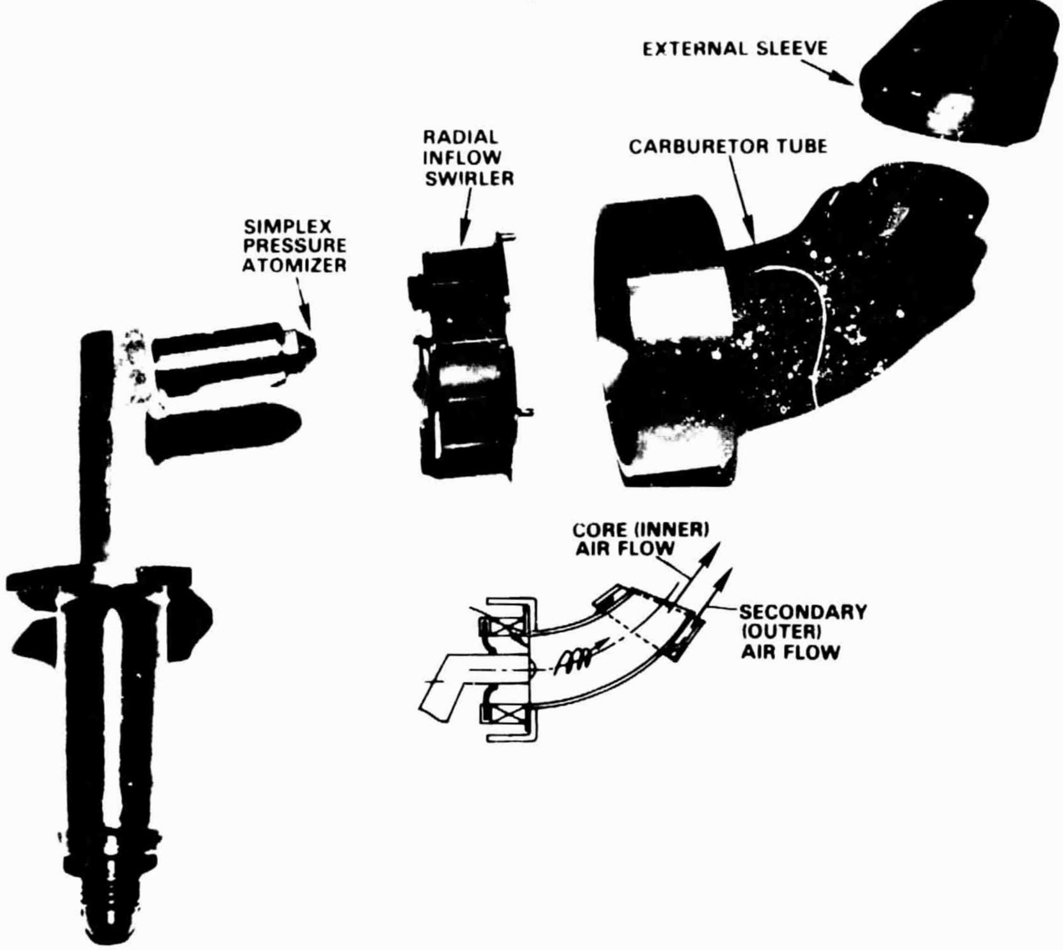

Figure 22   Main Zone Fuel Injector - Carburetor Tube Assembly Features

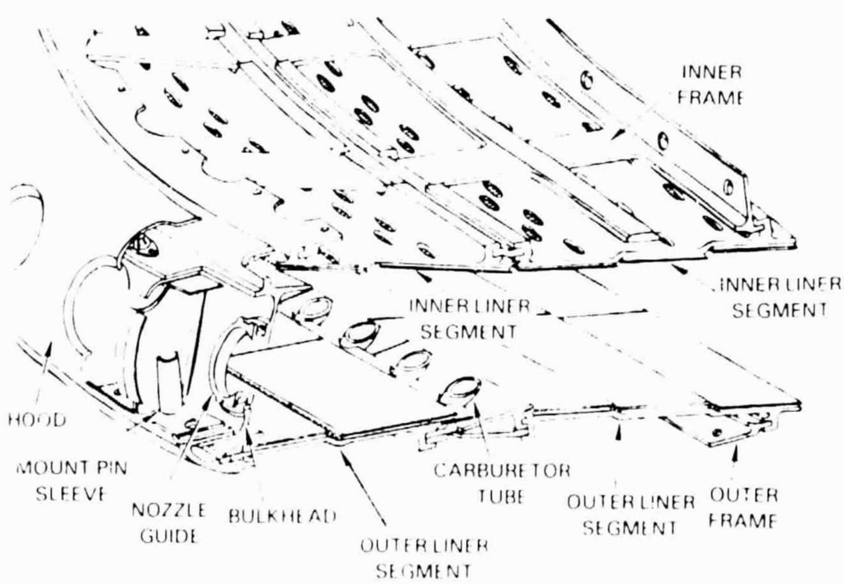

Figure 23 Isometric View of Segmented Liner Assembly

The segmented construction is incorporated in the Energy Efficient Engine combustor liner to eliminate hoop stress effects which would otherwise be the life-limiting failure mode. The liner segments are investment cast nickel base alloy with cooling air passages and seal slots electrochemically machined. The circumference of a full annular liner is divided into 24 segments. The segments are attached onto external frames by the integrally cast holes and lugs as shown in Figure 4-17. Air leakage between segments is minimized by feather seals.

4.2.2 Staged Combustor Test Configurations

Although the JT9D-7F had been selected as the reference engine for the Phase I program, the advanced Vorbix staged combustor was evaluated with components from the Energy Efficient Engine because of the availability of hardware from that program. Under the Energy Efficient Engine (E^3) program, a combustor sector rig had been fabricated and used in an extensive effort to evolve and optimize the configuration and performance characteristics of the combustor in the E^3 engine. This effort, documented in References 8 and 9, involved high pressure testing of eighteen configurations with Jet A fuel and led to a well established optimum configuration. Because of the thorough nature of this recent effort on the staged combustor concept, the activity under Phase I of the Broad Specification Fuels Combustion Technology program was restricted to an assessment of the sensitivity of this concept to fuel composition. This sensitivity assessment, in combination with the preceding rigorous development effort, provided an adequate base for assessing the viability of the staged combustor concept relative to the other concepts being screened in the Phase I program and no additional perturbations of this concept were evaluated.

Figure 24 shows the airflow distribution in Configuration AV-1 of the advanced Vorbix staged combustor. This configuration was installed in the sector rig to evaluate the performance, emissions and durability characteristics of the staged combustor with various test fuels at high pressure operating conditions representative of the Energy Efficient Engine. The airflow distribution is identical to the distribution in the final sector rig configuration of the combustor as it was evolved under the Energy Efficient Engine program (Configuration 2/15B, Run 21 of Reference 8). The pilot zone airloading is very low: it consists only of the airflow through the pilot stage fuel injector, its insert guide and some portion of the pilot zone cooling air. This leads to equivalence ratios in the pilot zone of the order of unity at idle which is conducive to low carbon monoxide and unburned hydrocarbon emissions. At high power levels the majority of the fuel is consumed in the main zone and the pilot stage equivalence ratio is reduced. The pilot to main stage fuel split schedule is a primary test variable for a staged combustor and the reoptimization of this schedule for operation with ERBS fuel was investigated during the evaluation.

Because of the timetable for the Energy Efficient Engine combustor development program, the evaluation of the ignition and altitude stability characteristics of the staged combustor concept were conducted at an earlier date using a different combustor configuration (Configuration 1/8A, Run 12 of Reference 8). This configuration is designated AV-2: the geometry and airflow distribution are shown in Figure 25. The differences in ignition and stability characteristics between this configuration and Configuration AV-1 are small and would not be expected to have a significant effect.

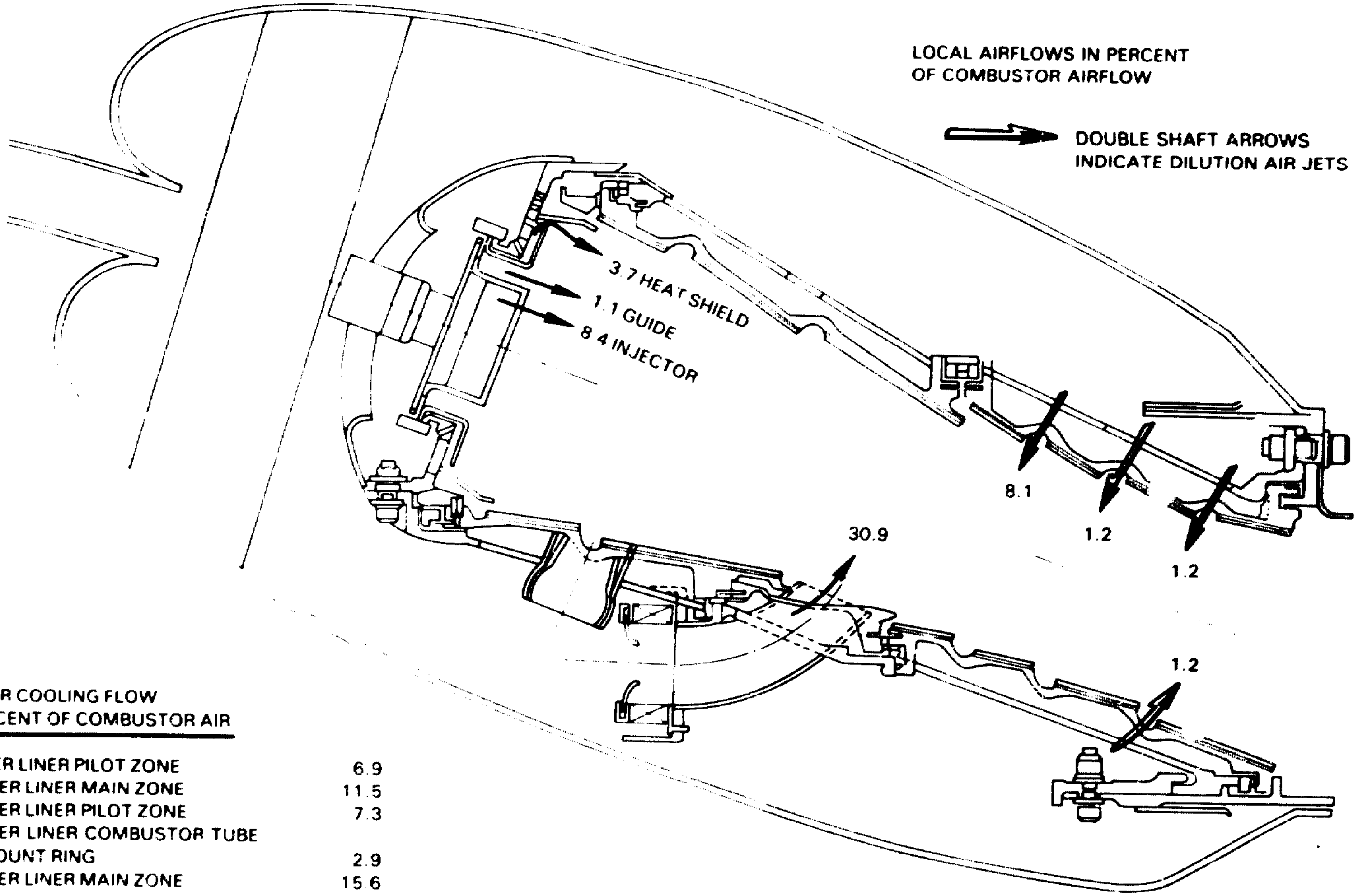

LINER COOLING FLOW
PERCENT OF COMBUSTOR AIR

INNER LINER PILOT ZONE	6.9
OUTER LINER MAIN ZONE	11.5
OUTER LINER PILOT ZONE	7.3
OUTER LINER COMBUSTOR TUBE MOUNT RING	2.9
OUTER LINER MAIN ZONE	15.6

Figure 24 Airflow Distribution in Advanced Vorbix Combustor Configuration AV-1

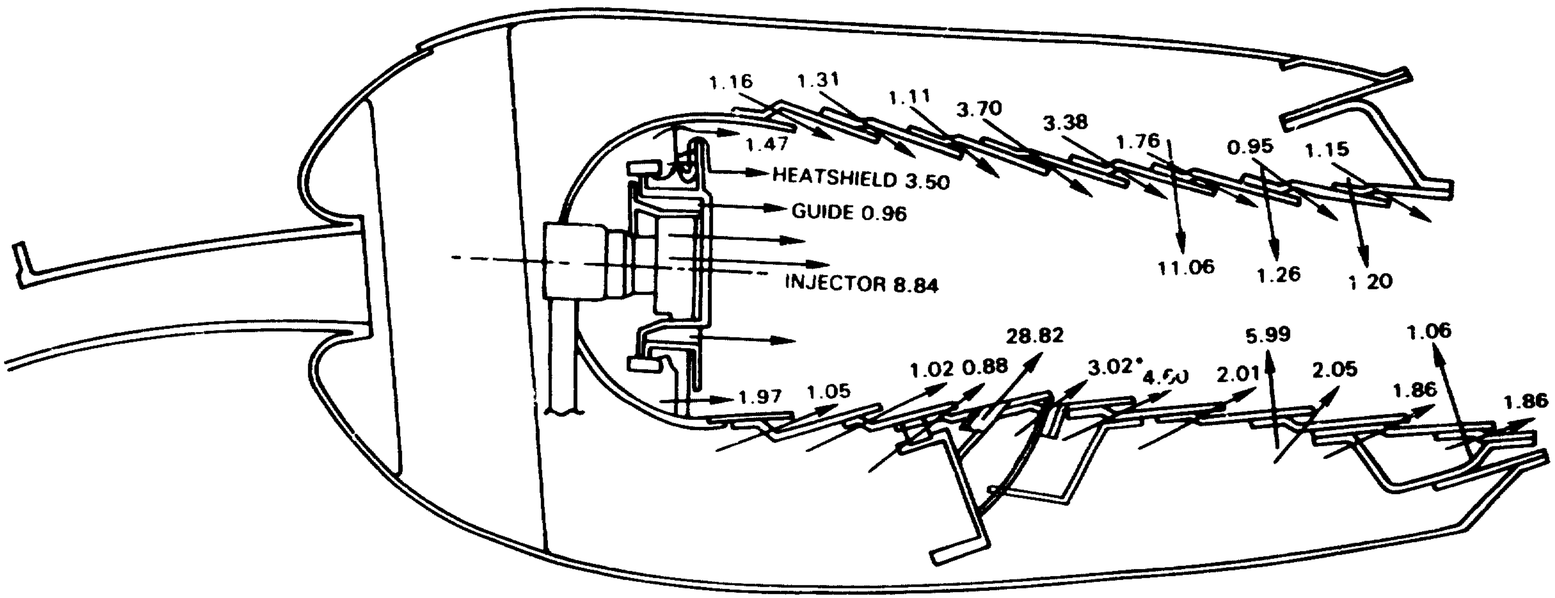

*MOUNT RING
*COOLING AIR BETWEEN COMBUSTOR TUBES

Figure 25 Airflow Distribution in Advanced Vorbix Combustor Configuration AV-2

Configuration AV-2 was evaluated after the combustor had been developed sufficiently for the pilot zone of the combustor to become well established. The fuel injectors in Configurations AV-1 and AV-2 were identical. The louver cooled liner used in the latter to facilitate modifications during the initial phases of the Energy Efficient Engine development program had the same geometric envelope and local cooling flows comparable to those in the final segmented liner. Comparison of Figures 24 and 25 shows that the pilot zone airflow distributions in these configurations are also similar.

4.3 VARIABLE GEOMETRY COMBUSTOR

Recent studies (References 10 and 11) have indicated that variable geometry combustors, in which the airflow distribution is shifted with operating conditions to achieve optimum stoichiometry over a range of power levels, may offer significant advantages in meeting performance and emissions requirements. As in the staged combustor concept, the enhanced control of stoichiometry could be used to advantage in operating with broadened properties fuels. Consequently, the variable geometry combustor was selected as the third and most advanced combustor concept for the Phase I program.

4.3.1 Conceptual Definition

Figure 26 shows the conceptual definition of the most general type of variable geometry combustor, hereafter referred to as "fully modulated" because the airflow to both the primary combustion zone and the dilution zone can be varied simultaneously. Airflow control is provided by butterfly valves rotating about radial axes in the air supply ducts adjacent to the outer combustor liner. Actuation of these valves diverts air from one combustor zone to the other while holding the overall flow resistance and hence pressure drop across the system reasonably invariant. The fully modulated variable geometry is capable of producing the rather massive shifts in combustor airflow required to maintain optimum equivalence ratios in the primary combustion zone over the entire engine operating range. To minimize carbon monoxide and unburned hydrocarbon emissions, the primary combustion zone must operate at an equivalence ratio of about unity at low power levels. At high power levels, a low primary zone equivalence ratio, of the order of 0.5, is required to minimize NO_x emissions, smoke formation and radiant heat transfer to the combustor liner. The airflow shifts needed to achieve these optimum equivalence ratios are rather massive; the primary combustion zone requires about 15 percent of combustor airflow at idle and 65 percent at takeoff.

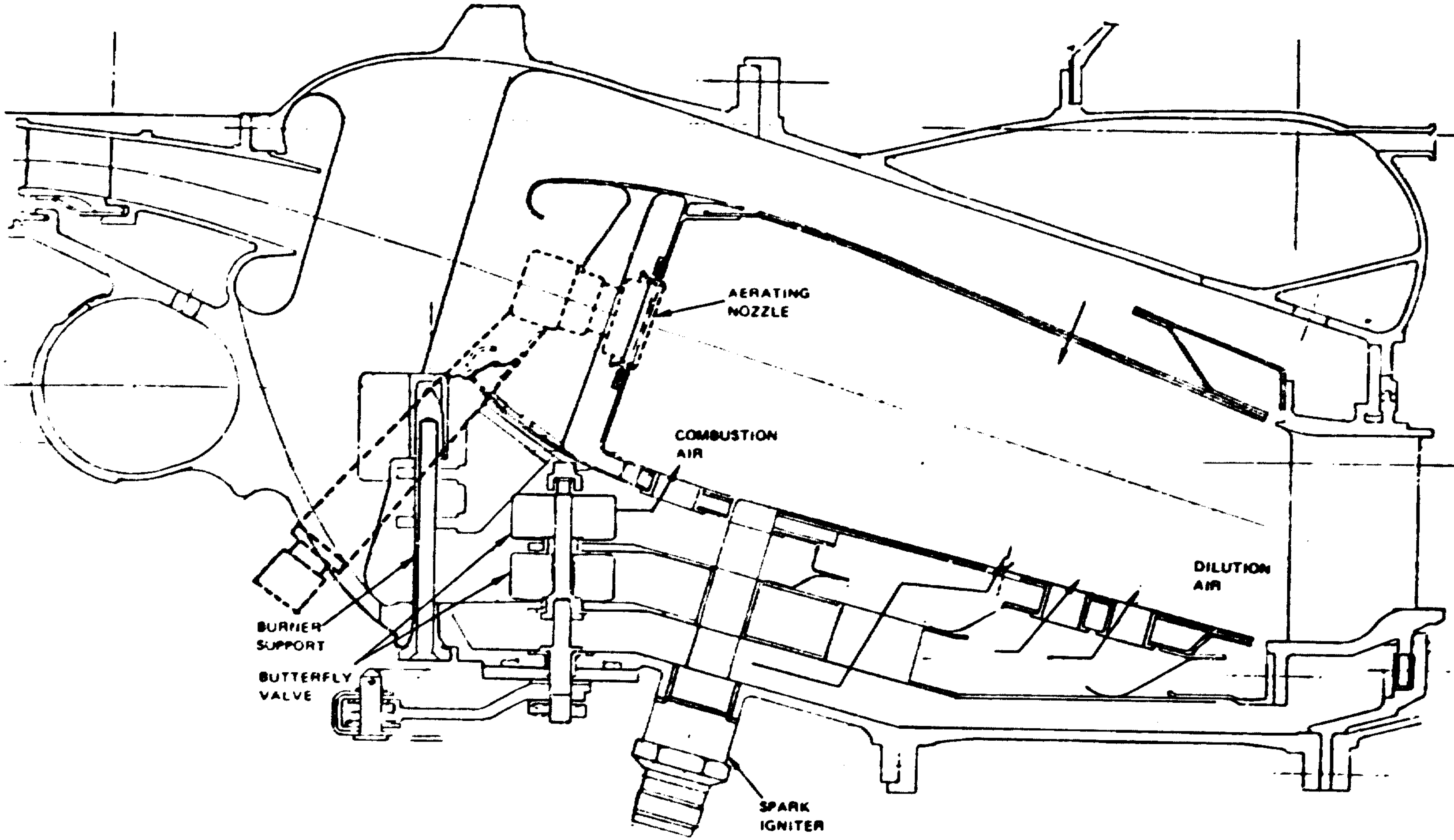

Figure 26 Fully Modulating Variable Geometry Combustor Concept

Other potential advantages of a variable geometry combustor include reduced residence time, a simplified fuel system, and improvements in thrust specific fuel consumption:

- Because the primary combustion zone is operated at the optimum equivalence ratio to minimize formation of carbon monoxide at low power and smoke at high power, the residence time required to oxidize these species is reduced. This could lead to decreases in combustor length, reducing the surface area which must be cooled and thereby permitting more of the combustor airflow to be used to control the exit temperature pattern factor and radial profile. The reduced residence time in the shorter combustor would also lead to lower NO_x emissions.

- Variable geometry can be used to enrich the primary zone at ignition and low power altitude operating conditions. This reduces demand on the low flow atomization characteristics of fuel injectors and encourages the use of single pipe injectors. The fuel system could then be simplified relative to duplex injectors or staged fuel systems. This also eliminates the risk of carbon deposition in inactive high power stage injectors, a decided advantage when operating on broadened properties fuels with lower thermal stability.

- Through appropriate scheduling of airflow areas with engine power level, variations in the net inlet flow area of the combustor (and hence pressure drop) may be used to advantage. Opening the combustor area at cruise and other intermediate power levels would increase the fraction of engine air passing through the combustor and reduce the turbine cooling air. This would increase turbine efficiency and reduce burner section pressure loss, thus improving thrust specific fuel consumption.

The major disadvantage of a variable geometry combustor is the increased complexity and cost introduced by the air management system. This system must be designed to provide the required airflow scheduling without introducing variations in combustor section pressure drop that could adversely affect the combustor liner or turbine inlet vane cooling. The airflow shifts between the primary zone and dilution zone of the combustor are massive and must be accomplished without compromising the combustor exit temperature pattern factor or radial profile. The reliability of the air management system and its actuation mechanisms will also be of paramount concern and fail safe operation of the combustor must be assured.

Alternate variable geometry concepts that are less complex than the combustor shown in Figure 26 could also be envisioned. One approach is to modulate only the airflow entering the primary combustion zone through variable apertures on the burner hood, bulkhead or liner. A combustor of this type would probably not have sufficient airflow transfer capability to produce the extremely lean primary zone equivalence ratios required to achieve very low NO_x output at high power and would experience sizable variations in total pressure drop when the system was actuated. However, this approach could be used to establish favorable tradeoffs between low power carbon monoxide and unburned hydrocarbon emissions, enhanced ignition and reduced high power smoke formation.

Another approach involves the use of a variable geometry aerating fuel injector. The stoichiometry of regions immediately downstream of the fuel injector face is critical to the formation of smoke and the consumption of unburned hydrocarbons. Variation in the quantity of air admitted through the injector can affect this local stoichiometry. Changes in the quantity, direction or velocity of air in the aerating passages of the injector can also affect the spray angle and atomization characteristics of the fuel injector. Variation in injector spray angle can be exploited to optimize emissions, smoke formation, ignition and liner heat load considerations. The requisite changes in injector airflow could be accomplished by axially translating sections of the injector or by rotating blockage rings. The injector components could be moved by mechanical linkages, air pressure drop forces or they could be hydraulically driven by the fuel pressure in the injector.

4.3.2 Variable Geometry Combustor Test Configurations

Because the design and evaluation of a fully modulating variable geometry combustor was beyond the scope of the Phase I program, the effort was restricted to assessing the effect of variations in combustor airflow distribution using fixed geometry combustor configurations. By evaluating combustor configurations with progressive changes in airflow distribution, the data required to optimize airflow scheduling with engine power level could be obtained. This information was sufficient to achieve the Phase I objective of screening the variable geometry combustor relative to the other concepts evaluated. If this screening indicated that the variable geometry concept was a viable approach to accommodating the use of broadened properties fuels, the design and evaluation of a variable geometry combustor could be conducted in Phase II of the program.

The JT9D-7 advanced bulkhead combustor used in the majority of the single stage combustor configurations was used as the basic combustor for the variable geometry concept. A total of eight configurations, the main features of which are listed in Table 7, were evaluated. These included a baseline or reference configuration, a configuration with a modified fuel injector and a pair of configurations that simulated the use of a variable geometry fuel injector. Four configurations were allocated to investigating the characteristics of a fully modulated variable geometry combustor by evaluating combustor geometries that were representative of the extremes of airflow shifting. These configurations are described in more detail in the remainder of this section. Data on the size of air admission apertures on the combustors are listed in Appendix A.

Table 7

Variable Geometry Combustor Test Configurations

Configuration Number	Combustor Type	Fuel Injector	Primary Zone Equivalence Ratio Idle/Takeoff	Primary Zone Length - cm (in)[1]	Comments	
VG-1	Bulkhead	Aerated	0.44/0.98	13.7 (5.4)	Established baseline with single pipe fuel injection.	
VG-2	Bulkhead	Modified Aerated	0.44/0.98	13.7 (5.4)	Effect of modified fuel injector relative to Configuration VG-1.	
VG-3	Bulkhead	Variable Open Position	0.44/0.98	13.7 (5.4)	Simulate variable geometry fuel injector	
VG-4	Bulkhead	Variable Closed Position	0.44/0.98	13.7 (5.4)		
VG-5	Bulkhead	Aerated	0.27/0.60	Note 2	High Power	Simulate fully modulated variable geometry combustor. Configuration VG-1 available for mid power range.
VG-6	Bulkhead	Aerated	0.94/2.13	17.5 (6.9)	Low Power	
VG-7	Bulkhead with Finwall®	Variable Closed Position	0.74/1.67	13.7 (5.4)	Low Power	Second simulation of fully modulated variable geometry combustor.
VG-8	Bulkhead with Finwall®	Variable Closed Position	0.25/0.57	Note 2	High Power	

1 - From fuel injector face to leading edge of first dilution hole in liner.
2 - Not applicable; no dilution air in these configurations.

Reference Configuration

An aerated single pipe fuel injector was used in all of the variable geometry combustor configurations. Use of this injector reduces the complexity of the fuel supply system, thus offsetting the additional complications of actuating the variable combustor components. It also minimizes the risks of deposition with the potentially lower thermal stability of broadened properties fuels. The greatest drawback with single pipe aerating injectors is the effect on combustor operation at low fuel flow rates where atomization could be poor relative to that achieved with duplex injectors. Areas of concern include ignition, low power stability and idle emissions. Configuration VG-1 was evaluated to measure these impacts. The combustor liner and the airflow distribution were identical to Configuration SS-2. The duplex pressure atomizing primary/aerated secondary fuel injector used in Configuration SS-2 was operated with all of the fuel flowing through the aerated secondary system to simulate a single pipe fuel injector. Comparison of the results of this evaluation with those of Configuration SS-2 established the increments associated with use of the single pipe injector as opposed to a duplex injector.

Modified Fuel Injector

As indicated in Section 4.1.3, a modified version of the duplex pressure atomizing primary/aerated secondary injector had been constructed and found to offer enhanced fuel atomization in the aerating secondary system. This modified fuel injector was evaluated in the single pipe mode in Configuration VG-2 to investigate the effect of these modifications on the single pipe/duplex injector trade. To facilitate comparison all other features of the combustor were identical to Configuration VG-1.

Variable Geometry Fuel Injector

Figure 27 shows a schematic view of a simulated variable geometry fuel injector which was fabricated with an injector body and outer aerating passage components identical to those used in the modified duplex fuel injector of Configuration VG-2. The central primary fuel injection body was replaced with interchangeable pintles that duplicated the extreme positions of an axially translatable variable position pintle. The conical shoulder on the pintle interacted with the lip of the fuel filming surface to meter the flow in the inner aerating air passage and vary the angle at which this airflow impinged on the fuel film. Figure 28 shows the assembled injectors with the long and short pintles installed to simulate the open and closed positions.

Airflow calibrations of these injectors indicated that with the pintle in the extended or open position, the airflow capacity was identical to the baseline duplex pressure atomized/aerated injector while the retracted length pintle used to produce the closed position geometry reduced the airflow capacity by 12 percent. The retracted or closed position produced a swirl strength 1.15 times that of the baseline injector while in the open position the swirl strength was 66 percent of that of the baseline injector. The combination of a high swirl strength and low airflow was thought to be conducive to improved ignition, while higher airflow would be expected to lean the critical smoke production region near the injector face at high power levels.

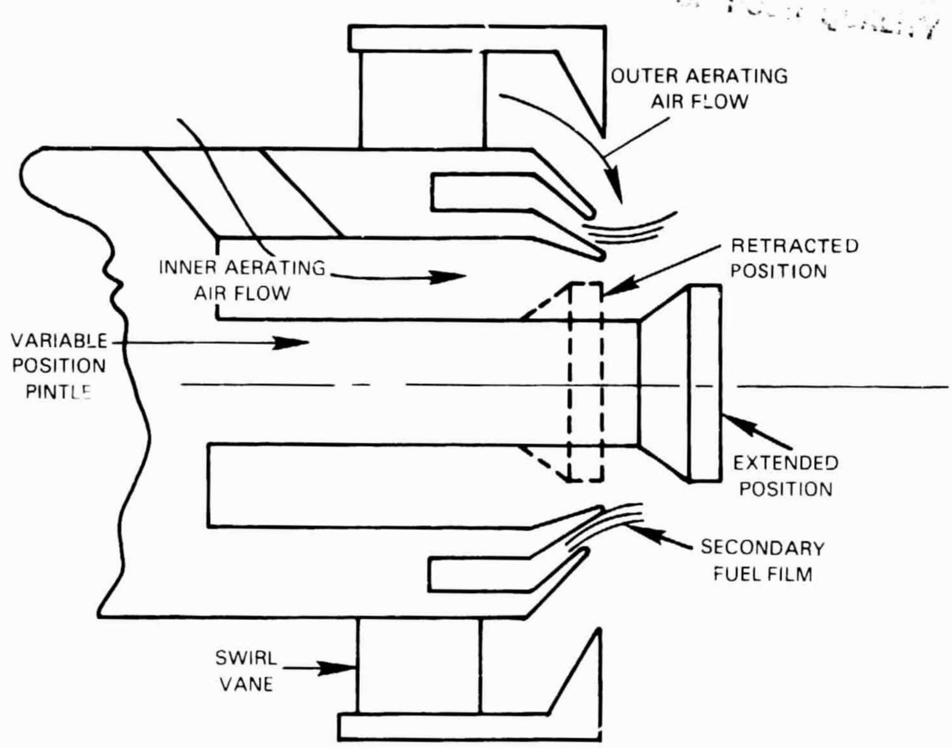

Figure 27 Schematic Cross Section of Single Pipe Variable Geometry Fuel Injector

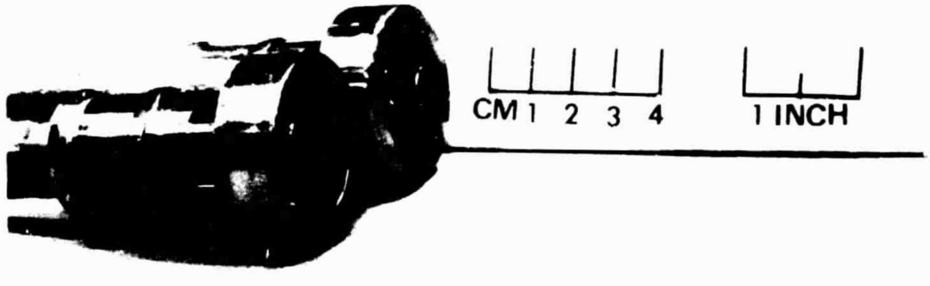

Figure 28 Variable Geometry Fuel Injectors with Pintles in Closed Position (Foreground) and Open Position (Background)

Spray characterization tests conducted on these injectors (reported in Appendix B) indicated that changes in the position of the pintle altered the spray angle with the closed position producing higher spray angles. The spray was also more dispersed, i.e., the cone width was larger when the pintle was in the open position. Relative to the baseline injector in a single pipe mode, the variable injector demonstrated reductions in Sauter Mean Diameter in more than half of the fuel/operating condition/geometry variations evaluated and reductions in peak density droplet size in nearly all of these variations.

The simulated variable geometry injector was evaluated in Configuration VG-3 with the injector pintle in the open position and Configuration VG-4 with the pintle in the closed position. The remaining combustor components and the airflow distribution in these configurations were identical to Configurations VG-1 and VG-2. This provided a common basis for comparison of all the single pipe fuel injectors.

Variable Airflow Distribution; Initial Series

Configurations VG-5 and VG-6 represented the extremes of lean and rich primary zone operation in a fully modulated variable geometry combustor. Other details of the combustor, such as the type of fuel injector, remained common with Configuration VG-1 so that this configuration could be considered representative of the fully modulated combustor with the air management system at an intermediate position.

Figure 29 shows the airflow distribution in the three configurations in the sequence. Configuration VG-5 represents the variable geometry combustor with all of the available air admitted to the primary combustion zone to the extent that there is no dilution air available to control the exit temperature distribution. This airflow distribution produces a primary zone bulk equivalence ratio of about 0.6 at takeoff which is conducive to low NO_x and particulate formation. At the opposite extreme, Configuration VG-6 represents the fully modulated variable geometry combustor with the valve in the primary zone air supply duct closed and the valve in the duct to the dilution zone open to produce the rich primary zone stoichiometry required for ignition and low power stability and emissions. The net flow area for air admission into each of the three configurations in this sequence was essentially the same. Consequently, the pressure drop and distribution of air to the cooling louvers and fuel injectors was nearly invariant between configurations.

Variable Airflow Distribution - Final Series

Configurations VG-7 and VG-8 also represent the extremes of rich and lean primary zone operation in a fully modulated variable geometry combustor. Figure 30 shows the airflow distribution in these configurations. Configurations VG-7 and VG-8 differed from Configurations VG-5 and VG-6 in the following respects:

- Configurations VG-7 and VG-8 were constructed with Finwall® replacing the louvers in the primary zone. As indicated in the description of Configuration SS-7 (Section 4.1.3) this feature led to a reduction in the liner cooling air requirement and produced a leaner bulk equivalence ratio in the primary zone of Configuration VG-8.

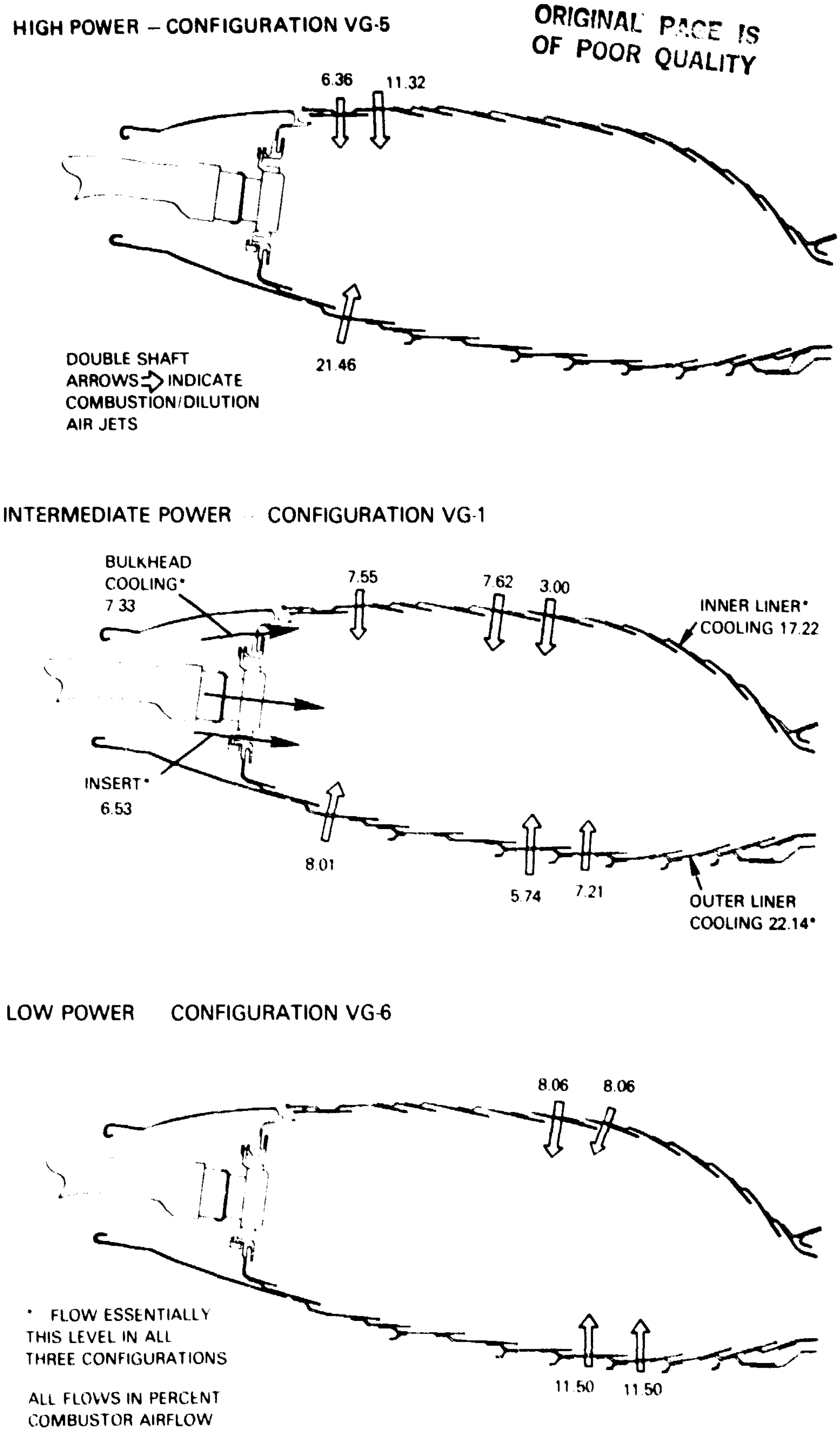

Figure 29 Airflow Distribution in Initial Series of Combustor Configurations Simulating a Fully Modulated Variable Geometry Combustor

ORIGINAL PAGE IS
OF POOR QUALITY

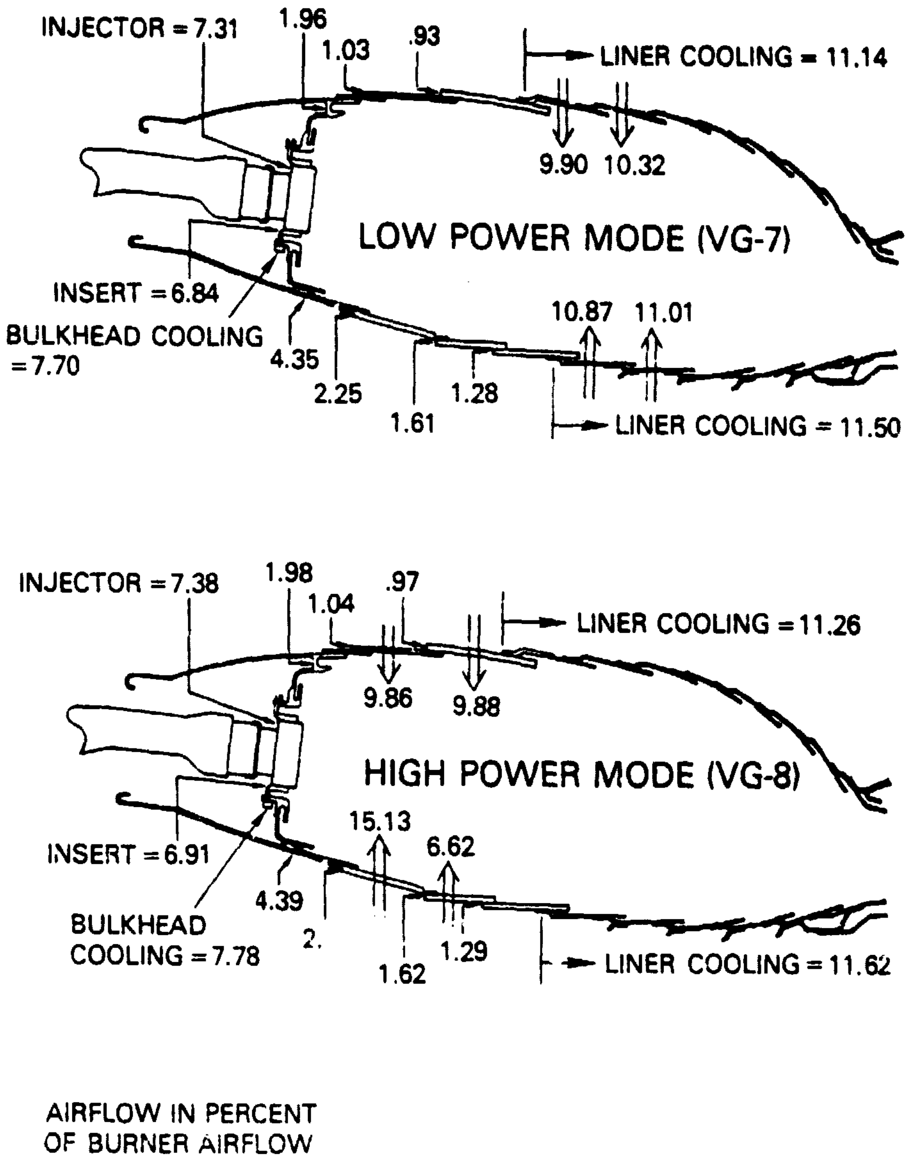

Figure 30 Airflow Distribution in Final Variable Geometry Combustor Configurations

o The airloading on the primary zone was increased and the length of the primary zone decreased in Configuration VG-7 relative to VG-6. Both of these configurations represent the low power operating mode of the combustor.

- The sequencing of the combustion air holes in the liner of Configuration VG-8 was altered to correct an apparent jet mixing limitation encountered in Configuration VG-5. Combustion air was admitted through both the inner and outer liner with two axially spaced sets of holes. The downstream set was positioned circumferentially so that jets entered the primary zone immediately downstream of the fuel injectors to encourage mixing with the reaction regions behind the injectors. The relative position of these combustion air holes can be seen in Figures 18 and 19 and in the data of Appendix A.

- Configurations VG-7 and VG-8 incorporated the "variable" fuel injector with the pintle in the closed position. This does not imply that a variable geometry fuel injector was envisioned in addition to the hypothetical fully modulated variable air distribution system. Rather, this particular injector, as a fixed geometry component, had been found to be the best single pipe fuel injector evaluated in prior configurations.

As in the case of Configurations VG-5 and VG-6, the net flow area of the combustor was nearly the same in Configurations VG-7 and VG-8 so the pressure drop and distribution of cooling and fuel injector air was not substantially altered when the primary zone/dilution zone airflow split was shifted.

SECTION 5.0

EXPERIMENTAL APPARATUS

This section contains the results of analysis of the physical and chemical properties of the test fuels used during the evaluation of the combustor concepts. Also included are descriptions of the test rigs, instrumentation, and the test facilities employed in the program.

5.1 TEST FUELS

Four different test fuels were used during the program. The principal test fuel was Experimental Referee Broad Specification (ERBS) fuel, which was used in the evaluation of every combustor configuration. The majority of the configurations were also evaluated with commercial Jet A fuel at selected operating conditions. In addition, two blended fuels were used in limited quantities to extend the range of fuel composition during the more critical tests of the initial and final configuration of each combustor. These two fuels were produced by adding a blending stock to the ERBS fuel to reduce its hydrogen content to 12.3 and 11.8 percent, respectively.

The Jet A fuel was supplied from the standard source at each test facility. The ERBS fuel and the two lower hydrogen content blended fuels were procured by NASA from Suntech, Inc. of Marcus Hook, Pa. These fuels were delivered to the Pratt and Whitney Aircraft test facility in Middletown, Connecticut in single lots of sufficient quantity for the entire Phase I program. The lower hydrogen content fuels were blended to the required proportions at the refinery before delivery. The ERBS fuel was stored in a dedicated tank in the tank farm near the test facility. The lower hydrogen content blended fuels were stored in leased tanker trailers parked near the test stand. Both the permanent storage tank and the trailers were drained and steam cleaned before the test fuel was delivered.

It was originally intended that the small amounts of test fuel required for the combustor ignition tests and fuel injector spray evaluations would be taken from the bulk lots. However, it became expedient to conduct some of these tests before the bulk lots were delivered. Thus, a portion of the ERBS fuel and the blending stock required to produce the 11.8 percent hydrogen content fuel were obtained from a stockpile maintained by NASA Lewis at the Plum Brook facility in Sandusky, Ohio. Since the required quantities were only on the order of 378 to 756 liters (100 to 200 gallons), the fuel was transported in convenient 208 liter (55 gallon) drums. When small deviations were noted between the ERBS fuel from the Plum Brook stockpile and the bulk lot delivered to the high pressure test facility, it was decided that all ignition testing would be conducted with fuel from the Plum Brook stockpile to maintain the continuity of the tests.

Samples of the test fuels were taken for analysis in the Materials Engineering Research Laboratory at the Pratt and Whitney Aircraft Middletown test facility. Extensive analyses were conducted to determine the physical properties and chemical composition of the four test fuels using samples extracted during the high pressure test of the first combustor configuration. Additional analyses of more limited scope were conducted on samples of the Jet A fuel used in the high pressure test facility over the duration of that program element. Likewise, samples of the fuels obtained from the Plum Brook stockpile for the ignition tests were analyzed. The results of these analyses are presented in the remainder of this section.

5.1.1 High Pressure Test Fuels

Table 8 shows the results of the analysis of the composition and properties of the bulk lots of the ERBS and lower hydrogen content test fuels that were used in all of the high pressure combustor tests. Also shown is the corresponding analysis of a sample of the Jet A fuel that was being used in the high pressure test facility at the time the first combustor configuration, Configuration SS-1, was evaluated. The table also lists the American Society for Testing and Materials (ASTM) Standard Procedure used to measure the indicated property. In general, the procedure is that stipulated in the ASTM D1655 specification for Jet A fuel. However, in the case of a few parameters, alternate analysis methods were preferred and are so indicated in this table.

In addition to being listed in Table 8, the distillation temperature distributions for the four fuels are plotted in Figure 31. The conventional hydrocarbon structure definition was supplemented by mass spectroscopic analysis of the ERBS and the two lower hydrogen content test fuels. The results of these analyses are shown in Table 9.

The Jet A fuel is shown to be well within the current ASTM D1655 specification except that the aromatic content exceeds the specification limit of 20 percent by volume. Likewise the smoke point, at 20mm, is at the limit of the specification consistent with the measured napthalene content. However, since 1976, footnotes to the specification have permitted use of Jet A fuels with aromatic contents up to 25 percent volume on a reportable basis. This Jet A was in the reportable category.

The ERBS fuel was prepared by Suntech, Inc. to approach the limits on critical parameters of the specification of Table 1, and consisted of a blend of kerosene and catalytic gas oil. The principal composition controlling parameter in the ERBS specification is the hydrogen content and it has been maintained in the desired range of 12.8 $\pm$ 0.2 percent. Relative to the Jet A sample this has been accomplished by an increase of the order of ten percent by volume in both the total aromatics and the napthalenes. This implies that the concentration of single ring aromatics in the ERBS is comparable to that in the Jet A and that the higher level of total aromatics in the ERBS is due primarily to high concentrations of multi-ring aromatics. This is substantiated to some extent by the mass spectrographic analysis data of Table 8, which indicates that the alkylnapthalenes are by far the highest concentration aromatic group. These shifts in chemical composition would be expected to alter the combustion characteristics of the fuel and this alteration is evident on comparison of the smoke points of the Jet A and ERBS fuel.

Table 8

Properties of Fuels Used in High Pressure Tests

Composition	Jet A*1	ERBS	12.3% Hydrogen	11.8% Hydrogen	ASTM Procedure
Aromatic content - % vol	20.6	31.5	40.4	52.2	D1319
Napthalene content - % vol	1.06	11.7	13.5	15.4	D1840*3
Olefin content - % vol	0.3	0.2	0.2	0.2	D1319
Sulfur content - % wt	0.16	0.04	0.04	0.05	D3120
Hydrogen content - % wt	13.62	12.93	12.37	11.80	*2
Hydrogen/Carbon Ratio	1.89:1	1.77:1	1.59:1	1.59:1	*2
Physical Properties					
Viscosity, cs. @ 249°K (-10°F)	5.50	8.57	7.23	6.48	D445
@ 299°K (80°F)	1.70	2.16	1.95	1.82	
@ 338°K (150°F)	1.00	1.19	1.11	1.06	
Surface Tension - dynes/cm @ 298°K (77°F)	29.3	30.3	30.7	30.8	D971
Gravity, °API, 289°K (60°F)	41.4	36.9	34.8	32.6	D1298
Specific Gravity, 289/289°K (60/60°F)	0.8184	0.8403	0.8509	0.8623	D1298
Heat of Combustion - MJ/kg, Net	42.96	42.59	42.26	41.97	D2382
Gross	45.85	45.33	44.89	44.47	
- (Btu/lb) Net	(18,490)	(18,330)	(18,190)	(18,060)	
Gross	(19,730)	(19,510)	(19,320)	(19,140)	
Flash Point - °K (°F) Open Cup	--	347 (165)	327 (130	336 (145)	D92
Closed Cup	318 (114)	318 (114)	308 (96)	311 (100)	D93
Freezing Point °K (°F)	215 (-71.5)	243 (-21.1)	244 (-19.3)	244 (-20.2)	D2386
Smoke Point - mm	20	12	11	9	D1322
Distillation					
Temperatures - °K (°F) Initial	422 (300)	422 (336)	413 (284)	420 (297)	D86
10%	447 (346)	471 (389)	453 (357)	447 (346)	
20%	456 (361)	479 (403)	468 (383)	459 (368)	
30%	463 (375)	485 (414)	476 (397)	471 (389)	
40%	471 (388)	490 (423)	486 (416)	485 (414)	
50%	478 (401)	498 (438)	496 (434)	498 (438)	
60%	484 (413)	506 (451)	507 (453)	511 (461)	
70%	492 (427)	514 (466)	517 (472)	524 (484)	
80%	501 (442)	528 (492)	530 (495)	539 (512)	
90%	512 (462)	550 (531)	555 (540)	561 (551)	
Final	544 (521)	594 (611)	597 (615)	603 (626)	
Recovery - % vol	99.0	98.5	98.0	98.5	
Residue - % vol	0.9	1.4	1.3	1.0	
Loss - % vol	0.1	0.1	0.7	0.5	
Carbon Residue 10% Bottoms - % wt	0.5	0.19	0.22	0.24	D524

*1 - Jet A analysis is for sample obtained at high pressure facility during test of Configuration SS-1.
*2 - Perkin-Elmer Model 240 Elemental Analyzer.
*3 - Specification D-1840 modified for napthalene contents above 5% volume.

Table 9

Mass Spectrographic Analysis of High Pressure Test Fuels

Fuel	Volume Percent of Total Sample ERBS	12.3% H2	11.8% H2
Saturates Analysis			
Paraffins	42.9	39.1	32.9
Non-condensed Cycloparaffins	19.0	14.4	10.1
Condensed Dicycloparaffins	6.5	6.4	5.2
Condensed Tricycloparaffins	0.6	1.1	0.8
Alkylbenzenes	0.5	0.0	0.0
Total Saturates	69.5	61.0	49.0
Aromatic Analysis			
Alkanes	0.5	0.6	0.9
Cycloparaffins	0.0	0.3	0.3
Alkylbenzenes	3.7	10.5	15.7
Indanes-Tetralins	5.7	7.0	6.7
Indanes-Dihydronapthalenes	1.6	2.1	1.9
Napthalene	0.1	0.2	0.2
Alkylnaphthalenes	13.2	11.4	16.6
Benzothiophenes	0.1	0.1	0.0
Acenaphthenes	0.9	2.0	1.7
Acenaphthylene-Fluorenes	1.3	1.5	1.9
Phenanthrenes	1.8	2.1	3.1
Total Aromatics	28.9	37.8	49.0

Comparison of the distillation temperature characteristics of ERBS and Jet A in Table 8 or Figure 31 indicates that the boiling temperature of ERBS is about 20 to 25°K (35 to 45°F) higher than that of Jet A across the entire distillation range. Despite this increase, the flash points of the two fuels are identical, implying comparable volatility. Relative to the specification limit of Table 1, the viscosity of the ERBS test fuel was very moderate and even complied with the specification for Jet A shown on this table. The combination of comparable volatility, and only a moderately higher viscosity of ERBS relative to Jet A, implies that the use of this fuel should not have a profound effect on such atomization and evaporation dependent processes as ignition and combustion stability.

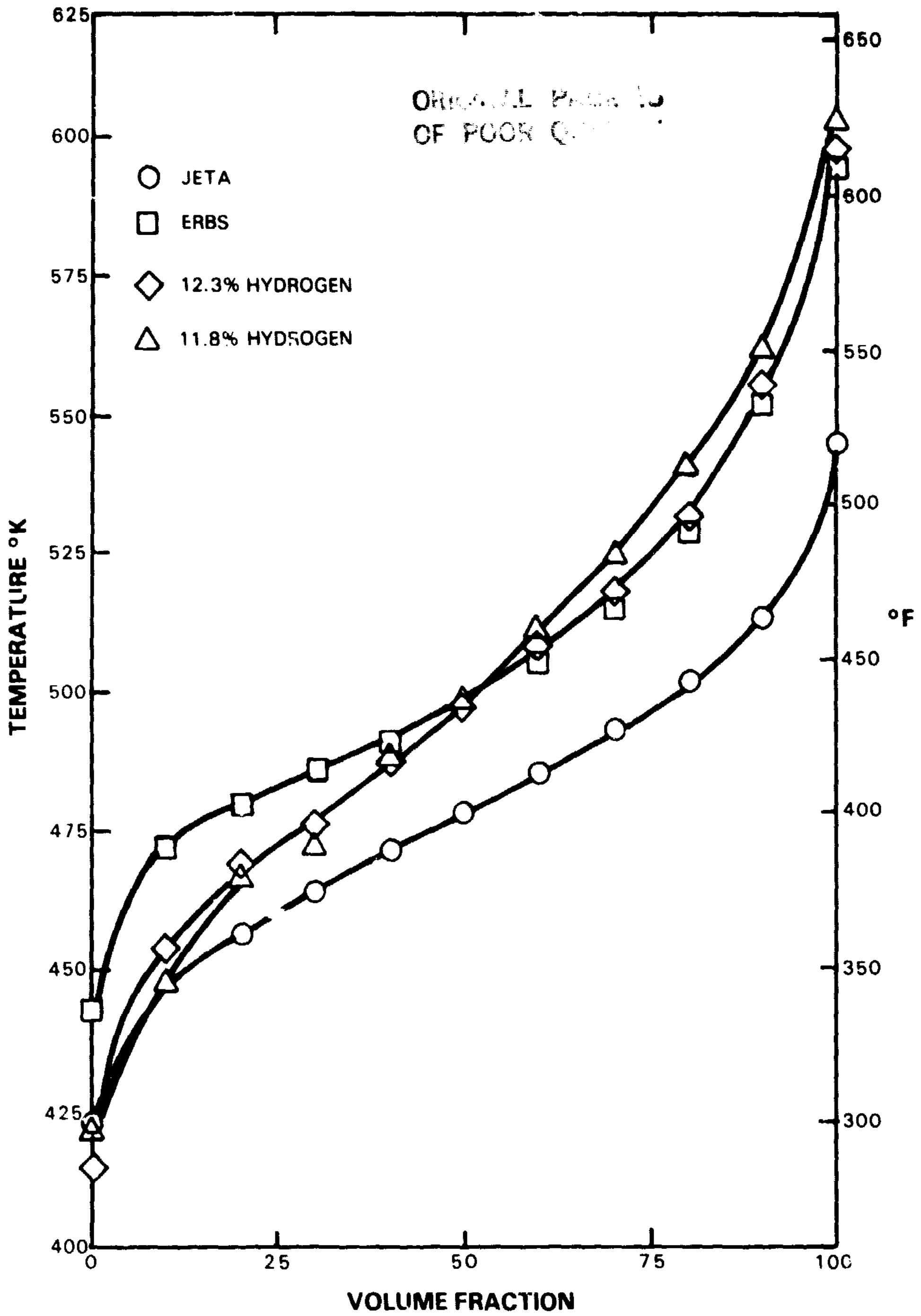

Figure 31 Distillation Characteristics of Test Fuels for High Pressure Tests

The two lower hydrogen content test fuels were produced by addition of progressively greater quantities of a blending stock to the basic ERBS fuel. The blending stock consisted of catalytic gas oil and xylene tower bottoms and had an aromatic content in excess of 80 percent. The blend proportions had been selected to produce fuels with nominally one half percent, and one percent, lower hydrogen content than the ERBS; i.e., 12.3 and 11.8 percent hydrogen, respectively. As shown in Table 8, each of these increments required increases of the order of 10 percent volume in the total aromatic content of the fuel.

The combination of the four high pressure test fuels has the desirable feature of a variation of nearly two percent in hydrogen content and a range of aromatic contents from about 20 to more than 50 percent. However, whereas the decrease in hydrogen content between Jet A and ERBS reflected primarily a difference in multi-ring aromatics, the concentration of napthalenes in the blended fuels are not substantially different from that in ERBS. This implies that the increase in total aromatic content of the blended fuels is primarily due to changes in the concentration of single ring aromatics. This is obviously consistent with the use of xylene tower bottoms in the blending stock and is further confirmed by the progressive increase in the alkylbenzines in the mass spectrographic analyses of the aromatic constituents of these fuels in Table 9. The increase in the aromatic content of the blended test fuels is shown to produce a progressive decrease in the smoke point, although the rate of decrease is significantly less than in the initial Jet A to ERBS increment.

Figure 31 shows that while the addition of the blending stock to the ERBS produced some increases in the distillation temperature of the higher fractions, the dominant effect was a reduction of the distillation temperatures for the early fractions. This resulted in a progressive increase in volatility as evidenced by the lower flash points of the 12.3 and 11.8 percent hydrogen test fuels relative to ERBS. The blending stock also had a relatively low viscosity which produced progressively lower viscosity of these fuels relative to ERBS. As indicated above, the combination of volatility and viscosity relate to the ignition and stability characteristics of the combustor. The trend of both these properties in the ERBS and the blended fuels is toward enhanced ignition/stability with decreasing hydrogen content. This characteristic is counter to expectations in that one would anticipate a shift toward higher distillation temperatures and increased viscosity with the higher aromatic concentrations that produced the reduction in hydrogen content. This phenomena is apparently due to the production of the low hydrogen content fuels by the blending of narrow and unique cuts rather than with a broader distillation of a complete crude.

5.1.2 Jet A Fuel for High Pressure Tests

The Jet A fuel used for the high pressure tests of the combustor concepts was drawn from the tank farm at the Middletown test facility. The farm serves as a fuel source for the entire test operation at Middletown and not just the high pressure combustor test facility. Consequently, there was no opportunity to control the Jet A fuel that was being used over the duration of the program.

However, the composition and properties of the Jet A fuel were monitored by conducting analyses of samples collected at various times during the course of the high pressure test sequence.

Table 10 presents the results of the analyses of these four fuel samples. Sample A was obtained during the test of Configuration SS-1 and is the Jet A fuel of Table 8. The other samples were obtained during the testing of configurations which served as either reference or baseline configurations of each combustor concept, as well as at spaced intervals over the duration of this element of the program.

Table 10

Properties of Jet A Fuel Used at the High Pressure Facility

Sample	A	B	C	D
Configuration Tested	SS-1	SS-2/VG-1	SS-5/AV-1	SS-7/VG-7
Aromatic Content - % vol	20.6	25.0	21.0	20.1
Napthalene Content - % vol	1.06	1.54	1.19	1.60
Hydrogen Content - % wt	13.62	13.49	13.82	13.78
Smoke Point - mm	20	20	20	21
Heat of Combustion, Net				
MJ/kg	42.96	42.91	43.01	43.06
(BTU/lb)	(18,490)	(18,470)	(18,510)	(18,530)
Specific Gravity @ 289/289°K				
(60/60°F)	0.8184	0.8208	0.8160	0.8128
Viscosity, CS @ 299°K (80°F)	1.70	1.72	1.85	1.75

With the exception of the aromatic content of Sample B, which is at the limit of acceptability under the footnotes in the current ASTM D1655 specification, the samples are reasonably consistent in their composition and properties.

5.1.3 Ignition Test Fuels

As indicated above, the ERBS and 11.8 percent hydrogen test fuels used for the ignition test sequences were obtained in drum lots from a stockpile maintained by Lewis Research Center, rather than from the bulk lot used for the high pressure tests. In addition, the 11.8 percent hydrogen content fuel used in the ignition tests was blended on site, rather than at the refinery, by mixing ERBS fuel with the high aromatic content blending stock in the stipulated proportions prior to each test.

Table 11 lists the measured composition and properties of the fuels used in the ignition testing of the advanced vorbix combustor, while the corresponding data on the fuels used in the evaluation of the JT9D based single stage and variable geometry concepts are shown on Table 12. The tests on the advanced vorbix combustor concept were conducted earlier in the program and comparison of the data of Table 11 with that of Table 8 indicated that the composition and the majority of the physical properties of these ignition test fuels were comparable with those of the bulk lot. However some deviations are evident in the distillation characteristics.

ORIGINAL PAGE IS
OF POOR QUALITY

Table 11

Fuels Used in Ignition Tests of Advanced Vorbix Combustor Concept

Fuel	Jet A	ERBS	11.8% Hydrogen
Aromatic Content - % vol	21.4	31.5	58.0
Hydrogen Content - % wt	13.78	12.95	11.88
Specific Gravity 289/289°K (60/60°F)	0.8104	0.8398	0.8602
Viscosity - cs @ 299°K (80°F)	1.73	2.05	1.78
Distillation - °K (°F)			
Initial	437(327)	448(348)	423(302)
10%	457(364)	463(375)	443(338)
20%	464(377)	468(384)	451(353)
30%	471(389)	475(396)	462(372)
50%	483(411)	488(420)	488(419)
80%	507(454)	527(490)	538(509)
90%	520(477)	567(561)	566(560)
Final	551(533)	618(653)	610(640)

Table 12

Fuels Used in Ignition Tests of Single Stage and Variable Geometry Combustor Concepts

Fuel	Jet A	ERBS	11.8% Hydrogen
Aromatic Content - % vol	18.8	30.8	49.3
Hydrogen Content - % wt	13.72	12.90	11.84
Specific Gravity 289/289°K(60/60°F)	0.8146	0.8418	0.8633
Viscosity - cs @ 299°K(80°F)	1.67	2.26	1.90
Distillation - °K(°F)			
Initial	437(310)	457(364)	426(307)
10%	449(349)	475(396)	449(350)
20%	457(364)	482(408)	461(371)
30%	464(376)	487(417)	475(396)
50%	477(400)	502(444)	503(447)
80%	502(444)	533(501)	543(518)
90%	513(464)	559(547)	566(560)
Final	547(525)	598(618)	604(628)

The data of Table 8 and Figure 31 indicate that, over the 10 to 50 percent recovered range critical to volatility, the boiling temperature of the ERBS is about 22°K (40°F) higher than that of Jet A implying the ERBS to be substantially less volatile. However, in the case of the test fuels of Table 11 the boiling temperature of the Jet A and the ERBS are much closer together over this range and the differences in volatility are minimized. Furthermore, since the 11.8 percent hydrogen content fuel was produced by blending with this particular lot of ERBS fuel, the volatility of that test fuel is improved to the extent that it, rather than the Jet A, is the most volatile of the three test fuels. These differences must be recognized in interpreting the results of the ignition tests on the advanced vorbix combustor.

The drums of ERBS fuel and stock used to blend the 11.8 percent hydrogen fuel for the ignition tests on the single stage and variable geometry combustor concepts were drawn from the stockpile at Lewis research Center nearly a year later than those used in the evaluation of the advanced vorbix combustor. Table 12 shows the properties and composition of the ERBS and the 11.8 percent hydrogen blended fuel mixed from this lot, as well as those of the Jet A fuel used in the ignition tests on these concepts. The data in this table indicate that the composition and the properties, including the distillation characteristics, of these ignition test fuels were comparable with those of Table 8 and Figure 31.

5.2 TEST APPARATUS - JT9D BASED COMBUSTOR CONCEPTS

Both the single stage and the variable geometry combustor concepts were based on JT9D-7 components and were evaluated in the same rig and test facility. This section includes a description of this test apparatus.

5.2.1 JT9D Combustor Test Rig

Figure 32 shows the JT9D combustor test rig which duplicates the internal contours of a segment of the JT9D-7 engine diffuser and burner case with the majority of the rig walls having been fabricated from actual engine components. The JT9D engine combustor has 20 fuel injectors and this rig, with a 72 degree sector width, includes four fuel injectors. The JT9D engine diffuser case incorporates ten service struts, two of which are reproduced in the test rig and are located 18 degrees to either side of the plane of symmetry, i.e., outboard of the two center fuel injectors. The fuel injector support locations and pad details duplicate those of the production JT9D-7 engine and production fuel injector supports and igniter are employed. Orifices are installed in the rear bulkhead of the rig to simulate the extraction of turbine cooling air from the combustor section. These orifices were sized to duplicate the turbine cooling flow of the JT9D-7F engine at sea level takeoff.

The combustor liners and front end were fabricated by cutting the required 72 degree sector from existing full annular production or experimental louver cooled JT9D burner assemblies. Flanges were welded to these liner sectors to attach them to radial endwalls. The photographs of the combustor concepts in Figures 8 and 10 show the complete liner sector/endwall assemblies. Figure 33 shows a liner sector with the endwall removed to show the louver cooling on the endwall. The combustor sector is installed in the rig case from the rear and is retained by rails on the endwall that slide on tracks on the case. This accommodates differential thermal expansion while constraining the liner in a curved position to minimize buckling deflections of the outer liner.

Leads from thermocouples and pressure taps on the combustor liner are bundled at the rear of the liner and are routed out of the rig by passthroughs adjacent to the rear bulkhead. The passthroughs are removable from the rig case with the liner sector to minimize damage to the instrumentation leads during teardown/assembly and hardware reoperation. Figure 34 shows the fully assembled segment combustor and rig casing.

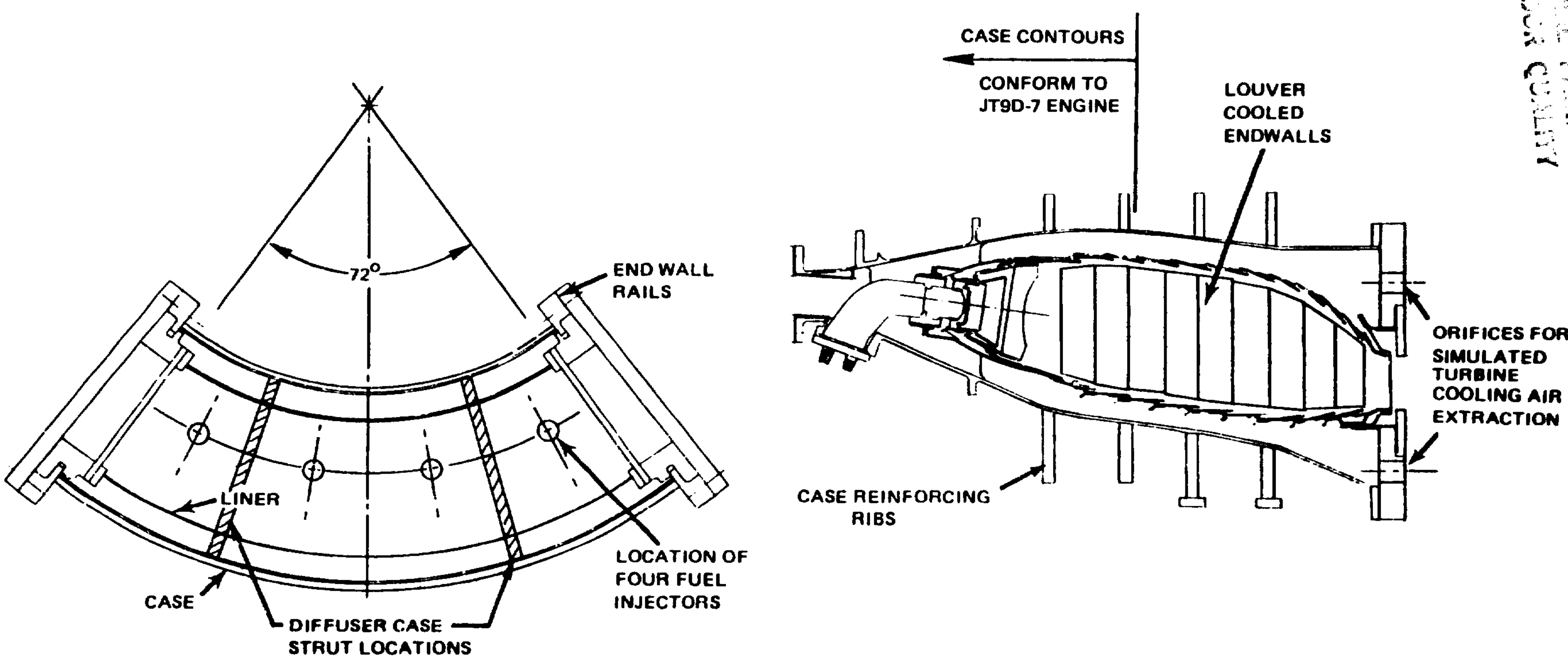

Figure 32 JT9D-7 72° Segment Burner Rig

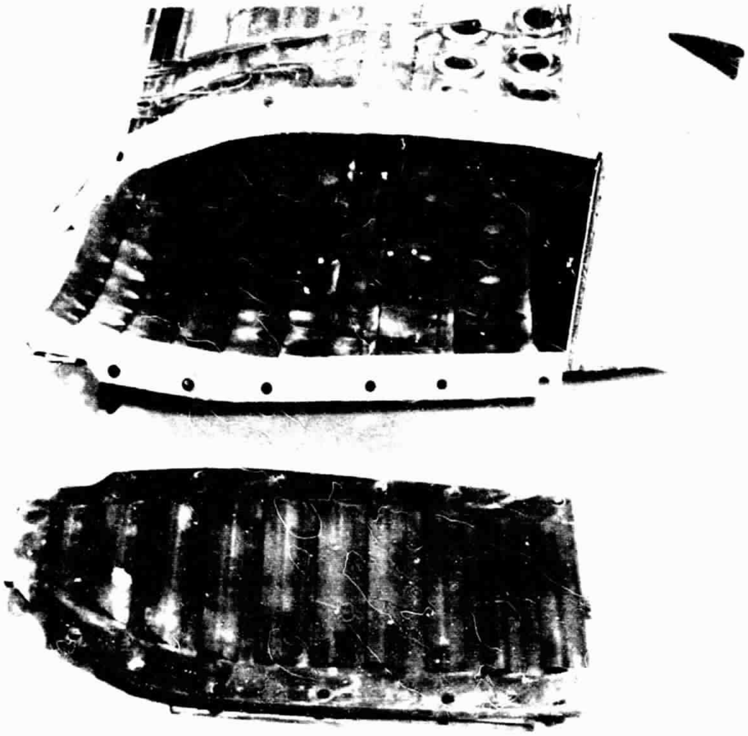

Figure 33 JT9D Combustor Sector Endwall

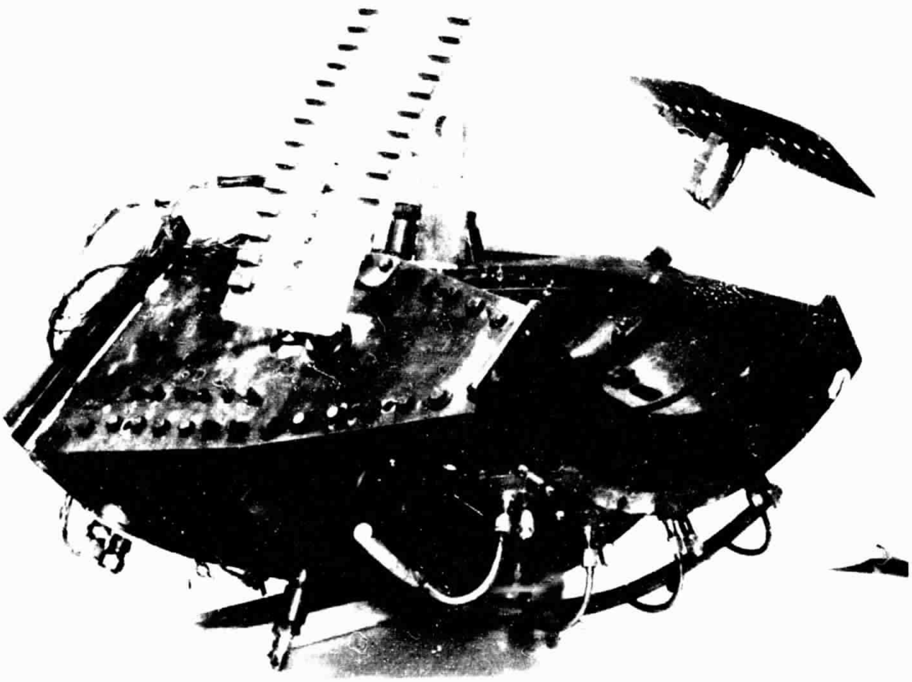

Figure 34 Assembled JT9D Combustor Sector Rig

5.2.2 JT9D Combustor Test Facility

All of the high pressure tests on the JT9D based combustor concepts were conducted in X-960 Stand of the Pratt & Whitney Aircraft Middletown test facility. X-960 is a new test facility with an airflow capacity of up to 45.5 kilograms/ second (100 pounds/second) with inlet temperatures and pressures up to 923°K (1200°F) and 4.14 MPa (600 psia) respectively, thereby permitting testing of representative combustor segments of current and anticipated high airflow size engines in a nonvitiated environment to full operating pressure.

Figure 35 shows a schematic diagram of the airflow system in X-960. An FT4A gas turbine drives a free turbine which powers two series mounted compressors. The rig inlet air is preheated to the appropriate combustor inlet temperature in two indirectly fired nonvitiating preheaters. The preheaters operate in parallel and the rig inlet airflow measurements are made in venturis in both of these lines. The airflow measurement is redundant in that venturis are located both upstream and downstream of the air preheater. The upstream venturis provide the primary airflow measurement and are designed for sonic operation with an airflow measurement accuracy of $\pm$0.5 percent.

Figure 36 shows the segment JT9D sized rig installed in the X-960 Stand. The test rig is enclosed inside a breech locked pressure tank that is pressurized above the rig operating pressure to avoid large bursting loads on the rig cases. The tank pressurization air and cooling air for the combustor exit instrumentation rake are bled from the stand inlet air duct upstream of the air preheater and the venturis. The rig inlet air duct provides an accelerating flow field in the transition from a cylindrical to an annular segment shape upstream of the combustor section inlet plane. The annular segment is 72 degrees in width at the rig inlet plane to be compatible with the burner rig.

The circumferentially traversing combustor discharge rake, described in more detail in Section 5.2.3 following, is mounted on a shaft rotating about the centerline of the combustor annulus. The traverse shaft extends through the rear wall of the exhaust chamber and is turned by an externally mounted actuator.

The pressure level in the test rig is regulated by a water cooled back pressure valve and the combustion products are quenched by a water spray before discharging to the atmosphere in a silencer pit.

When a test is completed, the entire pressure vessel enclosing the rig and the transition section of the inlet duct can be disconnected from the air supply ducts in the test cell and moved to a dressing area adjacent to the test cell for removal of the combustor rig proper. Two such pressure vessels are available at this facility so that, while a rig is being operated in the test cell proper another rig can be installed in the second vessel in the dressing area.

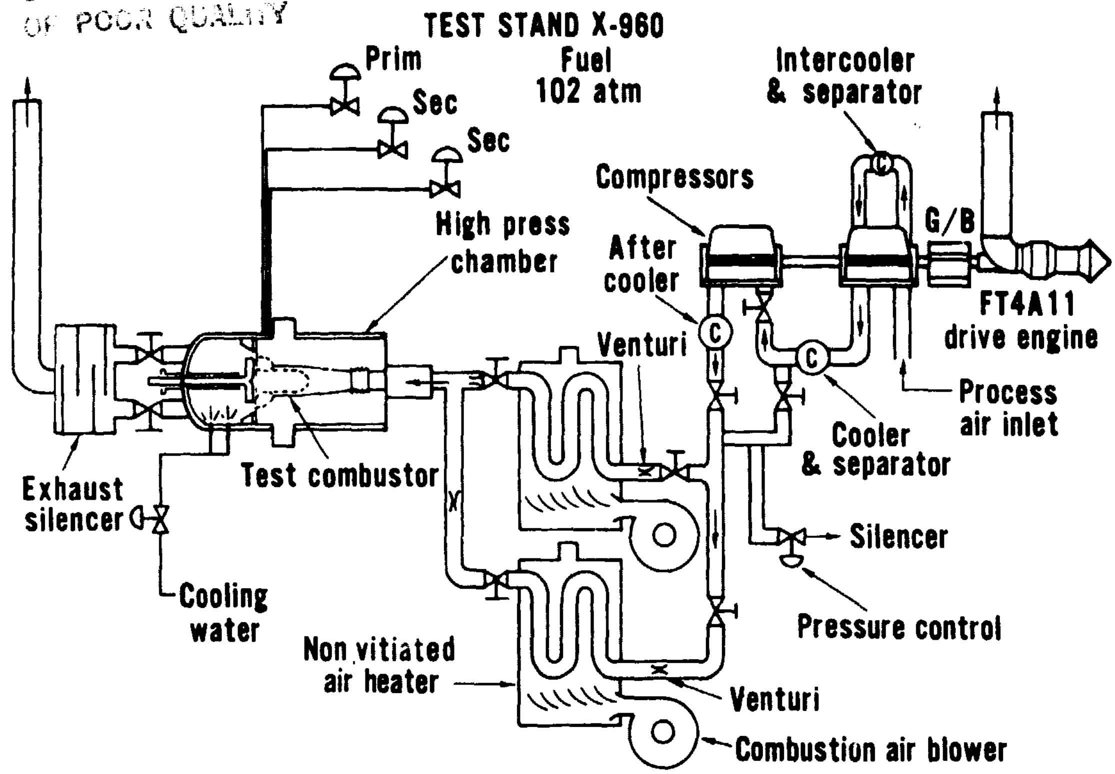

Figure 35 X-960 High Pressure Combustor Research Facility

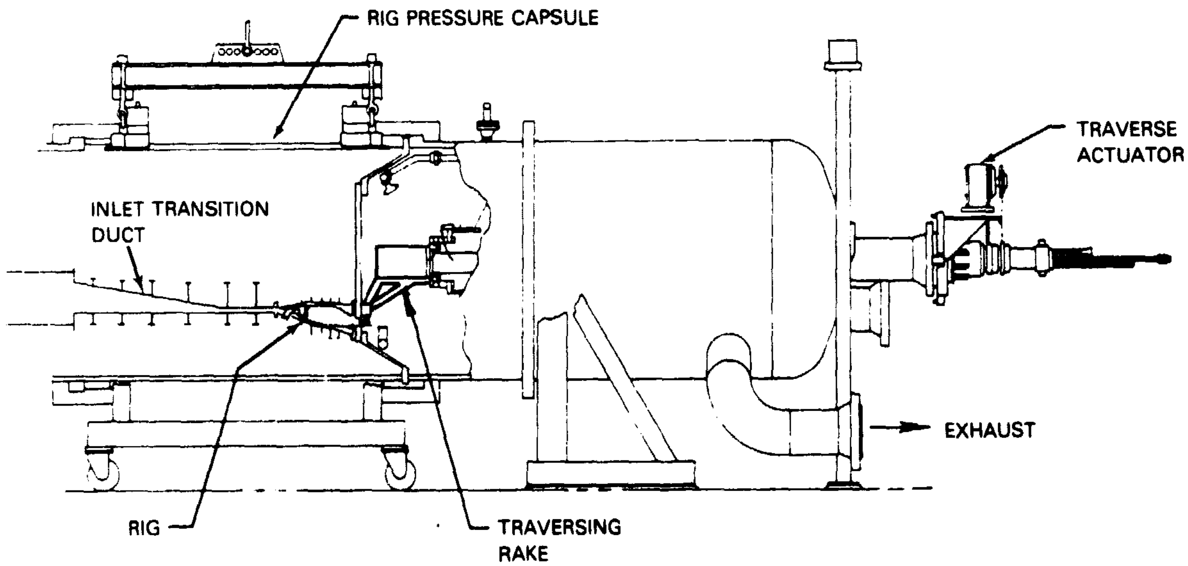

Figure 36 JT9D-7 Segment Rig Installation in X-960 High Pressure Combustor Facility

The control room immediately adjacent to the test cell contains all of the facilities and emissions equipment necessary to operate the rig. Rig control to maintain test parameters is effected by means of a Rig Supervisory Control system (RSC). The RSC is a digital computer control unit with appropriate input and output signal circuits. Pertinent input signals are compared to preprogrammed levels within the computer, then through the output circuits the necessary action is taken to trim the facilities equipment as required. In addition to being used to set test conditions, it also controls the facility during transients between test points, monitors rig and facility safety parameters permitting early detection of problems in the facility or rig, and institutes a controlled shutdown if required.

The data acquisition system incorporates, in addition to the standard pressure and temperature instrumentation, analytical instruments for emission measurements consistent with those specified in the latest EPA requirements. Steam-traced emission sampling lines are routed to the emission console located in the control room, where they can be manifolded as desired.

The fixed-station emission measurement system is designed to measure exhaust constituents from the high-pressure burner facility. The instrumentation and sample-handling system were designed to conform to specifications in SAE ARP-1256, subsequently adopted, with some exceptions by the Environmental Protection Agency (References 11 and 12). The laboratory is self-contained and incorporates gas analysis instruments for measurement of the following:

- Carbon dioxide and carbon monoxide are measured with Beckman Model 865 Non-Dispersive Infrared (NDIR) instruments.
- Nitrogen dioxide is measured with a Beckman Model 255A Non-Dispersive Ultraviolet (NDUV) analyzer.
- Nitric oxide and total oxides of nitrogen are measured with a TECO Model 14D Chemiluminescence analyzer.
- Oxygen is measured with a Scott Model 250 Paramagnetic O2 analyzer.

The combustor rig exhaust gas sample is distributed to the various instruments, with each instrument having its own flow metering system. The sample handling is shown schematically in Figure 37.

Emissions analysis systems are regularly calibrated against a complete set of standard gases. Where possible, these gases are traceable to the National Bureau of Standards through a set of Standard Reference Materials including:

SRM 1673-1675 Carbon Dioxide in Nitrogen
SRM 1677-1681 Carbon Monoxide in Nitrogen
SRM 1665-1669 Propane in Air.

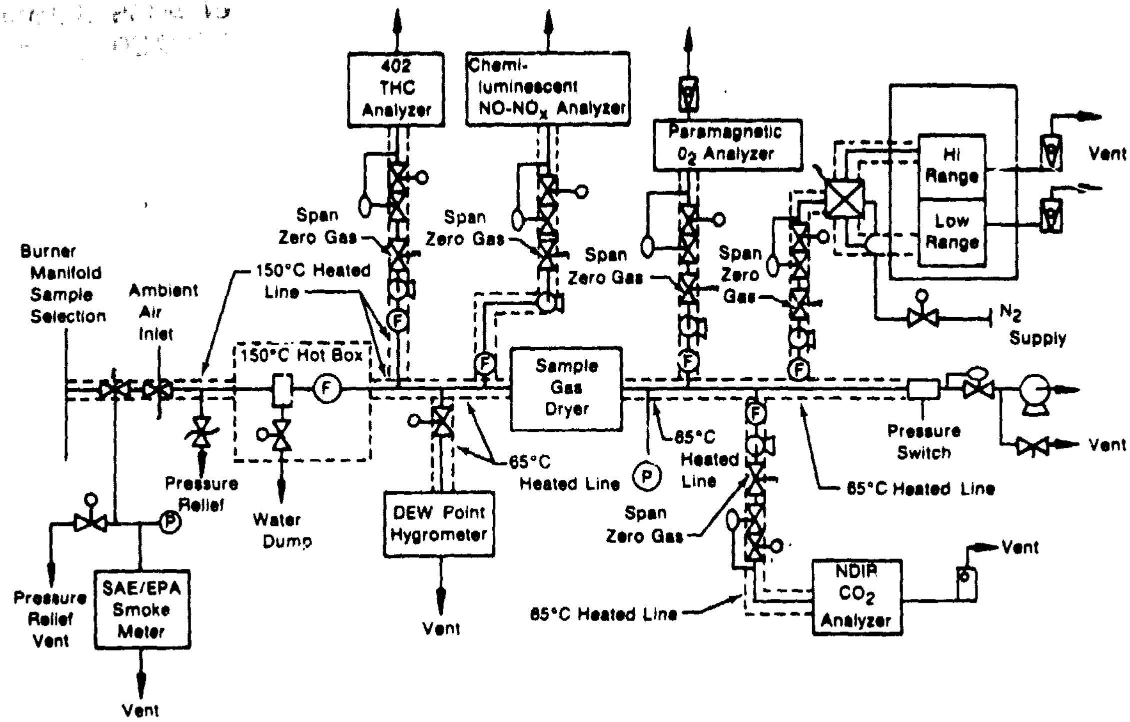

Figure 37   Gas Emissions Measuring System

Burner exhaust smoke measurements were obtained through use of a smoke measuring system that conforms to specifications of the Society of Automotive Engineers Aerospace Recommended Practice, ARP-1179. Figure 38 shows the smoke measuring system, or smoke meter, which is a semiautomatic electromechanical device. It incorporates a number of features to permit the recording of smoke data with precision and relative ease of operation. The unit is designed to minimize variability resulting from operator-to-operator differences. One of these features is a time-controlled solenoid-activated main sampling valve (Valve A of Figure 38) having "closed," "sample" and "bypass" positions. This configuration permits close control of the sample size over relatively short sample times. In addition, this timing system operates a bypass system around a positive displacement volume measurement meter to ensure that the meter is in the circuit only when a sample is being collected or during the leak check mode. Other design features include automatic temperature control for the sample line and filter holder, and silicon rubber filter holders with support screens for ease of filter handling.

The filter holder has been constructed with a 2.54 cm (1.0 in) diameter spot size, a diffusion angle of 7.25 degrees and a converging angle of 27.5 degrees.

A Photovolt Model 670 reflection meter with a type Y search unit conforming to ASA Ph 2.17-1958 "Standard for Diffuser Reflection Density" is used to determine the reflectance of the clean and stained filters. A set of Hunter Laboratory reflectance plaques, traceable to the National Bureau of Standards, is used to calibrate the reflection meter.

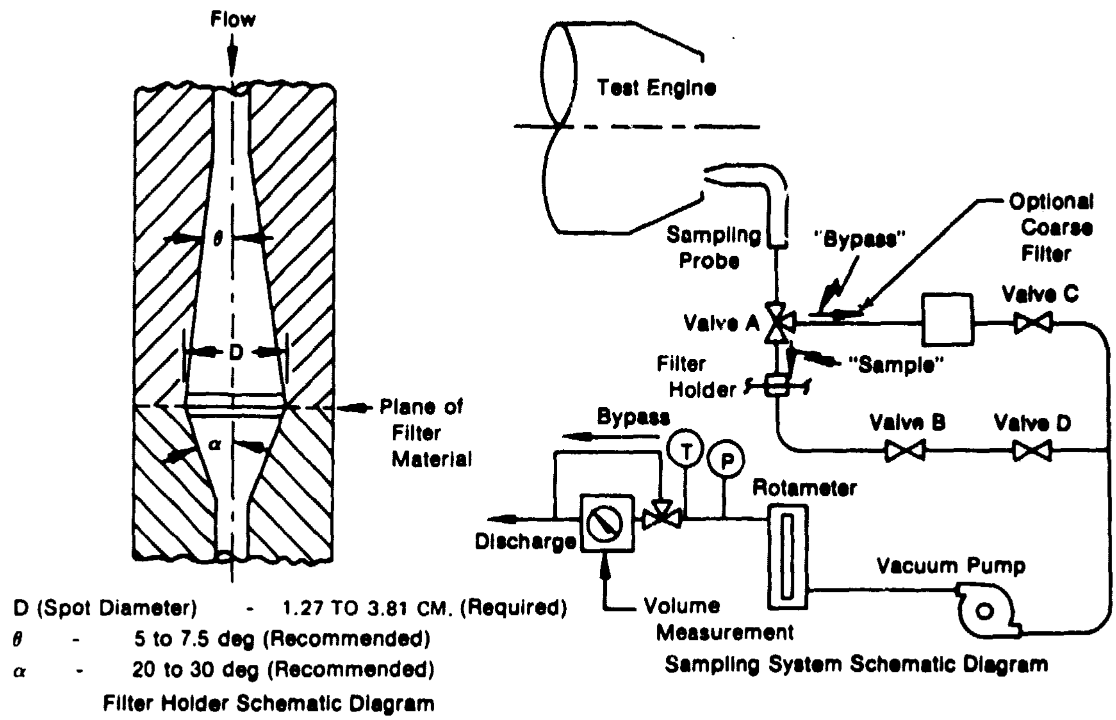

Figure 38 Smoke Meter

The burner test stand complex in the Middletown Test Facility is equipped with a computer controlled automatic data acquisition system. All data with the exception of that related to radiometer and smoke measurements, are processed through an on-line Univac computer that provides near real time data analysis. The data reduction program processes all data into engineering units and computes combustor operating parameters such as diffuser inlet Mach Number, fuel/air ratio, ideal temperature rise and emission indices with the latter averaged over the circumferential rake scan. Preselected critical parameters including those derived from emissions analysis are presented on a scope in the control room for screening to establish data validity before proceeding to the next point in the test program. Hard copy printout of the entire data reduction program output is available at a printer terminal in the Engineering Building in East Hartford within minutes after the data are acquired.

The Jet A fuel for X-960 Stand was drawn directly from the tank farm at the Middletown test facility. The Experimental Referee Broad Specification Fuel (ERBS) was drawn from a 20,000 gallon storage tank near the test facility.

The two lower hydrogen content test fuels were stored in tank trailers at a transfer station near the test complex. Figure 39 shows a simplified schematic diagram of the fuel supply system. Transfer and high pressure pumps are located in the line from each fuel source and the desired fuel was selected by operating the appropriate pumps and opening the selector valve in that line. A single pipe delivers the fuel from the selector valve to the rig. The total flow to the test rig is measured and the system is split into two separate branches with independent flow control to feed the primary and secondary fuel manifolds on the rig. Switching of fuels during testing was accomplished by activating the pumps in the line from the second source and bringing the fuel pressure up to the level in the system after which the selector valves were actuated. The selector valves are on-off type valves and the control system is set up so that only one of the four selector valves can be open at a time. The entire pump and selector valve operation sequence is actuated from the control room of the test stand and was accomplished with the rig operating. Check valves in the lines upstream of the selector valves prevent backflow through the lines which could contaminate the fuel in storage tanks. A timed delay bypass valve downstream of the high pressure pump diverts fuel to a dump tank for several minutes to avoid long system purge times after a change in test fuel.

The fuel flow to the combustor was measured with turbine type flow meters. One meter was used to measure the fuel flow to a manifold feeding the primary orifices of the injectors. The fuel flow to the secondary fuel manifold passed through either of two parallel metering paths which differed in the flow capacity of the control valves and flowmeters. The dual range system was required to obtain accurate fuel flow rate measurements over a wide range when the combustor was operated with single pipe fuel injectors. A fourth fuel flow meter was employed to provide a redundant measurement of the total fuel flow to the rig. Each meter was calibrated over the anticipated range of fuel flows prior to the initiation of testing. Appropriate correction factors for the differences in specific gravity and viscosity of the test fuels, derived from the laboratory analysis of these fuels, were incorporated in the data reduction programs. Fuel supply temperatures were measured with immersion type thermocouples in the fuel system and the fuel supply pressures were measured at the primary and secondary manifolds immediately upstream of the injectors.

5.2.3 JT9D Combustor Rig Instrumentation

Figure 40 shows the location of fixed instrumentation on the combustor rig inlet duct and rig cases. Four multihead Kiel type total pressure rakes and five multihead total temperature rakes are installed in the inlet duct. The total temperature and total pressure rakes are located 1.5 and 2.7 annular duct heights respectively, upstream of the equivalent axial location of the burner diffuser inlet plane in the rig as shown in Figure 41. Each total pressure and total temperature rake has four radially spaced sensors. The air temperature probes have shielded Chromel-Alumel thermocouples. Four static pressure taps are circumferentially spaced on the inner radius wall of the inlet duct at the same circumferential location as the total pressure rakes. Static pressure taps were installed on the combustor rig case. In conjunction with pressure measurements from instrumentation on the combustor liners these data permitted computation of the airflow distribution in the combustor and simulated turbine cooling air bleed system. A hydrocarbon sniffer was installed on a port on the outer burner case to detect fuel in the burner shroud in the event of fuel system malfunction, damage or aspiration from the combustor.

ORIGINAL PAGE IS
OF POOR QUALITY

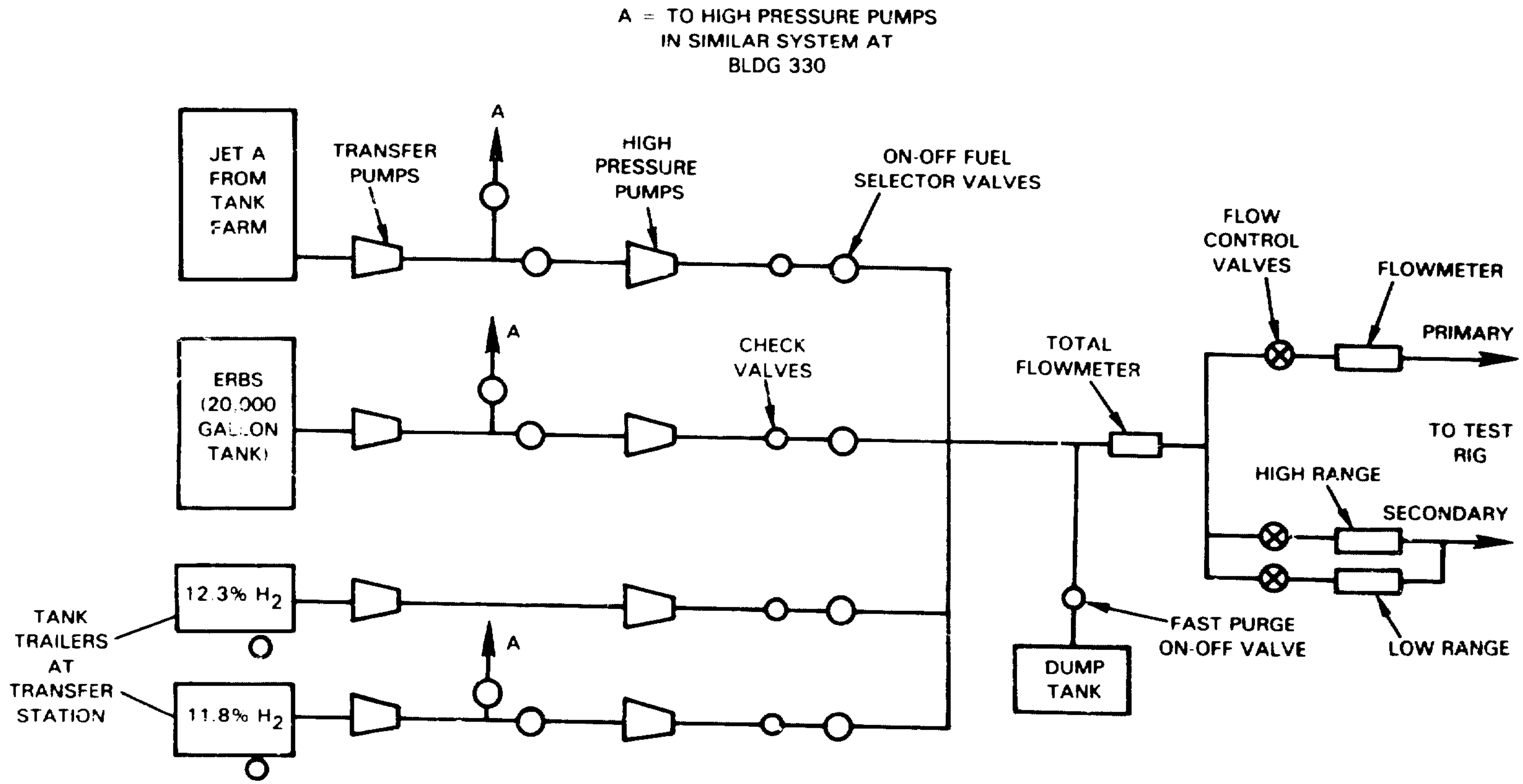

Figure 39 Simplified Schematic Diagram of Fuel Supply System for X-960 Test Stand

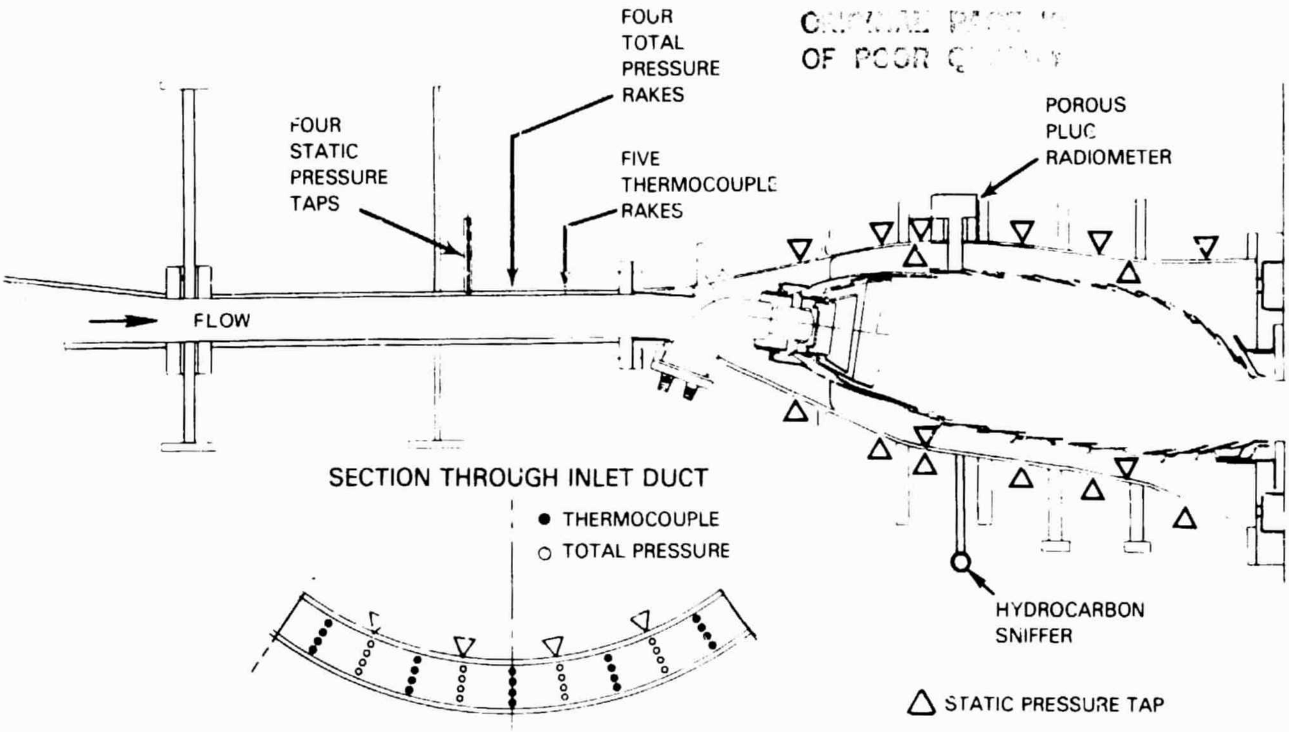

Figure 40 Combustor Rig Inlet and Case Mounted Instrumentation

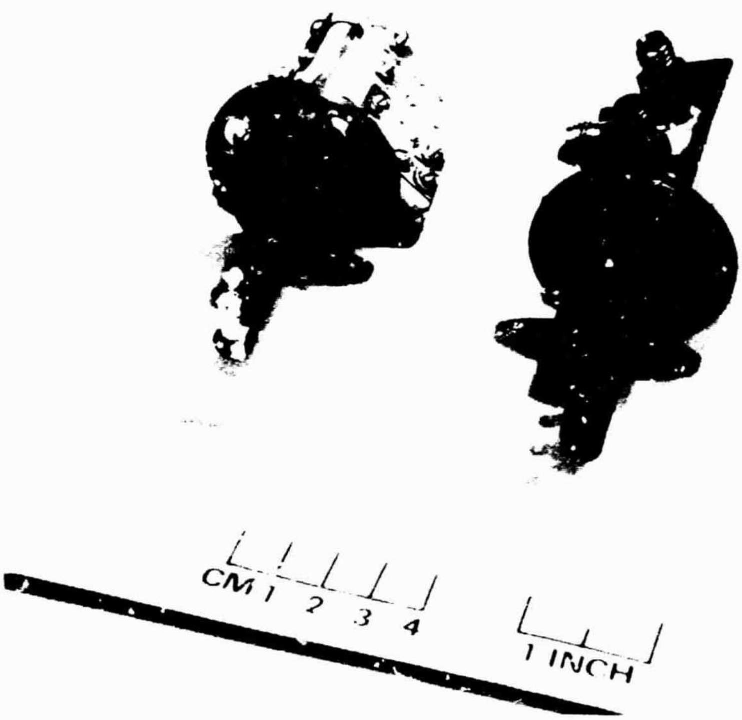

Figure 41 JT9D Combustor Rig Inlet Rakes for Temperature (Left) and Pressure (Right)

Since the effect of fuel composition on liner temperature and durability was a major concern in the program, the combustor liners were extensively instrumented with metal temperature thermocouples. Typically, thirty to forty Chromel-Alumel thermocouples were installed on each liner sector. The thermocouples were installed by welding the junction directly to the cold side surface of the liner. Figures 42, 43 and 44 show the location of these thermocouples on the three JT9D combustor liner sectors employed during the program. Figure 45 shows a photograph of the outer liner of the basic bulkhead combustor sector after the installation of the thermocouples and is representative of the lead routing on all of the sectors. On the liner proper, the thermocouples were installed with the junctions positioned near the weld between a film cooled panel and the riser of the following louver. Since the temperature gradient between this region and the cooler louver knuckle is critical to cyclic fatigue, the measurements were relevant to liner life. In the case of the bulkhead combustor of Figure 43, several thermocouples were also located on the cold knuckle of a louver to verify the temperature in this region. The readings from these thermocouples were excluded from any "average" metal temperature definition. The circumferential distribution of thermocouples generally favored positions downstream of the two center fuel injectors and midway between these injectors. Two or three of the thermocouples on the liners could not be connected to the data acquisition system because they were used for condition monitoring purposes by the supervisory control system in the test facility. Thermocouples located near the endwalls of the liner sectors were generally allocated to this purpose.

When the instrumentation was installed on the bulkhead combustor sector of Figure 43, an intermediate region of the liners was left devoid of thermocouples. The dilution air orifices are located in this region of the combustor, and the configuration changes that were to be made on this sector required repeated reoperation of the liners in this area to alter or relocate these apertures. Since the instrumentation would be susceptible to damage during these reoperations, it was concentrated in the primary and dilution zones upstream and downstream of these areas. Likewise measurement of meaningful metal temperatures in the Finwall® panels of the combustor liner of Figure 44 would require immersing the thermocouple junctions in the hot wall of the panels. Because of the complexity of such an installation, no thermocouples were installed on the Finwall® panels. However, the density of thermocouples on the bulkhead of the combustor was increased to provide a better indication of primary zone heat load effects.

A porous plug radiometer was installed in the test rig to provide direct measurement of the radiation heat transfer to the liner during the evaluation of selected configurations. As shown in Figure 40 the radiometer was mounted in a boss on the rig case with the sensing surface protruding through a hole in the combustor liner in order to sense the radiant heat load in the primary combustion zone. Figures 42 and 43 show the location of the radiometer probe in the combustors.

SCHEMATIC VIEW FROM UPSTREAM SHOWING CIRCUMFERENTIAL POSITION OF INSTRUMENTATION

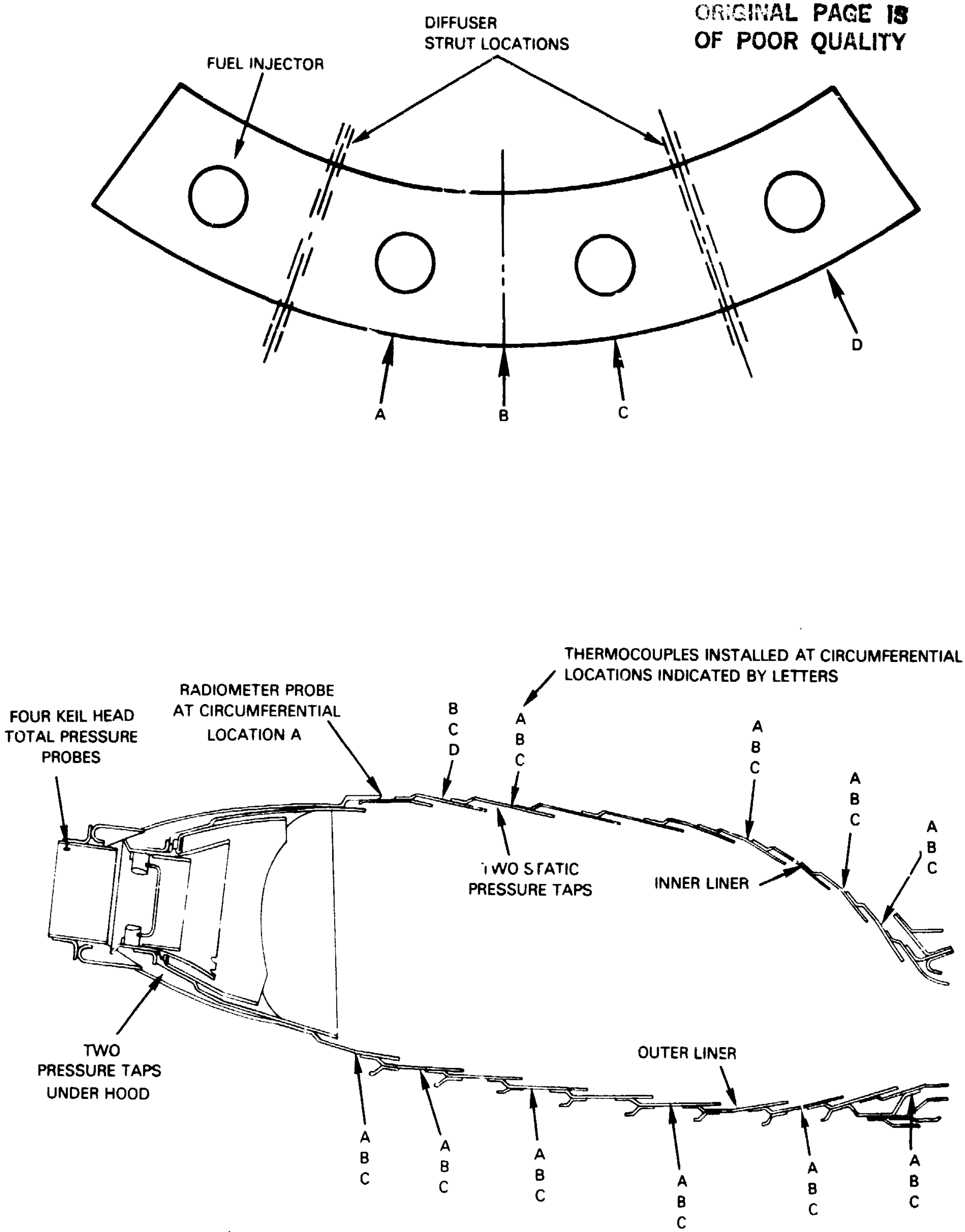

Figure 42 Instrumentation on the Production JT9D Combustor Liner (Configuration SS-1)

SCHEMATIC VIEW FROM UPSTREAM SHOWING CIRCUMFERENTIAL POSITION OF INSTRUMENTATION

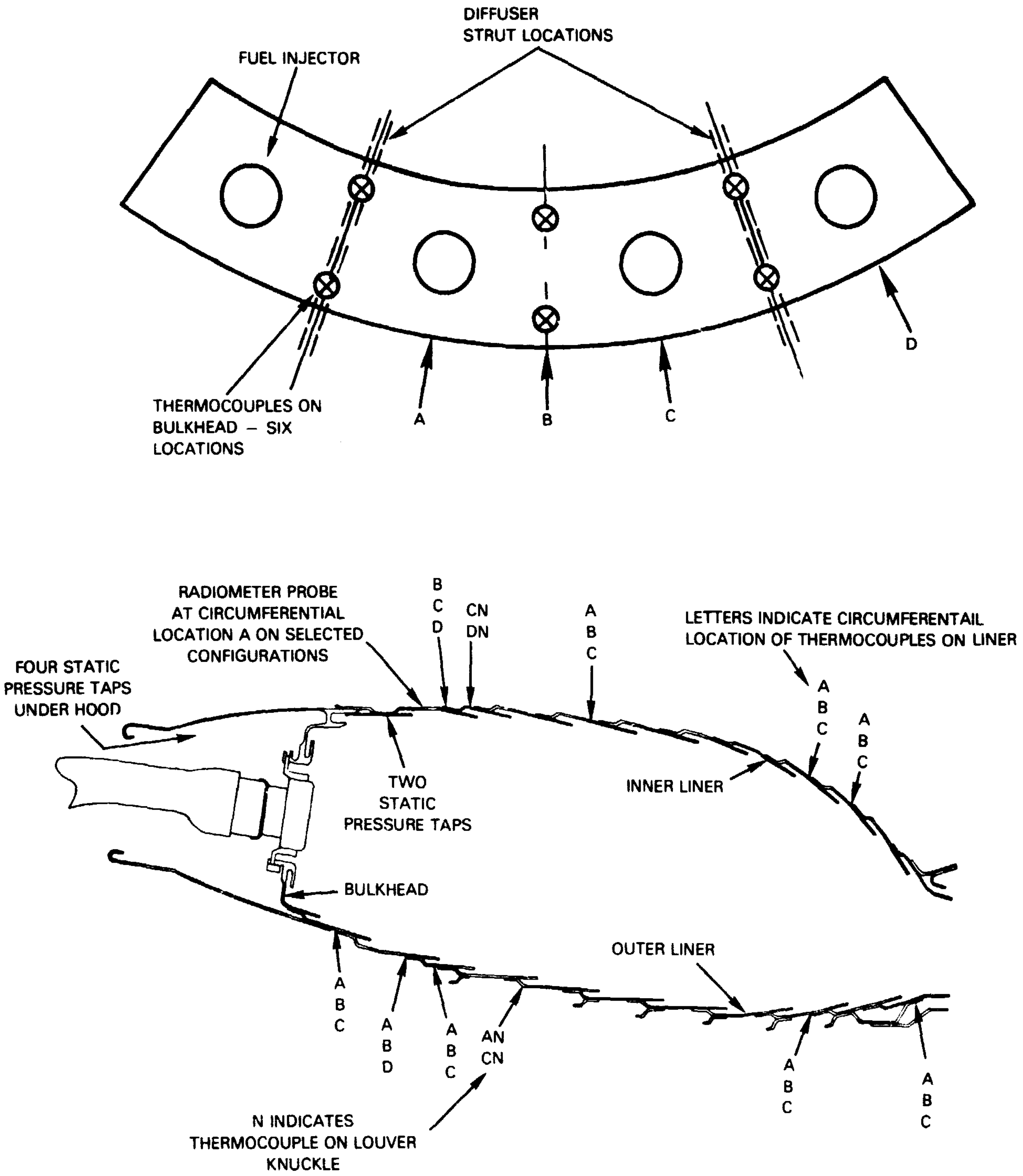

Figure 43 Liner Instrumentation on Bulkhead Combustor Configurations

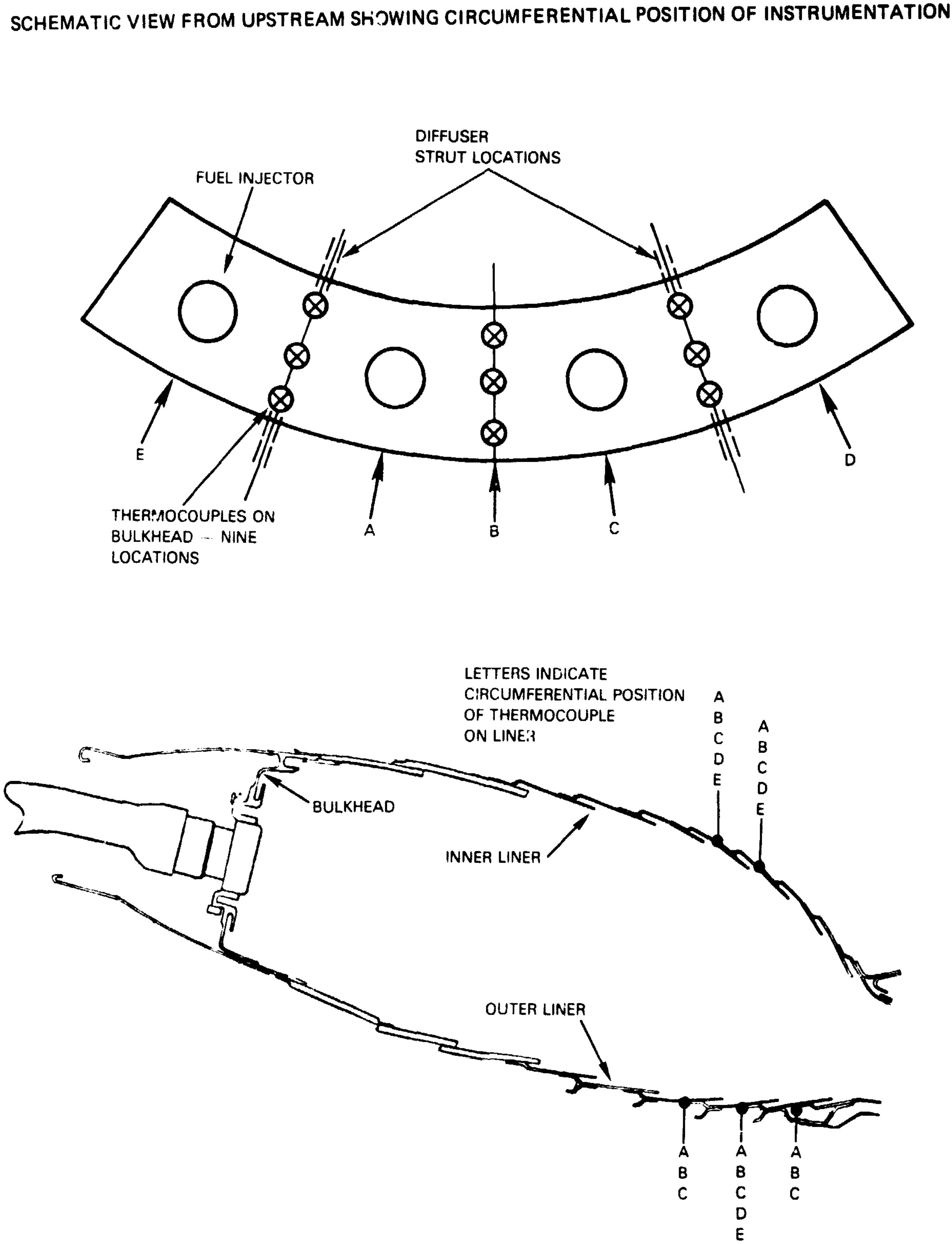

Figure 44 Liner Instrumentation Locations on Bulkhead Combustor with Finwall® Liner Panels

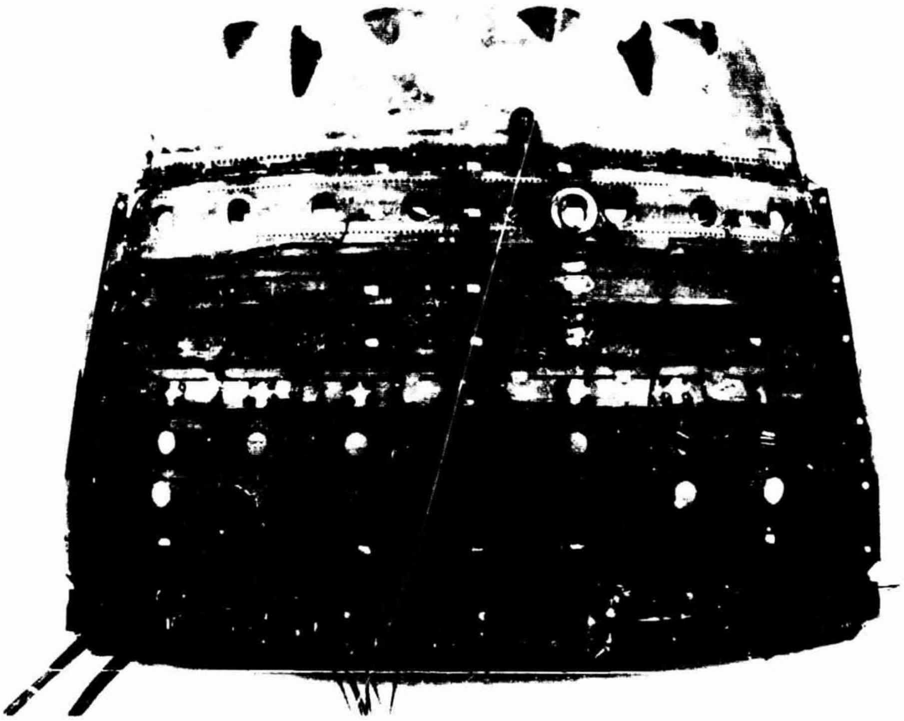

Figure 45 JT9D Bulkhead Combustor Outer Liner Sector After Installation of Thermocouples

Figure 46 shows a cross section view of the porous plug radiometer, which is a transpiration cooled device designed to measure incident total hemispherical radiation in the presence of strong convective conditions. These radiometers use a controlled flow of transpiration cooling through the sensor to blow the free stream thermal boundary layer from the front surface of the probe. This technique allows a direct measurement of the radiant heat flux without complication from convective or reactive effects. The sensing element consists of a thin porous plate through which a precisely metered quantity of transpirant gas of filtered shop air or bottled nitrogen is passed. A differential Chromel-constantan thermocouple measures the temperature difference between the gas and the plate, which is related to the heat flux into the porous plug. The probe was calibrated prior to use to establish the relationship between incident heat flux, gas flow rate and gas temperature rise. During test, the output from the differential thermocouples in the sensor was processed on a digital millivoltmeter that is incorporated in a portable Hewlett Packard computer. Preprogrammed calibration data on the radiometer was used to provide real time readout of the heat flux and sensor surface temperature.

The combustor exit conditions were measured with the exit rake shown in Figure 47. The rectangular flange of the rake attaches to a flat on the side of the traverse drive shaft on the centerline of the exhaust chamber, as shown in Figure 36. The radial arms support the sensors at the radius of the combustor exit annulus. Figure 48 shows the details of the rake head which consists of four gas sampling/total pressure probes and five shielded gas temperature thermocouple probes spaced radially across the combustor exit annulus in two circumferentially spaced rows. The mount arm and the gas sample/total pressure tubes are cooled with high pressure air bled from the rig inlet supply duct upstream of the airflow measurement venturis.

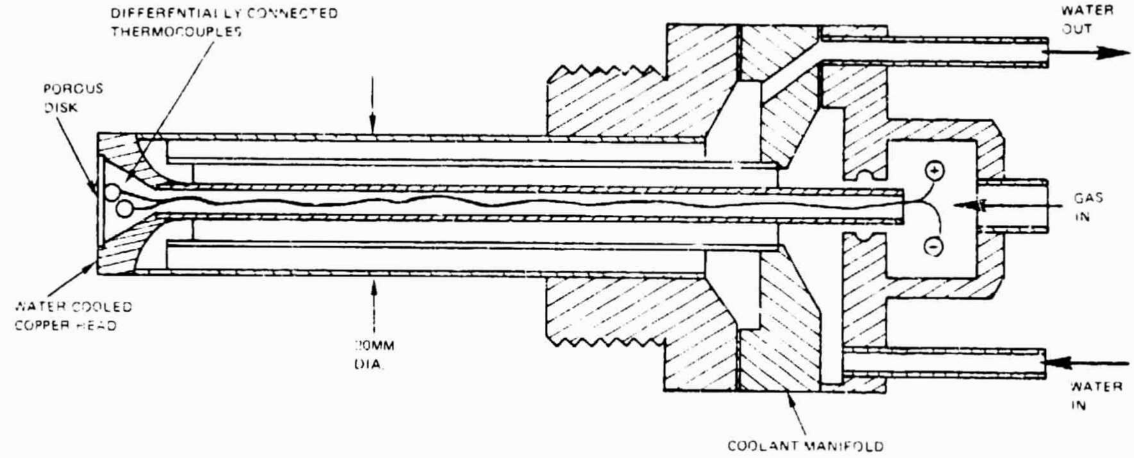

Figure 46 Porous Plug Radiometer

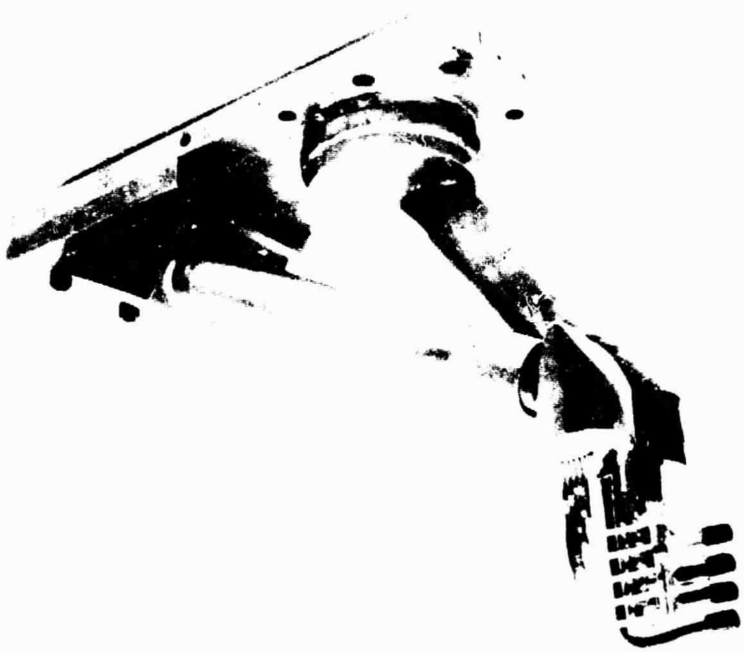

Figure 47 JT9D Combustor Exit Rake Assembly

ORIGINAL PAGE IS OF POOR QUALITY

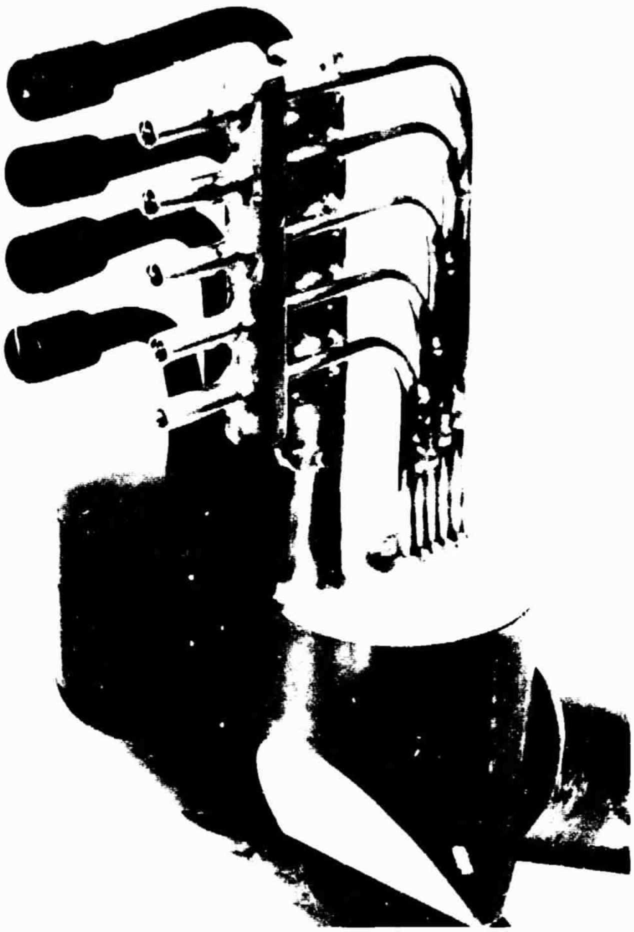

Figure 48   JT9D Combustor Exit Rake Head Details

The gas temperature thermocouples in the rake employ a grounded immersion type of junction with ISA Type B thermocouple wire (Platinum, six percent Rhodium vs Platinum, 30 percent Rhodium). The calibration of this wire is accurate to 1975°K (3100°F). The gas sampling heads were made from Platinum - 20% Rhodium alloy while the remainder of the lines were made from stainless steel tubing. When emissions or smoke is measured, the samples from various sensors, as selected by valves in the sample lines, are mixed in a manifold and feed to the analysis equipment. All of the emissions or smoke samples analyzed during this program were extracted from all four heads on the rake and mixed to produce a single representative average sample for the particular circumferential position. Temperature measurements on this type of air cooled rake have shown that the gas samples are quenched to 425 to 475°K (300 to 400°F) by the cooling air in the rake and the sample lines between the rake and the analysis equipment are heated to maintain the sample temperature at about 425°K (300°F). When these sensors are used to measure total pressure the sample lines are dead ended by closing the selector valves, and the pressure is recorded on a transducer in the automatic data recording system.

5.3 TEST APPARATUS - ENERGY EFFICIENT ENGINE COMBUSTOR CONCEPTS

The advanced Vorbix combustor concept was designed for the NASA/Pratt & Whitney Aircraft Energy Efficient Engine and the evaluation of this combustor involved use of rig components sized for geometric compatability with that engine. This rig, the test facility and instrumentation were essentially identical to those employed during the evolution of this combustor under the Energy Efficient Engine program (Reference 9). This section provides a description of this experimental apparatus.

5.3.1 Energy Efficient Engine Combustor Test Rig

The Energy Efficient Engine combustor test rig was a sector rig which incorporated many of the design features of the JT9D combustor rig (see Section 5.2.1). The rig cases describe a 90 degree sector and enclose a 75 degree sector of the combustor proper. This is sufficient to include five of the 24 diffuser case struts and pilot stage fuel injectors of the full annular combustor section, and ten of the 48 carburetor tubes. Figure 49 shows a cross section of this rig. While the JT9D combustor rig had been fabricated from an engine diffuser case, the aerothermal definition of the engine gaspath was incomplete at the time construction of this rig was initiated. Consequently, it consists of basic structural cases with removable fillers and inserts used to reproduce the case contours in the prediffuser, dump and burner shroud regions. The rig incorporates manifolds for extracting simulated turbine cooling and service bleed air and, in operation, the airflow rates in these systems were metered and controlled to duplicate those in the engine.

For development flexibility, the pilot and main stage fuel injectors were mounted on individual supports rather than on the modular supports that would be used in the full annular engine combustor. The rig is compatible with the use of either the segmented Finwall® combustor liner sector or a liner sector with conventional sheet metal louver construction. Either liner is attached to louver cooled endwalls similar to those shown on the JT9D combustor sector in Figure 33. Like the JT9D rig construction, the burner sector is mounted on rails on the endwalls of the case that constrain the liners in a curved position while accommodating thermal expansion.

5.3.2 Energy Efficient Engine Combustor Test Facility

The high pressure tests on the Energy Efficient Engine combustor rig were conducted in X-903 Test Stand. X-903 is one of four high pressure combustor development stands located in the Building 330 test complex at the Pratt & Whitney Aircraft Middletown plant. Normally, airflows up to 11.4 kg/sec (25 lb/sec) at pressure levels up to 4.3 MPa (625 psia) are provided in this stand by two steam driven two stage turbocompressors and one six stage steam driven boost compressor. However, this airflow was inadequate to provide combustor inlet Mach number similarity in the sector rig at the inlet pressure levels of the Energy Efficient Engine cycle at high power levels. For these operating conditions the air was supplied from the compressors at X-960 Stand in the adjacent building. As indicated in Section 5.2.2 these compressors were capable of providing air flow rates up to 45.5 kg/sec (100 lb/sec) which was more than adequate for operation of the sector rig. Regardless of the source of the air, it was preheated to the required combustor inlet temperature in an indirect fired heat exchanger prior to delivery to the test rig.

ORIGINAL PAGE IS
OF POOR QUALITY

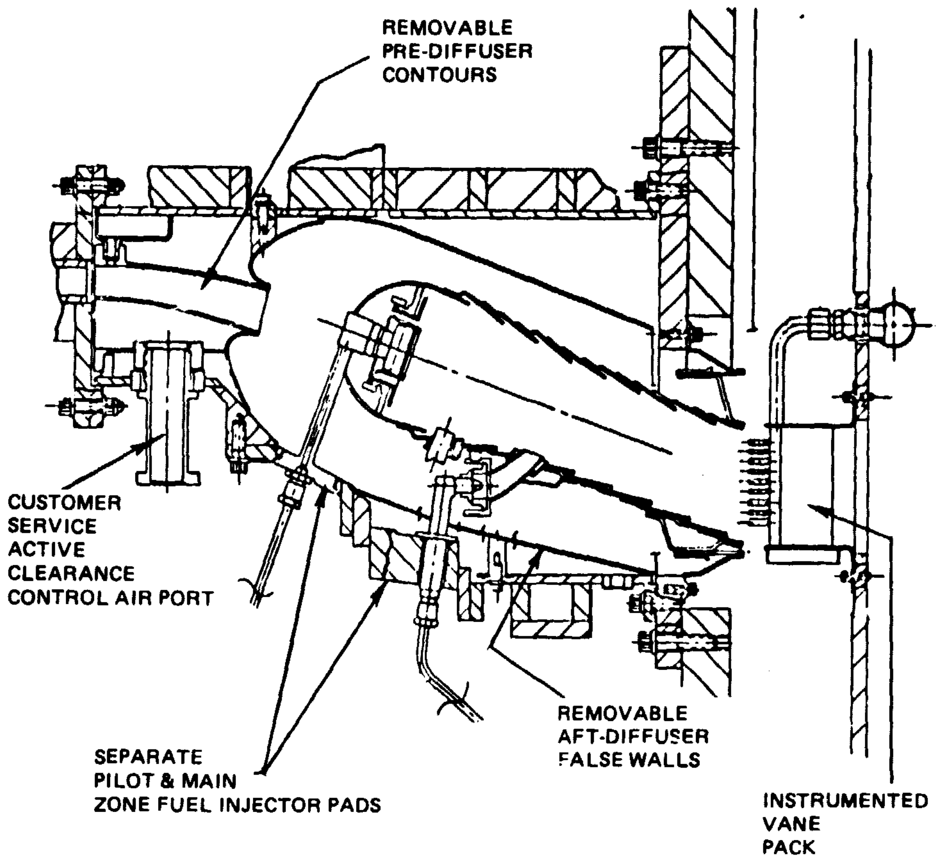

Figure 49 Energy Efficient Engine Combustor Sector Rig

The combustor test rig is mounted within a cylindrical pressure tank. Tank pressurization is automatically controlled to 0.04 MPa (6 psi) above rig pressure. In this manner, the pressure load is supported by the facility pressure vessel, permitting experimental hardware to be of relatively light construction. A retractable tank section with a quick-disconnect breech-lock seal is provided to enable easy access to the test rig. Exhaust gases are collected in a water-cooled exhaust chamber and ducted underground to an expansion and liquid separation pit at the base of the main exhaust stack. X-903 Stand is serviced by an automated data acquisition and recording system similar to that in X-960. All necessary data required for configuration analysis are recorded and processed in real time on the central Univac computer. The computer reduces the data, converts it to engineering units, and displays the results on a data display scope at the test facility. The data can then be reviewed, after which printed output can be obtained at the test location or at the computing center. The printed output includes raw and reduced data for both performance and gas analysis evaluation.

The emissions and smoke collection and analysis system serving X-903 and the other test stands in Building 330 is similar to that in X-960 and employs identical instruments. This system was described in Section 5.2.2 and shown in Figures 37 and 38.

During the high pressure test sequence, the advanced Vorbix combustor was operated on Jet A, Experimental Referee Broad Specification fuel (ERBS) and the 11.8 percent hydrogen test fuel. These fuels were supplied through the fuel system in X-960 Stand in the adjacent building. As shown in Figure 39 the legs of the distribution system carrying these three fuels are branched downstream of the transfer pumps. The branch lines route to Building 330, where X-903 Stand is located, and feed three independent high pressure pumps. The remainder of the fuel supply system in X-903 Stand, i.e., that downstream of the high pressure pumps, was essentially the same as that shown in Figure 39 for the X-960 Stand .

5.3.3 Energy efficient Engine Combustor Rig Instrumentation

Table 13 provides a list of the fixed instrumentation installed on the inlet duct and the cases of the Energy Efficient Engine combustor rig. When installed in the test facility the airflow entered the rig through a transition duct followed by an inlet duct which had a constant annular sector cross section. The inlet total pressure and total temperature rakes were installed in this duct upstream of the prediffuser inlet plane. The rig was instrumented extensively with static pressure taps, many of which had been required to accomplish the early development objectives of the Energy Efficient Engine program. These included the static pressure taps in the prediffuser, and the strut mounted total pressure rakes at the prediffuser exit which had served to document the performance of this component. Likewise the static pressure taps in the burner shrouds and under the pilot stage hood provided substantiation of the pressure recovery in these passages but were used in the present evaluation primarily to confirm the combustor airflow distribution.

Table 13
Instrumentation on Energy Efficient Engine Combustor Rig Cases

Location	Measurement/Type	Quantity
Inlet Duct	4-Element total pressure rakes	6
	4-Element total temperature rakes	5
	ID/OD wall static pressure taps	5/5
Prediffuser	ID/OD wall static pressure taps	2 rows of 6/6
Diffuser Case Struts	5 element total pressure rakes	4 struts
Outer Shroud	Wall static pressure taps	2 rows of 4
	Hydrocarbon sniffer	1
Inner Shroud	Wall static pressure taps	2 rows of 6
	Hydrocarbon sniffer	1
Combustor Hood	Static pressure taps	2

When the segmented liner combustor sector was first assembled for evaluation under the Energy Efficient Engine program 40 Chromel-Alumel thermocouples were installed on the liner segments. Thirty-six of these were located on the hot side surface of the segments. Their installation involved milling a slot into the hot side wall of the Finwall® and imbedding the junction in the metal while routing the leads off the segment without disrupting the cooling airflow. The four remaining thermocouples were installed on the hooks which attached the segments to the liner structural case. Figure 50 shows the location of these thermocouples on the sector burner liner.

The combustor exit conditions were measured with instrumentation mounted on a fixed vane pack. The pack consisted of 14 radial vanes spanning the combustor exit annulus and spaced at 5.7 degree increments as shown in Figure 51. The vanes have flat parallel sides with semicircular leading and trailing edges and are 0.95 cm (0.375 in) thick. The vane leading edge is constructed of a 0.95 cm (0.375 in) tube that connects to a manifold on the opposite side. The manifold covers the remaining cross-sectional area of the vane. The vanes are air cooled, and film cooling holes, 0.635 mm (0.025 in) in diameter, are located in a 3.8 mm (0.150 in) staggered array. The holes are canted on the sides 30 degrees to downstream. The cooling air flows through the leading edge tube into the manifold at the opposite end from which it is directed into the rear cavity of the vane and is discharged through the film cooling holes on the remainder of the vane surface.

Gas temperature thermocouples and gas sampling heads are installed on the leading edge of the eight vanes in the center of the combustor exit sector. Five shielded thermocouples are spaced radially across the combustor exit annulus on these vanes and incorporate a grounded immersion type of junction with ISA Type B thermocouple wire (Platinum, six percent Rhodium vs Platinum, 30 percent Rhodium). The calibration of this wire is accurate to 1975°K (3100°F). Four gas sampling heads are located radially between the thermocouples on each of these eight vanes. The gas sampling heads are uncooled and are fabricated in a convergent-divergent shape from a Platinum-20% Rhodium alloy. The sample lines inside the vane body are fabricated from stainless steel tubing and the sample was quenched by the cooling air inside the vane. The sample lines between the rig and the analysis equipment are heated to maintain the sample temperature at about 425°K (300°F). When emissions or smoke are measured the samples from various sensors,as selected by valves in the sample lines, are mixed in a manifold and feed to the analysis equipment. All of the emissions or smoke samples analyzed during this program were extracted from all 32 gas sample heads on the vane pack and mixed to produce a single representative average sample for the particular combustor operating condition.

Four vanes in the pack were instrumented with five radially spaced total pressure Kiel head probes. Two of these vanes were located on each side of the exit annulus adjacent to the central array of eight vanes with thermocouple probes and gas sampling heads. The vanes closest to each endwall of the rig were not instrumented.

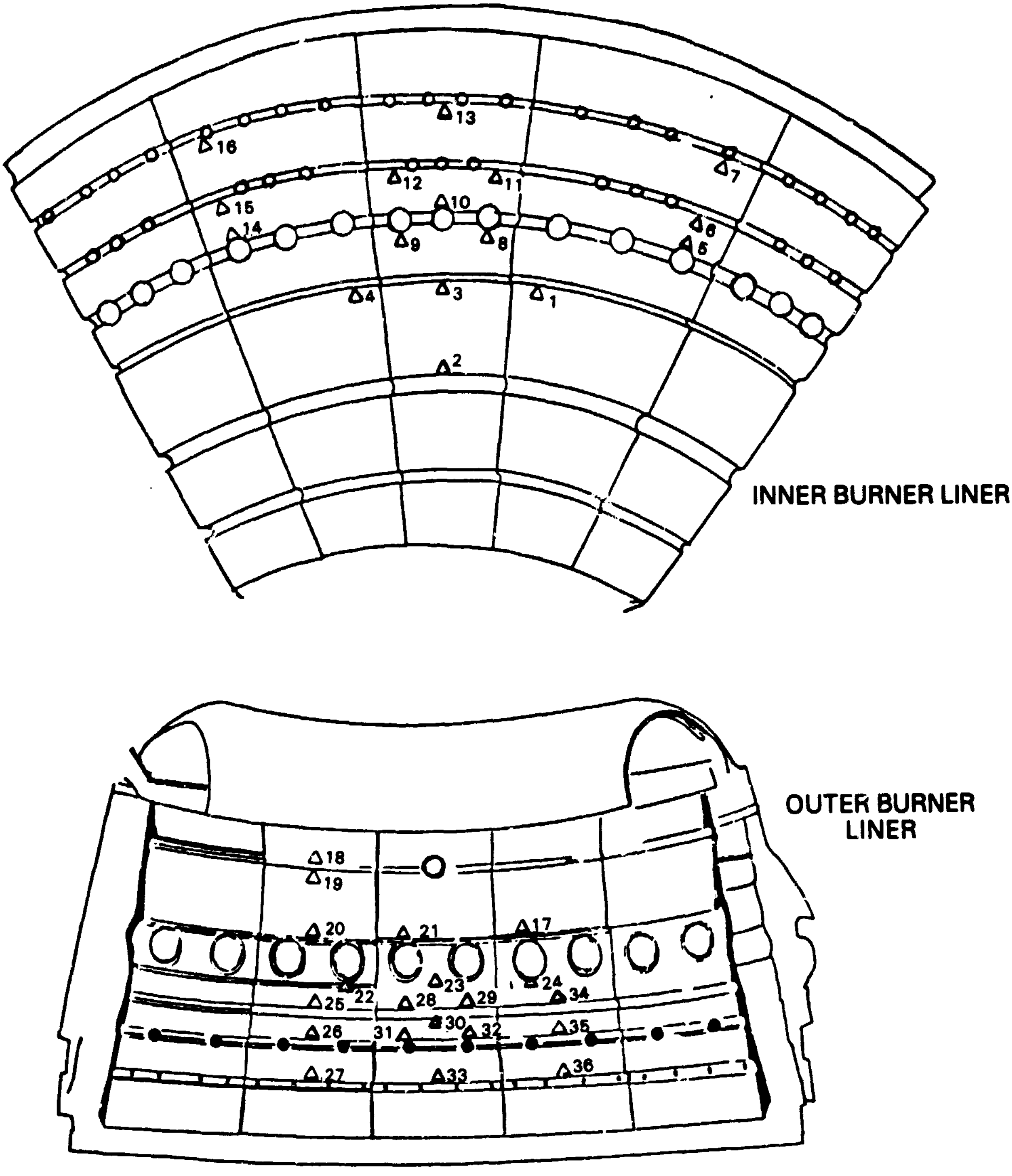

Figure 50 Thermocouple Sensor Locations on Segmented Liner

5.4 ALTITUDE TEST FACILITY

The final configuration of each of the three combustor concepts was evaluated for altitude and sea level ignition capability and stability in an altitude facility at X-336 Stand in the Experimental Test Airport Laboratory at Pratt & Whitney Aircraft's East Hartford facility. X-336 is a subatmospheric pressure test stand equipped with inlet air and fuel coolers and air dryers. The exhaust duct in this stand can be evacuated to pressures as low as 0.007 MPa (1 psia) by a combination of vacuum pumps, and refrigerated air can be supplied at temperatures as low as 224°K (-60°F) and dried to a water content of less than 1 gm/kg.

Figure 51 Combustor Exit Instrumentation Vane Pack

For ignition testing the entire combustor rig and the inlet duct section containing the burner inlet instrumentation is removed from the high pressure facility and installed in X-336 Stand. The fuel supply system permits drawing fuel from either the standard facility Jet A supply or, through manually actuated valves from barrels of special test fuels.

The existing rig inlet rakes and the venturi in the facility inlet duct are used to establish combustor air inlet conditions. Ignition is detected by Chromel-Alumel immersion type thermocouple probes installed in the combustor exit plane with one probe located axially downstream of each fuel injector. The signals from these thermocouples, the frequency count from a turbine type flowmeter in the primary fuel supply line, the output from a pressure transducer in the primary fuel manifold and the igniter pulses are all recorded on a Visicorder strip chart to document the transients during the ignition process.

SECTION 6.0

EXPERIMENTAL PROCEDURES

6.1 INTRODUCTION

This section presents a definition of the parameters used in assessing the performance and emissions characteristics of the combustors. Also contained in this section are the test procedures and the test conditions.

The various combustor performance and emissions parameters that are discussed as program results are listed in Table 14. Definitions of the calculated parameters are presented in Section 6.2 and 6.3 while the symbols are defined in the Nomenclature List.

Table 14

Summary of Combustor Performance Parameters

Parameter	Symbol	Units	Measured	Calculated
Total Airflow	W_{at}	Kg/sec (lb/sec)	X	
Burner Airflow	W_{a0}	Kg/sec (lb/sec)		X
Inlet Total Pressure	P_{Tin}	MPa (psia)	X	
Inlet Total Temperature	T_{Tin}	°K (°F)	X	
Reference Velocity	V_{Ref}	m/sec (ft/sec)		X
Total Fuel Flow	W_F	Kg/sec (lb/sec)	X	
Fuel Flow Split	% of W_F	%	X	
Fuel/Air Ratio	F/A	--		X
Burner Total Pressure Loss	$\Delta P/P_{Tin}$	% of P_{Tin}	X	
Metal Temperature		°K (°F)	X	
Fuel Temperature	T_{fuel}	°K (°F)	X	
Pattern Factor	PF	--		X
Carbon Balance Fuel/Air Ratio	FA_{CB}	--		X
Emissions Index	EI	g/kg		X
Combustion Efficiency	η_c	%		X
EPA Parameter	EPAP	g/kN		X

6.2 PERFORMANCE PARAMETER DEFINITIONS

The definition of several combustor performance parameters require the identification of average combustor inlet and exit total pressure and total temperature. The combustor inlet total temperature and total pressure, T_{Tin} and P_{Tin} are the numerical averages of the measured values from the rakes in the rig inlet duct immediately upstream of the diffuser. Likewise the exit total temperature and total pressure T_{Texit} and P_{Texit} are the numerical

C-2

averages of all measurements obtained at the combustor exit plane. In the case of the JT9D based single stage and variable geometry combustor concepts this data included measurements at nineteen (19) positions of the circumferentially traversing combustor exit rake. As shown in Figure 52 these positions were evenly spaced three degrees apart across the majority of the 72 degree width of the sector.

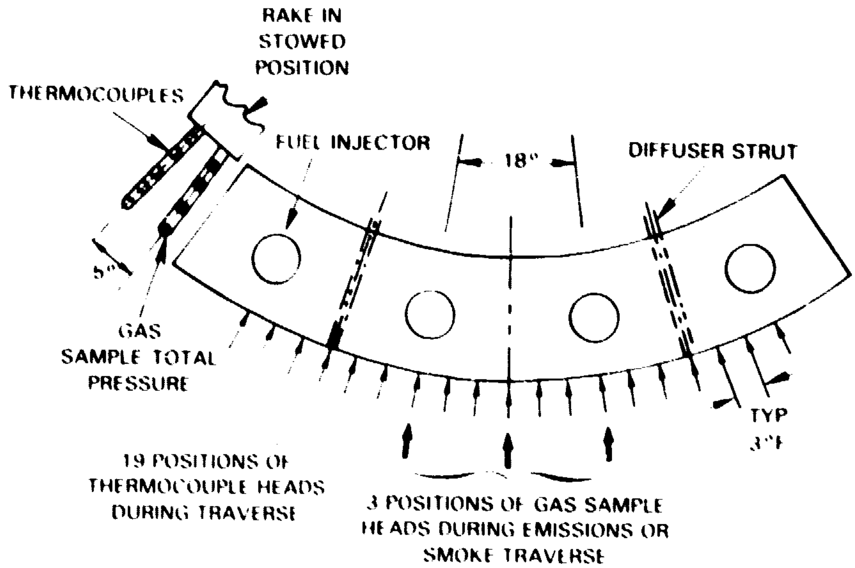

Figure 52 Schematic Front View of JT9D Combustor Sector Showing Exit Rake Circumferential Positions

The advanced Vorbix combustor test rig incorporated fixed position combustor exit instrumentation mounted on a vane pack. The combustor exit temperature was the numerical average of the measurements from forty (40) gas temperature thermocouples mounted on eight vanes in the center of the combustor exit sector as described in Section 5.3.3. Likewise, the combustor exit total pressure was the numerical average of the measurements from twenty (20) total pressure probes mounted on four of the vanes in the combustor exit sector.

Combustor performance parameters computed from this and other data are described below.

Combustor Airflow

The combustor airflow W_{ab} is calculated by subtracting the measured inner and outer turbine cooling air bleed flows and the estimated combustor liner sidewall cooling airflow from the measured total rig airflow.

Reference Velocity

The reference velocity is defined as that flow velocity that would result if the total combustor airflow, at the compressor discharge temperature and static pressure, were passed through the combustor liner at the maximum cross sectional area. This area is 717 cm^2 (111.2 in^2) for the JT9D based combustor concepts and 357 cm^2 (55.4 in^2) for the Energy Efficient Engine combustor sector.

Total Pressure Loss

The total pressure loss across the burner section includes losses in the diffuser as well as those across the burner proper and is referenced to the average burner section inlet total pressure as:

$$\frac{\Delta P_T}{P_{Tin}} = \frac{P_{Tin} - P_{Texit}}{P_{Tin}} \qquad \text{(Eq. 1)}$$

Pattern Factor

The combustor exit temperature nonuniformity is characterized by the pattern factor which is defined as:

$$P.F. = \frac{T_{Texit\ max} - T_{Texit}}{T_{Texit} - T_{Tin}} \qquad \text{(Eq. 2)}$$

where:

$T_{Texitmax}$ = maximum temperature measured at exit

Metered Fuel/Air Ratio

The metered fuel/air ratio is the ratio of the total combustor fuel flow, as defined by turbine meters in the fuel supply system, to the combustor airflow, Wab.

6.3 EMISSIONS ANALYSIS PARAMETERS

Carbon Balance Fuel Air Ratio

The carbon balance fuel/air ratio was computed using the equation:

$$F/A_{CB} = \frac{M_C + \alpha M_H}{M_{AIR}} \quad \frac{N_{CO} + N_{CO_2}}{100 - \left(\frac{1}{2} + \frac{\alpha}{4}\right) N_{CO} - \frac{\alpha}{4} N_{CO_2}} \qquad \text{(Eq. 3)}$$

where: M_x is the molecular weight of the x^{th} specie
N_x is the mole fraction of the x^{th} specie
α is the hydrogen to carbon ratio of the fuel

and the measured species concentrations.

Emissions Indices

Concentrations of emissions constituents were reduced to emission indices in the form of grams of constituent per kilogram of fuel. Generally the carbon balance fuel/air ratio of the sample was used to make the conversion from concentrations since it is considered more representative of the actual fuel air ratio at the site of combustion. However, a malfunction of the carbon dioxide measurement apparatus occured during the test of configurations VG-3 and VG-4. Since this precluded accurate computation of the carbon balance fuel air ratio the metered fuel air ratio was used for the conversion of this data. Data obtained from other configurations which would be compared against that of configurations VG-3 and VG-4, such as VG-1 and SS-2 were converted to emissions indicies using both fuel air ratios and both sets of results are tabulated in Appendix C. However, except in situations where comparison with the emissions data from configurations VG-3 and VG-4 is being made, the emissions characteristics cited are those computed with the carbon balance fuel air ratio.

In evaluating the JT9D based combustor concepts, involving the use of a circumferentially traversing emissions sampling rake, an average emissions index was computed by numerically averaging the individual readings at three circumferential positions. These three positions are shown in the schematic diagram of Figure 52. The evaluation of the Energy Efficient Engine-based advanced Vorbix combustor concept involved use of a combustor exit vane pack with thirty two (32) discrete gas sampling heads. In operation, a single mixed sample produced by extracting simultaneously and at nearly equal flow rates through all sample ports was used. The mixed sample was analyzed for composition and the computed carbon balance fuel air ratio and emissions indices is a representative average.

Corrections were applied to the emissions indices to account for deviation of the test condition from standard conditions. These included correction of NO_x emissions for inlet humidity and of all constituents for deviations of the inlet total pressure relative to the appropriate engine cycle. Except for the operation of the advanced Vorbix combustor at climb and takeoff conditions these inlet pressure deviations were small and consisted only of experimental inaccuracies in setting the test conditions. These correction factors are:

$$\text{Corrected } EI_{HC} = \text{Measured } EI_{HC} \times \left(\frac{P_{T_{meas}}}{P_{T_{corr}}}\right) \qquad \text{(Eq. 4)}$$

$$\text{Corrected } EI_{CO} = \text{Measured } EI_{CO} \times \left(\frac{P_{T_{meas}}}{P_{T_{corr}}}\right) \qquad \text{(Eq. 5)}$$

$$\text{Corrected } EI_{NO_x} = \text{Measured } EI_{NO_x}\left(\sqrt{\frac{P_{T_{corr}}}{P_{T_{meas}}}}\right) \exp\ 0.0188\ (H_{meas} - H_{corr}) \qquad \text{(Eq. 6)}$$

where: H = Inlet specific humidity

The specific humidity reference is 6.34 gm/kg.

ORIGINAL PAGE IS OF POOR QUALITY

Combustion Efficiency

Combustion efficiency is calculated from gaseous emissions data on a deficit basis using the average carbon monoxide and total unburned hydrocarbon emissions. The calculation is based on an assumption that the total concentration of unburned hydrocarbons can be assigned the heating value of methane (CH_4) and the equilibrium concentration of carbon monoxide is negligible. The equation is:

$$\eta_C = 1 - \left(\frac{10\ EI_{CO} + 50.2\ EI_{THC}}{1000\ HV} \right) \qquad \text{(Eq. 7)}$$

where: HV = heating value of the fuel (kJ/kg)

EPA Weighted Emissions Parameter

The average emissions at the idle, approach, climb and takeoff conditions are used to compute the EPA parameter for a landing and takeoff cycle in the form:

$$EPAP = \frac{\sum_j EI_j\ W_{fj}\ t_j}{Fn} \qquad \text{(Eq. 8)}$$

where:
- EI = Emission Index (gm/kg of fuel)
- Wf = Fuel flow (kg/hr)
- t = Time in mode (hrs)
- j = Mode, i.e., idle, approach, climb and takeoff
- F_n = Rated engine thrust (kilonewtons)

This equation reduces to the form:

$$EPAP = \sum_j A_j\ EI_j \qquad \text{(Eq. 9)}$$

where Aj is a coefficient unique to the particular engine cycle. Table 15 lists the values of the coefficients for the JT9D-7F and Energy Efficient Engine cycles.

Table 15

Value of EPAP Coefficients

Mode	Time In Mode (minutes)	Coefficient A for JT9D-7F Cycle	Coefficient A for Energy Efficient Engine Cycle
Idle	26.0	1.63	1.10
Approach	4.0	0.72	0.57
Climb	2.2	1.12	0.97
Takeoff	0.7	0.44	0.38

6.4 HIGH PRESSURE TEST PROCEDURES

The single stage and variable geometry combustors were evaluated over test matrices structured around the combustor operating conditions in the JT9D-7F engine as listed on Table 3. The rig operating conditions were identical to those of that table except that the combustor airflow was 20 percent of that listed to correspond to the 72 degree sector width of the rig. Because of the program objective of evolving the combustor concepts toward operation on broadened properties fuels the majority of the test points involve operation with ERBS fuel. The basic matrix includes operation with ERBS fuel at the combustor design condition at each of the four power levels in the Environmental Protection Agency landing and takeoff cycle and at the cruise aerodynamic design point of the engine. Comparative data were also obtained with Jet A fuel and parametric variations conducted at the idle and takeoff conditions. A second and more extensive test matrix was used for evaluation of the performance of selected single stage and variable geometry combustor configurations. This test matrix parallels the structure of the basic matrix with the principal feature being the inclusion of test points with additional low hydrogen content fuels. The matrix involved operation of the combustors on both Jet A and ERBS at the five major operating conditions, i.e., the four conditions in the EPA landing and takeoff cycle and the cruise condition. Operating with the two lower hydrogen content test fuels was limited to the idle, cruise and takeoff operating conditions. The matrix also included parametric variations which were conducted with both ERBS fuel and the 11.8 percent hydrogen blended test fuel.

The high pressure tests on the advanced Vorbix combustor were conducted at combustor inlet and operating conditions representative of the Energy Efficient Engine cycle as listed in Section 4.3. However, because experience with operation of the test rig with the segmented Finwall® combustor liner was limited, the total pressure at the climb and takeoff operating conditions was reduced to 92 and 86 percent respectively of the design engine pressure level at these conditions. Table 16 presents a summary of the operating parameters of the Energy Efficient Engine combustor rig as it was run under the present program.

In conducting the high pressure tests, efforts were made to conserve the ERBS and other special test fuels. Since it required considerable running time to complete a major change of combustor inlet conditions and achieve thermal stabilization in the high pressure test facility, the combustors were operated on Jet A fuel during these transitions as well as during the initial startup. The remote test fuel selection system was used to switch operation to ERBS or one of the lower hydrogen content fuels only after inlet condition stabilization had been achieved at the desired test conditions.

The data of Section 5.1 indicate that the heating value of the test fuels decreases with decreasing hydrogen content. In operating an engine on lower hydrogen content fuels the fuel/air ratio of the combustor would have to be increased to maintain the net energy release constant at each power setting. However, the difference in the heating value of Jet A and ERBS was less than one percent and increments in the fuel/air ratio of this magnitude would be less than the accuracy to which rig operating conditions could be maintained.

ORIGINAL PAGE IS
OF POOR QUALITY

Table 16

Operating Conditions of the Energy Efficient Engine
Sector Combustor Rig

Engine Operating Condition	Inlet Total Pressure MPa (psia)	Inlet Total Temperature °K (°F)	Combustor Sector Airflow kg/sec (lb/sec)	Combustor Fuel/Air Ratio
Ground Idle (6% Thrust)	0.434 (63)	472 (391)	2.76 (6.06)	0.0098
Approach (30% Thrust)	1.159 (168)	620 (659)	5.89 (12.94)	0.0150
Climbout (85% Thrust)	2.647 (384)*	775 (934)	12.01 (26.42)**	0.0217
Sea Level Takeoff (100% Thrust)	2.760 (400)*	805 (991)	12.31 (27.06)**	0.238
Max. Cruise (10,688 m/35,000 ft, M = 0.8)	1.400 (203)	754 (899)	6.44 (14.13)	0.0231

* Reduced from design level
**Reduced from equivalent engine level to maintain diffuser inlet Mach number at reduced inlet pressure.

High power operation of both the JT9D and the Energy Efficient Engine combustor rigs was potentially limited by the temperature capability of the combustor exit instrumentation. In the case of the Energy Efficient Engine combustor rig with its fixed exit vane pack, the fuel/air ratio at takeoff was restricted to 0.022, as opposed to the design value of 0.0238, by this limitation. The traversing combustor exit rake used on the JT9D combustor rig could be rotated to a stowed position outside of the combustor exit annulus as shown in Figure 52. This permitted more flexible operation in situations where local gas temperatures were excessive in that after exit temperature and emissions traverses were conducted at the highest allowable fuel/air ratio, the rake could be moved out of the gaspath while the fuel/air ratio was increased to the design level to acquire data on liner temperatures or heat flux at that condition.

6.5 ALTITUDE IGNITION TEST PROCEDURES

Ignition and stability evaluations were conducted on the final configuration of each of the three combustor concepts. The single stage and variable geometry combustor concepts were evaluated at conditions representative of those encountered in the JT9D-7F engine while the advanced Vorbix combustor was tested at simulated operation of the Energy Efficient Engine. Table 17 provides a list of the combustor operating conditions at each point in the altitude relight/cold start test sequences. These are referenced to the flight and relight envelopes of Figure 53 which shows three superimposed lines of constant airflow that are constructed from the windmilling characteristics of the compressor in the appropriate engine. These lines are spaced across the entire flight envelope rather than just the airstart envelope to provide substantiation of the ignition characteristics over a wider range of combustor inlet conditions including the lower flight Mach numbers at which the combustor inlet temperature is lower.

Table 17

Altitude Ignition/Stability Test Conditions

Airflow Line on Figure 6-2	Sector Rig Airflow kg/hr (lb/hr)	Inlet Total Temperature °K (°F)	Inlet Total Pressure	Wfuel kg/hr (lb/hr)
JT9D-7F Engine				
1	1920 (4233)	242 (-23)	Varied	57.8 (127)
2	2944 (6483)	258 (5)	Varied	57.8 (127)
3	4180 (9200)	272 (30)	Varied	57.8 (127)
Energy Efficient Engine				
1	364 (800)	243 (-22)	Varied	59 (130)
2	726 (1600)	250 (-10)	Varied	59 (130)
3	1456 (3200)	288 (60)	Varied	59 (130)

In evaluating the altitude ignition capability, the airflow to the combustor rig was established on one of these lines and ignition attempts made at progressively lower combustor inlet pressures, corresponding to higher altitudes, until the limit of ignition was reached. These tests were conducted at a fixed inlet temperature corresponding to the upper boundary of the relight envelope. The ignition attempts were made at a fuel flow rate corresponding to the minimum scheduled fuel flow of the appropriate engine.

The minimum pressure blowout condition was also established on each airflow line. In these tests, the combustor was fired at a low simulated altitude, i.e., at high pressure, and after combustion was stabilized the pressure was progressively decreased at constant inlet temperature, fuel flow and airflow until blowout was encountered.

ORIGINAL PAGE IS
OF POOR QUALITY

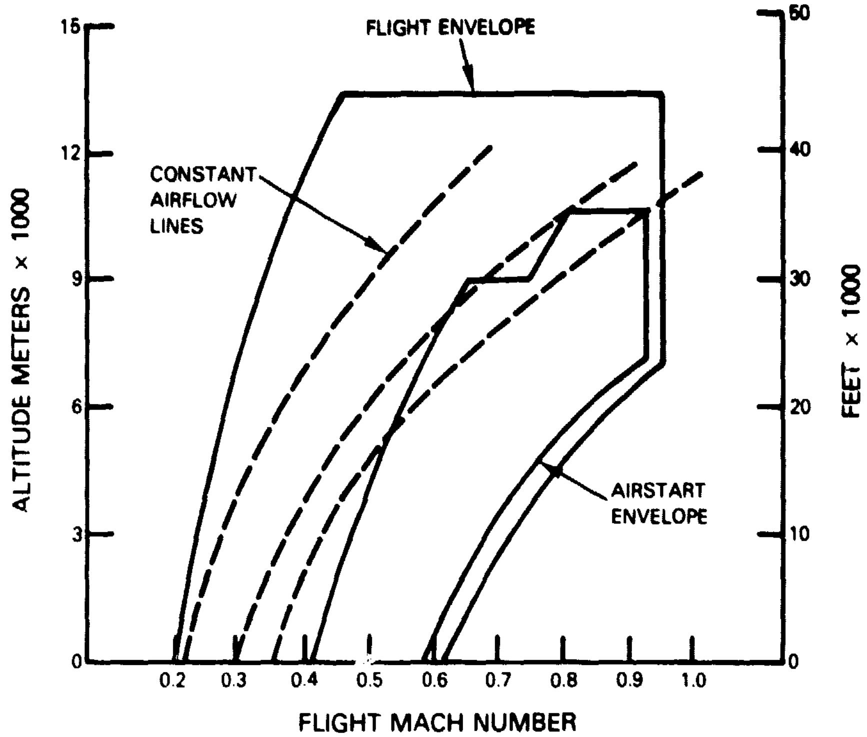

Figure 53 Altitude Relight Test Conditions Superimposed on the JT9D-7 Flight Envelope

Cold ignition tests were also conducted by operating with both the inlet air and the fuel cooled to simulate 245 to 250°K (0 to -10°F) ambient temperatures. The rig airflow duplicated the compressor discharge Mach number at sea level cranking conditions. The time to achieve ignition was recorded over a range of starting fuel flow rates.

The altitude relight, minimum pressure blowout and cold start tests were conducted with Jet A, ERBS and the 11.8 percent hydrogen test fuels.

SECTION 7.0

EXPERIMENTAL RESULTS

During the experimental investigation, a total of sixteen combustor configurations were evaluated in the high pressure test facility, requiring more than 200 hours of facility operation. In addition, ignition and stability characteristics of one configuration of each combustor concept were evaluated in the altitude test facility. Data from these tests is tabulated in Appendix C and results are discussed in this section. Section 7.1 presents results of the evaluation of three single stage combustor configurations which are similar to production combustors used in various models of the JT9D engine. These results are significant because they establish the sensitivity of these combustors to fuel composition. Section 7.2 evaluates the test results for the remaining configurations of the single stage combustor concept. These configurations involved perturbations to primary zone stoichiometry, fuel injectors and more effective liner cooling; they were tested primarily with ERBS fuel. Results of the evaluation of the advanced Vorbix staged combustor concept are presented in Section 7.3 while configurations representing different modes of operation of variable geometry combustor concepts are discussed in Section 7.4. The sensitivity of the ignition and stability characteristics of selected combustor configurations is discussed in Section 7.5.

7.1 FUEL SENSITIVITY OF BASELINE COMBUSTORS

Three combustor configurations, SS-1, SS-2 and VG-1, were selected as baseline configurations. Configuration SS-1 is the current production combustor for the JT9D-7F engine and hence is representative of an in-service combustor. Configuration SS-2 duplicates the advanced bulkhead type combustor which had been developed for the JT9D-7F engine. It is conceptually identical to the combustor used in more advanced JT9D engine models such as the JT9D-7R4. Configuration VG-1 had been designated as the initial configuration of the variable geometry concept. However, it is identical to Configuration SS-2 except for operation of the duplex fuel injector in the single pipe mode through the aerated secondary fuel system. Consequently, the effect of single pipe versus duplex fuel injection could be isolated by comparing these two configurations. Further, since Configuration VG-1 was evaluated with all four test fuels at the most critical operating conditions (whereas Configuration SS-2 was restricted to operation on Jet A and ERBS fuel) its inclusion as one of the baseline configurations extends the evaluation of the basic bulkhead combustor over the entire range of fuel composition. The fuel sensitivity of these three configurations is discussed in the remainder of this section.

7.1.1 Liner Heat Load

Fuels with lower hydrogen content have been found to form higher concentrations of carbonaceous particulates in the initial combustion zone. These particles become luminous when heated to near stoichiometric temperatures by the combustion gases and radiant heat transfer to the liner becomes a significant part of the net heat load. In the test program, radiant

ORIGINAL PAGE IS
OF POOR QUALITY

heat flux to the combustor liner was measured at a single position on the inner liner immediately downstream of the fuel injector in each baseline combustor configuration. Figure 54 shows the relation between radiant heat flux and the hydrogen content of the fuels. The magnitude of the measured heat fluxes is qualitatively consistent with accepted empirical models of the combined gas/luminous particle radiation process (Reference 13). The data show a general trend of increasing heat flux with decreasing hydrogen content. The use of ERBS fuel (12.93 percent hydrogen) rather than Jet A (13.62 percent hydrogen) leads to increases in heat flux of up to thirty percent depending on the combustor configuration and operating mode.

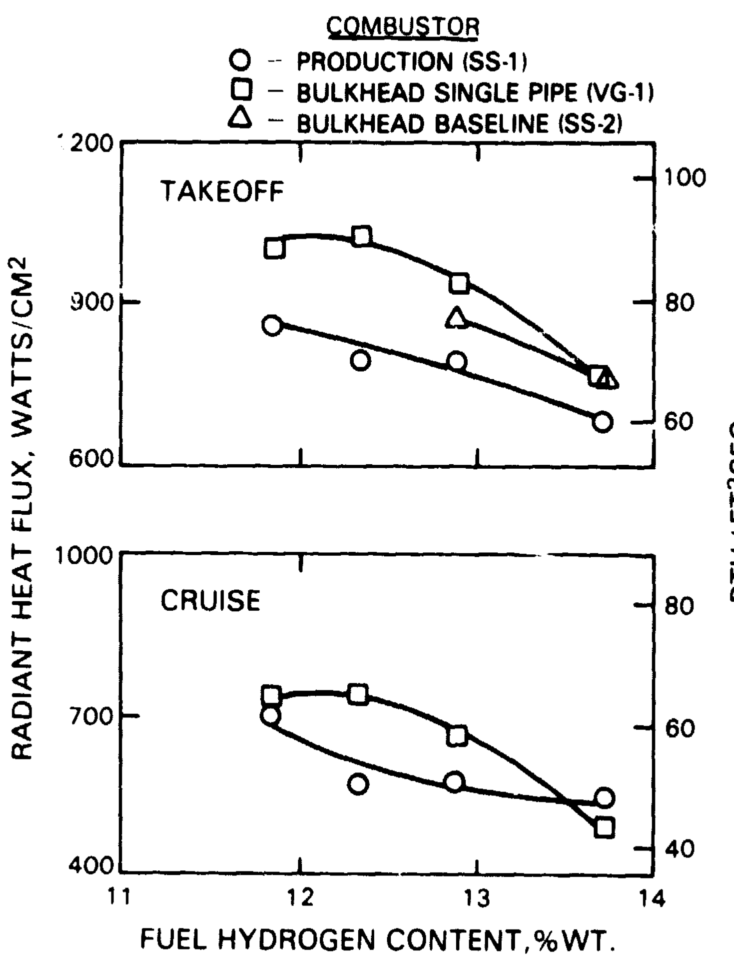

Figure 54 Radiant Heat Flux to Liner in Primary Zone of the Three Baseline Single Stage Combustors

The level of heat flux in the current production combustor (Configuration SS-1) is generally lower than in the bulkhead combustor. These measurements may have been influenced by the position of the radiometer or caused by locally leaner mixtures in the production combustor. In the bulkhead combustors, the entire primary combustion region downstream of the fuel injector face could be sensed by the radiometer, whereas in the production combustor the probe was located downstream of the "cone-annular" transition and did not sense radiation from the regions inside the flame stabilizing cones (see Figures 42 and 43). Alternatively, these differences may have been caused by locally leaner mixtures in the production combustor. There is minimal difference in the heat flux levels encountered in the bulkhead combustor configurations with the fuel injector operating in the normal duplex mode and in the single pipe injection mode. This is to be expected because, at takeoff, ninety percent of the total fuel flow passes through the aerated secondary system of the duplex fuel injector.

The data in Figure 54 show a general trend toward greater sensitivity of heat flux to fuel hydrogen content in the Jet A to ERBS range, i.e., hydrogen contents of 13.6 to 12.9, than in the low hydrogen content range. The single exception to this trend occurred in the production combustor at cruise. This leveling of radiant heat flux at low hydrogen content could be caused by a single factor or a combination of several factors, including (1) delayed heat release, (2) saturated particulate concentrations, or (3) fuel composition effects. A brief description of each factor follows.

1. Delayed Heat Release

   The lower hydrogen content fuel could be burning at a slower rate because of more complex chemistry. This could cause the point of highest heat release to move downstream in the combustor, diminishing heat flux at the radiometer location. However, this does not appear to be the case because a downstream shift was not detected by the thermocouples on the liners.

2. Saturated Particulate Concentrations

   Combustion of lower hydrogen content fuels leads to progressively higher production of particulates in the primary combustion zone. Leveling could be caused by saturation of the number density of luminous particles at which, according to current empirical models such as that of Reference 13, the "effective emissivity" of the combustion products exponentially approaches that of a blackbody radiator and there is no further increase in heat transfer.

3. Fuel Composition Effects

   As shown by the data of Table 8, the difference in hydrogen content between Jet A and ERBS fuel essentially results from an increase in the napthalene content, i.e., double ring aromatics, of about 10 percent by volume. Conversely, when the two lower hydrogen content fuels were blended the hydrogen content was reduced primarily by adding single ring aromatics to the basic ERBS fuel. Since multi-ring aromatics have a greater propensity for particulate formation than single ring components, the proportionately larger increase in heat flux produced by the Jet A to ERBS increment may have been due to these differences in fuel composition which are not evident when fuel is characterized on the basis of hydrogen content.

Further research beyond the scope of this program would be required to better isolate the cause of these differences in the response of radiant heat flux to fuel composition.

7.1.2 Liner Metal Temperatures

Use of lower hydrogen content fuels increases radiant heat flux which increases local metal temperatures in the combustor liner, reducing structural life. As indicated in Section 5.2.3, thermocouples were installed in the JT9D combustor liner sectors to measure these temperature increments. The thermocouple junctions were positioned near the weld between a film cooled panel and the riser of the following louver. Since the temperature gradient between this region and the cooler louver knuckle is critical to cyclic fatigue the measurements were relevant to liner life.

The incremental changes in metal temperature associated with different fuels are most evident at the cruise condition and trends are best delineated with data obtained at cruise. Figure 55 maps the measured temperature distribution in the liner of the current production JT9D-7F combustor at cruise. Local metal temperatures observed during operation on Jet A fuel and the incremental increases in metal temperature encountered with ERBS fuel and the 11.8 percent hydrogen content fuel are presented. The data demonstrate a progressive increase in local metal temperatures with decreasing hydrogen content. The incremental increases in liner temperature are also more pronounced in the primary zone than in the dilution zone. Evidently, the radiant heat transfer to the liner from luminous particles is more intense on those surfaces with a close proximity to, and hence a high view factor from, the primary reaction zone where particulate concentrations are the highest.

Within the primary zone, the increases in liner temperature appear to be global in nature. For example, use of ERBS fuel produced temperature rises in the narrow range of 11° to 16°K (20° to 29°F) at all primary zone thermocouple locations on the inner liner and 18° to 25°K (32° to 45°F) on the nominally hotter outer liner. This uniform temperature increase is consistent with a diffuse radiant source and shows no evidence of an axial shift in the position of the zone of highest radiant heat release.

Figure 56 shows the corresponding temperature distribution in the baseline advanced bulkhead combustor sector at cruise. It includes measured temperatures with Jet A fuel and the local incremental temperature increases encountered with ERBS fuel. While the nominal temperature levels in the liner are comparable to those in the current production combustor (see Figure 55), the temperature distribution also shows high temperature streaks downstream of the fuel injectors. The increases in temperature with ERBS fuel rather than Jet A are also larger than those encountered in the current production combustor.

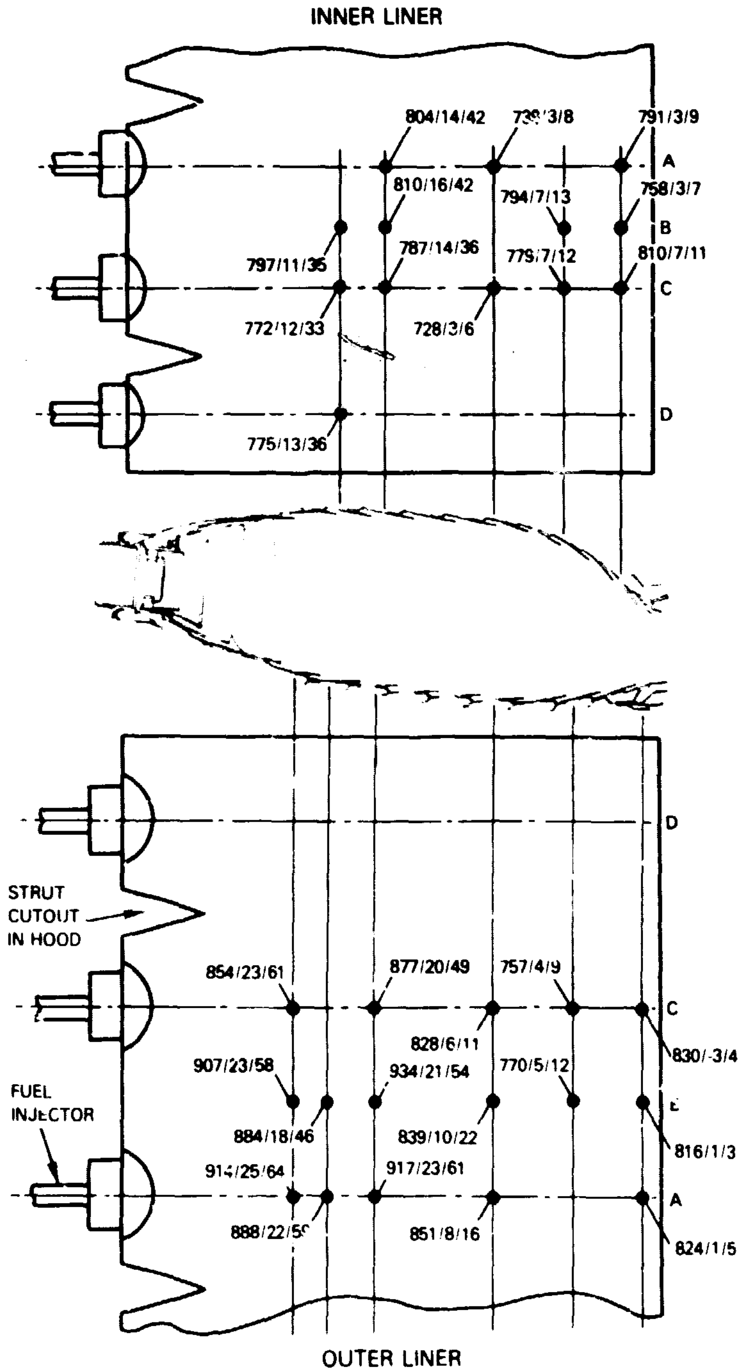

TEMPERATURES XXX/YY/ZZ IN °K
XXX = TEMPERATURE WITH JET A FUEL, YY = INCREMENTAL INCREASE JET A TO ERBS, ZZ = INCREMENTAL INCREASE JET A TO 11.8%H_2

Figure 55 Liner Temperature Distribution of Production JT9D Combustor (SS-1) at Cruise

ORIGINAL PAGE IS
OF POOR QUALITY

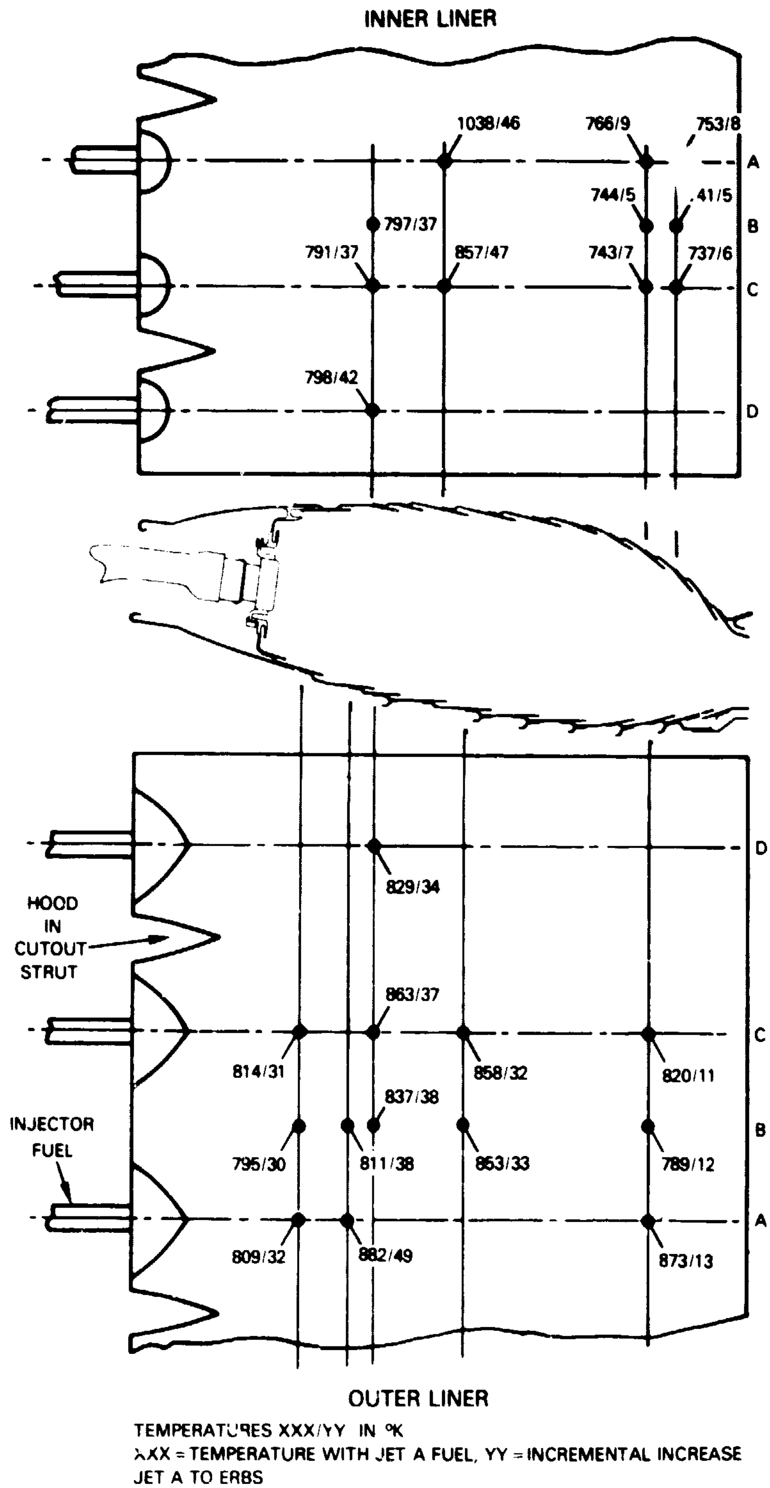

Figure 56 Liner Temperature Distribution in Advanced Bulkhead Combustor at Cruise

An empirical parameter for correlating fuel effects on liner temperature was developed in Reference 14; this parameter has found acceptance and substantiation in other investigations of the effect of fuel properties on liner temperature. Its use involves establishing the incremental change in maximum liner temperature at cruise relative to that observed with a reference JP-4 fuel with a nominal hydrogen content of 14.5 percent. Since this level was beyond the range of hydrogen content in the test fuels used in the program, the relationship between maximum liner temperature and hydrogen content was extrapolated to establish the liner temperature with JP-4 fuel. In Figure 57 the correlation parameter is used to show the variation of liner temperature at cruise in the three baseline single-stage combustor configurations. There is little variation among the three configurations; the only pronounced departure from a single characteristic is the bulkhead combustor with the single pipe fuel injector operating on ERBS fuel. The data also fit well within the band established by prior tests of other single stage engine combustors reported in Reference 14. This correlation implies that the incremental increase in liner temperature associated with a change in fuel composition will be larger in a combustor which has higher initial liner temperature levels.

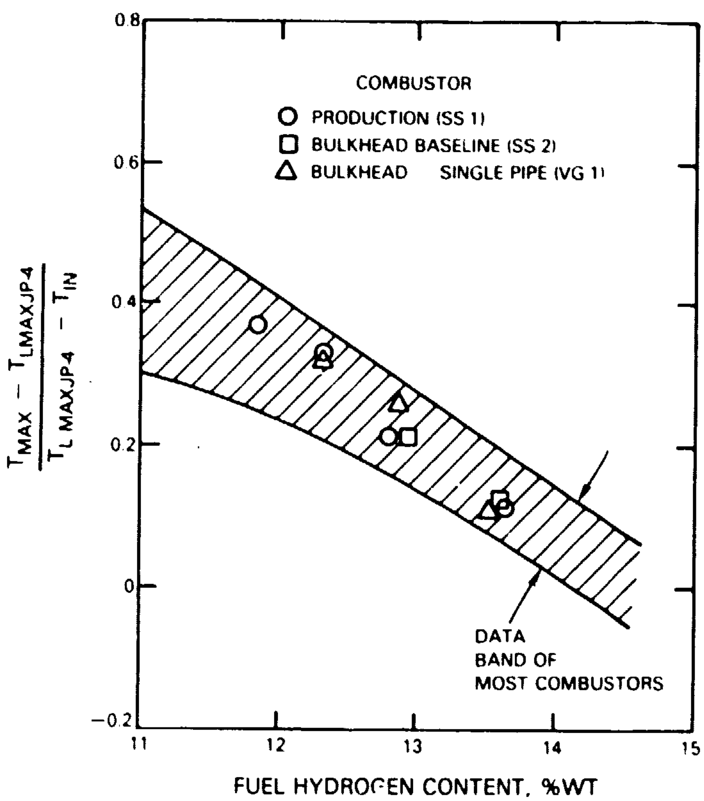

Figure 57 Correlation of Maximum Cruise Liner Temperature in the Reference Single Stage Combustor Configurations

While liner temperature is most sensitive to fuel composition at intermediate operating conditions such as cruise, the life limiting failure mode of current combustor liners is fatigue arising from cyclic exposure to elevated temperatures. The highest liner temperatures are encountered at takeoff. Thus an assessment of the impact of different fuels on combustor liner life must be based on changes in metal temperature at this condition. These temperature increments are generally not as pronounced as those encountered at cruise because the pressure level in the combustor, and hence the total (radiant and convective) heat flux to the liner, is substantially higher. Consequently the incremental change in radiant heat flux associated with a different fuel is a smaller fraction of the total heat load.

Figure 58 shows the temperature distribution and temperature increments in the liner of the advanced bulkhead combustor of the JT9D-7F engine at takeoff. The temperature distribution with Jet A fuel parallels that observed at cruise (Figure 56). The nominal level is 50 to 75°K (90 to 135°F) higher; the highest temperatures occur in the streak downstream of the fuel injector at circumferential position A. The incremental changes in liner temperature associated with ERBS fuel or the 11.8 percent hydrogen test fuel relative to Jet A are significantly smaller than those observed at cruise. In fact, no detectable increases were observed at many thermocouples on the inner liner enclosing the dilution zone of the combustor.

Despite the reduction in the magnitude of liner temperature increments in the primary zone at takeoff relative to those at cruise, they retain their global nature in that the magnitudes are in a narrow band. The single exception is a thermocouple in the streak region on the fourth louver of the inner liner. The thermocouple indicated a metal temperature of 1169°K (1641°F) during operation with Jet A fuel; this thermocouple was apparently at the hottest location in the liner. With ERBS fuel, liner temperature increased 40°K (72°F) at this location. This increase is more than three times the temperature increase encountered at the other measurement locations in the primary zone. However, it must be considered a unique local phenomenon associated with the high temperature streak.

Figure 59 shows the temperature distribution in the liner of the current production JT9D combustor sector (Configuration SS-1) at takeoff with Jet A fuel. As with the bulkhead combustor, the local metal temperatures are 50° to 75°K (90° to 135°F) higher than the temperatures encountered at cruise (Figure 55). However, the increments associated with the lower hydrogen content test fuels are very small and in many instances negative. On the basis of this data, it appears that the nominal magnitude of the temperature increments must be approaching zero and that the residual positive and negative increments are indicative of the uncertainty arising from defining the increments as the difference of two experimental measurements. In regard to the accuracy of the measurements, all liner temperature data reported herein have been adjusted to compensate for any deviations in combustor inlet total temperature relative to the nominal inlet temperature of Table 3 or Table 17. No adjustments were made to account for differences in the combustor fuel/air ratio between test points, but efforts were made to minimize these variances.

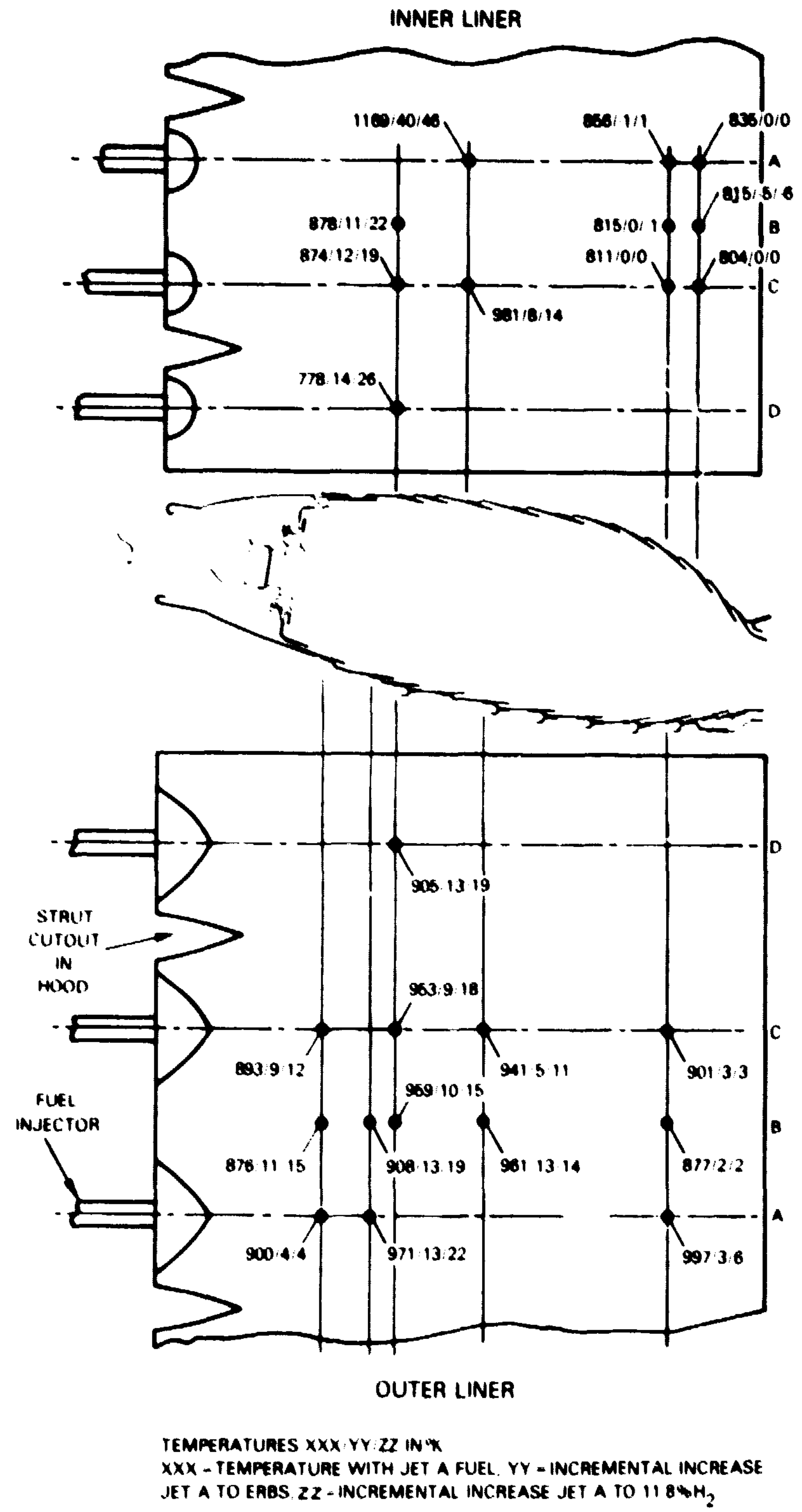

Figure 58 Liner Temperature Distribution in Advanced JT9D Bulkhead Combustor at Takeoff

ORIGINAL PAGE IS
OF POOR QUALITY

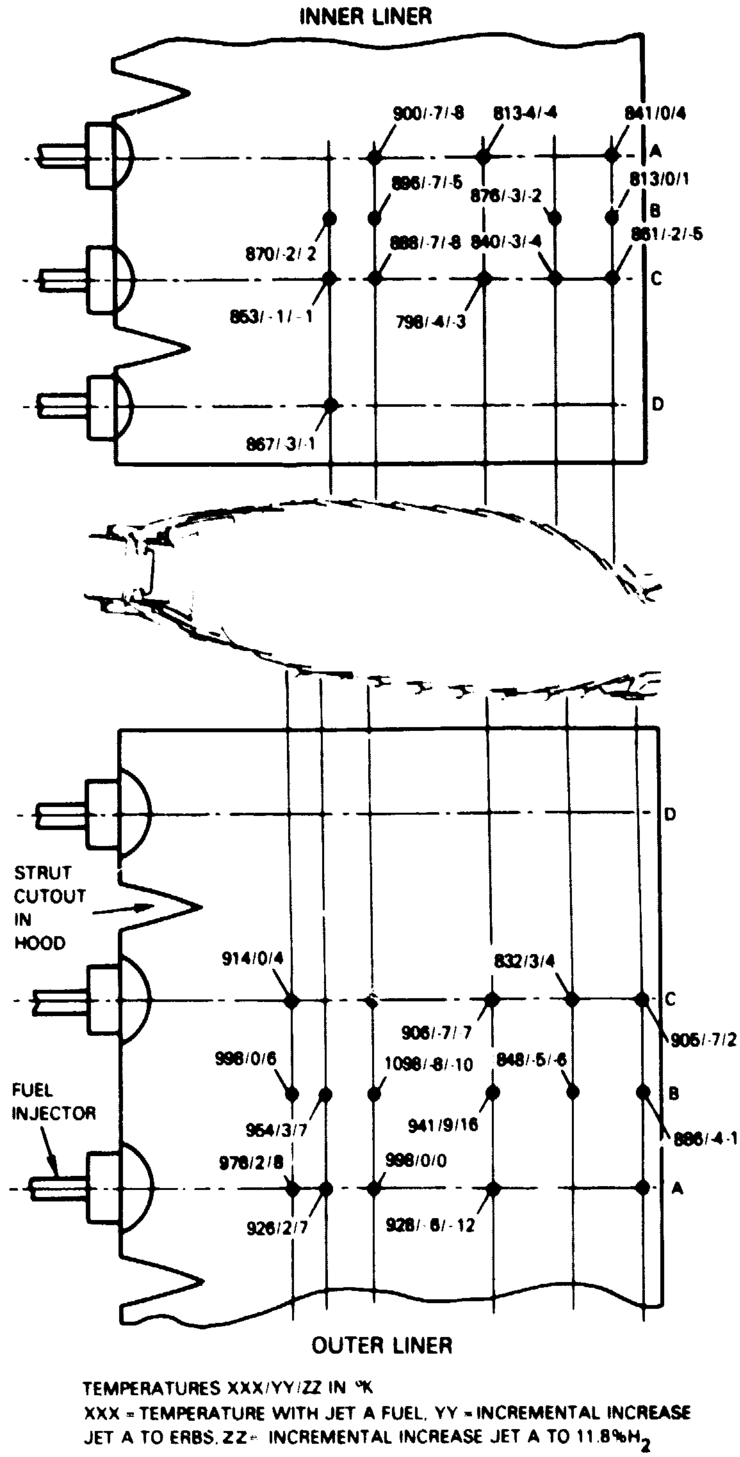

Figure 59 Liner Temperature Distribution in Production JT9D Combustor (Configuration SS-1) at Takeoff

The minimal increases in liner temperature are inconsistent with the data of the preceding section in which radiant heat flux to the combustor liner at takeoff was shown to increase continuously with progressively lower hydrogen content fuels. It is possible that the absence of liner temperature increases resulted from compensating changes in convective heat transfer produced by introducing the lower hydrogen content fuels. An alternative explanation is that the convective heat load in this particular combustor is high and that the incremental increase in radiant heat load produced by these fuels did not produce a sufficient increase in total heat load to elevate liner temperature significantly.

Figure 60 provides an overview of the impact of fuel composition on liner temperature in the three reference combustor configurations. The metal temperatures cited are averages of all thermocouples in the primary zone and dilution zone of the combustor. Positioning these thermocouples near the weld region of the louver makes the measurements a representative indicator of temperatures in the life limiting region and not an average metal temperature for the entire liner surface. It is evident from the figure that liner temperature in the dilution zone is generally insensitive to variations in fuel hydrogen content. The effect of hydrogen content is also more pronounced at cruise than at takeoff. The insensitivity of liner temperature in the current production combustor, cited above, is also illustrated.

There is also some difference in the nominal temperature level in the liner of the advanced bulkhead combustor when it is operated at cruise with the duplex pressure atomizing primary/aerating secondary fuel injector in the normal duplex mode (Configuration SS-2) and in the single pipe aerated mode (Configuration VG-1). These differences result from changes in the overall mean temperature level rather than variations in the intensity of hot streaks on the liner. Data from the spray evaluation of the fuel injectors used in these configurations (presented in Appendix B) indicate that the single pipe mode produced a wider spray angle at higher power levels than the normal duplex mode. This increase in spray angle could have localized combustion closer to the liner surfaces and caused the increases in nominal temperature level. Despite this difference in overall temperature level with fuel injection mode, the increments in liner temperature associated with the use of ERBS fuel rather than Jet A are comparable.

Stress analysis of louver sheet metal liners, in combination with empirical data on the fatigue strength of Hastelloy X liner material provides correlation between the temperature gradient across the louver knuckle at takeoff and the cyclic fatigue life of this region. Measured temperature increases in the weld region of louvers in the primary zone of the advanced bulkhead combustor at takeoff have been used to calculate the reduction in liner life for several situations. These data are summarized in Table 18.

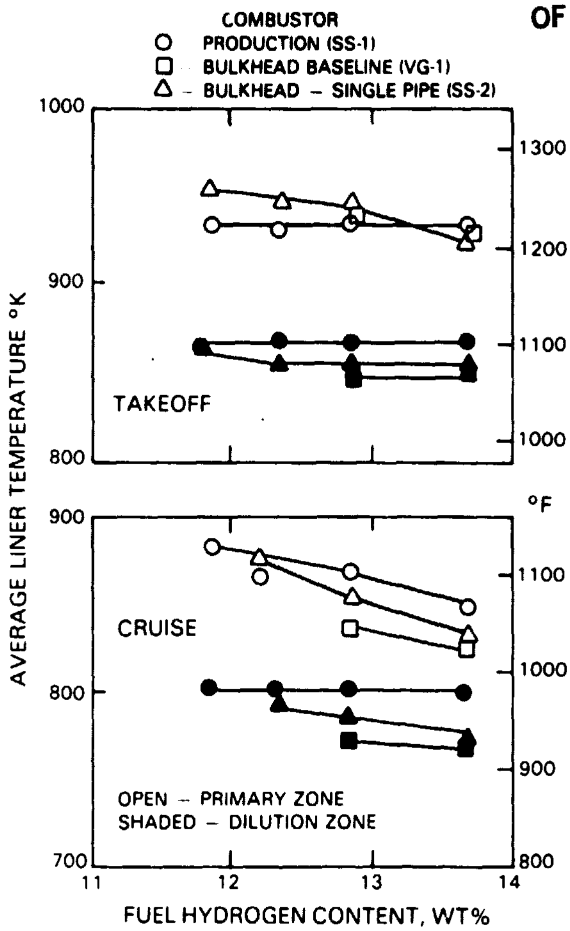

Figure 60 Effects of Fuel Composition on Average Liner Temperatures in the Three Reference Combustors

Table 18

Projected Effect of Use of ERBS Fuel vs Jet A on Life of Advanced Bulkhead Combustor Liner

Configuration	SS-2	VG-1
Fuel Injection Mode	Duplex	Single Pipe
Based on Average Liner Temperature Increase		
Temperature Increase °K (°F)	7 (12)	12.3 (22)
Reduction in Life - %	6	11
Based on Maximum Liner Temperature Increase		
Temperature Increase °K (°F)	15 (27)	40 (72)
Reduction in Life - %	13.5	36

These projections indicate that liner life is less sensitive to fuel composition when the fuel injector is operated in the normal duplex mode (Configuration SS-2). As the data in Appendix B demonstrate, this lack of sensitivity should not be attributed to a significant difference in the sensitivity of the spray geometry or atomization characteristics of the injector to fuel composition. Projected liner life increments differ by factors of 2 or 3 when based on the measured average temperature increase in the critical weld region as opposed to the single maximum observed temperature increase. For a direct back to back comparison of the use of the two fuels in existing hardware the larger life increments associated with the maximum temperature increases must be incorporated. However, the life increments based on average temperature increases indicate that there is a significant incentive to reduce the sensitivity of liner life to fuel composition by reducing the magnitude of the increments at these isolated locations. In both combustor configurations these maximum liner temperature increases occur at the point of highest nominal liner temperature in the streak region behind a fuel injector. It will be shown in Section 7.2 that use of a modified fuel injector reduced not only the nominal temperature level in the streak region but also the Jet A to ERBS temperature increment at that location.

7.1.3 Emissions

Figures 61 and 62 show the measured carbon monoxide and unburned hydrocarbon emissions from the current production combustor (Configuration SS-1) and the advanced bulkhead combustor (Configuration VG-1) at the idle combustor inlet conditions. In the bulkhead combustor, the fuel injector operated in the aerated single pipe mode. Data are presented for a range of fuel/air ratios centered about the design proportions. The data indicate a general trend toward decreasing emissions output with increasing fuel/air ratio. The data also indicate that the emissions output levels off at fuel/air ratios near 0.015. As indicated in Section 4.1, the bulk primary zone equivalence ratios in both combustors were about 0.5 at the design idle fuel/air ratio. Hence, a fuel/air ratio of 0.015 would produce mixture strengths approaching stoichiometric and carbon monoxide and unburned hydrocarbon emissions would be expected to be minimal. Data obtained with the ERBS fuel and 11.8 percent hydrogen test fuel over a wide range of fuel/air ratios show substantially similar characteristics. In general, emissions output is most divergent at lean fuel/air ratios where emissions rise abruptly, indicating declining combustion efficiency as lean blowout is approached. With the exception of carbon monoxide emissions from the current production JT9D combustor (Figure 61), the differences in emissions with ERBS and 11.8 percent hydrogen fuels diminish as fuel/air ratio is increased; there are virtually no differences at fuel/air ratios of about 0.015. These findings suggest that combustors with rich primary zone mixture strengths, i.e., approaching stoichiometric at idle, may not only produce the lowest nominal carbon monoxide and unburned hydrocarbon emissions at this condition but that these emissions characteristics may also be least sensitive to fuel composition.

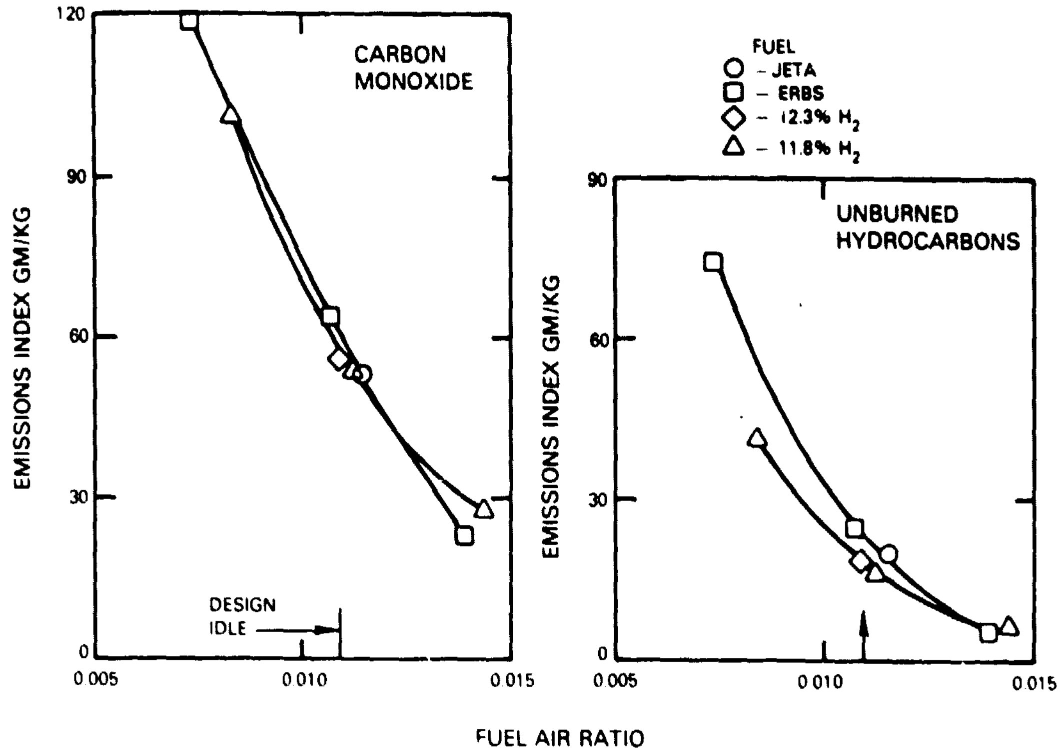

Figure 61 Idle Emissions Characteristics of Current JT9D Production Combustor (Configuration SS-1)

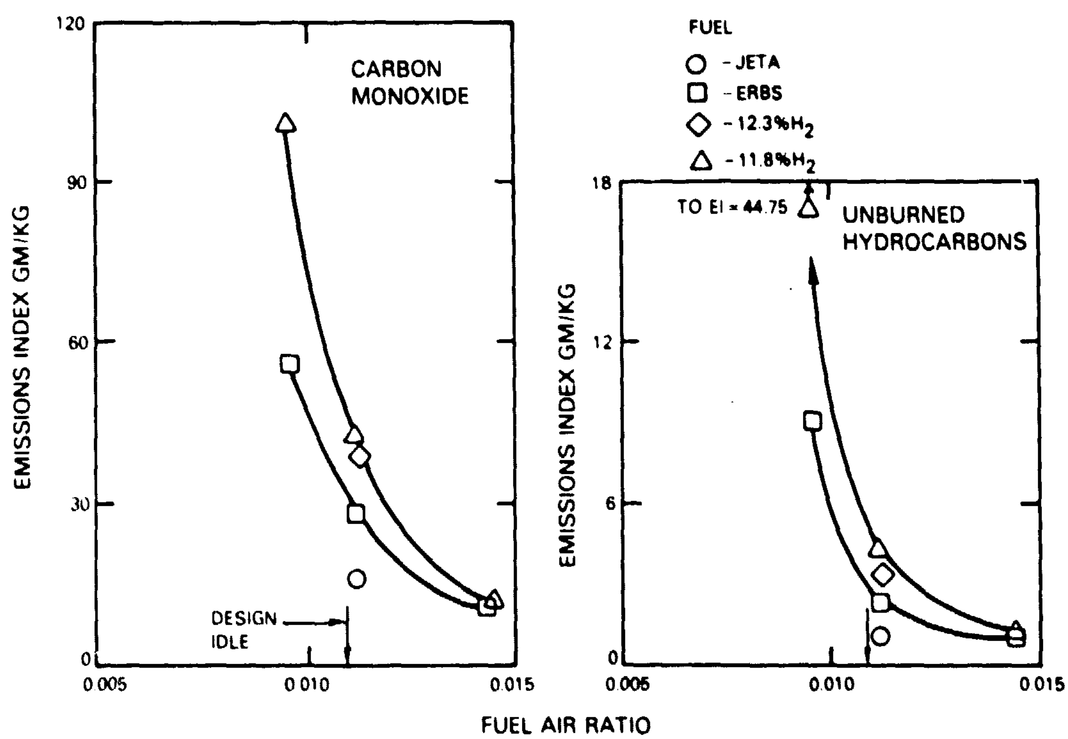

Figure 62 Idle Emissions Characteristics of JT9D Bulkhead Combustor with Single Pipe Fuel Injector (Configuration VG-1)

ORIGINAL PAGE IS
OF POOR QUALITY

The effects of fuel composition on the emissions from these combustors at the design idle fuel/air ratio are demonstrated in Figures 63 and 64, which were constructed from a crossplot of the data of Figures 61 and 62. Also shown in these figures are the emissions characteristics of Configuration SS-2, the baseline advanced bulkhead combustor operating in the normal duplex fuel injection mode. At the design idle fuel flow rate, about half of the fuel passed through the pressure atomizing primary system and the remainder through the aerated secondary system. Goals for these constituents are shown in the figures. To comply with the proposed 1981 Environmental Protection Agency standards (Table 2), these goals must be met at idle and typically low levels must be achieved at higher power conditions.

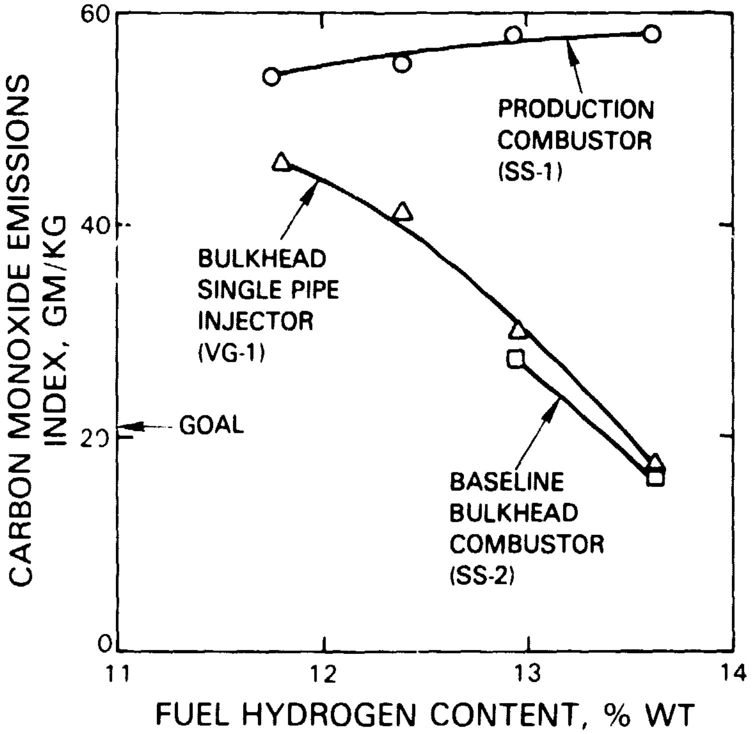

Figure 63 Carbon Monoxide Emissions Characteristics of the Baseline Single Stage Combustors at Idle

The nominal level of carbon monoxide emissions from the current production combustor is high but sensitivity to fuel composition is minimal. The bulkhead type combustor exhibits a much stronger sensitivity to fuel composition; carbon monoxide emissions increase with reduction in hydrogen content. When operating on Jet A fuel (13.62 percent hydrogen), carbon monoxide emissions are below the goal level. However, the emissions characteristics are sensitive enough to cause carbon monoxide output to increase significantly above the goal with ERBS fuel (12.93 percent hydrogen). The data also indicate that carbon monoxide emissions from the advanced bulkhead combustor are independent of fuel injection mode; the single pipe and the baseline duplex modes produce essentially the same emissions levels with Jet A and ERBS fuels.

ORIGINAL PAGE IS OF POOR QUALITY

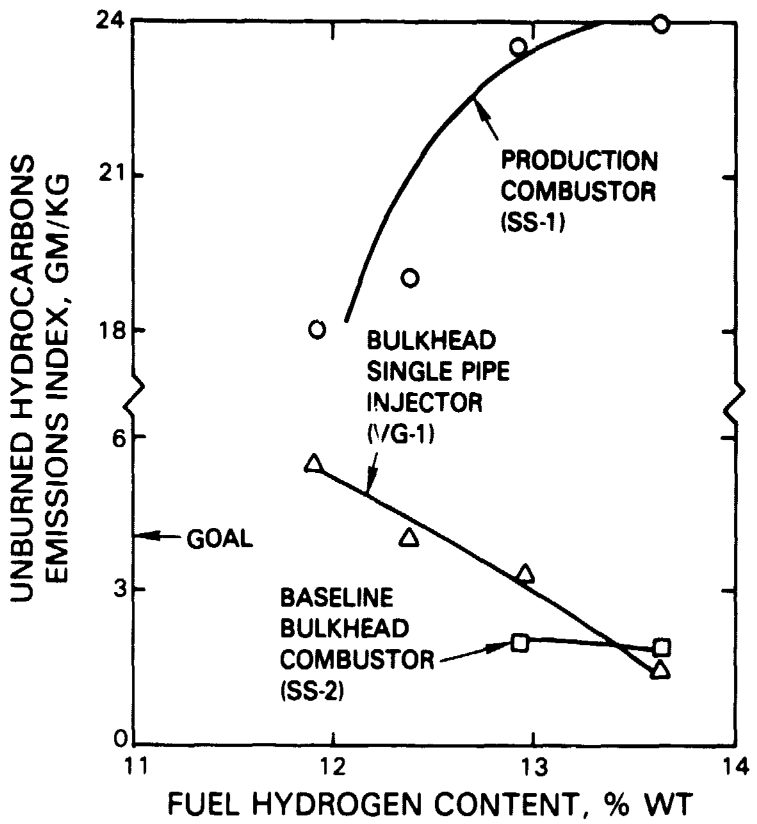

Figure 64 Unburned Hydrocarbon Emissions Characteristics of the Baseline JT9D Single Stage Combustors at Idle

The unburned hydrocarbon emissions characteristics of the three single stage combustors shown in Figure 64 are qualitatively similar to those for carbon monoxide. The overall level of emissions from the current production combustor is substantially above the goal, but the two lower hydrogen content test fuels produce reductions of the order of 25 percent relative to Jet A and ERBS. This improvement in performance was probably caused by the unusual viscosity and volatility characteristics of the two fuels. As indicated in Section 5.1.1, these fuels had lower viscosity and greater volatility than would have been expected for their hydrogen contents relative to the trends deduced from the properties of the Jet A and ERBS fuel. These characteristics could have enhanced atomization and vaporization, producing the observed reduction in unburned hydrocarbon emissions. Conversely, both the unburned hydrocarbon and carbon monoxide emissions characteristics of the bulkhead type combustor reflect an apparent sensitivity to fuel composition, i.e., its hydrogen content or hydrocarbon structure, and not the physical properties relevant to vaporization (see Configuration VG-1 on Figures 63 and 64). This may result from the construction of the bulkhead combustor. Cooling air remains more remote from the initial reaction zones, minimizing quenching reactions and making the combustion process less sensitive to the rate of evaporation.

ORIGINAL PAGE IS OF POOR QUALITY

The data of Figure 64 indicate that the goal for unburned hydrocarbon emissions can be achieved with substantial margin by the advanced bulkhead combustor operating on Jet A fuel (13.62 percent hydrogen content). Unburned hydrocarbon emissions vary somewhat with fuel injection mode. The duplex mode, with half of the fuel passing through a pressure atomizing system at high pressure drop, is less sensitive than the single pipe mode. However, regardless of the injection mode the goal for unburned hydrocarbon emissions can be met with ERBS fuel.

Similar measurements of the carbon monoxide and unburned hydrocarbon emissions characteristics of the baseline single stage combustor were obtained at approach (30% takeoff thrust) and higher power levels. These measurements were consistent with development experience in that the emissions were low and the combustion efficiency exceeded 99.9 percent with all combinations of test fuel and power level (above approach) investigated.

While the proposed EPA emissions standards (Reference 12) do not stipulate maximum levels for emissions of oxides of nitrogen from single stage combustors, the sensitivity of these emissions was investigated during the evaluation of the three baseline combustors. Figure 65 shows the variation in NO_x emissions from these combustors at simulated takeoff conditions for the JT9D engine. Data were acquired at takeoff combustor inlet conditions but at a fuel/air ratio of 0.0193 rather than the design fuel/air ratio of 0.0248 due to temperature limitations on the combustor exit rake. Despite similar primary zone stoichiometry, the NO_x output of the bulkhead combustor configurations is significantly higher than the output of the current production combustor.

Data from all three combustors indicate a progressive increase in NO_x emissions with decreasing hydrogen content. This has generally been attributed to the increase in adiabatic flame temperature caused by the reduced hydrogen content of the fuel. In Reference 4 an interpretation was advanced in which kinetic analysis of the NO_x formation in a combustor led to the following relation between NO_x emissions and flame temperature:

$$\frac{EINO_x}{EINO_{x\ ref}} = \left(\frac{Tf}{Tf_{ref}}\right)^{-0.53} \exp\left(\frac{67{,}400}{Tf_{ref}} - \frac{67{,}400}{Tf}\right) \qquad \text{(Eq. 10)}$$

In the single stage combustors, with their swirl stabilized combustion zone, diffusion is the dominant mode of combustion and the majority of reactions occur at or near stoichiometric proportions. The theoretical variation of NO_x emissions with hydrogen content was determined from Equation 10 using computed flame temperatures at an equivalence ratio of unity and combustion of Jet A fuel as the reference condition. The solid lines on Figure 65 show the theoretical variation for each combustor. Measurements from the current production combustor follow the theoretical variation closely while the measurements from the bulkhead combustor indicate that this combustor is less sensitive than predicted in both fuel injection modes. Nonetheless, this theoretical approach appears to be qualitatively substantiated and can be of use in establishing a limit on the potential increase in NO_x emissions.

ORIGINAL PAGE IS
OF POOR QUALITY

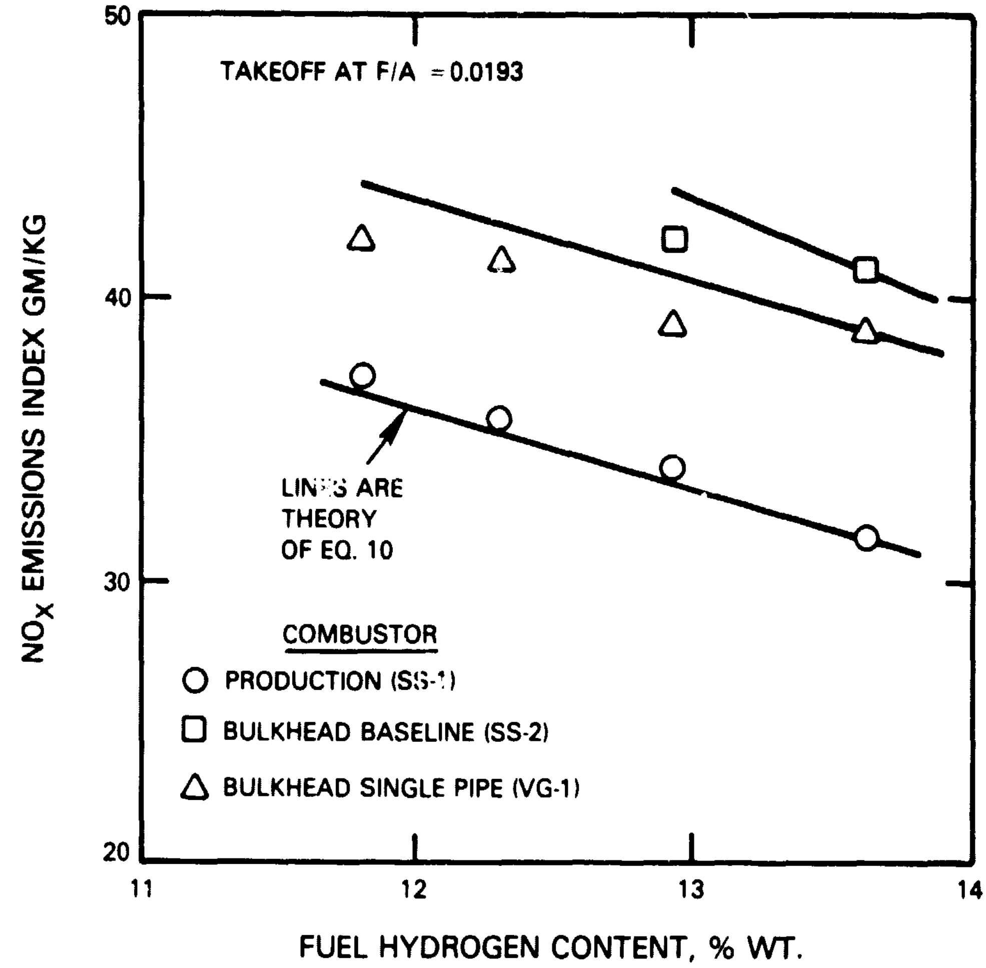

Figure 65 Takeoff NO_x Emissions Characteristics of the Baseline JT9D Single Stage Combustors

7.1.4 Smoke

Unless they are oxidized in the remainder of the combustor, the carbon particulates formed in the primary zone are emitted with the other combustion products in the form of visible smoke. The smoke output of the baseline combustors was measured at selected high power operating conditions. The magnitude of the SAE smoke number was low: less than 5 under all combinations of operating conditions and test fuels. While the experimental uncertainty of comparative measurements of such small magnitudes is high, the data from all three baseline combustor configurations demonstrated a consistent trend. Figure 66 shows the variation in measured SAE Smoke Number with fuel hydrogen content at combustor inlet conditions consistent with takeoff operation of the JT9D engine but at reduced fuel/air ratios imposed by the exit rake temperature limitations. There is a definite similarity in the sensitivity of smoke output to fuel composition in the current production combustor and the advanced bulkhead combustors. Additional confirmation is provided by the measurement obtained in Configuration VG-I with the reduced reference velocity. This perturbation of inlet conditions increased the residence time in the combustor, allowing more complete oxidation of the particulates and producing the observed reduction in the Smoke Number.

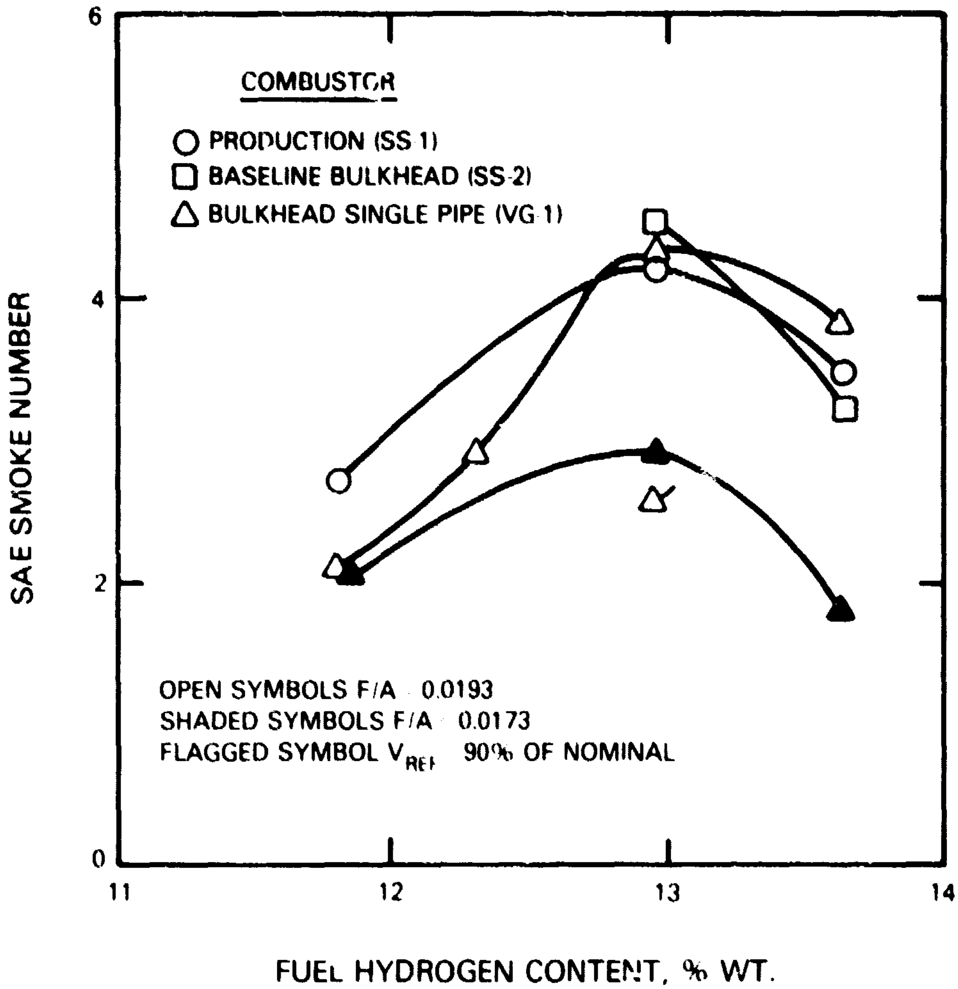

Figure 66 Smoke Characteristics of JT9D Baseline Single Stage Combustors at Takeoff

At the higher fuel/air ratios all three configurations produced about the same smoke output. The change from Jet A to ERBS fuel was accompanied by an increase in SAE Smoke Number on the order of 15 to 25 percent. The reductions in Smoke Number that occurred with the 12.3 and 11.8 percent hydrogen test fuels was unexpected given the composition and hydrocarbon structure of the fuels. The unusual viscosity and volatility characteristics of these fuels, cited previously is the only evident factor which would explain these results. Smoke output has been shown to be sensitive to fuel atomization and vaporization processes in unique situations involving combustors operating at low power levels, but this type of sensitivity would not appear likely in the high pressure and temperature environment of the JT9D combustor at takeoff.

7.1.5 Combustor Exit Temperature Distribution

While refining the combustor exit temperature distribution to achieve the program goals for pattern factor and radial profile was not a major objective of the Phase I effort, the sensitivity of these parameters to variations in fuel composition was investigated. Figure 67 shows a representative comparison of combustor exit temperature distribution with Jet A and ERBS fuel. These data were obtained from the baseline advanced bulkhead combustor (Configuration SS-2) operating at JT9D takeoff conditions with the fuel/air ratio reduced to 0.0193 because of exit rake temperature limitations. There was a fifth gas temperature thermocouple on the combustor exit rake, located near the inner radius at 8 percent radial span. However, the data from this thermocouple were not included in the analysis of the exit temperature. It appears that erroneously low readings were produced by the water spray in the facility exhaust chamber which forced cooling air flow from the simulated inner vane platform onto this thermocouple. Exclusion of the readings was justified by consideration of the energy balance on the combustor, i.e., the enthalpy rise across the combustor relative to the heat of combustion of the fuel consumed.

The data of Figure 67 indicate that the use of ERBS fuel rather than Jet A did not have a significant impact on the overall combustor exit temperature distribution. The temperature distribution is dominated by hot regions downstream of, but displaced about three degrees from, the centerline of the fuel injectors. The peak behind the fuel injector at the 27° circumferential position represents the maximum temperature; this point is coincident with the circumferential locations of the thermocouples which indicate the highest liner metal temperatures. The pattern factor of 0.454 ±0.003 is dictated by the high gas temperature which occurred at the same circumferential position with both fuels. Had the high temperature streaks not occurred downstream of one of the injectors, the exit pattern factor with both test fuels would have been less than 0.20.

The tendency for the combustor exit temperature distribution to be insensitive to fuel composition was also evident in the other baseline single stage combustor configurations. Table 19, which lists combustor exit temperature pattern factors for these configurations at JT9D takeoff combustor operating conditions, demonstrates this insensitivity. With the exception of the bulkhead combustor operating in the single pipe mode with 12.3 percent hydrogen fuel, pattern factor deviations are ±.022 or less.

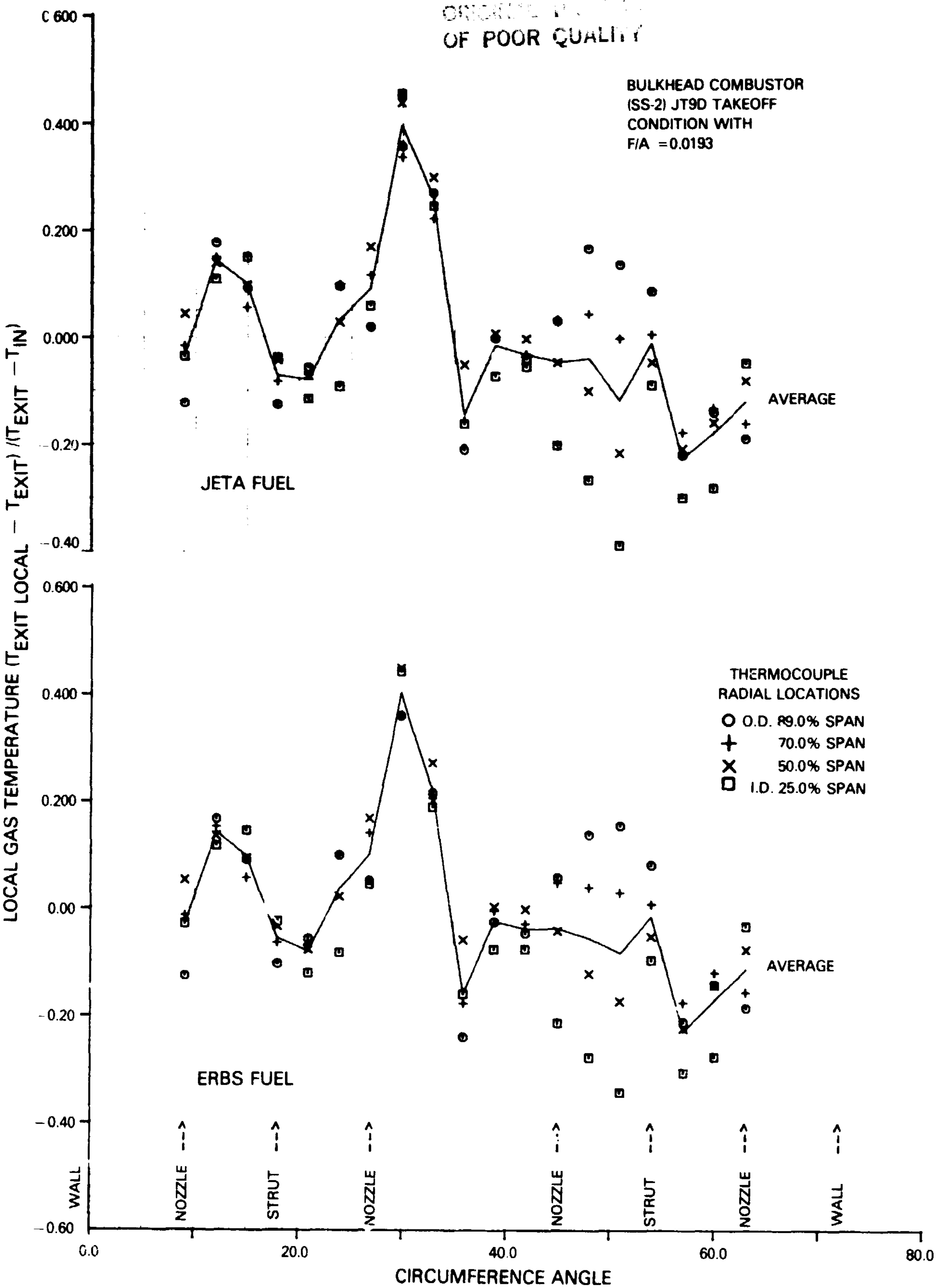

Figure 67 Exit Temperature Distribution of Baseline Bulkhead Combustor (Configuration SS-2) at Takeoff

ORIGINAL PAGE IS
OF POOR QUALITY

Table 19

Exit Temperature Pattern Factors of Baseline
Single Stage Combustors at JT9D Takeoff

Combustor Configuration	Jet A	ERBS	12.3% H_2	11.8% H_2
Current Production (SS-1) @ F/A = 0.0206	0.433	0.440	0.460	0.477
Baseline Bulkhead (SS-2) @ F/A = 0.0193	0.456	0.451	--	--
Bulkhead Single Pipe (VG-1) @ F/A = 0.0193	0.462	0.476	0.541	0.491

To achieve the required turbine blade life, the circumferentially averaged radial temperature profile at the combustor exit must comply with the target profile defined in Figure 5. Figure 68 shows the radial temperature profiles obtained from the exit temperature distribution for all of the baseline single stage combustor/test fuel combinations listed in Table 19. The data indicate that the radial temperature distribution at the exit of each combustor configuration is essentially insensitive to fuel composition except in the previously cited case of the bulkhead combustor operating in the single pipe mode on 12.3 percent hydrogen fuel. In this exceptional case, the data indicate that the profile has been shifted by a reduction in the average temperature at the 89 percent span location, i.e., near the outer periphery of the gas path. The data also demonstrate that the radial profiles produced by all three baseline combustors are considerably less peaked than the target profile and would require additional refinement to achieve the target.

It must be noted that these observations about the combustor exit temperature distribution are based on short duration testing which only reflects the effect of different test fuels on fuel spray or combustion characteristics. Combustor exit temperature distribution can also deteriorate from alterations in the fuel injector spray characteristics caused by deposits in or on the injector. Investigation of the effect of fuel composition on this deterioration mechanism was beyond the scope of the program but must be considered in establishing turbine life impacts.

7.1.6 Combustion Stability

The lean blowout fuel/air ratios of the baseline single stage combustors were measured at the JT9D idle inlet condition. This parameter indicates the risk of blowout during engine deceleration and provides a qualitative or relative measure of the altitude stability and ignition characteristics of the combustor. Table 20 lists the fuel/air ratio at blowout for each combustor. It can be seen from the table that the ratio is a function of combustor configuration but independent of fuel composition. The current production combustor (Configuration SS-1) and the baseline bulkhead combustor with the duplex fuel injector (Configuration SS-2) have nearly the same blowout fuel/air ratio. Since the stability of both of these combustors has been found to be adequate in engine operation, the idle blowout fuel/air ratio must be

ORIGINAL PAGE IS OF POOR QUALITY

considered satisfactory. The single pipe injector system used in Configuration VG-1 relies on aerated fuel atomization rather than the pressure atomized primary system used in the other two configurations. Higher lean blowout fuel/air ratios were encountered with this configuration, indicating a need for further development.

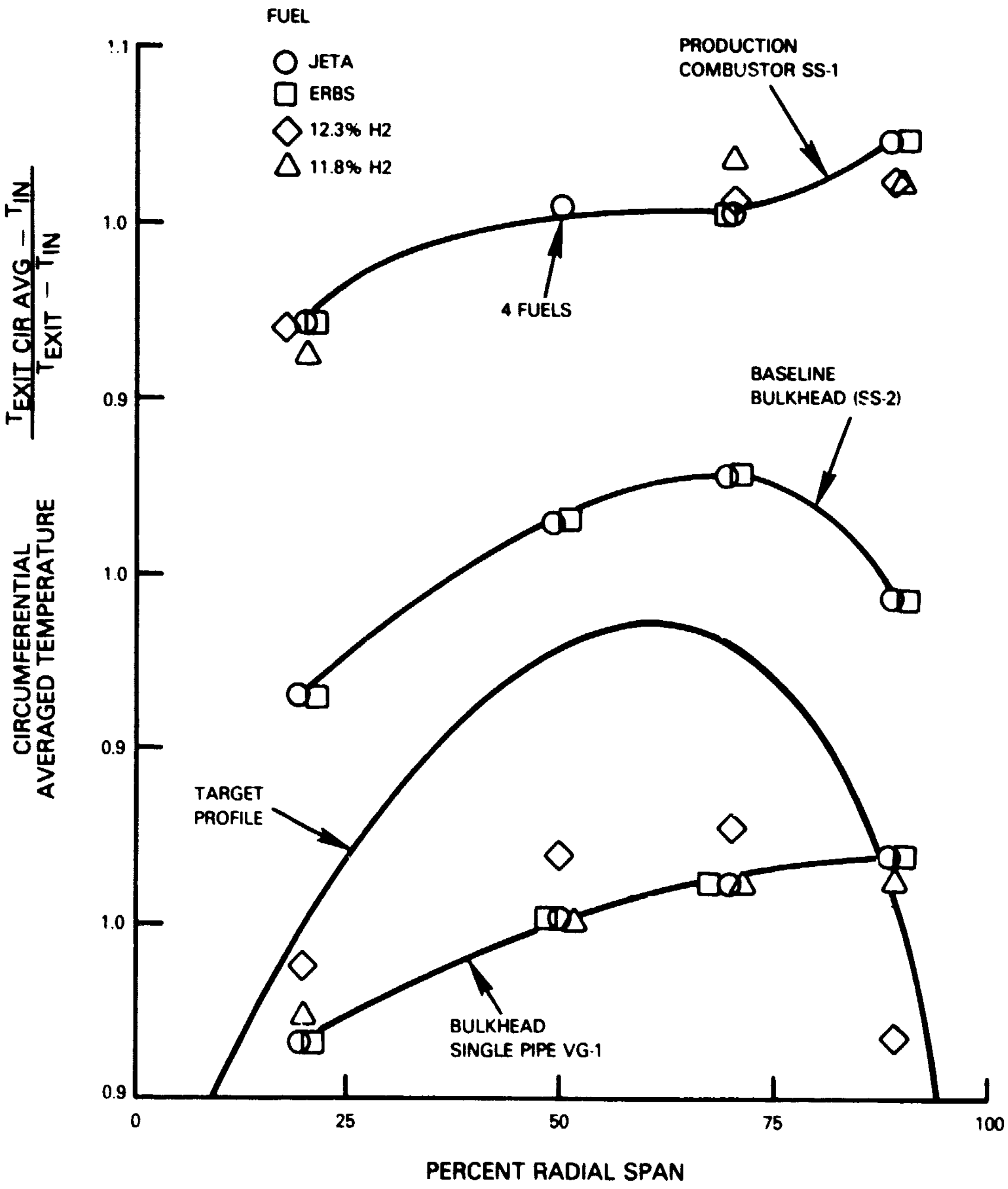

Figure 68 Radial Exit Temperature Profiles of Baseline Single Stage Combustors

Table 20

Lean Blowout Fuel/Air Ratio of Baseline
Single Stage Combustors at JT9D Idle

Combustor Configuration		Jet A	ERBS	11.8% H_2
Current Production	(SS-1)	0.0042	0.0042	0.0043
Baseline Bulkhead	(SS-2)	0.0044	0.0046	--
Bulkhead Single Pipe	(VG-1)	0.0061	0.0063	0.0060

7.1.7 Carbon Deposition

Since the tests were short, the full impact of carbon deposition on the burner liners and external surfaces of fuel injectors could not be assessed. However, the tests were monitored to detect any serious deficiencies. Figure 69 shows the inside of the current production combustor sector (Configuration SS-1) after testing. There is some evidence of carbon deposition on the surfaces of the flame stabilization cone, but the material had a soft powdery texture and was not considered to be a significant problem. Figure 70 shows the inside of the advanced bulkhead combustor sector. The photograph was taken after the sector had been operated in the baseline configurations (SS-2 and VG-1) and after various fuel injector perturbations had been evaluated. Consequently this sector was subjected to more than 100 hours of operation before being photographed. There is no evidence of carbon deposition on the bulkhead or the liner of this combustor. When this combustor operated with the standard duplex pressure atomizing/aerated fuel injector there was no evidence of carbon formation on the injector face. However some deposition was observed on the alternate fuel injector and the variable geometry injector.

7.1.8 Status of Single Stage Combustor Concept

The results presented in this section summarize the capabilities of state-of-the-art single stage combustors to accommodate the use of broadened property fuels. The advanced bulkhead combustor construction was shown to represent a significant advance over the cone stabilized annular combustor in that low power emissions goals were met with Jet A fuel. Test results indicate that increased liner temperatures, caused by increased radiant heat load, are a major obstacle in accommodating broadened property fuels. Reductions in liner life of 13.5 percent are projected with ERBS fuel. Use of broadened property fuels was also shown to increase emissions output. There is particular concern about carbon monoxide emissions at idle; ERBS fuel has been found to increase emissions output beyond acceptable levels. The modifications to the basic single stage combustor which are discussed in Section 7.2 were designed to reduce the sensitivity of these parameters to fuel composition.

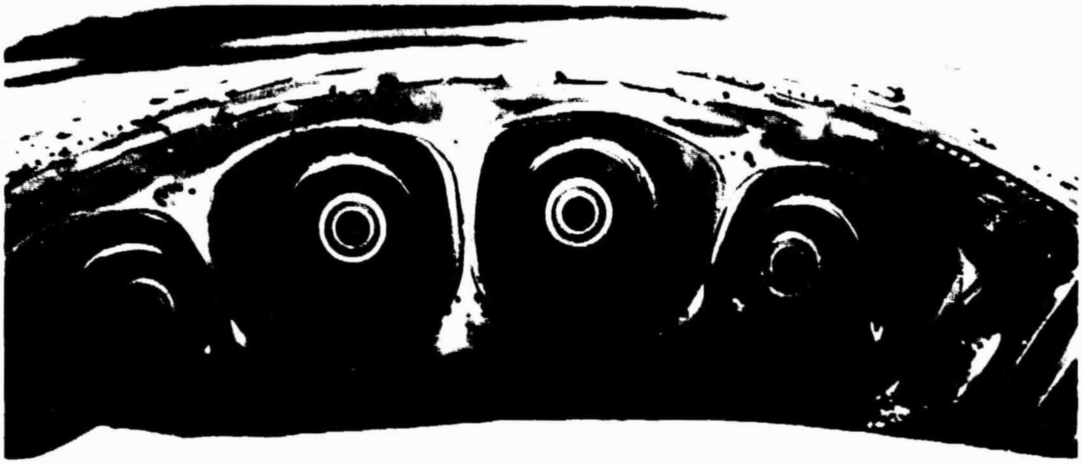

Figure 69 Interior of Current Production JT9D Combustor (Configuration SS-1) after Testing

Figure 70 Interior of Advanced Bulkhead Combustor (Configuration VG-1 and SS-2) after Testing

Including Configuration VG-1 as a baseline single stage combustor configuration provided the opportunity to assess the potential of a single pipe aerated fuel injector relative to the conventional, but more complex, duplex system. In general, the performance of the single pipe approach was comparable to the duplex system. The single exception was the area of combustion stability in which the lean blowout fuel/air ratio was notably higher than achieved by a duplex injectors with a pressure atomized primary system. This finding implies that further refinement may be required to develop a viable single pipe fuel injection system with the required stability and ignition capability. However, single pipe fuel injection offers distinct advantages in reducing the propensity for deposition and coking in the fuel system. In view of the reduced thermal stability which is expected with broadened property fuels, the advantages of the single pipe fuel injection approach may justify the effort required to develop adequate combustion stability and ignition margin.

7.2 MODIFICATIONS TO SINGLE STAGE COMBUSTOR CONCEPT

After the baseline single stage combustors had been evaluated, test effort was focused on advanced single stage combustor configurations which incorporated a variety of modifications designed to enhance the performance and emissions characteristics of the basic single stage combustor. Particular emphasis was placed on those modifications which would offset the deficiencies encountered with operation on broadened properties fuels. These revisions included use of modified fuel injectors, variations in combustor stoichiometry and use of advanced liner cooling concepts. The tests indicated that advanced technology features could lead to fundamental improvements in the performance of combustors operating on broadened properties fuels. Test results are discussed in more detail in the remainder of this section. Unless indicated otherwise all data reported in this section were obtained with ERBS fuel.

7.2.1 Modified Fuel Injector

As described in Section 4.1.3, the first variation to the advanced single stage combustor, Configuration SS-4, incorporated a modified version of the duplex pressure atomizing primary/aerated secondary fuel injector used in the bulkhead combustor. This injector was operated in the normal duplex mode during the evaluation. The effect of the modification was deduced by comparing test results from Configuration SS-4 with results from the baseline Configuration, SS-2. The modified fuel injectors were also evaluated in the single pipe mode in Configuration VG-2. Results were compared with data from Configuration VG-1 to determine the effect of the modification.

Table 21 summarizes the results of the evaluation of the relevant combustor configurations. The effect of the injector modification can be determined by comparing the data for the baseline and modified configurations obtained with ERBS fuel. Corresponding data for the baseline combustors operating on Jet A fuel are also provided. These data can be used to distinguish the changes in combustor performance caused by the fuel injector modification from the changes caused by the switch from Jet A to ERBS fuel.

The data obtained at idle indicate that, despite the improvement in fuel atomization observed in bench tests, the modifications to the fuel injector did not reduce carbon monoxide and unburned hydrocarbon emissions significantly. While there was a decrease in carbon monoxide emissions of about 10 percent when the baseline and modified injectors were operated in the single pipe mode, the modified injectors increased carbon monoxide emissions by about the same amount when operated in the duplex mode. The emissions of unburned hydrocarbons were found to increase when the modified fuel injectors were used. With the duplex fuel system, the unburned hydrocarbon emissions are low enough to meet the goal of a maximum emissions index of 4.0 gm/kg as defined in Figure 64. However, larger increases in unburned hydrocarbon emissions were encountered in the single pipe aerating mode and this goal was exceeded.

ORIGINAL PAGE IS
OF POOR QUALITY

Table 21

Effect of Modified Fuel Injector on Performance of
Single Stage Combustor

	Duplex			Single Pipe		
Operating Mode	Baseline	Baseline	Modified	Baseline	Baseline	Modified
Fuel Injector	SS-2	SS-2	SS-4	VG-1	VG-1	VG-2
Configuration						
Fuel	Jet A	ERBS	ERBS	Jet A	ERBS	ERBS
Performance at Idle						
Carbon Monoxide Emissions - gm/kg	16.8	27.5	31.6	16.0	28.0	25.5
Unburned Hydrocarbon Emissions - gm/kg	1.9	2.0	3.2	1.1	2.3	5.1
Lean Blowout Fuel/Air Ratio	0.0042	0.0042	0.0049	0.0061	0.0063	0.0058
Performance at Takeoff (F/A = 0.0193)						
NO_x Emissions - gm/kg	41.0	42.0	37.7	38.6	39.0	30.8
SAE Smoke Number	3.2	4.5	2.7	3.8	4.3	2.4
Exit Pattern Factor	0.457	0.451	0.281	0.462	0.543	0.250
Primary Zone Liner Temperatures - °K (°F)						
Maximum at Cruise	979 (1303)	1003 (1346)	924 (1204)	1035 (1404)	1082 (1489)	931 (1216)
Average at Cruise	845 (1063)	851 (1073)	846 (1064)	832 (1038)	853 (1076)	843 (1058)
Maximum at Takeoff	1141 (1595)	1157 (1623)	1020 (1377)	1168 (1644)	1233 (1760)	1024 (1384)
Average at Takeoff	928 (1212)	931 (1216)	932 (1219)	928 (1211)	945 (1242)	931 (1217)

The modified fuel injectors had opposing effects on lean stability characteristics at idle. The lean blowout fuel/air ratio increased in the duplex mode (all of the fuel passed through the pressure atomizing primary system of the injector at this fuel/air ratio). Conversely, lean blowout improved in the single pipe mode. These results are qualitatively consistent with the results of the spray characterization tests reported in Appendix B. The modifications to the fuel injector at best failed to improve fuel atomization in the primary system whereas they enhanced atomization in the secondary system of the injector.

Data obtained at takeoff indicate that modified fuel injectors substantially improve high power performance. When interpolated to a common fuel/air ratio, the data of Table 21 indicate significant reductions in NO_x emissions (on the order of ten percent), smoke output and exit gas temperature pattern factor. The reductions in NO_x emissions and smoke output are both greater than the increments associated with the change from Jet A to ERBS fuel. They also imply that the modifications to the injectors affected fuel dispersion in the primary combustion zone. Apparently, a more uniform dispersion is achieved at high power levels and fuel concentration is moderated in the locally rich regions where NO_x and smoke are formed in greater quantities.

Figure 71 shows the temperature distribution at the exit plane of Configuration SS-4 at takeoff conditions. Comparing these data with the distribution from the baseline configuration (Figure 67) indicates that the temperature levels of the hot regions downstream of the fuel injectors are more nearly consistent. The single high temperature region behind the injector at the 27 degree position, which dictated the high pattern factor in Configuration SS-2, has been eliminated.

Table 21 also lists maximum and average liner temperatures in the primary zone of the combustors. The most obvious effect of the modification to the fuel injectors is the large reduction in maximum liner temperature at both cruise and takeoff conditions. In the baseline configurations, the maximum temperatures occurred at positions in line with a fuel injector (but not the same injector in all cases). In most cases, attenuation of the metal temperatures in the regions immediately downstream of the fuel injectors is sufficient to reduce the average temperature of the liner enclosing the primary zone by increments comparable to those produced by the transition from Jet A to ERBS fuel in the baseline configurations.

In summary, the modified fuel injector substantially improved combustor performance at high power conditions, even though it did not provide the gains in low power emissions expected from its improved atomization characteristics. Improvements included reduced NO_x and smoke output, reduced liner temperatures in the most critical regions, and a more uniform exit temperature distribution. These improvements are attributed to the enhanced fuel dispersion characteristics of the fuel injector which apparently resulted in more uniform mixture strengths in the primary zone.

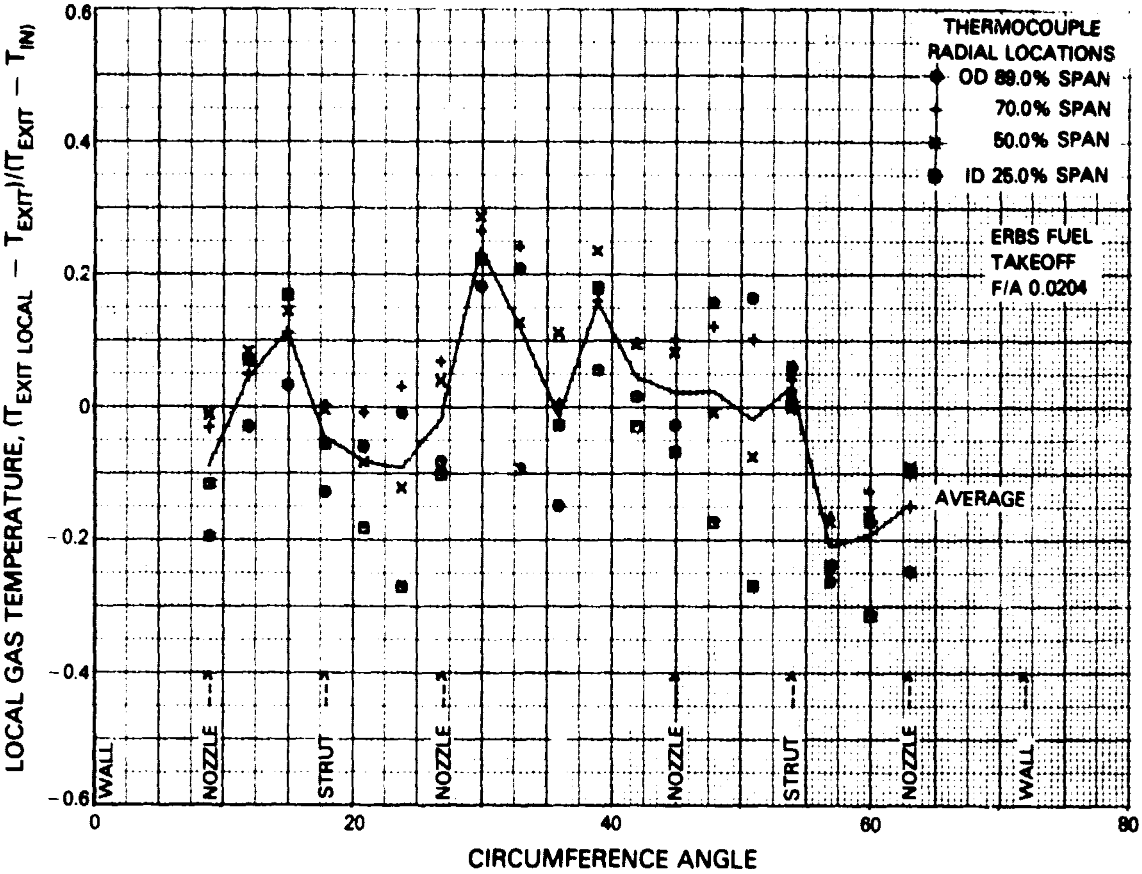

Figure 71 Exit Temperature Distribution of Configuration SS-4 with Modified Fuel Injector

7.2.2 Increased Primary Zone Residence Time

The dilution jet orifices on the liner of Configuration SS-3 were moved downstream relative to the baseline Configuration (SS-2) to investigate the effect of primary zone residence time on combustor performance. This change was made because ERBS fuel had increased carbon monoxide emissions to a level which exceeded the goal for the baseline combustor configurations. This approach offered an opportunity to oxidize more of this constituent in the primary zone. Table 22 compares the results of the evaluation of Configuration SS-3 with those of the baseline configuration.

Table 22

Effect of Primary Zone Residence Time on
Performance of Single Stage Combustor

	Baseline Configuration (SS-2)	Extended Primary Zone Configuration (SS-3)
Fuel	ERBS	ERBS
Emissions Indices at Idle - gm/kg		
Carbon Monoxide	27.5	20.4
Unburned Hydrocarbons	2.0	1.0
Performance at Takeoff (F/A=0.0193)		
NO_x Emission Index - gm/kg	42.0	42.1
SAE Smoke Number	4.5	2.1
Exit Pattern Factor	0.451	0.460
Average Liner Temperatures °K (°F)		
Cruise; Primary Zone	851 (1073)	844 (1062)
Dilution Zone	769 (925)	784 (950)
Takeoff; Primary Zone	931 (1216)	940 (1232)
Dilution Zone	848 (1067)	870 (1106)

The emissions characteristics measured at idle indicate that extending the length of the primary zone successfully reduced carbon monoxide emissions below the goal of 21 gm/kg. Unburned hydrocarbon emissions, which were already at an acceptable level in Configuration SS-2, were also reduced. Similarly, measurements of the SAE Smoke Number at takeoff indicate that the increase in primary zone residence time permitted more particulates to be oxidized in the combustor, further reducing detectable smoke at the combustor exit. Increasing the length of the primary zone would be expected to increase oxides of nitrogen, but this type of increase was not detected in the measurements obtained at takeoff.

Displacement of the dilution air orifices toward the discharge of the combustor reduced the space available for penetration and mixing, which control the exit temperature distribution. However, as shown in the table, the combustor exit temperature pattern factor was not altered significantly. In fact, the overall gas temperature distribution retained the dominant features of the distributions for the baseline Configuration (Figure 67).

As shown in Table 7-5 the average of the sixteen individual liner metal temperature measurements in the primary zone did not change by more than 9°K (16°F) at either cruise or takeoff when the dilution air orifices were moved downstream. The shifts which did occur were random; the average temperature decreased at cruise and increased at takeoff. In the dilution zone, the changes in average temperature were larger and more consistent. Readings from the nine operating thermocouples in this section of the liner showed that average temperature increased 15°K (25°F) at cruise and 22°K (39°F) at takeoff. Evidently, shifting the dilution air jets downstream delays quenching of the luminous particulates in the combustion products, exposing the liner at the rear of the combustor to a significantly higher radiant heat load. Consequently, while increasing residence time in the primary combustion zone appears to be a viable approach to reducing emissions constituents and smoke in order to accommodate broadened properties fuels, consideration must also be given to the durability of the aft sections of the combustor liner.

7.2.3 Primary Zone Stoichiometry Variations

The bulk equivalence ratio in the primary zone is a controlling parameter in the combustion process; the influence of this parameter was assessed in Configurations SS-5 and SS-6 of the single stage combustor concept. Primary zone airloading in these configurations was perturbated above and below the nominal loading level for the baseline bulkhead combustor (Configuration SS-2) by altering the airflow through the combustion air orifices in the liner enclosing the primary zone. The perturbations in airflow to the primary zone were moderate to remain realistic with respect to the operational constraints on a single stage combustor. Further, a corresponding change was made to the flow entering the dilution zone orifices in order to maintain the same overall combustor section total pressure drop.

Figure 72 shows the effect of variations in primary zone airloading on the emissions characteristics of the single stage combustor. In the baseline bulkhead combustor (Configuration SS-2), 37 percent of the combustor air flowed through the primary zone, producing a bulk equivalence ratio of 0.44 at the design idle fuel/air ratio. As shown in the figure and indicated in Section 7.1, the baseline configuration met the program goal for unburned hydrocarbon emissions, but narrowly missed the goal for carbon monoxide emissions. However, since carbon monoxide emissions decrease with reductions in primary zone airloading, a small reduction should enrich this zone enough to achieve the program goal with ERBS fuel. Conversely, an increase in primary zone airloading, which would produce lean mixture strengths at high power levels, leads to large increases in both unburned hydrocarbon and carbon monoxide emissions. It is evident that the baseline bulkhead combustor was designed at the minimum primary zone equivalence ratio consistent with low emissions at idle.

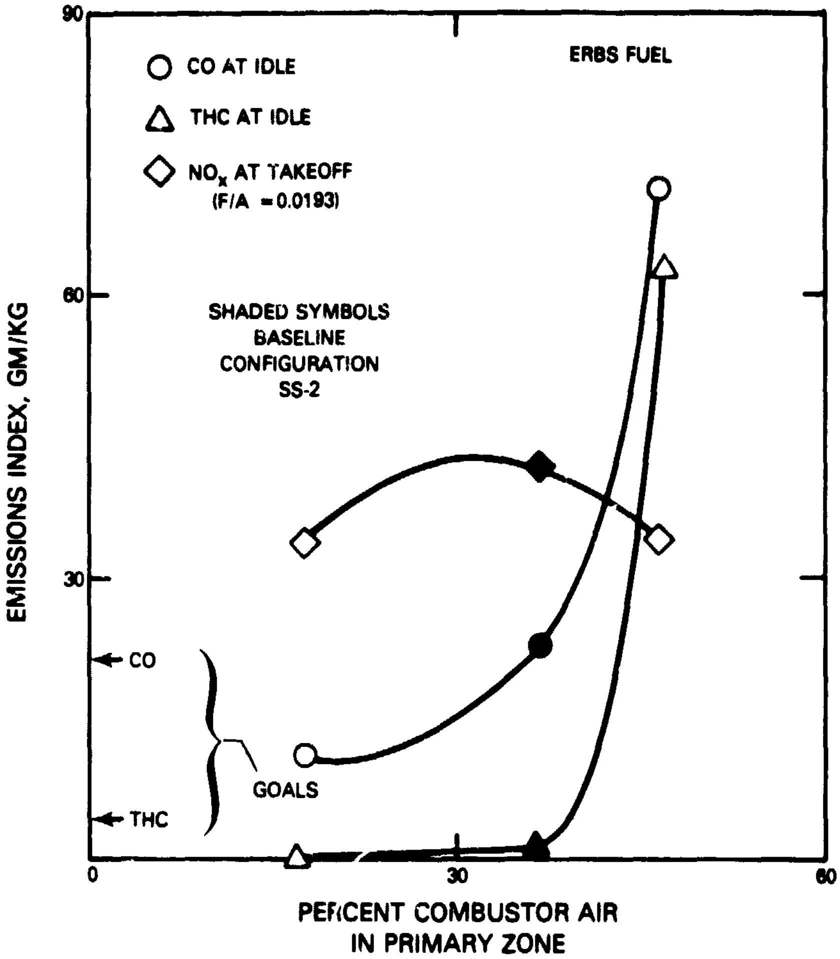

Figure 72 Effect of Primary Zone Airloading on Emissions Characteristics of Single Stage Combustor

Measurements of combustion stability at idle indicated that enriching the primary zone through reduced airloading improved the lean blowout fuel/air ratio from 0.0046 in Configuration SS-2 to 0.0025 in Configuration SS-6. However, in Configuration SS-5 increased airloading led to significantly higher carbon monoxide and unburned hydrocarbon emissions which usually imply a shift toward the lean stability limit, but the lean blowout fuel/air ratio remained essentially unchanged.

Figure 72 also shows the variation in NO_x emissions at normal takeoff inlet conditions but with a reduced fuel/air ratio relative to the engine design condition. At this fuel/air ratio, the bulk equivalence ratio in the primary combustion zone would be unity at a primary zone airloading of about thirty percent. As shown in the figure, the NO_x emissions characteristic is consistent in that there is a maximum at thirty percent and emissions decline at both lower and higher primary zone airloadings. Measurements of the SAE Smoke Number at the modified takeoff conditions were inconclusive: experimental uncertainties between combustor configurations were equal in magnitude to the low nominal smoke output from the single stage combustor.

Changes in primary zone equivalence ratio also affect heat loads on the liner, as demonstrated in Figure 73. Average readings from thermocouples installed on the primary and dilution zone liner louvers and the front bulkhead of the combustor are shown as a function of primary zone airloading. Due to attrition of thermocouples on the liner during the course of the program, the number of measurements is limited to those thermocouples which produced accurate readings in all three configurations. (The thermocouples on the bulkhead were not installed on the baseline configurations.) Despite some deviations, metal temperatures decrease with increases in primary zone airloading. When the combustor operates at a fixed overall fuel/air ratio and pressure drop, the variations in primary zone equivalence ratio would not be expected to affect the thermal environment in the dilution zone of the combustor. Although the thermal environment was generally unaffected at takeoff, there were unexplained deviations at cruise with low primary zone airloading producing metal temperatures throughout the dilution zone which were higher than expected.

Since life limiting liner metal temperatures occur in the primary zone, increasing primary zone airloading to produce leaner mixtures at high power may be an effective method of maintaining liner life with broadened properties fuels. In Section 7.1.2, the average liner temperature in the primary zone of the baseline bulkhead combustor (Configuration SS-2) was shown to increase 6°K (12°F) at takeoff when ERBS fuel was substituted for Jet A. Assuming that the variation in bulkhead temperature with primary zone airloading at takeoff shown in Figure 73 is a representative primary zone liner response, a four percent increase in combustor airflow would be enough to reduce the metal temperatures to the levels encountered with Jet A fuel, thus maintaining liner life. If the analysis is based on the change in maximum rather than average liner temperature, the increment is 16°K (27°F) and a 9.5 percent increase in combustor airflow is required to offset the change in liner temperature.

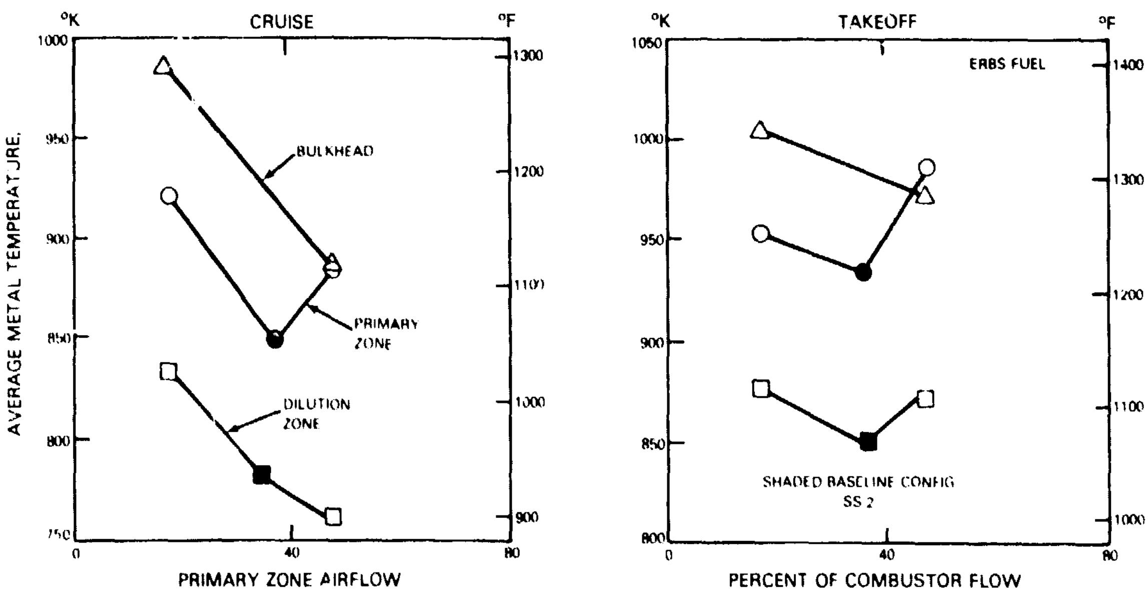

Figure 73 Effect of Primary Zone Airloading on Liner Temperature in the Single Stage Combustor

However, as the data of Figure 72 indicate, even an increase of four percent of combustor airflow to the primary zone would have a serious impact on emissions output at idle. Carbon monoxide emissions would rise from close to the goal to more than 50 percent above, while unburned hydrocarbon emissions would also exceed acceptable levels.

Increases in primary zone airloading would also be expected to adversely affect combustor exit temperature distribution due to the reduction in available dilution air. Table 23 shows the variation in combustor exit temperature pattern factor for the relevant combustor configurations. There is a progressive increase in pattern factor as airflow is diverted from the dilution air jets to the primary combustion zone. Based on the tabulated data, the 4 percent and 9.5 percent increases in primary zone airloading required to maintain liner life with ERBS fuel would increase the pattern factor by 0.03 and 0.07 respectively. While it is possible that development effort could reduce these increments and optimize the dilution process with the lower airflow, the potential for increases in pattern factor of this magnitude must be recognized.

Table 23

Effect of Primary Zone Airloading on Combustor Exit Temperature Distribution

Configuration	SS-5	SS-2	SS-6
Airflow Distribution ~ % Wab			
Primary Zone	17.0	32.5	41.3
Dilution Air Jets	39.1	23.6	14.8
Combustor Exit Distribution			
Pattern Factor	0.405	0.451	0.516

In summary, altering combustor stoichiometry by shifting primary zone airloading produces desirable characteristics which could be used to enhance the performance of single stage combustors with broadened properties fuels. The change in airloading had the strongest impact on emissions output at idle and liner heat load. Lean stability characteristics and exit temperature distribution were influenced to a lesser extent and both of these elements would be favorably affected by enriching the primary zone. Unfortunately, the key factors - idle emissions and liner heat load - require opposing changes in primary zone airloading. For this reason it appears that changing current design practice to alter primary zone stoichiometry in single stage combustors is not an attractive generic approach to accommodating broadened properties fuels. However, this approach may be of value in accomodating unique combinations of combustors and fuels.

7.2.4 Improved Liner Cooling

As shown in Section 4.1.3, Configuration SS-7 incorporated Finwall® construction in the liner enclosing the primary zone. The modified fuel injector used in Configuration SS-4 was also included in Configuration SS-7 in order to reduce liner temperature streaks and produce a lower exit temperature pattern factor. Table 24 summarizes the emissions and performance characteristics of Configuration SS-7; corresponding data from several other configurations is included for reference. Configuration SS-2 is the baseline single stage combustor while Configuration SS-4 incorporated the modified fuel injector in an otherwise baseline combustor.

Table 24

Effect of Improved Liner Cooling and Modified Fuel Injector on Single Stage Combustor Performance

Configuration	SS-2	SS-2	SS-4	SS-7
Injector	Baseline	Baseline	Modified	Modified
Liner	Baseline	Baseline	Baseline	Finwall®
Fuel	Jet A	ERBS	ERBS	ERBS
Idle Emissions Indices - gm/kg				
Carbon Monoxide	16.8	27.5	31.6	36.0
Unburned Hydrocarbons	1.9	2.0	3.2	6.7
Performance at Takeoff (F/A = 0.0193)				
NO_x Emissions Index gm/kg	41.0	42.0	37.7	47.5
SAE Smoke Number	3.2	4.5	2.7	1.7
Exit Pattern Factor	0.457	0.451	0.281	0.309
Average Metal Temperatures - °K (°F)				
Cruise				
Bulkhead	---	911 (1180)*	---	985 (1315)
Liner - Primary Zone	845 (1063)	851 (1073)	845 (1064)	---
Liner - Dilution Zone	766 (920)	769 (925)	767 (922)	792 (967)
Takeoff				
Bulkhead	---	986 (1315)*	---	1047 (1425)
Liner - Primary Zone	928 (1212)	930 (1216)	931 (1219)	---
Liner - Dilution Zone	852 (1074)	848 (1067)	841 (1054)	865 (1098)

*Estimated from data for Configurations SS-5 and SS-6.

The data indicate that Configuration SS-7 generated significantly higher carbon monoxide and unburned hydrocarbon emissions at idle than the baseline combustor operating on ERBS fuel. However, as discussed in Section 7.2.1 and shown in the table, use of the modified fuel injector in Configuration SS-4 produced some increase in these constituents. The remainder of the increase may have been caused by a shift in airflow in Configuration SS-7 relative to the baseline configuration. Incorporating the advanced Finwall® construction in the primary zone liner reduced the cooling air requirements; about two percent of the combustor airflow which was saved was diverted into the primary combustion air jets. As shown in Figure 72 and discussed in Section 7.2.3, even small increases in primary zone airloading relative to the baseline configuration could increase idle emissions to the levels encountered. One of the potential advantages of an advanced liner which requires less cooling air is the reduced propensity for quenching carbon monoxide or hydrocarbon consuming reactions through contact with low temperature cooling air. While Configuration SS-7 did not demonstrate this benefit, it was also evident from the low nominal level of the emissions of these constituents and their response to other perturbations that reaction quenching by liner cooling air was not a significant mechanism in the bulkhead type combustor.

The modified fuel injector had been selected for Configuration SS-7 because of the superior high power performance demonstrated in Configuration SS-4. The data of Table 24 show that this advantage was sustained in Configuration SS-7; in fact, the SAE Smoke Number at takeoff was reduced even further. Similarly, the combustor exit temperature pattern factor remained low compared to the baseline configuration. The overall exit temperature distribution retained the dominant features demonstrated in Configuration SS-4 (see Figure 71). However, while introducing the modified fuel injector in Configuration SS-4 led to a 10 percent reduction in takeoff NO_x emissions relative to the baseline configuration, the NO_x emissions from Configuration SS-7 were about 10 percent higher than the baseline. The primary zone bulk equivalence ratio at the modified (reduced fuel/air ratio) takeoff condition used to tabulate NO_x emissions was about 0.75 and emissions output was increasing with overall combustor fuel/air ratio at this point. Consequently, while no specific evidence can be advanced, the increased NO_x emissions produced by Configuration SS-7 might be attributed to local enrichment of the primary reaction zone associated with the use of the Finwall® panels. For example, this local enrichment could have resulted from a change in the penetration characteristics of the primary combustion air jets in the Finwall® liner due to the grommets used on these apertures. It is noteworthy that higher than anticipated NO_x emissions were also encountered in Configurations VG-7 and VG-8 which used the same combustor liner sector.

The gas side metal temperatures in the Finwall® liner panels could not be measured directly due to the difficulties associated with installing thermocouples in these surfaces. However, the panels had been designed for operation on ERBS fuel at the same maximum metal temperature which would be encountered in a louver cooled liner with Jet A fuel. The panels were inspected after Configurations SS-7, VG-7 and VG-8 had been tested. There was no observed distress in the panels, providing qualitative verification that the panels had been cooled to the intended level.

Thermocouples were installed on the dilution zone liner and the bulkhead of the combustor sector in Configuration SS-7: the average metal temperatures are listed in Table 24. While more thermocouples were installed in Configuration SS-7 than in the liners of the previous configurations, the averages only include readings from thermocouple locations which were common to each combustor sector. Measured liner temperatures in Configuration SS-7 were found to be considerably higher than the temperatures in the preceding configurations. Metal temperatures in the dilution zone were 15 to 25°K (25 to 45°F) higher while those on the bulkhead were of the order of 50°K (100°F) higher. This variation was observed with all four test fuels. Examination of the pressure distribution around the combustor indicated that the temperature changes did not result from large scale shifts in local liner cooling air flow. However, it must be recognized that two different combustor sectors were involved. While efforts were made to install the thermocouples in a consistent manner and at the same locations, deviations were inevitable. These deviations may have contributed to the temperature differences.

While metal temperatures in the liner have been emphasized thus far, measurements obtained from Configuration SS-7 as well as Configurations SS-5 and SS-6 indicate that the highest temperatures were encountered on the bulkhead of the combustor. Configuration SS-7 was evaluated with all four test fuels; Figure 74 shows the variation in average bulkhead metal temperature at the takeoff combustor inlet condition. Metal temperature increases progressively with increasing fuel/air ratio and decreasing hydrogen content. At the design takeoff fuel/air ratio the transition from Jet A to ERBS fuel increases average bulkhead temperature 11°K (20°F), an increment comparable in magnitude to the increases in the hottest regions of the louver panels in the liner.

7.2.5 Improvement Potential of the Single Stage Combustor Concept

The analysis of test results presented in this section highlights areas in which development effort would be effective in enhancing the ability of single stage combustors to operate on broadened properties fuels. Changing the stoichiometry and residence time history in the combustor by revising airflow distribution has produced changes in emissions, smoke and performance characteristics which are consistent with accepted theory and experience with Jet A fuel. However, current combustor airflow schedules have been optimized to satisfy a number of opposing criteria and goals. Generic modification of combustor stoichiometry to accommodate a particular aspect of operation with broadened properties fuels is likely to compromise one or more other criteria with opposing requirements.

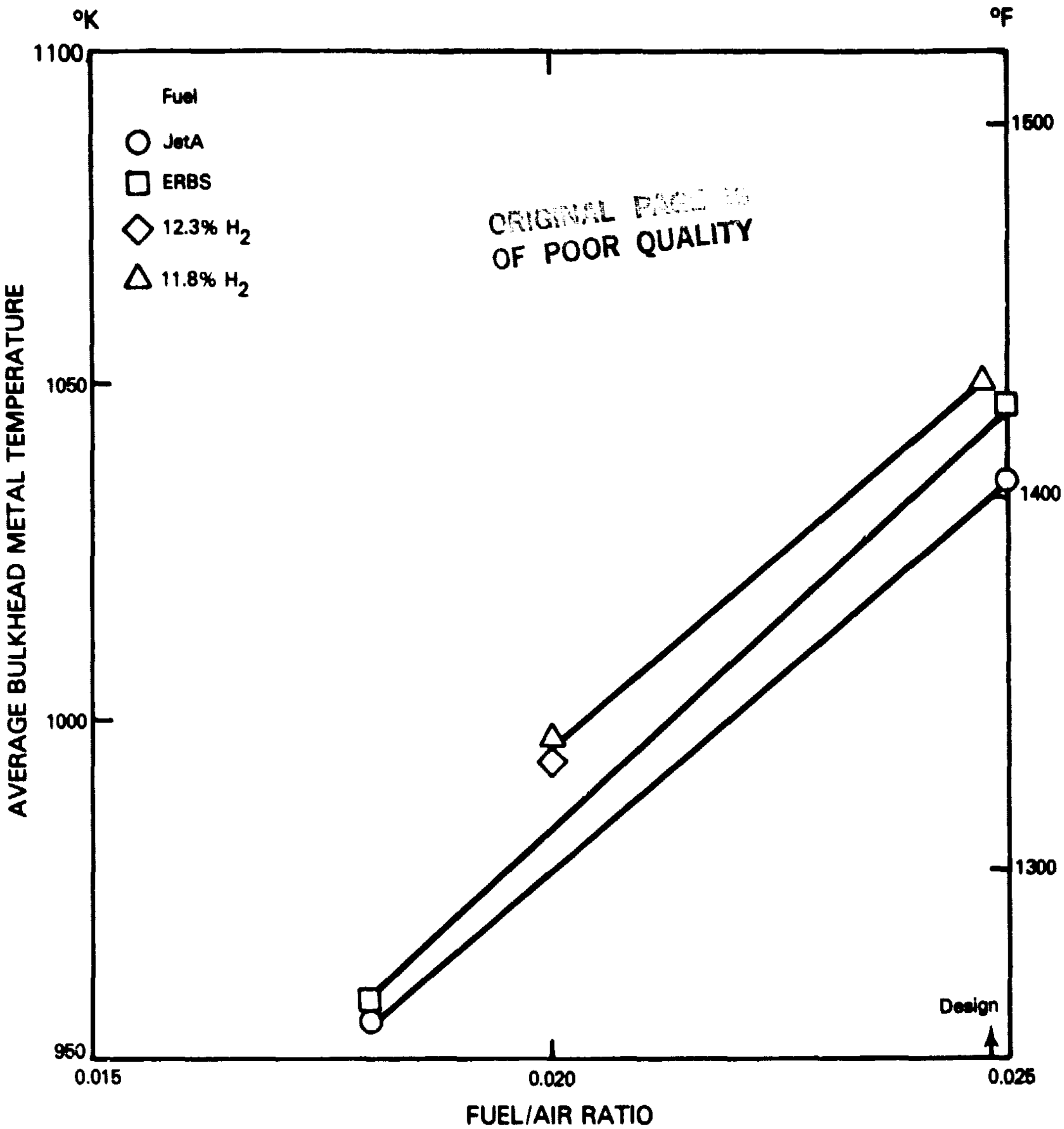

Figure 74 Sensitivity of Bulkhead Metal Temperature at Takeoff Condition

It appears that more fundamental improvements in combustor performance can be achieved by introducing advanced technology design concepts. In the current program, introduction of modified fuel injectors, which were produced with minimal development effort, led to significant improvements in high power performance including a reduction in peak liner temperatures, lower pattern factor and reduced smoke and NO_x ou put. With a properly structured development effort, the atomization characteristics and spray geometry of fuel injectors can be refined, providing optimum combustor performance with broadened properties fuels. While it was not demonstrated directly by the relevant combustor configuration, more advanced liner cooling concepts offer the potential for significant improvements in combustor performance. Advanced liners offset the increased heat load produced by broadened properties fuels without requiring increases in liner cooling air flow which would compromise performance and emissions characteristics.

7.3 STAGED VORBIX COMBUSTOR CONCEPT

The staged vorbix combustor was the second combustor concept evaluated in the Phase I program. With two distinct combustor zones, each serviced by an independent fuel system, this advanced technology combustor included the type of stoichiometry control that would be required if emissions of oxides of nitrogen were restricted in the airport vicinity. This flexibility of operation was expected to provide significant advantage over the single stage combustor concept in the accomodation of broadened properties fuels. The staged vorbix concept was evaluated with combustor rig components from the NASA/PWA Energy Efficient Engine Program and was operated at conditions representative of that engine.

7.3.1 Liner Temperatures

Fine wire thermocouples had been embedded in the hot wall of the internal convectively-cooled segments of the Vorbix combustor liner to monitor liner temperatures. Figure 75 shows the changes in liner temperature encountered at the cruise condition with the transition from Jet A to ERBS fuel. In this and subsequent figures, no effort is made to differentiate the data on the basis of the circumferential position of the thermocouples because no trends or tendencies toward streaking could be detected due to the high density of pilot zone fuel injectors and carburetor tubes.

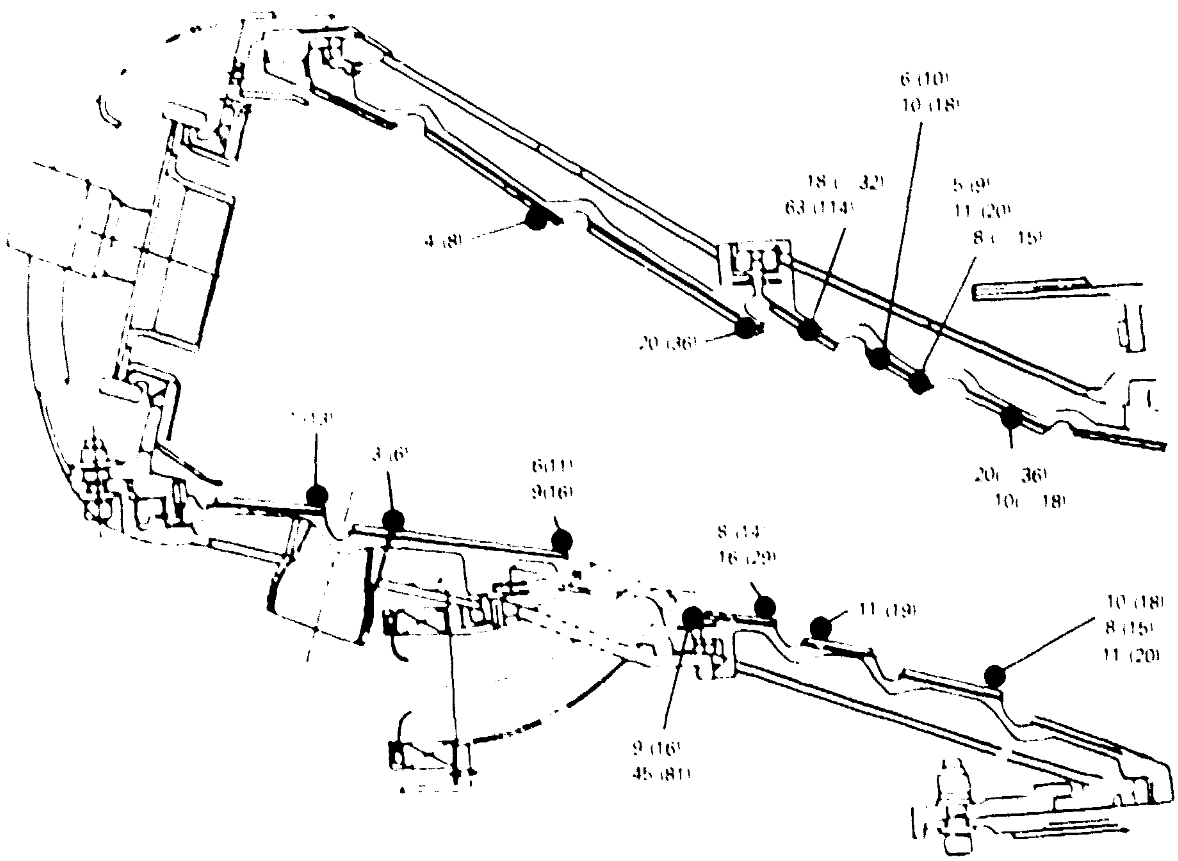

Figure 75 Effect of Fuel Composition on Liner Temperatures in the Staged Vorbix Combustor at Cruise

Within the pilot zone the increases in liner temperature are moderate, averaging only 6°K (11°F). This increase is significantly less than the 38°K (69°F) increase in average temperature observed in the louver cooled bulkhead type single stage combustor (Configuration SS-2). This reduced sensitivity may result from the staged operation of the combustor. The pilot zone is comparable to a single stage combustor operating at an equivalence ratio which is 20 to 30 percent of normal. This lean operation can minimize the initial formation of carbon particulates which cause shifts in radiant heat transfer to the liner. However, the internally cooled liner construction may also contribute to the reduced sensitivity of this combustor to fuel composition. By changing the overall energy balance on the liner surface, the incremental change in radiant heat transfer may have become a proportionately less significant contribution to the total heat load, thereby producing the smaller change in surface temperature.

Measured responses from the thermocouples in the secondary or main stage of the combustor with the transition from ERBS fuel to Jet A can be divided into two groups. Increases of 5 to 16°K (9 to 29°F) were observed in the first group, which included nearly all of the thermocouples on the outer liner segments and some of the thermocouples on the inner liner segments. The average increase is higher than the average in the pilot zone, but still considerably less than the increases encountered in the primary zone of a louver cooled single stage combustor. These thermocouples appear to be responding reasonably to the increase in radiant heat transfer associated with the combustion of ERBS fuel in the main stage. However, the second group, which included more than half of the thermocouples on the inner liner, shows a more erratic response to the change in fuel composition. In fact, a significant number of negative temperature increments were observed. These responses evidently result from the sensitivity of local convective heat transfer modes to fuel composition. During the development of the staged Vorbix combustor under the Energy Efficient Engine program, high temperature streaks were encountered in this region of the inner liner. It was thought that these streaks resulted from the interaction between the swirling flow from the pilot fuel injector and the jets from the carburetor tubes.

Similar temperature measurements were obtained with the combustor operating at the takeoff condition for the Energy Efficient Engine (with the exceptions noted in Section 6.4). Figure 76 shows the increases in local liner temperatures in the pilot stage with ERBS fuel and the 11.8 percent hydrogen content test fuel. As experience with the single stage combustor would indicate, the increases in liner temperature with ERBS fuel at takeoff were consistent with, but less than the increases observed at cruise. However, reducing the fuel hydrogen content further to 11.8 percent did not produce significant additional increases in local liner temperatures.

The response of the thermocouples in the main stage became chaotic at the takeoff condition: local temperature excursions in excess of ±55°K (100°F) were observed. The data obtained at takeoff are best presented in the alternate format of Figure 77. This figure graphically illustrates the response of each thermocouple for the entire Jet A/ERBS/11.8 percent hydrogen content fuel change sequence. Very few thermocouples show the response which would be anticipated with a progressive increase in radiant heat load, i.e., a modest increase in temperature with decreasing hydrogen content. Rather, pronounced increases and decreases in temperature were observed with ERBS fuel while only moderate increments (both positive and negative) were observed with further reduction in hydrogen content. With only two exceptions, temperatures on the outer liner increased and temperatures on the inner liner decreased as hydrogen content was reduced. This response reinforces the conclusion reached with cruise data that the liner temperature is responding to a strong change in convective heat load which is dependent on fuel composition. While a specific cause can not be identified, the sensitivity of the fuel dispersion and atomization processes which occur in the carburetor tubes to the physical properties of the fuel might produce this unusual response.

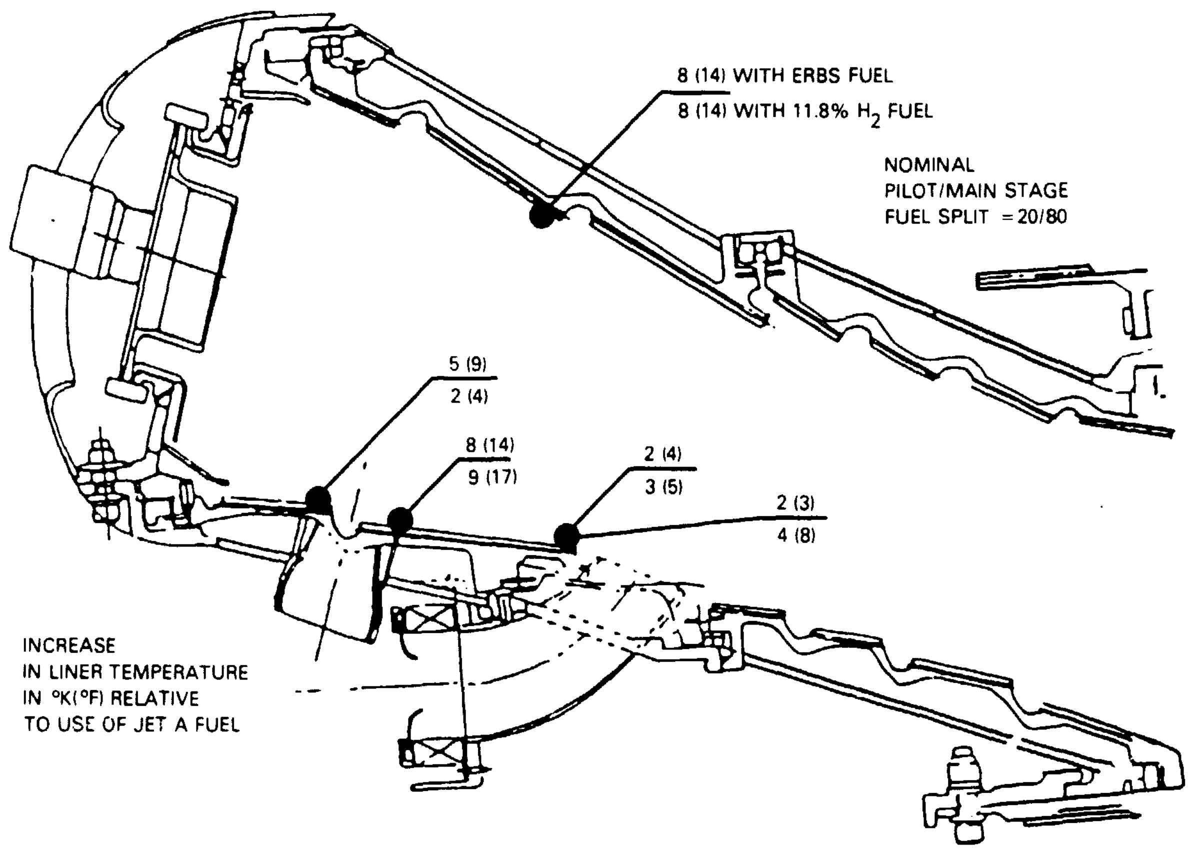

Figure 76 Effect of Fuel Composition on Liner Temperature in the Pilot Stage of the Advanced Vorbix Combustor at Takeoff

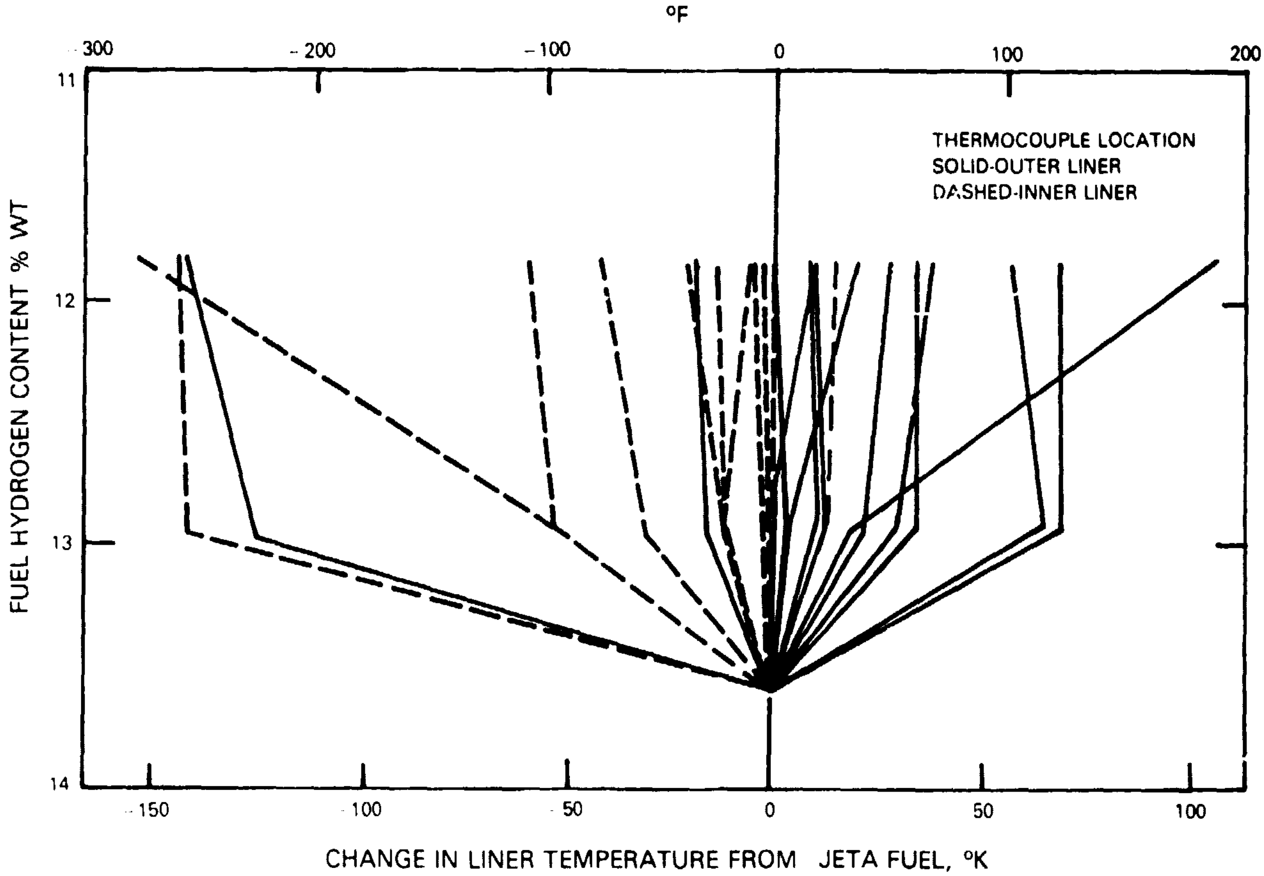

Figure 77 Effect of Fuel Composition on Liner Temperatures in the Main Stage of the Advanced Vorbix Combustor at Takeoff

The takeoff liner temperature data shown in Figures 76 and 77 were obtained at a pilot to main stage fuel split of 20/80. To investigate the effect of this split on liner temperature sensitivity more fuel was introduced to the pilot stage, even though this perturbation could increase high power NO_x emissions. Operation at a 30/70 pilot to main fuel split at takeoff increased the sensitivity of the pilot zone liner temperature to fuel hydrogen content. The corresponding reduction in main zone fuel flow also changed liner temperature responses to fuel composition. Most of the thermocouples on the inner liner, which show a decrease in temperature with fuel hydrogen content at a 20/80 fuel flow split (see Figure 77), showed increases of comparable magnitude at the 30/70 fuel flow split.

Structural analysis of the segmented liner (Reference 15) indicates that the life limiting failure mode is cyclic fatigue cracking of the hot surface of the liner segments. Consequently, the highest temperatures encountered during operation, i.e., those at takeoff, are most significant in determining liner life. While the structural analyses have not advanced sufficiently to determine the life decrement associated with specific increases in liner temperature, it would appear that the small temperature changes observed in the pilot stage of the advanced Vorbix combustor with ERBS fuel would not produce large life deficits. However, the large temperature excursions encountered in the main stage at takeoff would be expected to lead to excessive loss of liner life. These data indicate that the sensitivity of this configuration of the advanced Vorbix combustor to fuel composition is unacceptable. Further refinement of the main stage of the combustor is required to exploit what appears from liner temperature measurements in the pilot zone to be a potential advantage of staged combustors.

7.3.2 Emissions

Figure 78 shows the carbon monoxide and unburned hydrocarbon emissions characteristics of the advanced Vorbix combustor at the idle operating condition for the Energy Efficient Engine. The variation in the concentration of these constituents with fuel/air ratio is shown for the three test fuels evaluated. The goals which are shown in the figure are representative of the levels which must be achieved (in combination with comparable performance at higher power) to comply with the proposed standards of Table 2 for engines certified after 1984.

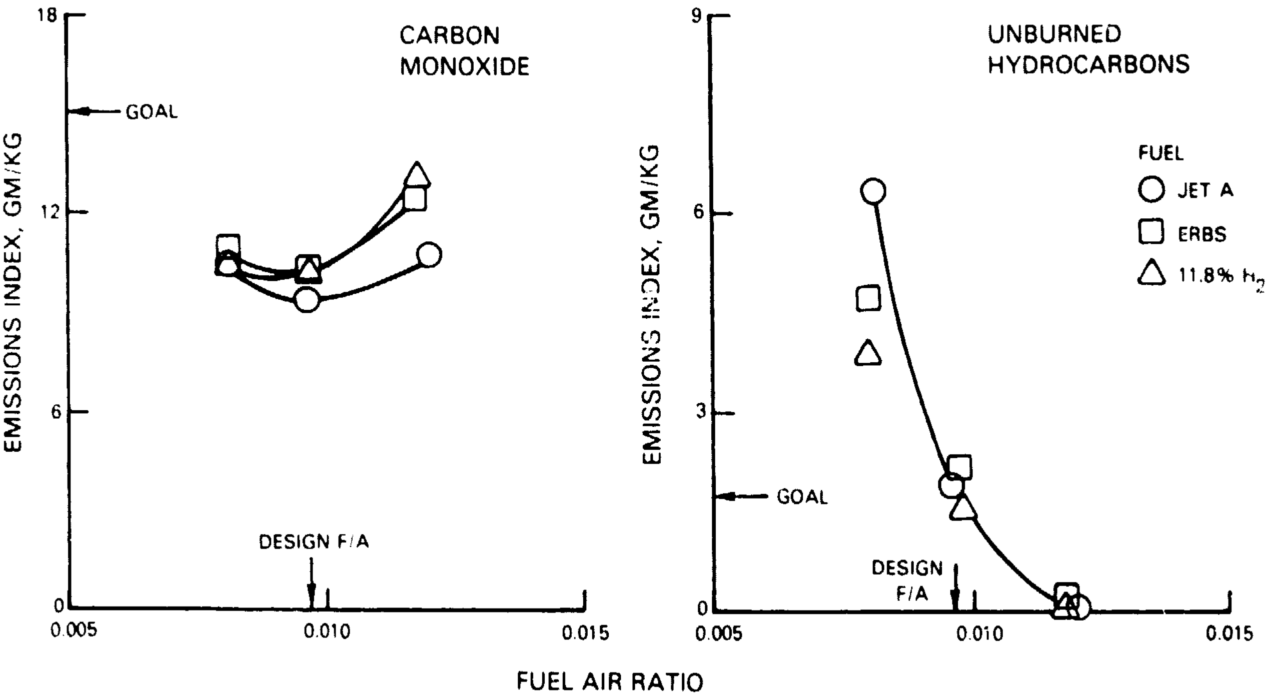

Figure 78 Emissions Characteristics of the Staged Vorbix Combustor at Idle

At the design fuel/air ratio, carbon monoxides emissions are slightly higher with the reduced hydrogen content fuels than they are with Jet A. However, emissions output with all three fuels is well below the goal. The variation in unburned hydrocarbon emissions with fuel/air ratio is more pronounced. This variation parallels trends observed in the single stage combustor, including higher emissions output and greater sensitivity to fuel composition at the lean fuel/air ratios. The performance improvements which accompany reductions in hydrogen content at the low fuel/air ratios may be due to the fuel volatility effect identified in Section 5.1.1. At the design idle fuel/air ratio, unburned hydrocarbon emissions with all three fuels are nearly identical and close to the goal.

To fully evaluate the emissions characteristics of staged combustors, carbon monoxide and unburned hydrocarbon output at approach must be considered in addition to emissions output at idle. Output of these constituents can be significant when the combustor is operating with both stages fired at the low overall fuel/air ratios encountered at approach. The alternative of operating on one stage is precluded by concern over engine acceleration capability. Figure 79 shows the variation in carbon monoxide and unburned hydrocarbon emissions at approach as a function of the pilot to main stage fuel flow split. Operation with ERBS fuel significantly increases the output of both constituents. The goal for carbon monoxide emissions can be achieved with Jet A fuel at all but the lowest pilot stage fuel fractions. Assuming a parallel variation in carbon monoxide output with pilot stage fuel flow fraction, it is doubtful that the goal can be achieved with ERBS fuel even at pilot stage fuel fractions approaching 90 percent. However, compliance with the proposed emissions standard is determined by weighting emissions output over the landing/takeoff cycle, and the levels which are cited as goals at idle and approach are an oversimplification of this weighted average. The actual EPA parameter for carbon monoxide emissions from the staged combustor operating on ERBS fuel is 22.67, which satisfies the goal of a maximum of 25. This parameter is computed with the carbon monoxide output levels shown in Figures 78 and 79 and the appropriate emissions output at higher power levels.

Unburned hydrocarbon emissions at approach are a more critical problem in that the levels observed with Jet A fuel already exceed the goal. In addition, emissions at approach and idle can not be traded to comply with the weighted average EPA parameter because they are already at or above the goal level at idle. Consequently, the unburned hydrocarbon emissions characteristics of the staged Vorbix combustor must be refined in order to meet the program goals with Jet A fuel. The introduction of ERBS fuel increases the need for refinement even further.

A major incentive for evaluating staged combustors is the capability of reducing oxides of nitrogen through lean combustion at high power levels. Figure 80 shows the effect of fuel composition on the NO_x emissions characteristics of the staged Vorbix combustor at the takeoff condition for the Energy Efficient Engine. As in the preceding figures, the emissions level cited as a goal is that which; in combination with a comparable level of emissions at lower power levels; would produce a weighted average EPA parameter that complies with the proposed standards for engines certified after 1984 (Table 2). Data obtained with Jet A fuel demonstrate the general emissions characteristics of the staged Vorbix combustor; the NO_x emissions index increases as overall fuel/air ratio rises. Shifting fuel from the main stage to the pilot stage produces proportionately greater increases in NO_x emissions due to the higher equivalence ratios in the pilot stage. While NO_x output with Jet A fuel is not low enough to meet the goal, emissions are substantially below the levels which could be achieved with a conventional single stage combustor in this high pressure ratio engine.

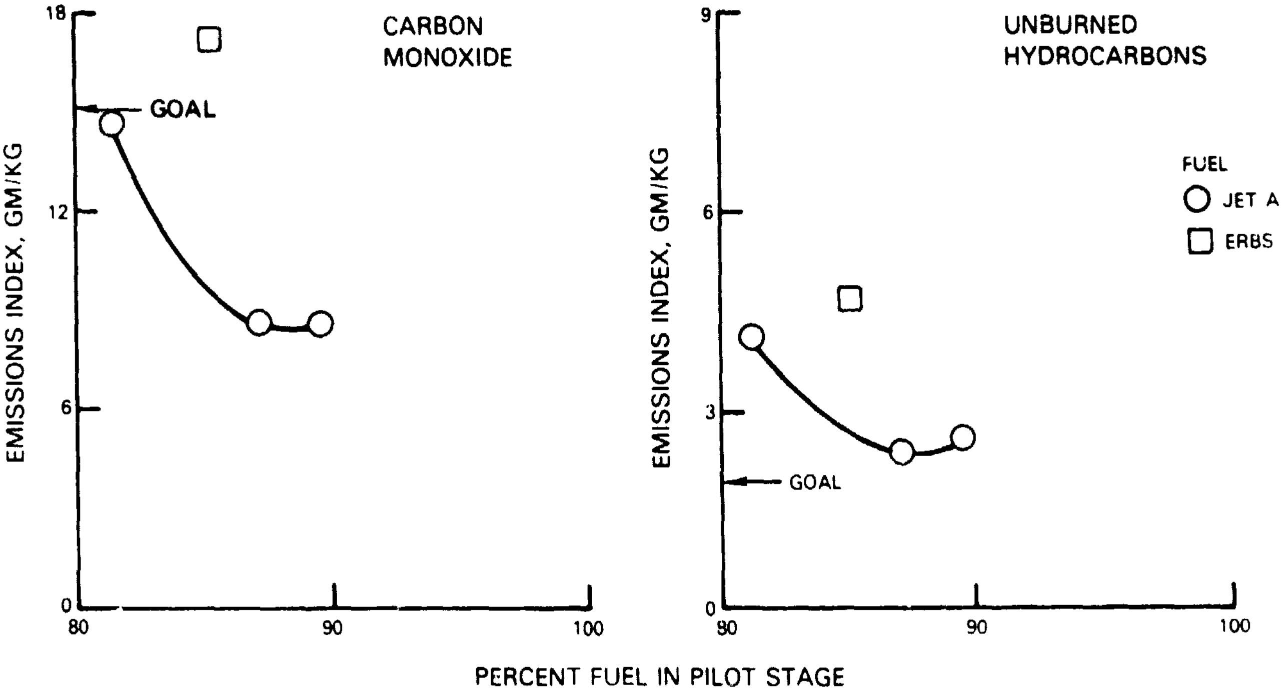

Figure 79 Emissions Characteristics of the Staged Vorbix Combustor at Approach

Operating the staged combustor on either ERBS fuel or the 11.8 percent hydrogen content fuel increases NO_x emissions at pilot zone equivalence ratios of both 0.45 and 0.65. This increase in emissions results from the higher flame temperatures produced by lower hydrogen content fuels which, as demonstrated in Section 7.1.3, increase the potential for formation of oxides of nitrogen. The fractional increases in NO_x emissions observed with the transition from Jet A fuel to the lower hydrogen content fuels are comparable in magnitude to the increases observed in single stage combustors (see Figure 65). Consequently, while staged combustion reduces nominal thermal NO_x emissions output, it does not reduce the sensitivity of the emissions characteristics to fuel composition.

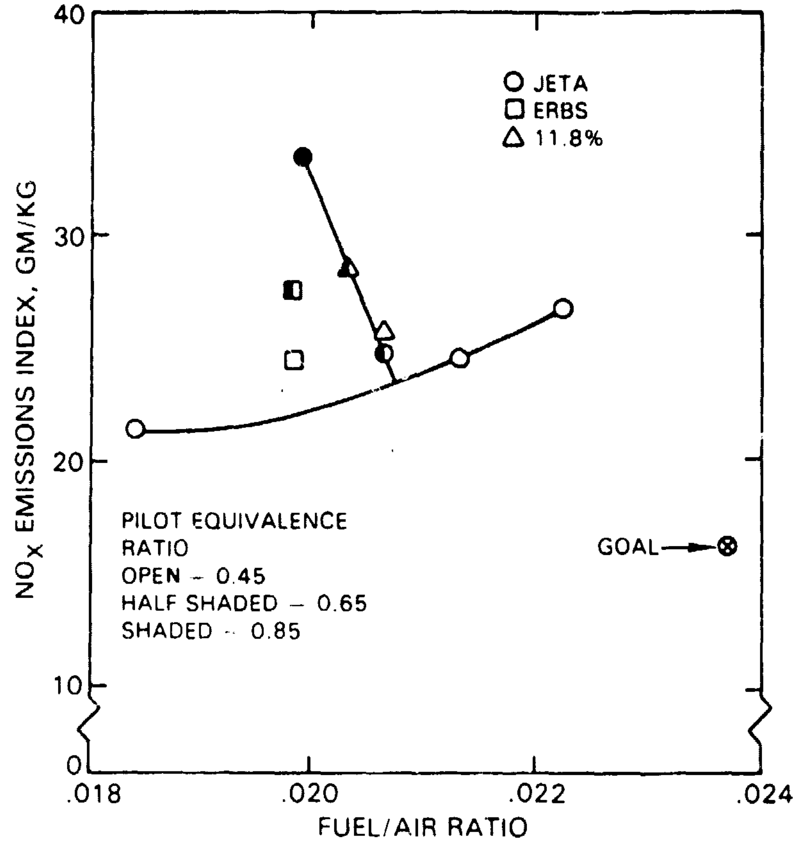

Figure 80 NO_x Emissions Characteristics of the Staged Vorbix Combustor at Takeoff

7.3.3 Smoke

The smoke output from the advanced Vorbix combustor was extremely low at all operating conditions. The SAE Smoke Number was less than unity at nearly all test points. No consistent variation in smoke output with fuel composition was observed.

7.3.4 Combustor Exit Temperature Distribution

The combustor exit temperature distribution was measured with fixed gas temperature thermocouples mounted on a vane pack behind the test combustor. Because the circumferential density of thermocouples was comparable to the density of the carburetor tubes in the power stage (vane spacing of 5.7° versus carburetor tube spacing of 7.5°) the features of the exit temperature distribution could not be correlated with the geometry of the combustor. When the combustor operated on Jet A fuel at simulated takeoff inlet conditions and a fuel/air ratio of 0.0213, the exit temperature pattern factor was 0.331.

This is somewhat higher than the 0.25 level observed in prior evaluations of the staged Vorbix combustor under the Energy Efficient Engine program. This increase has been attributed to higher than nominal fuel flow from the fuel injector in one carburetor tube in the main stage. When the combustor operated at the same conditions with the lower hydrogen content test fuels the high temperature streak produced by the injector still dominated the exit temperature distribution. Pattern factors of 0.305 and 0.368 were observed with ERBS fuel and the 11.8 percent hydrogen fuel respectively.

Circumferentially averaged radial temperature profiles constructed from these temperature distributions are shown in Figure 81. To achieve the required turbine blade life in the Energy Efficient Engine the entire temperature profile must be within the maximum local temperature envelope shown. The temperature profiles measured with all three fuels are characterized by a high temperature core and cool peripheral area, particularly at the outer radii. The elevated temperatures measured at the 30 percent span preclude achieving a satisfactory profile with any of the test fuels. Variations in the profile with fuel composition are shown to be small.

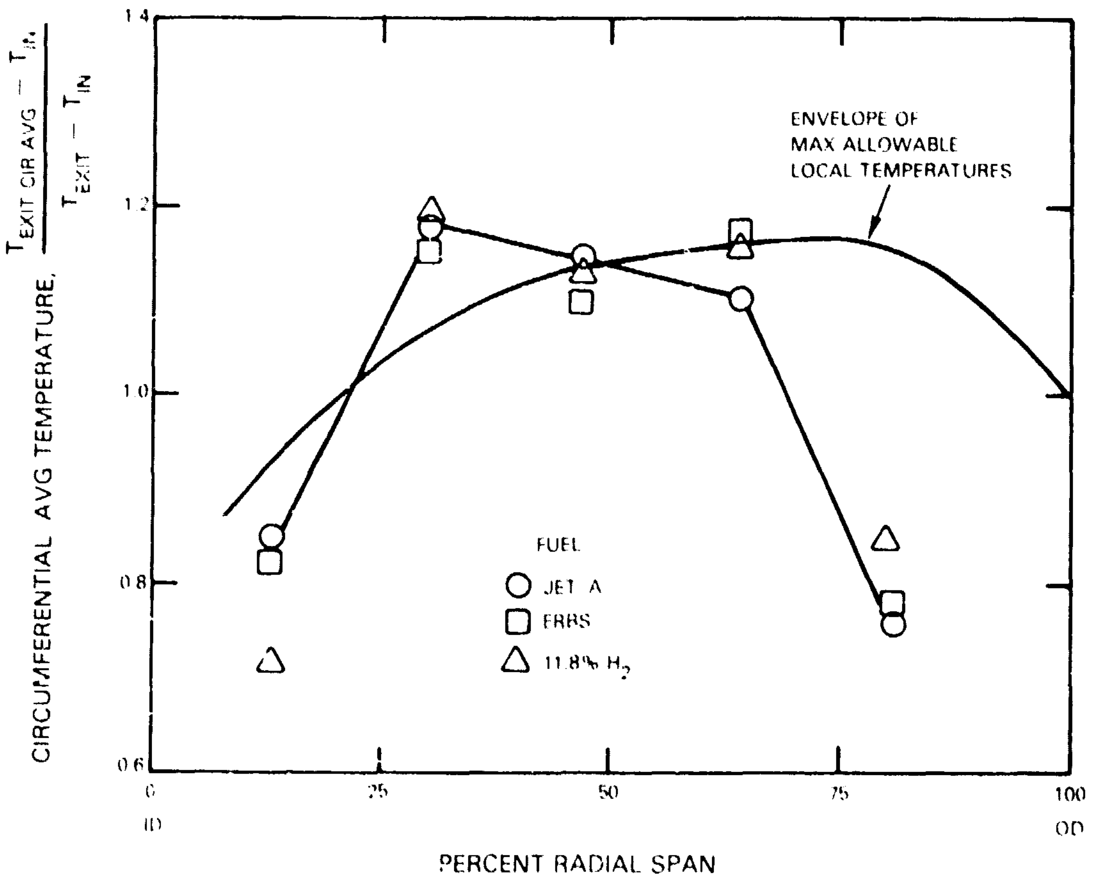

Figure 81 Exit Radial Temperature Profiles from the Staged Vorbix Combustor

Perturbations in the pilot to main stage fuel flow split at takeoff were investigated with all three test fuels. The pattern factor did not change more than +0.0015 relative to the values cited above and no significant shifts in radial temperature profile were observed.

7.3.5 Combustion Stability

The lean blowout fuel/air ratio was determined at idle inlet conditions with each test fuel to obtain a qualitative measure of the ignition and stability characteristics of the staged combustor. The measured lean blowout fuel/air ratio was 0.0057 with Jet A fuel, 0.0066 with ERBS fuel, and 0.0053 with 11.8 percent hydrogen content fuel. This sensitivity to fuel composition is moderate and follows the general trend of the combined viscosity and volatility characteristics of the fuels. The nominal level of the blowout fuel/air ratio is comparable to the level observed in the single stage combustor with a single pipe fuel injector.

7.3.6 Carbon Deposition

After the high pressure test of Configuration AV-1 had been completed, the test rig was opened and the components were inspected. There was no evidence of carbon deposition or any other distress on the liner segments, fuel injectors, or carburetor tubes.

7.3.7 Status of the Staged Combustor Concept

The high pressure tests indicate the advanced Vorbix combustor is capable of meeting the proposed carbon monoxide emissions standards for engines certified after 1984 with either Jet A or ERBS fuel. Unburned hydrocarbon emissions were low with both fuels but the levels are still marginal relative to the proposed standards. The use of staged combustion is a demonstrated method of achieving low NO_x emissions at high power. Although NO_x emissions were not reduced enough to satisfy the proposed standards, output was substantially below the level which could be achieved with a conventional single stage combustor in the high pressure ratio Energy Efficient Engine. In fact, the levels attained with the staged Vorbix combustor were the lowest in the program.

The effect of fuel composition on liner temperatures in the staged Vorbix combustor remains a paradox. Some of the data indicate that the increments in liner temperature associated with broadened properties fuels are considerably smaller than the temperature changes encountered in louver cooled single stage combustors. It is not clear whether these findings should be attributed to locally leaner combustion achieved with staging or a reduction in sensitivity to fuel composition due to internal convective cooling. However, the remaining data indicate that liner temperatures in the main stage are extremely sensitive to fuel composition. It appears that significant variations in the dispersion of fuel toward the inner liner altered the convective heat loads on these surfaces. The mechanisms causing these temperature excursions must be identified and densitized before the staged Vorbix combustor could be considered viable for extensive operation with broadened properties fuels.

7.4 VARIABLE GEOMETRY COMBUSTOR CONCEPT

The variable geometry combustor was selected as the third concept for evaluation in the Phase I program because the local stochiometry control accomplished by shifting the combustor airflow distribution could enhance the capability of operating with broadened properties fuels. Two basic variable geometry combustor design approaches were evaluated by conducting tests on fixed geometry combustor configurations respresentative of different positions of the variable components. The first design approach involved use of a variable-geometry single-pipe fuel injector while the second was a "fully modulated" variable geometry combustor in which massive quantities of combustor air could be shifted between the primary and dilution zones. Two variations of the "fully modulated" combustor were evaluated. These configurations were produced as perturbations of the baseline JT9D bulkhead combustor with the fuel injector operating in the single pipe mode as established by Configuration VG-1 and that configuration was the reference against which the performance of the different variable geometry approaches was evaluated.

7.4.1 Variable Geometry Fuel Injector

Combustor configurations VG-3 and VG-4 incorporated single-pipe fuel injectors with interchangeable central pintles that reproduced the extreme positions of a hypothetical axially-translatable variable-position pintle. As indicated in Section 4.3.2, prete t flow calibration and spray characterization had demonstrated that these changes in pintle position altered the injector airflow, its angular momentum and the spray angle. In both pintle positions the atomization characte istics were generally superior to the baseline injector operating in the single pipe mode. Table 25 presents a listing of the pertinent results of the high pressure evaluation of the combustor with the fuel injector pintle in both positions while operating on ERBS fuel. For comparison, the corr onding data obtained with the baseline combustor and single pipe fuel in... or in Configuration VG-1 is shown. The latter includes results obtained f. operation on both Jet A and ERBS fuel to provide indication of the ir ntal changes associated with that fuel transition.

The data obtained at idle indicate that the use of the variable geometry fuel injector, with the pintle in either position, had minimal effect on the carbon monoxide emissions at this power level. The concentration of this pollutant is slightly higher than that obtained with ERBS fuel in the baseline Configuration VG-1 with the fixed geometry fuel injector, and remains substantially above the level achieved with Jet A fuel in that configuration. Likewise, the unburned hydrocarbon emissions output at idle varies only slightly with the position of the pintle in the variable geometry injector and is higher than achieved in the baseline combustor with the same fuel.

However, use of the variable geometry fuel injector configurations led to significant improvement in the lean stability characteristics at idle. The lean blowout fuel air ratio with the pintle in either position is shown in Table 25 to be considerably lower than achieved with the baseline injector in

Table 25

Performance of Combustor with Variable Geometry Fuel Injector

Injector Type	Fixed Geometry		Variable Geometry	
Injector Position	Baseline	Single Pipe	Open	Closed
Configuration	VG-1	VG-1	VG-3	VG-4
Fuel	Jet A	ERBS	ERBS	ERBS
Performance at Idle				
Carbon Monoxide Emissions - gm/kg	16.0	28.0	29.5	30.5
Unburned Hydrocarbon Emissions gm/kg	1.1	2.3	3.6	3.8
Lean Blowout Fuel/Air Ratio	0.0061	0.0063	0.0041	0.0052
Performance at Takeoff (F/A = 0.0192)				
NOx Emissions - gm/kg	38.6	39.0	40.25	39.0*
SAE Smoke Number	3.8	4.3	2.6	3.0*
Exit pattern Factor	0.462	0.476	0.356	0.273
Primary Zone Liner Temperatures °K (°F)				
Max. at Cruise	1035 (1404)	1082 (1489)	1006 (1354)	947 (1245)
Average at Cruise	832 (1038)	853 (1076)	895 (1152)	855 (1080)
Max. at Takeoff	1168 (1644)	1233 (1760)	1101 (1523)**	1031 (1396)
Average at Takeoff	928 (1211)	945 (1242)	959 (1267)**	930 (1215)

* Extrapolated from higher fuel air ratio.
** Extrapolated from lower fuel air ratio.

Configuration VG-1. Curiously, use of the injector with the pintle in the open position; which admits more air through the injector and hence produces leaner local mixtures; produced a lower blowout fuel air ratio than the injector with the pintle retracted to restrict the airflow.

Shifting of the fuel injector pintle did not have a significant effect on the output of NOx emissions at takeoff. While extrapolation of the data from Configuration VG-4 was required to achieve a common fuel air ratio for comparison, the results presented on Table 25 indicate little variation in takeoff NOx emissions between the two configurations with the variable fuel injector and that with the baseline fixed geometry injector when they were operated on ERBS fuel. The SAE smoke number at takeoff was lower with the variable geometry injector in either position than it was with the baseline fixed geometry injector in Configuration VG-1 even when the latter was operated on Jet A rather than ERBS fuel. However, the nominal smoke output from all four fuel-configurational variations was small and the incremental differences are comparable to the experimental uncertainty.

Introduction of the variable geometry fuel injectors was found to have a significant effect on both the combustor exit temperature distribution and liner temperature levels at high power conditions. The improvement in exit temperature distribution is evident from the cited pattern factors which reduced progressively from the baseline Configuration VG-1 through Configurations VG-3 and VG-4. Figure 67 of Section 7.1 shows the combustor exit temperature distribution observed with Configuration VG-1. Evaluation of Configurations VG-3 and VG-4 indicated that the high temperature regions downstream of each fuel injector and in particular that behind the injector at the 27 degree circumferential position were progressively attenuated. Figure 82 shows the exit temperature distribution observed at takeoff with ERBS fuel in Configuration VG-4 and demonstrates that the high temperature streak that dominated the temperature distribution and established the pattern factor of Configurations VG-1 and VG-3 has been eliminated.

Similar effects are evident in the maximum liner metal temperature. This peak temperature occurred at the same location in all of the fuel-configurational variations listed on Table 25, i.e. downstream of a fuel injector on the third louver panel of the inner liner as shown in Section 7.1.2. The measurements indicated that use of the variable geometry fuel injector produced significant reductions in maximum liner temperature at both cruise and takeoff relative to the baseline Configuration VG-1 operating on the same ERBS fuel. When the injector pintle was in the open position the reduction in peak liner temperature at cruise was more than 70°K (140°F) which was nearly equal to the incremental change in peak liner temperature associated with the Jet A to ERBS transition in the baseline Configuration VG-1. Operation with the pintle in the closed position reduced these peak metal temperatures at cruise another 60°K (109°F).

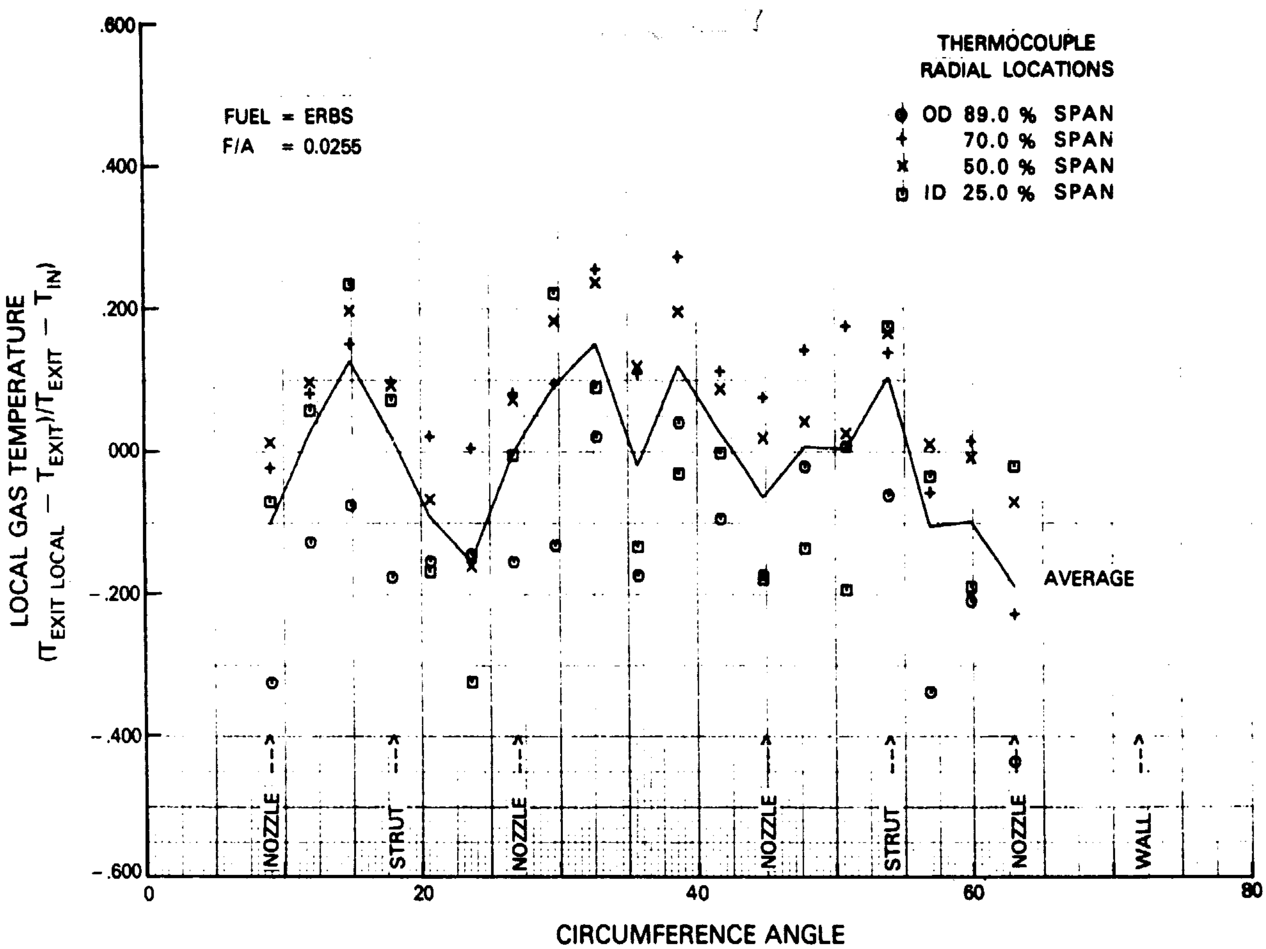

Figure 82 Combustor Exit Temperature Distribution at Takeoff With Variable Geometry Injector in Closed Position

Consideration of the listed average liner temperatures indicates that the mechanism of reduction of the maximum liner temperature differs with the position of the pintle in the variable geometry injector. When the pintle was in the closed position the average liner temperature in the primary zone was comparable to those in the baseline Configuration VG-1, implying that the use of this injector produced an attenuation of only the hot streaks downstream of the injector without causing a major shift in the heat load distribution on the remainder of the liner. Conversely use of the injector with the pintle in the open position led to increases in the average liner temperature in the primary zone while the reductions in maximum liner temperature were being achieved. This implies a more significant change in the heat load distribution on the liner.

The cause of the improved high power performance with the variable geometry injector is not evident. However, as described in Section 7.2.1 similar trends of reduced exit temperature pattern factors and peak liner temperatures were also observed in the single stage combustor configurations with the modified fuel injector. The geometry of the outer aerating air passage in the improved and the variable geometry injectors was identical and was a refinement relative to the baseline injector. It is suspected that this is the common aspect. Likewise, the cause of the lower liner temperatures and pattern factors with the variable geometry injector in the closed as opposed to open configuration cannot be positively identified, but the bench spray characterization tests described in Appendix B indicated that closing the pintle caused an increase in the spray angle which may have enhanced fuel dispersion.

Based on the data of Table 25 the viability of a variable geometry fuel injector with a translating pintle as simulated by Configurations VG-3 and VG-4 is questionable. The use of such an injector with the pintle in the closed position at high power would be desirable to achieve the exit temperature pattern factor and liner temperature advantages. However, there is little advantage to be gained by introducing a different injector geometry at low power.

Translating the pintle to the open position, as in Configuration VG-3, at low power appears to offer minute reductions in idle carbon monoxide and unburned hydrocarbon emissions and a 20 percent reduction in lean blowout fuel/air ratio with the latter having possible favorable implications regarding altitude stability and ignition. However, it is doubtful that the added complexity of a variable fuel injector could be considered acceptable for this small performance advantage. Rather the results of this evaluation indicate that the closed pintle injector of Configuration VG-4 should be considered in the context of a fixed-geometry single-pipe injector that offers considerable potential for use in either a single stage or another variable geometry combustor concept.

7.4.2 Fully Modulated Variable Geometry Combustor

Two sequences of combustor configurations were evaluated to assess the viability of a fully modulated variable geometry combustor as a means of accommodating the use of broadened properties fuels. The initial sequence included combustor Configurations VG-1, VG-5 and VG-6 which were variations of the baseline louver-cooled JT9D-7F bulkhead combustor with the baseline fuel injector operated in the aerated single pipe mode. The second sequence encompassed Configurations VG-7 and VG-8 and was representative of a more advanced design approach in that it employed Finwall® structure in the liners enclosing the primary combustion zone as described in Section 4.3.2. The variable fuel injector with the pintle in the closed position was used as a fixed-geometry single-pipe injector in this sequence of configurations. Both of these sequences included the entire range of variation of airflow distribution that could be accommodated in the hypothetical fully-modulated variable-geometry combustor which operated at an essentially invariant pressure drop so as to maintain constant liner cooling and fuel injector aerating airflow.

The results of the evaluation of these sequences were used initially to establish the optimum scheduling of the airflow distribution in the combustor: i.e. to define the fractions of combustor airflow the variable geometry mechanism should deliver to each zone of the combustor. The primary zone airloading - the fraction of combustor airflow entering the primary zone through both the fuel injector and its surrounding insert and collar and the primary combustion air orifices in the liner - is the principal variable in the optimization. Figure 83 shows the trend of critical emissions characteristics of the variable geometry combustor synthetized from Configurations VG-1, VG-5 and VG-6. Data are presented for the carbon monoxide and unburned hydrocarbon emissions at the idle condition of the JT9D-7F engine and for the oxides of nitrogen at the takeoff condition of that engine. The goals shown on the figure for each constituent are the levels that would have to be achieved at that operating condition to attain the proposed requirements of Table 2 for an engine certified after 1984 if consistent emissions levels are also maintained at other power conditions. The data indicate the carbon monoxide emissions dictate the optimum air loading at the idle condition. A primary combustion zone loading of 25 percent or less of the total combustor airflow would be required to achieve the goal for carbon monoxide emissions while operating on ERBS fuel. At that loading the goal for unburned hydrocarbon emissions would be satisfied by a comfortable margin. Of course, reducing the primary zone airflow further at low power levels, such as the 17 percent of total airflow incorporated in test Configuration VG-6, could be advantageously pursued to enhance low power combustion stability and provide wider margin for compliance with the carbon monoxide and unburned hydrocarbon emissions goals.

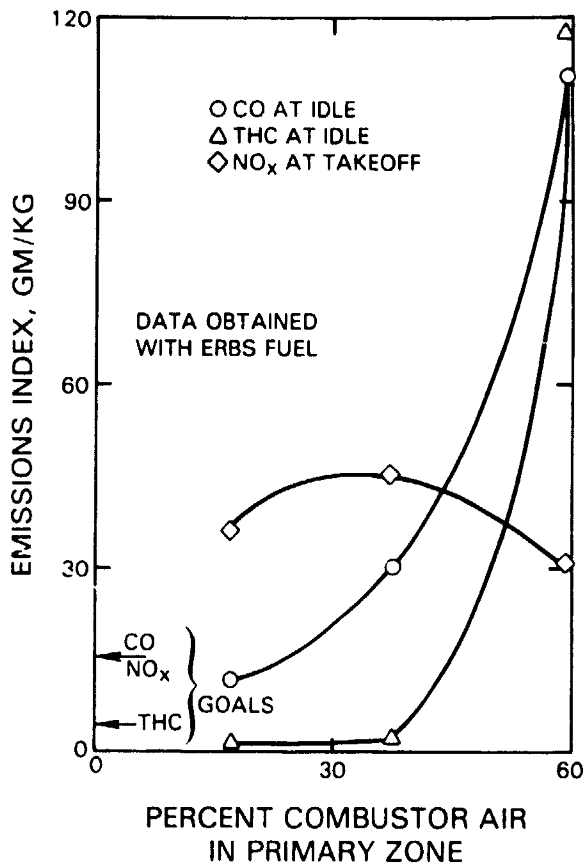

Figure 83 Emissions Characteristics of a Variable Geometry Combustor

The takeoff NOx emissions data of Figure 83 indicate that the trade with primary zone airflow, and hence bulk equivalence ratio, is very limited. The emissions peak at an air loading that corresponds to a bulk primary zone equivalence ratio of about unity at takeoff. Increasing this air load to the maximum practical level of about 60 percent (i.e. Configuration VG-5), at which all combustor air not used for liner cooling is admitted to the primary zone, produced a bulk equivalence ratio of about 0.6 in that zone at takeoff. However, this accomplished only a 30 percent reduction in the NOx emissions leaving the emissions index still at nearly twice the goal level. The inability to reduce NOx emissions by more substantial amounts with the introduction of massive quantities of additional primary zone air appears to be attributable to the strong recirculation zones formed by the air discharge from the aerated fuel injectors in the bulkhead type combustor. Apparently, the jets of additional combustion air introduced through aperatures in the liners immediately downstream of these injectors do not have sufficient momentum to effectively penetrate these recirculation zones. Consequently, while the bulk equivalence ratio of the primary zone is reduced, the mixture strengths in the NOx formation regions remained nearly invariant and little net reduction in NOx emissions was accomplished.

Based on the data of Figure 83, a variable geometry combustor synthesized from Configurations VG-1, VG-5 and VG-6 would not be attractive from the isolated point of view of emissions control. In fact, the data of this figure indicate that nearly as favorable emissions characteristics could be achieved by retaining a fixed geometry combustor with very low primary zone air loading. However, variation of primary zone stochiometry also has a significant effect on combustor liners heat load and the variable geometry features used to reduce NOx emissions at high power would also contribute to enhanced liner life. Figure 84 shows the measured average metal temperatures in the bulkhead and in liners enclosing the primary and the dilution zones of this sequence of combustor configurations. With the exception of some anomalies in the data from thermocouples on primary zone liner panels, the measurements exhibit a trend of substantial decrease in metal temperature with increasing primary zone air loading at both the cruise and takeoff operating conditions. The liner cooling air flow rates were maintained essentially invariant in these configurations and the reduced metal temperatures must be attributed to the lower bulk equivalence ratio in the primary zone. Even if, as deduced in the discussion above, the additional primary zone air was not participating in the reactions sufficiently to suppress NOx production, it was evidently effective in attenuating the heat load on the bulkhead and parts of the liner.

A comparison can be made between the liner metal temperature in a fixed and a variable geometry combustor, both of which operate with low primary zone air loadings; of the order of twenty percent of the combustor air flow; at low power levels in order to satisfy idle emissions, stability or ignition constraints. It is evident from the data of Figure 84 that, if the variable geometry combustor were capable of increasing the primary zone air loading to 60 percent of combustor airflow at high power levels it could potentially have local metal temperatures in the louvers enclosing the primary zone 28 to 42°K (50 to 75°K) lower than the fixed geometry combustor at takeoff. Temperature reductions of this magnitude could more than offset the increases associated with the use of broadened properties fuels in fixed geometry combustors such as those of Section 7.1 and could contribute to the viability of the fully modulated variable geometry combustor concept.

ORIGINAL PAGE IS
OF POOR QUALITY

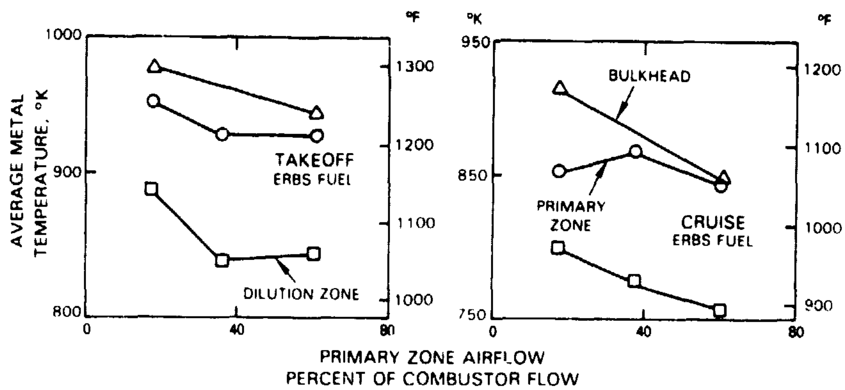

Figure 84 Effect of Primary Zone Air Loading on Liner Temperatures in Variable Geometry Combustor

Based on these considerations of the emissions characteristics and liner durability impacts in the first sequence of combustor configurations, the airflow schedule of the hypothetical fully modulated variable geometry combustor was refined prior to definition of the final sequence of configurations. To satisfy emissions constraints and meet ignition and stability requirements it was concluded that the primary zone airloading incorporated in Configuration VG-6 was close to optimum for low power levels and that the actuation of the variable geometry system to produce higher primary zone airloadings should occur in the range above the 30 percent thrust approach sea level power setting and be completed prior to attaining cruise conditions. It was also concluded that the primary zone airloading should be at the highest attainable level in the configuration simulating the high power operating mode of the combustor to emphasize reduction of the NOx emissions at these operating conditions. Consequently, in defining Configuration VG-8 the liner cooling air that had been eliminated by incorporating the Finwall® liner panels was diverted to the primary combustion air jets. The positioning of the combustion air holes in the liner in this configuration was altered to improve the interaction of these jets with the reaction zones inside the combustor.

Table 26 presents the performance characteristics of the two hypothetical fully-modulated variable-geometry combustors. The initial combustor is that synthesized from the performance of Configurations VG-1, VG-5 and VG-6 as described above, while the final version is that based on data obtained from Configurations VG-7 and VG-8. The table also shows the program goals relevant to the variable geometry combustor concept and the performance of the fixed geometry baseline Configuration VG-1 when it was operated on Jet A fuel.

Table 26

Performance Characterisitics of Fully Modulated Variable Geometry Combustors

		Program Goal	Baseline Single Stage	Fully Modulated Variable Geometry: Initial	Fully Modulated Variable Geometry: Final
Combustor Configuration		-	VG-1	VG-5/6	VG-7/8
Fuel Injector		-	Baseline Single Pipe	Baseline Single Pipe	Var. Closed Position
Liner Type		-	Louver	Louver	Finwall®
Airflow Distribution (% Wab)					
Primary/Dilution Zones	@ Idle/Approach	-	32.5/23.6	17.0/39.1	17.9/42.1
	@ High Power	-	32.5/23.6	56.1/0	60.0/0
Fuel		ERBS	Jet A	ERBS	ERBS
Idle Performance					
Carbon Monoxide Emissions (gm/kg)		14.0[1]	16.0	10.2	23.3
Unburned Hydrocarbon Emissions (gm/kg)		2.0[1]	1.1	1.0	5.3
Lean Blowout Fuel/Air ratio		Note 2	0.0061	0.0052	Note 3
Takeoff Performance (F/A = 0.0193)					
NOx Emissions (gm/kg)		16.0[1]	38.6	27.5	35.3
SAE Smoke Number		19.2	3.8	1.7	1.3
Exit Pattern Factor		0.25	0.462	0.473	0.359
EPA Emissions Parameters					
Carbon Monoxide		25.0	27.3	19.8	39.2
Unburned Hydrocarbons		3.3	1.8	1.63	8.7
Nitrogen Oxides		33.0	68.7	56.5	65.4
Average Liner Metal Temperatures °K (°F)					
	Bulkhead	No higher	870(1107)[4]	826(1027)	964(1277)
Cruise	Primary Zone	than	832(1038)	838(1050)	Note 5
	Dilution Zone	baseline	774(934)	754(899)	769(925)
		combustor			
	Bulkhead	with	952(1255)[4]	902(1164)	1047(1426)
Takeoff	Primary Zone	Jet A	928(1211)	940(1234)	Note 5
	Dilution Zone	Fuel	857(1084)	850(1072)	844(1061)

Notes: (1) Approximate goal to achieve EPA parameter if emissions at other power levels are consistent.
(2) Consistent with reference engine.
(3) Altitude stability and ignition capability evaluated. See Section 7.5.
(4) Estimated from measurements on Configurations VG-5 and VG-6.
(5) Finwall® panels not instrumented.

The data indicate that the baseline fixed geometry combustor could achieve the goals for unburned hydrocarbon emissions appropriate to post 1984 engine certification but was marginally deficient of the corresponding goal for carbon monoxide emissions. However, the initial version of the variable geometry combustor achieved the goals for both of these constituents by comfortable margins even when operating on ERBS rather than Jet A fuel. This was an obvious consequence of the enrichment of the primary combustion zone that can be accomplished at low power levels in the variable geometry combustor. The carbon monoxide and unburned hydrocarbon emissions characteristics of the final version of the variable geometry combustor were not as good as those of its predecessor with the goals for both of these constituents being exceeded. This version had incorporated the "variable" fuel injector with the pintle in the closed position from Configuration VG-4 and this deterioration in low power emissions characteristics had been anticipated on the basis of experience with that configuration.

The use of the variable geometry concept is shown to lead to improvement in the combustion stability at idle. The enrichment of the primary zone of the initial version of this combustor produced a 15 percent reduction in lean blowout fuel air ratio relative to the baseline fixed geometry combustor despite the use of ERBS rather than Jet A fuel. While the idle stability of Configuration VG-7 was not investigated, the experience of evaluating Configuration VG-4 with the same fuel injector implies that the fully modulated variable geometry combustor synthesized from this configuration should have even lower blowout fuel air ratios. Configuration VG-7 was however, subjected to a series of sea level and altitude ignition tests in an altitude test facility. The results of this evaluation are discussed in detail in Section 7.5 and demonstrate superior altitude ignition capability of the variable geometry combustor concept relative to a fixed geometry single stage combustor.

The NOx emissions characteristics of both versions of the fully modulated variable geometry combustor are below expectations for this type of combustor. Relative to the baseline fixed geometry combustor, the initial version of this combustor produced only a 29 percent reduction in NOx emissions at takeoff and an 18 percent decrease in the overall EPA parameter for oxides of nitrogen. As indicated previously in this section, the limited NOx emissions reduction achieved with this configuration appeared to be attributable to inadequate mixing in the primary combustion zone. While the positioning of combustion air jets in the primary zone had been altered to enhance mixing in Configuration VG-8, the high power NOx emissions and consequently the EPA parameter were even higher in the final variable geometry combustor. Similar higher than anticipated NOx emissions were observed in the evaluation of Configuration SS-7 which also incorporated the combustor liner sector with the Finwall® in the panels enclosing the primary zone. As indicated in Section 7.2.4 it was suspected that the use of the grommetted combustion air orifices in the Finwall® panels may have altered the penetration characteristics of the air jets. This could have further reduced their ability to mix with the combustion products inside the liner and led to richer local combustion.

Further evidence of this locally rich initial combustion is apparent in the measured temperatures on the combustor bulkhead as listed on Table 27. The average measured metal temperatures are shown for the final variable geometry combustor configurations - Configurations VG-7 and VG-8. Both of these incorporated the Finwall® liner panels but with widely different primary zone air loadings and hence equivalence ratios at takeoff. Comparison of the data for Configuration VG-8 with Configuration VG-5 having similar bulk primary zone equivalence ratio, but different liner construction and fuel injectors, indicates that the bulkhead was substantially cooler in the latter configuration. The temperature levels observed in Configuration VG-8 are comparable to those measured in Configuration VG-7, which had a significantly higher bulk equivalence ratio in the primary zone. This is further evidence that with the Finwall® liner construction and the closed position variable fuel injector the reaction zone stochiometry must be relatively independent of the bulk stochiometry of the primary zone despite the presence of massive quantities of additional air in the combustion air jets.

Table 27

Effect of Primary Zone Configuration on Bulkhead Temperatures with ERBS Fuel

Configuration	VG-5	VG-8	VG-7
Liner	Louver	Finwall®	Finwall®
Fuel Injector	Baseline	Var. Closed	Var. Closed
Primary Zone			
Airloading ~ % Wab	56.1	60.0	17.9
Bulk Equivalence Ratio at Takeoff	0.60	0.57	2.03
Avg. Bulkhead Metal Temperature °K (°F)			
at Cruise	826 (1027)	964 (1277)	980 (1304)
at Takeoff	902 (1164)	1047 (1426)	1051 (1433)

One of the major concerns in the operation of a fully modulated variable geometry combustor is the ability to control the combustor exit temperature distribution if all of the available combustion air is diverted to the primary combustion zone at high power levels. The results of the evaluation of the initial version of the variable geometry combustor in the high power mode; i.e. Configuration VG-5; indicated that the combustor exit temperature pattern factor at takeoff, while substantially above the program goal as shown as Table 26, was not much greater than that measured with the baseline fixed geometry combustor having considerable dilution zone airflow. The exit temperature distribution also retained the dominant features of that observed in the evaluation of the baseline combustor Configuration VG-1. Furthermore, measurements of the exit temperature distributions from the final version of the variable geometry combustor in the high power mode, i.e. Configuration VG-8, indicated a significantly lower pattern factor than that of Configuration VG-5. These trends are consistent with prior experience with the fuel injectors in these configurations and imply that the characteristics of the fuel injectors dominate the exit temperature distribution in this type of combustor. However, they do not serve to alleviate the basic concern over the ability to control the exit temperature distribution in the absence of dilution air.

7.4.3 Status of the Variable Geometry Combustor Concept

The results presented in this section provide an indication of the viability of two versions of a variable geometry combustor for accommodating the use of broadened properties fuels. The first version incorporated a variable geometry fuel injector capable of modulating the quantity of air admitted through the aerating passages. Its evaluation revealed that there were no significant advantages to be achieved from the point of view of emissions, durability or operational performance from this approach. However, the fixed geometry fuel injectors that were used to simulate the variable injector were found to produce significant improvements in combustor exit pattern factor, combustor stability margin and maximum liner temperature levels which could be used to advantage in more conventional single stage combustors with single pipe fuel systems.

The synthesis of the characteristics of fully modulated variable geometry combustors from the evaluation of appropriate fixed geometry configurations indicates this concept has considerable potential for accommodating the use of broadened properties fuels. The ability to enrich the primary combustion zone by restricting its airloading at low power levels has been found conducive to improved ignition and stability margin and to achieving carbon monoxide and unburned hydrocarbon emissions levels consistent with the proposed EPA standards for engines certified after 1984. Furthermore, by increasing the primary zone airloading to reduce the equivalence ratio at high power the heat load on the liners may be reduced. The associated incremental changes in liner metal temperature are more than adequate to offset those associated with a Jet A to ERBS transition.

Several major deficiencies were also observed in the evaluation of simulated fully-modulated variable-geometry combustors. Despite maintaining primary zone bulk equivalence ratios of 0.60 and less at takeoff, the NOx emissions characteristics were substantially higher than anticipated. This has been traced to incomplete mixing in the conventional swirl stabilized primary combustion zone but raised concern over the need for more complex combustor designs if a greater degree of mixture homogeneity is required for control of NOx emissions. There is also concern over operation of a variable geometry combustor at high power levels if all of the available combustor airflow is diverted into the primary zone since this would leave no mechanism for control of the combustor exit temperature distribution. These difficulties lead to questioning of the practicality of the full modulated airflow version of the variable geometry combustor. In particular, could a less complex variable geometry combustor in which only the primary zone airflow is modulated be more tractable and still offer the opportunity to enhance ignition, low power emissions and liner heat load while operating on broadened properties fuels? A variable geometry combustor of this type will be investigated in Phase II.

7.5 IGNITION AND STABILITY EVALUATION

The final version of each combustor concept was evaluated in an altitude test facility to assess the impact of broadened properties fuels on ignition and altitude stability characteristics. A brief description of each configuration follows:

- o Single Stage Combustor - Configuration SS-7 incorporated the advanced Finwall® liner construction in the primary zone and the modified duplex fuel injector.

- o Staged Combustor - Configuration AV-2, an advanced staged Vorbix combustor, had the same aerodynamics and stoichiometry as the high pressure test configuration but incorporated a louver cooled sheet metal liner.

- o Variable Geometry Combustor - Configuration VG-7 simulated a fully modulatable variable geometry combustor with a single pipe fuel injector. The airflow control system produced low primary zone airloading, i.e., a rich primary zone stoichiometry which would be desirable at ignition and other low power operating conditions.

The single stage and variable geometry combustor configurations were evaluated at representative conditions for the JT9D-7F engine, while the staged Vorbix combustor was evaluated under simulated operating conditions for the Energy Efficient Engine.

7.5.1 Altitude Ignition and Stability Characteristics

In Figure 85 the ignition boundaries and minimum pressure stability envelopes for Configuration SS-7 are superimposed on the required ignition envelope for the JT9D-7F engine, which was defined in Section 3.4. The overall ignition capability and blowout margin for this configuration are low relative to levels achieved with JT9D components during flight testing. However, previous experience correlating data from rig tests with data obtained during flight testing indicates that these findings are characteristic of JT9D combustors. Rig data accurately reflects the incremental changes in ignition capability or stability margin produced by a combustor modification but generates consistently pessimistic absolute levels.

When the results of the fuel sensitivity evaluation are interpreted on this basis, it can be seen that the ERBS fuel and the 11.8 percent hydrogen content test fuel produce some reduction in the altitude ignition capability of the single stage combustor. However, the minimum pressure stability envelope is shown to be independent of fuel composition.

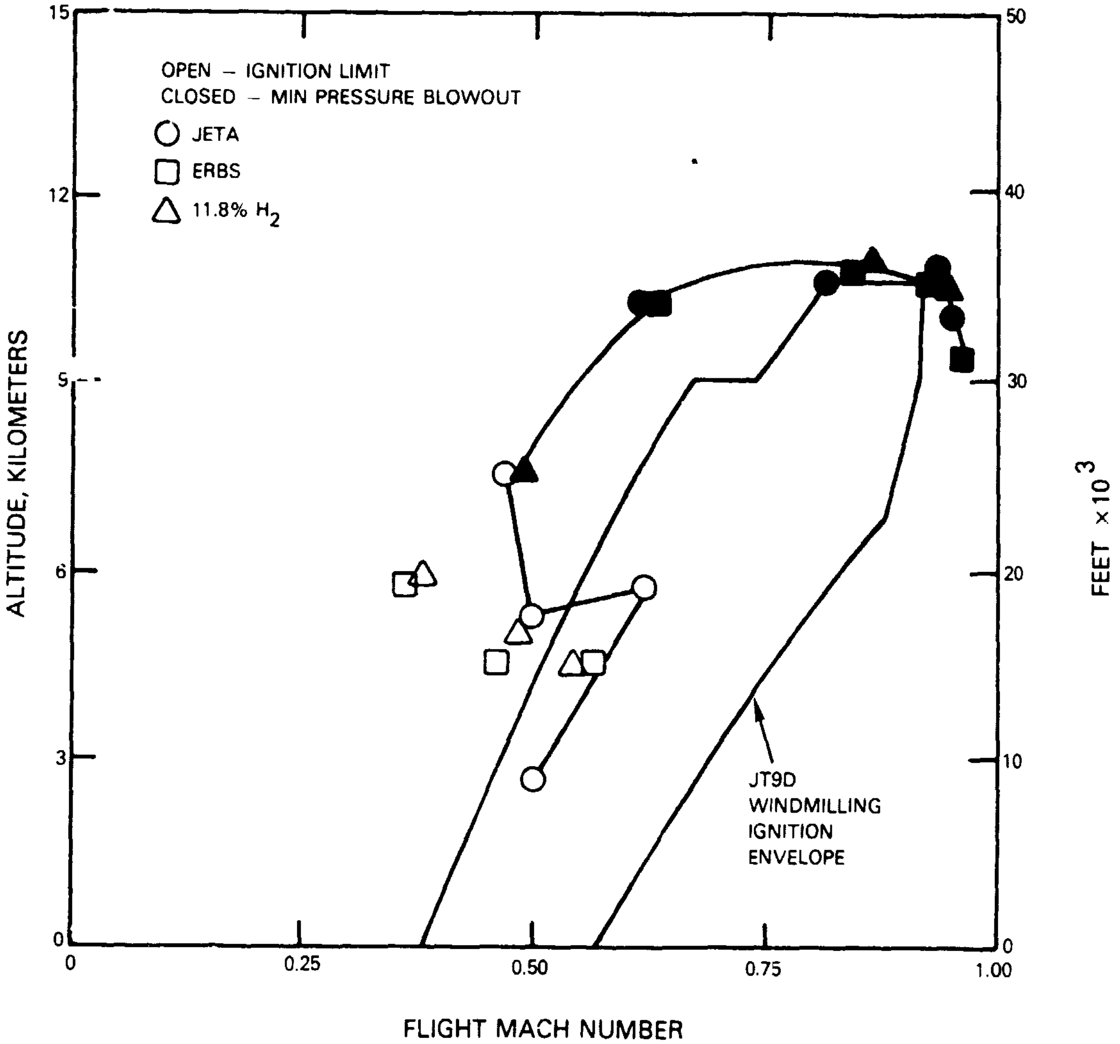

Figure 85 Altitude Ignition and Stability Characteristics of Configuration SS-7

Figure 86 shows the ignition characteristics of the advanced Vorbix combustor relative to the required ignition envelope for the Energy Efficient Engine. The combustor could be ignited at all attainable conditions within the envelope. In addition, ignition was achieved with all three test fuels at the critical points shown in the figure. However, the fuel control schedule for the Energy Efficient Engine calls for richer fuel/air ratios at ignition than the JT9D-7F, which may have facilitated starting. Attempts to document a minimum pressure stability boundary for the staged Vorbix combustor were unsuccessful; blowout could not be produced at the minimum scheduled fuel flow over the range of vacuum capabilities in the facility, which included simulated altitudes in excess of 13.5 kilometers (45,000 feet).

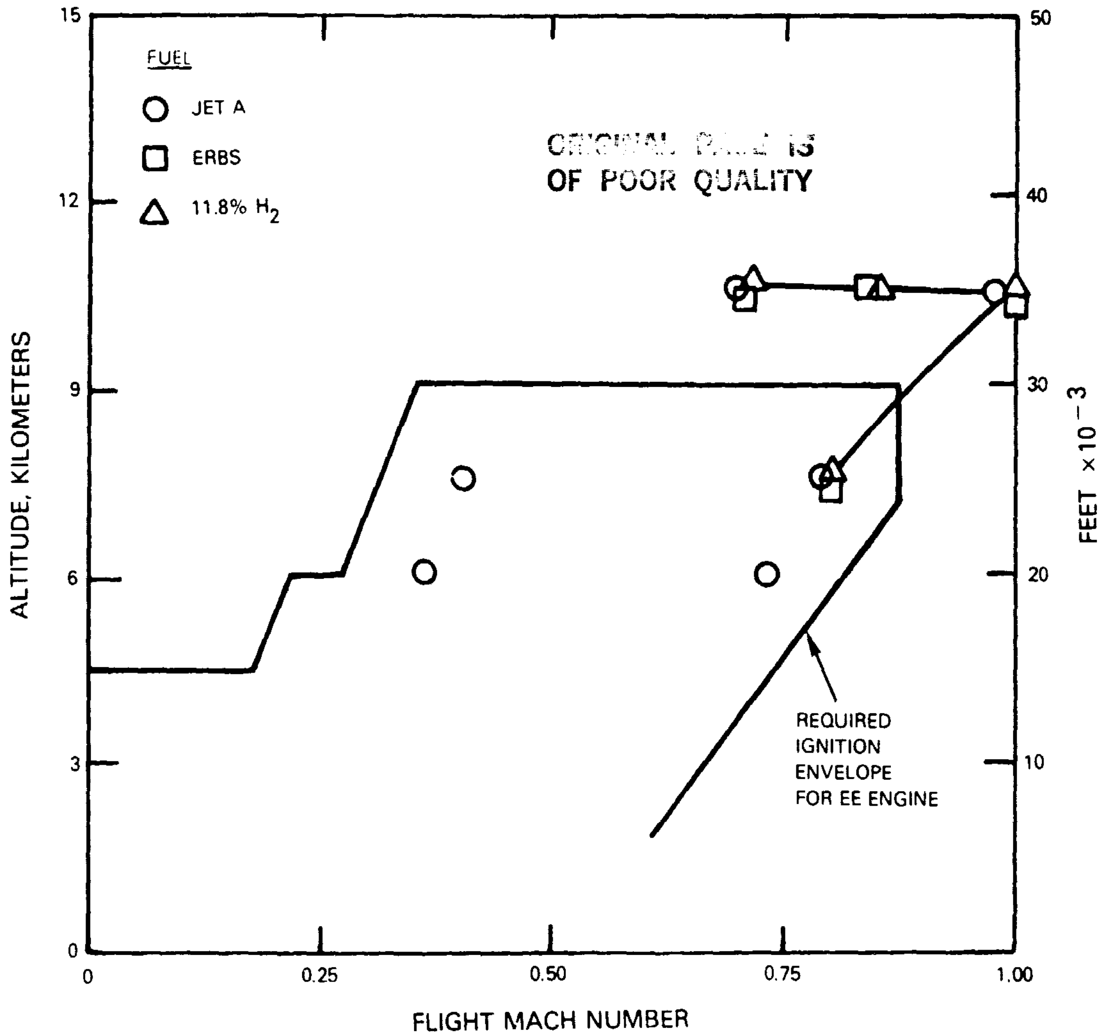

Figure 86 Ignition Characteristics of Configuration AV-2

The measured ignition envelope for the advanced variable geometry combustor, Configuration VG-7, is shown in Figure 87. A comparison with Figure 85 indicates, ignition capability with Jet A fuel improved somewhat relative to the single stage combustor. The data presented in Appendix B do not support this finding in that fuel atomization characteristics with the single pipe aerated injector used in the variable geometry combustor are significantly poorer at ignition than the characteristics of the pressure atomizing primary system of the duplex injector used in the single stage combustor. Evidently the richer primary zone stoichiometry of the variable geometry combustor in the low primary zone airloading mode is sufficient to overcome the atomization deficiency and produce the cited improvement in ignition capability.

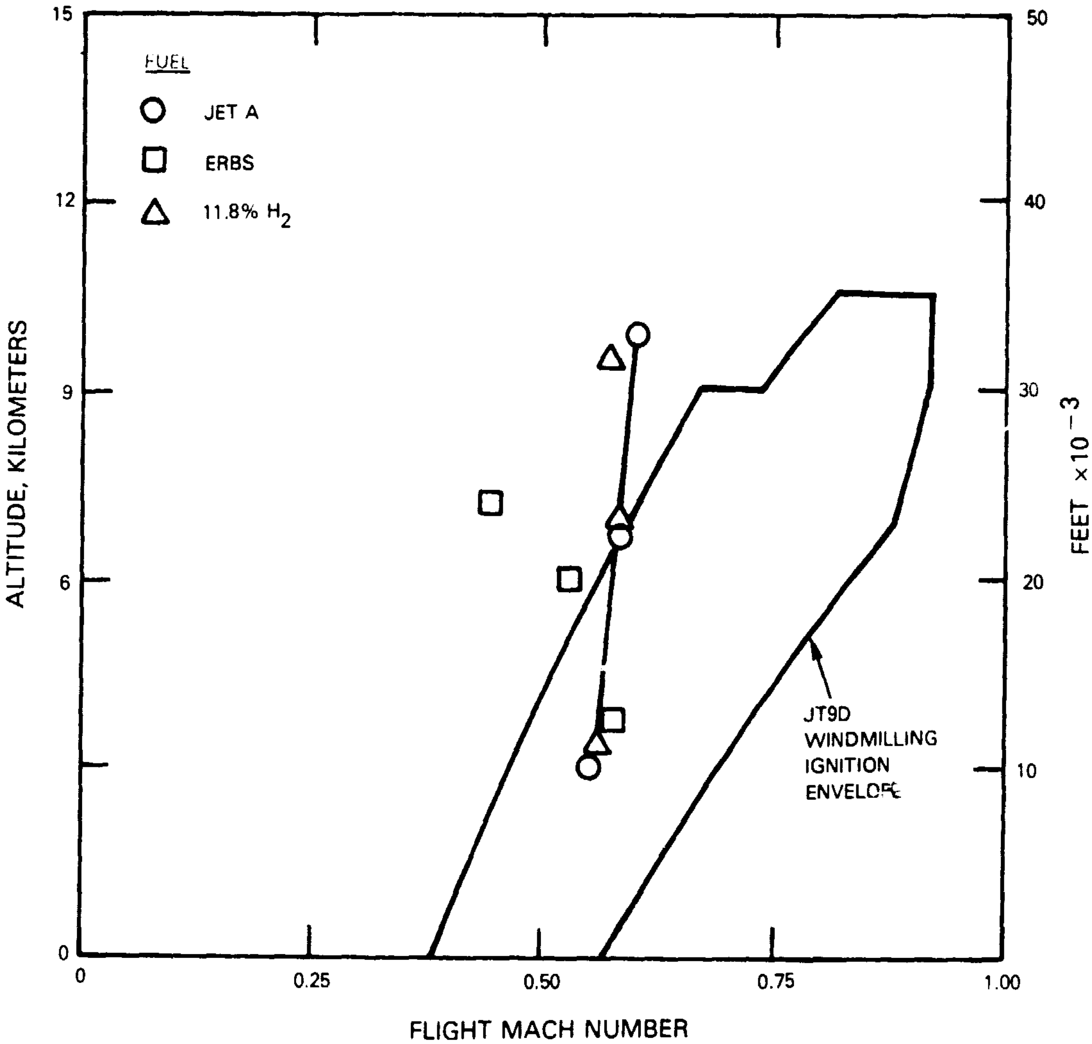

Figure 87 Ignition Characteristics of Configuration VG-7

While the ignition boundaries of the variable geometry combustor are nearly identical with Jet A fuel and the 11.8 percent hydrogen content test fuel, the ignition boundary observed with ERBS fuel is somewhat lower. This difference may be due to the viscosity and volatility trends of these fuels, cited previously (Section 5.1). As shown in Table 12, the viscosity and low volume distillation temperature ranges of Jet A fuel and the 11.8 percent hydrogen content fuel are comparable, implying that the atomization and vaporization characteristics, which are critical to ignition, are similar. The viscosity and low volume distillation temperatures of the ERBS fuel are higher which tends to impede fuel vaporization and hence ignition.

7.5.2 Sea Level Ignition Evaluation

The impact of fuel composition on the sea level ignition capabilities of the three combustor concepts was also evaluated. The JT9D-based single stage and variable geometry combustors were evaluated at air and fuel temperatures of 250°K (-10°F), while the advanced Vorbix combustor was evaluated at an air temperature of 278°K (40°F) and a fuel temperature of 273°K (0°F) due to high ambient humidity at the time of the test.

Results of the evaluation of the single stage combustor, Configuration SS-7, are presented in Figure 88. In most instances, rapid ignition was achieved with Jet A fuel at 85 percent of nominal ignition flow. Progressively higher fuel flow rates were required to achieve consistent ignition with the ERBS fuel and the 11.8 percent hydrogen content fuel, implying a sensitivity to fuel composition. However, the incremental increases required to achieve ignition with the broadened properties fuels were small and satisfactory results could be achieved without exceeding the nominal ignition flow. Similar results were observed with the staged Vorbix combustor (Configuration AV-2) and the variable geometry combustor (Configuration VG-7). Ignition capability was somewhat sensitive to fuel composition, but each combustor had an adequate ignition margin with Jet A fuel to accommodate this sensitivity.

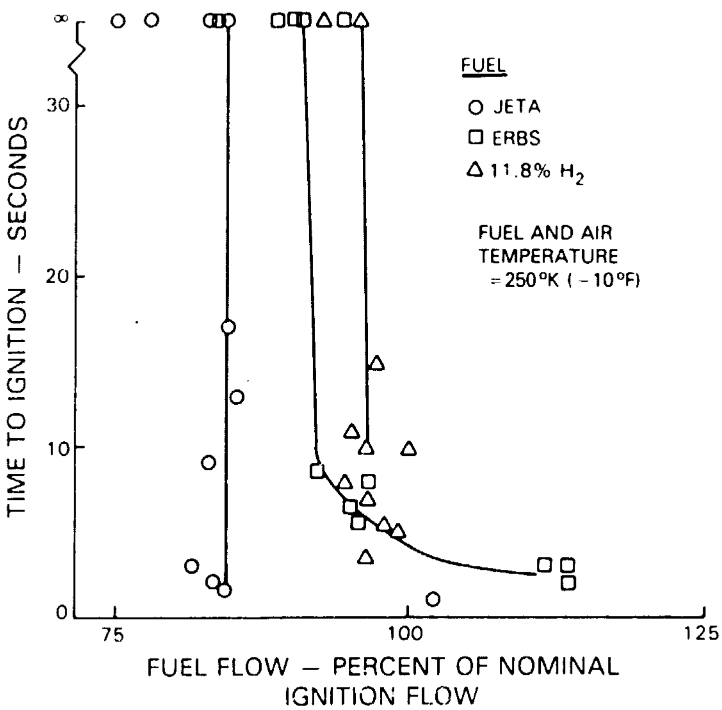

Figure 88 Sea Level Ignition Characteristics of Single Stage Combustor Configuration SS-7

7.5.3 Summary of Ignition and Stability Effects

The evaluation of the final configuration of each combustor concept indicates that ignition capability can be affected by fuel composition. Although the differences were moderate, they indicate a general sensitivity to fuel viscosity and volatility effects at simulated altitude ignition conditions. Conversely, sea level ignition also appeared to be sensitive to fuel composition, implying a different controlling mechanism.

The staged Vorbix combustor demonstrated better altitude ignition capability than the advanced version of the single stage combustor, but this improvement may be due in part to differences in the engine cycle. Use of variable geometry to enrich the primary zone of an otherwise single stage combustor also improved ignition capability.

SECTION 8.0

CONCLUDING REMARKS

The results of Phase I of the Broad Specification Fuels Combustion Technology Program have demonstrated that the use of Experimental Referee Broad Specification (ERBS) fuel rather than Jet A fuel can have a significant impact on the operation of conventional single stage JT9D combustors. Reductions in liner life of about 13 percent are anticipated from the data as are higher carbon monoxide and unburned hydrocarbon emissions and some deterioration in ignition capability. The program results also indicate that advanced combustion technology offers the potential for reducing these sensitivities. Modest reductions with the least configurational impact appear attainable with the introduction of improved fuel injectors and advanced liner constructions. More advanced technology combustor concepts, such as staged and variable geometry combustors, are less sensitive to changes in fuel composition and offer more flexibility of operation. However, the technical risks associated with the development and use of these complex combustor concepts are large. If these advanced technology combustors were required solely for the purpose of accommodating a particular broadened properties fuel, the costs and risks involved would become major factors in a cost-benefit analysis of the acceptability of that fuel.

While not addressed specifically in the Phase I program, consideration of the use of broadened properties fuels also leads to concern over deterioration in thermal stability with increased propensity for carbon deposition in fuel injectors and their supports. The use of duplex and staged fuel systems in which parts of the system are not operational at low power levels are of particular concern because of the risk of thermal decomposition of stagnant fuel in the absence of the convective cooling produced by flowing fuel. This concern can be a major factor in establishing the acceptability of a particular combustor concept and must be recognized in future evolution of advanced technology combustors.

The incentive to incorporate advanced combustor concepts could be improved, and consequently the economic impact of their introduction reduced, if these concepts were also exploited to enhance important engine operation aspects such as combustor and turbine airfoil durability and specific fuel consumption.

REFERENCES

1. R. Roberts, A. Peduzzi, and G. E. Vitti, "Experimental Clean Combustor Program, Phase II, Alternate Fuels Addendum," NASA CR-134970, July 1976.

2. C. C. Gleason and D. W. Bahr, "Experimental Clean Combustor Program, Alternate Fuels Addendum, Phase II Final Report," NASA CR-134972, January 1976.

3. J. P. Longwell, Editor, "Jet Aircraft Hydrocarbon Fuels Technology," Proceedings of Workshop held at NASA Lewis June 7-9, 1977, NASA Conference Publication 2033, 1978.

4. R. P. Lohmann, E. J. Szetela, A. Vranos, "Analytical Evaluation of the Impact of Broad Specification Fuels on High Bypass Turbofan Combustors," NASA CR-159454, December 1978.

5. R. Roberts, A. Peduzzi, G. E. Vitti, "Experimental Clean Combustor Program, Phase I, Final Report," NASA CR-134756, October 1975.

6. R. Roberts, A. Peduzzi, G. E. Vitti, "Experimental Clean Combustor Program, Phase II, Final Report," NASA CR-134969, November 1976.

7. R. Roberts, A. Fiorentino, W. Greene, "Experimental Clean Combustor Program, Phase III, Final Report," NASA CR-135253, October 1977.

8. D. J. Dubiel, W. Greene, C. V, Sundt, S. Tanrikut, M. H. Zeisser, "Energy Efficient Engine Sector Combustor Rig Test Program Technology Report," NASA CR-167913, September 1982.

9. W. Greene, S. Tanrikut, D. Sokolowski, "Development and Operating Characteristics of an Advanced Two Stage Combustor," American Institute of Aeronautics and Astronautics Paper 82-0191, 1982.

10. A. J. Fiorentino, W. Greene, J. Kim, "Lean Premixed Prevaporized Fuel Combustor Conceptual Design Study," NASA CR-159647, August 1979.

11. T. R. Clements and R. R. Kazmar, "Variable Geometry Combustor Development," Air Force Aeropropulsion Laboratory Report AFWAL-TR-80-2102, October 1980.

12. Environmental Protection Agency, "Control of Air Pollution from Aircraft and Aircraft Engines," Federal Register 40 CFR Part 87 (43 FR 12615), March 24, 1978.

13. A. H. Lefebvre and M. V. Herbert, "Heat Transfer Processes in Gas Turbine Combustion Chambers," Proceedings of the Institute of Mechanical Engineers, Vol. 174, No. 12, 1960.

14. W. S. Blazowski and T. A. Jackson, "Evaluation of Future Jet Fuel Combustion Characteristics," AFAPL-TR-77-93, July 1978.

15. S. Tanrikut, R. L. Marshall, D. E. Sokolowski, "Improved Combustor Durability - Segmented Approach with Advanced Cooling Techniques," AIAA Paper 81-1354, July 1981.

NOMENCLATURE

A	Flow Area cm^2 (in^2)
C_D	Discharge Coefficient
CO	Carbon Monoxide
EI	Emission Index gm/kg
F/A	Fuel to Air Ratio
g_c	Gravitational Constant m/sec^2 (ft/sec^2)
NO_x	Oxides of Nitrogen
P_S	Static Pressure MPa (psia)
P_T	Total Pressure MPa (psia)
THC	Total Unburned Hydrocarbons
T_f	Flame Temperature °K (°F)
T_T	Total Temperature °K (°F)
V_{ref}	Velocity at a Cross Section of the Burner in the Absence of Combustion m/sec (ft/sec)
W_A	Airflow kg/sec (lb/sec)
W_{AB}	Burner Airflow kg/sec (lb/sec)
W_F	Burner Fuel Flow kg/sec (lb/sec)
η_c	Combustion Efficiency

SUBSCRIPTS

ca	Circumferential Average
exit	Average at Combustor Exit Plane
in	Average at Combustor Section (diffuser) Inlet

APPENDIX A
COMBUSTOR LINER HOLE PATTERNS

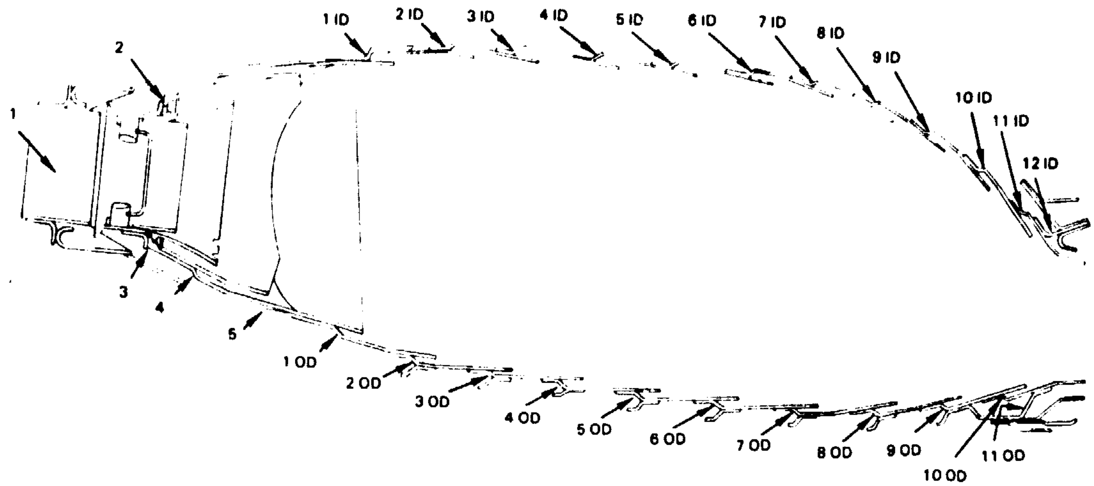

	SHORT CONE HOOD	AREA* CM²	AREA* IN²
1	FUEL NOZZLE AND SWIRLER	13.94	2.160
2	SKIRT COOLING	5.01	0.777
3	FALSE HEAD COOLING	7.61	1.180
4	CROTCH COOLING	11.10	1.721
5	MOUNT LUG COOLING	0.37	0.057

*Acd

BYPASS AIR	AREA CM²	AREA IN²
OD TURBINE COOLING AIR	31.06	4.814
ID TURBINE COOLING AIR	30.89	4.787
ENDWALL COOLING AIR	17.42	2.700

LINER COOLING					
INNER LINER			OUTER LINER		
LOUVER	AREA CM²	AREA IN²	LOUVER	AREA CM²	AREA IN²
1 ID	3.365	.5215	1 OD	3.809	.5904
2 ID	2.601	.4031	2 OD	3.853	.5972
3 ID	2.989	.4632	3 OD	3.192	.4947
4 ID	2.578	.3995	4 OD	3.191	.4946
5 ID	1.716	.2660	5 OD	4.209	.6524
6 ID	2.346	.3636	6 OD	2.226	.3449
7 ID	0.779	.1208	7 OD	2.950	.4573
8 ID	0.841	.1303	8 OD	3.289	.5098
9 ID	1.743	.2701	9 OD	3.631	.5627
10 ID	1.259	.1952	10 OD	4.558	.7065
11 ID	2.129	.3299	11 OD	3.352	.5195
12 ID	4.729	.7329			

LOUVER NUMBER	AIR TYPE	PENETRATIONS				
		NUMBER	TYPE	SIZE CM	SIZE IN	SPACING
1 OD	COMBUSTION	8	PLUNGED HOLE	1.702D	670D	BETWEEN
4 OD	DILUTION	8	SLOT	3.078 X1.422	1.212 X .560	INLINE
1 ID	COMBUSTION	8	PLUNGED HOLE	2.228D	.877D	BETWEEN
4 ID	DILUTION	8	SLOT	4.989 X 1.179	1.964 X .464	INLINE

Figure A-1 Combustor Hole Pattern in JT9D-7 Production Burner; Configuration SS-1

PRECEDING PAGE BLANK NOT FILMED

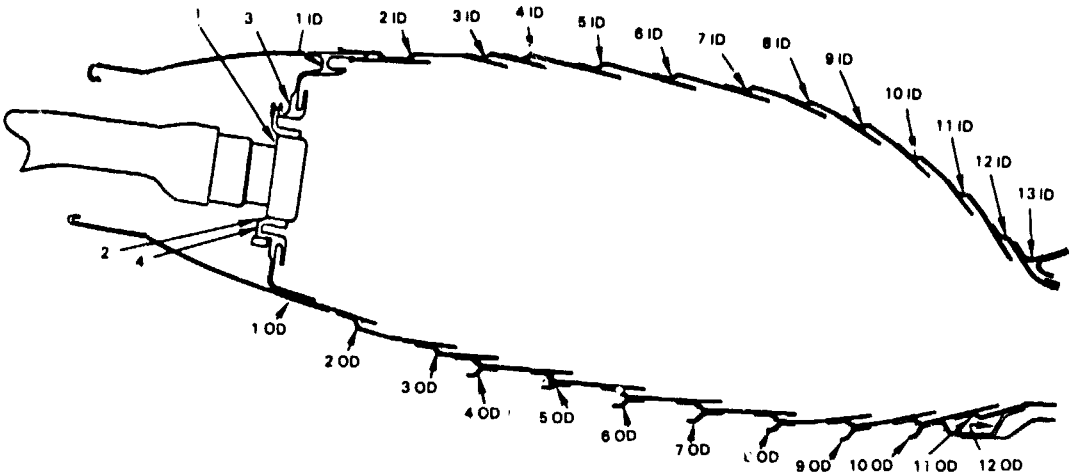

BULKHEAD HOOD		AREA CM²	AREA IN²
1	FUEL NOZZLE	9.03*	1.400*
2	INSERT	7.48*	1.160*
3	BULKHEAD COOLING	6.23	0.965
4	INSERT COOLING	6.45	0.999

*Acd

BYPASS AIR	AREA CM²	AREA IN²
OD TURBINE COOLING AIR	31.06	4.814
ID TURBINE COOLING AIR	30.89	4.787
ENDWALL COOLING AIR	17.42	2.700

LINER COOLING					
INNER LINER			OUTER LINER		
LOUVER	AREA CM²	AREA IN²	LOUVER	AREA CM²	AREA IN²
1 ID	4.929	.7640	1 OD	5.523	.8560
2 ID	4.808	.7452	2 OD	3.814	.5912
3 ID	2.737	.4242	3 OD	3.093	.4794
4 ID	3.507	.5436	4 OD	3.767	.5838
5 ID	5.165	.8006	5 OD	7.033	1.0900
6 ID	4.768	.7390	6 OD	6.497	1.0070
7 ID	3.754	.5818	7 OD	5.007	.7760
8 ID	2.608	.4042	8 OD	4.418	.6848
9 ID	2.336	.3620	9 OD	2.878	.4460
10 ID	3.121	.4838	10 OD	2.905	.4502
11 ID	1.696	.2628	11 OD	4.558	.7064
12 ID	2.128	.3298	12 OD	3.352	.5196
13 ID	4.728	.7328			

LOUVER NUMBER	AIR TYPE	PENETRATIONS				
		NUMBER	TYPE	DIAMETER CM	DIAMETER IN	SPACING
2 OD	COMBUSTION	8	PLUNGED HOLE	1.664	.655	BETWEEN
5 OD	DILUTION	7	SHARP EDGE HOLE	1.905	.750	INLINE
6 OD	DILUTION	7	SHARP EDGE HOLE	1.700	.669	INLINE
2 ID	COMBUSTION	8	PLUNGED HOLE	1.857	.731	BETWEEN
4 ID	DILUTION	7	SHARP EDGE HOLE	2.065	.813	INLINE
5 ID	DILUTION	7	SHARP EDGE HOLE	1.270	.500	INLINE

Figure A-2 Combustor Hole Pattern in JT9D-7 Bulkhead Burner for Configurations SS-2, SS-4, and VG-1 through VG-4

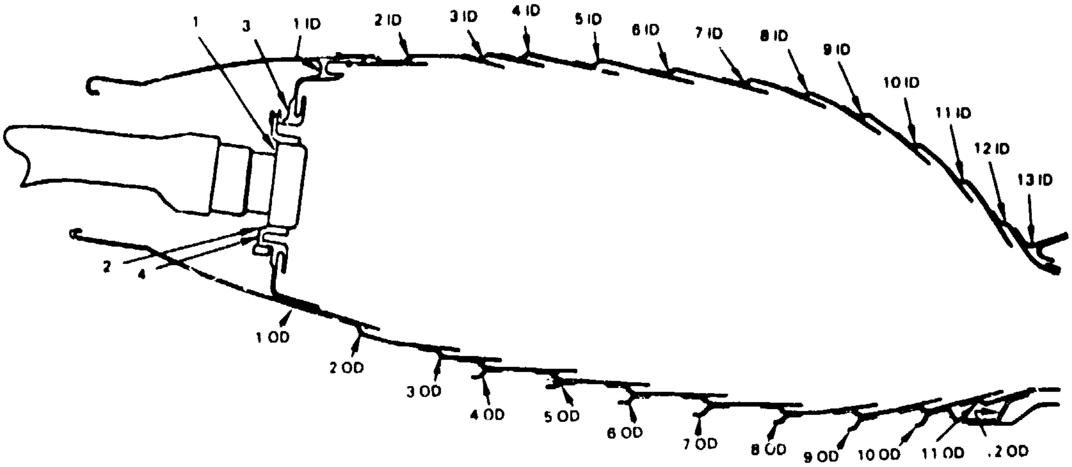

	BULKHEAD HOOD	AREA CM²	AREA IN²
1	FUEL NOZZLE	9.03*	1.400*
2	INSERT	7.48*	1.160*
3	BULKHEAD COOLING	6.23	0.965
4	INSERT COOLING	6.45	0.999

*Acd

BYPASS AIR	AREA CM²	AREA IN²
OD TURBINE COOLING AIR	31.06	4.814
ID TURBINE COOLING AIR	30.89	4.787
ENDWALL COOLING AIR	17.42	2.700

LINER COOLING					
INNER LINER			OUTER LINER		
LOUVER	AREA CM²	AREA IN²	LOUVER	AREA CM²	AREA IN²
1 ID	4.929	7640	1 OD	5.523	.8560
2 ID	4.808	.7452	2 OD	3.814	.5912
3 ID	2.737	.4242	3 OD	3.093	.4794
4 ID	3.507	.5436	4 OD	3.767	.5838
5 ID	5.165	.8006	5 OD	7.033	1.0900
6 ID	4.768	.7390	6 OD	6.497	1.0070
7 ID	3.754	.5818	7 OD	5.007	.7760
8 ID	2.608	.4042	8 OD	4.418	.6848
9 ID	2.336	.3620	9 OD	2.878	.4460
10 ID	3.121	.4838	10 OD	2.905	.4502
11 ID	1.696	.2628	11 OD	4.558	.7064
12 ID	2.128	.3298	12 OD	3.352	.5196
13 ID	4.728	.7328			

LOUVER NUMBER	AIR TYPE	PENETRATIONS				
				DIAMETER		
		NUMBER	TYPE	CM	IN	SPACING
2 OD	COMBUSTION	8	PLUNGED HOLE	1.664	.655	BETWEEN
6 OD	DILUTION	7	SHARP EDGE HOLE	1.700	669	INLINE
7 OD	DILUTION	7	SHARP EDGE HOLE	1.905	.950	INLINE
2 ID	COMBUSTION	8	PLUNGED HOLE	1.857	731	BETWEEN
6 ID	DILUTION	7	SHARP EDGE HOLE	2.065	813	INLINE
7 ID	DILUTION	7	SHARP EDGE HOLE	1.270	500	INLINE

Figure A-3 Combustor Hole Pattern in JT9D-7 Bulkhead Burner; Configuration SS-3

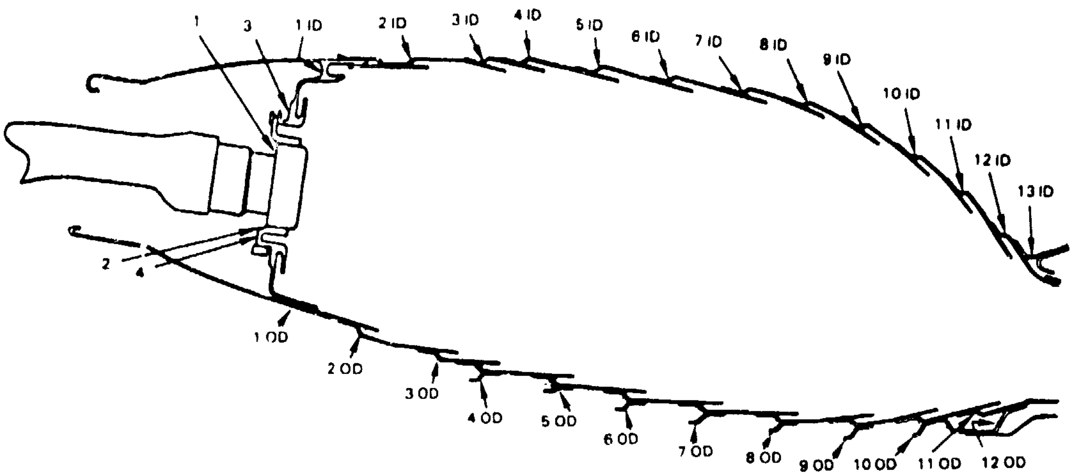

	BULKHEAD HOOD	AREA CM²	AREA IN²
1	FUEL NOZZLE	9.03*	1.400*
2	INSERT	7.48*	1.160*
3	BULKHEAD COOLING	6.23	0.965
4	INSERT COOLING	6.45	0.999

*Acd

BYPASS AIR	AREA CM²	AREA IN²
OD TURBINE COOLING AIR	31.06	4.814
ID TURBINE COOLING AIR	30.89	4.787
ENDWALL COOLING AIR	17.42	2.700

LINER COOLING					
INNER LINER			OUTER LINER		
LOUVER	AREA CM²	AREA IN²	LOUVER	AREA CM²	AREA IN²
1 ID	4.929	.7640	1 OD	5.523	.8560
2 ID	4.808	.7452	2 OD	3.814	.5912
3 ID	2.737	.4242	3 OD	3.093	.4794
4 ID	3.507	.5435	4 OD	3.767	.5838
5 ID	5.165	.8006	5 OD	7.033	1.0900
6 ID	4.768	.7390	6 OD	6.497	1.0070
7 ID	3.754	.5818	7 OD	5.007	.7760
8 ID	2.608	.4042	8 OD	4.418	.6848
9 ID	2.336	.3620	9 OD	2.878	.4460
10 ID	3.121	.4838	10 OD	2.905	.4502
11 ID	1.696	.2628	11 OD	4.558	.7064
12 ID	2.128	.3298	12 OD	3.352	.5196
13 ID	4.728	.7328			

LOUVER NUMBER	AIR TYPE	PENETRATIONS				
		NUMBER	TYPE	DIAMETER CM	DIAMETER IN	SPACING
6 OD	DILUTION	7	SHARP EDGE HOLE	2.065	.813	INLINE
7 OD	DILUTION	7	SHARP EDGE HOLE	2.065	.813	INLINE
5 ID	DILUTION	7	SHARP EDGE HOLE	1.905	.750	INLINE
6 ID	DILUTION	7	SHARP EDGE HOLE	1.905	.750	INLINE

Figure A-4 Combustor Hole Pattern in JT9D-7 Bulkhead Burner; Configurations SS-5 and VG-6

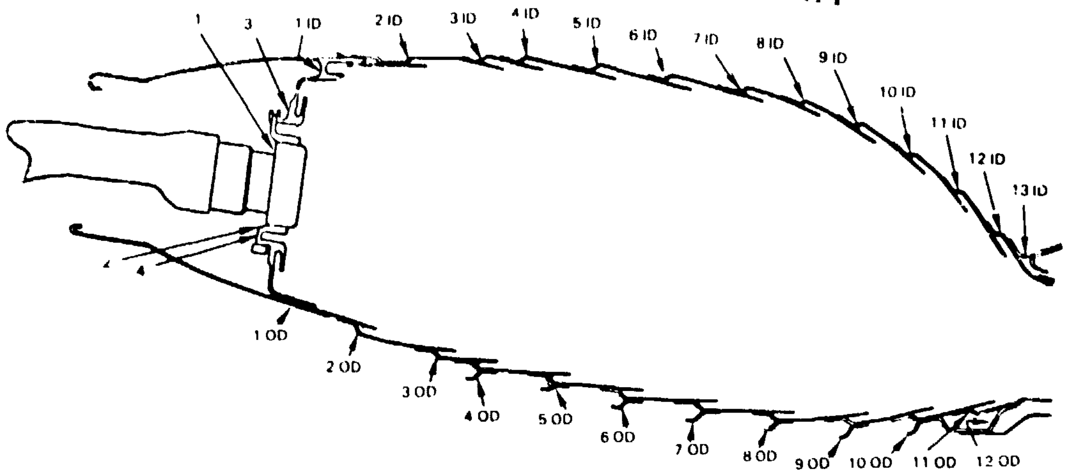

	BULKHEAD HOOD	AREA CM²	AREA IN²
1	FUEL NOZZLE	9.03*	1.400*
2	INSERT	7.48*	1.160*
3	BULKHEAD COOLING	6.23	0.965
4	INSERT COOLING	6.45	0.999

*Acd

BYPASS AIR	AREA CM²	AREA IN²
OD TURBINE COOLING AIR	31.06	4.814
ID TURBINE COOLING AIR	30.89	4.787
ENDWALL COOLING AIR	17.42	2.700

LINER COOLING					
INNER LINER			OUTER LINER		
LOUVER	AREA CM²	AREA IN²	LOUVER	AREA CM²	AREA IN²
1 ID	4.929	.7640	1 OD	5.523	.8560
2 ID	4.808	.7452	2 OD	3.814	.5912
3 ID	2.737	.4242	3 OD	3.093	.4794
4 ID	3.507	.5436	4 OD	3.767	.5838
5 ID	5.165	.8006	5 OD	7.033	1.0900
6 ID	4.768	.7390	6 OD	6.497	1.0070
7 ID	3.754	.5818	7 OD	5.007	.7760
8 ID	2.608	.4042	8 OD	4.418	.6848
9 ID	2.336	.3620	9 OD	2.878	.4460
10 ID	3.121	.4838	10 OD	2.905	.4502
11 ID	1.696	.2628	11 OD	4.558	.7064
12 ID	2.128	.3298	12 OD	3.352	.5196
13 ID	4.728	.7328			

LOUVER NUMBER	AIR TYPE	PENETRATIONS				
		NUMBER	TYPE	DIAMETER CM	DIAMETER IN	SPACING
2 OD	COMBUSTION	6	PLUNGED HOLE	2.540	1.000	BETWEEN
6 OD	DILUTION	7	SHARP EDGE HOLE	1.905	.750	INLINE
2 ID	COMBUSTION	6	PLUNGED HOLE	2.540	1.000	BETWEEN
5 ID	DILUTION	7	SHARP EDGE HOLE	2.065	.813	INLINE

Figure A-5 Combustor Hole Pattern in JT9D-7 Bulkhead Burner; Configuration SS-6

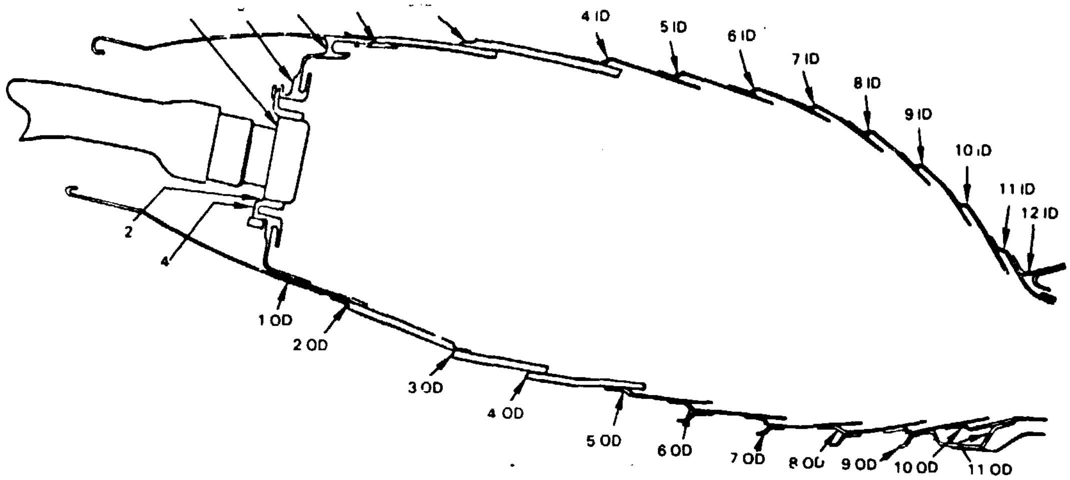

	BULKHEAD HOOD	AREA CM²	AREA IN²
1	FUEL NOZZLE	8.65*	1.340*
2	INSERT	7.48*	1.160*
3	BULKHEAD COOLING	6.23	0.365
4	INSERT COOLING	6.45	0.999

*Acd

BYPASS AIR	AREA CM²	AREA IN²
OD TURBINE COOLING AIR	31.06	4.814
ID TURBINE COOLING AIR	30.89	4.787
ENDWALL COOLING AIR	17.42	2.700

LINER COOLING					
INNER LINER			OUTER LINER		
LOUVER	AREA CM²	AREA IN²	LOUVER	AREA CM²	AREA IN²
1 ID	2.465	.3820	1 OD	5.523	.8560
2 ID	2.089	.3237	2 OD	3.843	.5957
3 ID	1.947	.3017	3 OD	2.752	.4265
4 ID	5.165	.8006	4 OD	2.181	.3380
5 ID	4.768	.7390	5 OD	6.497	1.0070
6 ID	3.754	.5818	6 OD	5.007	.7760
7 ID	2.608	.4042	7 OD	4.418	.6848
8 ID	2.336	.3620	8 OD	2.878	.4460
9 ID	3.121	.4838	9 OD	2.905	.4502
10 ID	1.696	.2628	10 OD	4.558	.7064
11 ID	2.128	.3298	11 OD	3.352	.5196
12 ID	4.728	.7328			

LOUVER NUMBER	AIR TYPE	PENETRATIONS				
		NUMBER	TYPE	DIAMETER CM	DIAMETER IN	SPACING
2 OD	COMBUSTION	9	SHARP EDGE HOLE	1.905	.750	BETWEEN
5 OD	DILUTION	7	SHARP EDGE HOLE	1.905	.750	INLINE
6 OD	DILUTION	7	SHARP EDGE HOLE	2.035	.801	INLINE
2 ID	COMBUSTION	8	SHARP EDGE HOLE	1.905	.750	BETWEEN
4 ID	DILUTION	7	SHARP EDGE HOLE	2.065	.813	INLINE
5 ID	DILUTION	7	SHARP EDGE HOLE	1.715	.675	INLINE

Figure A-6 Combustor Hole Pattern in JT9D-7 Bulkhead Burner; Configuration SS-7

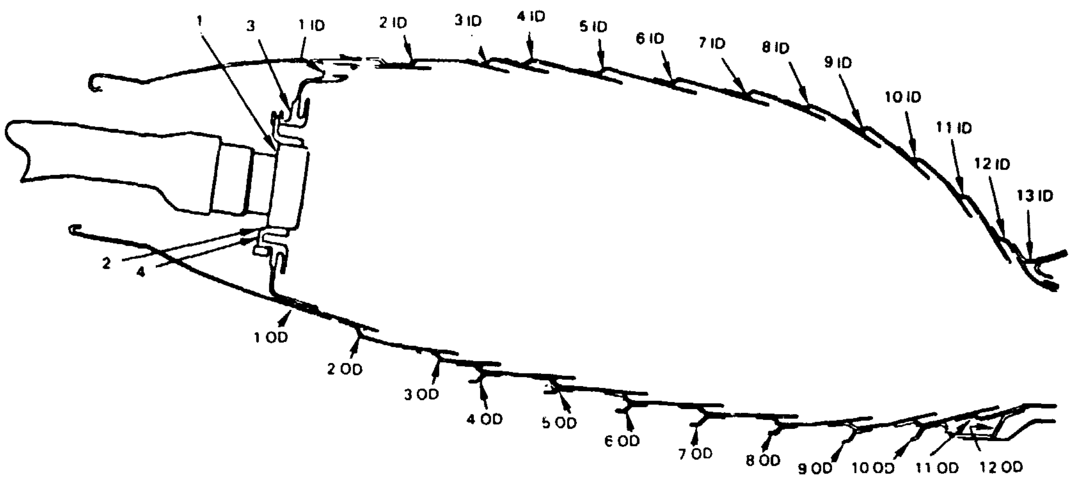

BULKHEAD HOOD		AREA CM²	AREA IN²
1	FUEL NOZZLE	9.03*	1.400*
2	INSERT	7.48*	1.160*
3	BULKHEAD COOLING	6.23	0.965
4	INSERT COOLING	6.45	0.999

*Acd

BYPASS AIR	AREA CM²	AREA IN²
OD TURBINE COOLING AIR	31.06	4.814
ID TURBINE COOLING AIR	30.89	4.787
ENDWALL COOLING AIR	17.42	2.700

LINER COOLING					
INNER LINER			OUTER LINER		
LOUVER	AREA CM²	AREA IN²	LOUVER	AREA CM²	AREA IN²
1 ID	4.929	.7640	1 OC	5.523	.8560
2 ID	4.808	.7452	2 OD	3.814	.5912
3 ID	2.737	.4242	3 OD	3.093	.4794
4 ID	3.507	.5436	4 OD	3.767	.5838
5 ID	5.165	.8006	5 OD	7.033	1.0900
6 ID	4.768	.7390	6 OD	6.497	1.0070
7 ID	3.754	.5818	7 OD	5.007	.7760
8 ID	2.608	.4042	8 OD	4.418	.6848
9 ID	2.336	.3620	9 OD	2.878	.4460
10 ID	3.121	.4838	10 OD	2.905	.4502
11 ID	1.696	.2628	11 OD	4.558	.7064
12 IC	2.128	.3298	12 OD	3.352	.5196
13 [illegible]	4.728	.7328			

LOUVER NUMBER	AIR TYPE	PENETRATIONS				
				DIAMETER		
		NUMBER	TYPE	CM	IN	SPACING
2 OD	COMBUSTION	8	SHARP EDGE HOLE	3.175	1.250	BETWEEN
1 ID	COMBUSTION	8	SHARP EDGE HOLE	[illegible].905	.750	[illegible]
2 ID	COMBUSTION	8	SHARP EDGE HOLE	2.540	1.000	BETWEEN

Figure A-7 Combustor Hole Pattern in JT9D-7 Bulkhead Burner; Configuration VG-5

ORIGINAL PAGE IS
OF POOR QUALITY

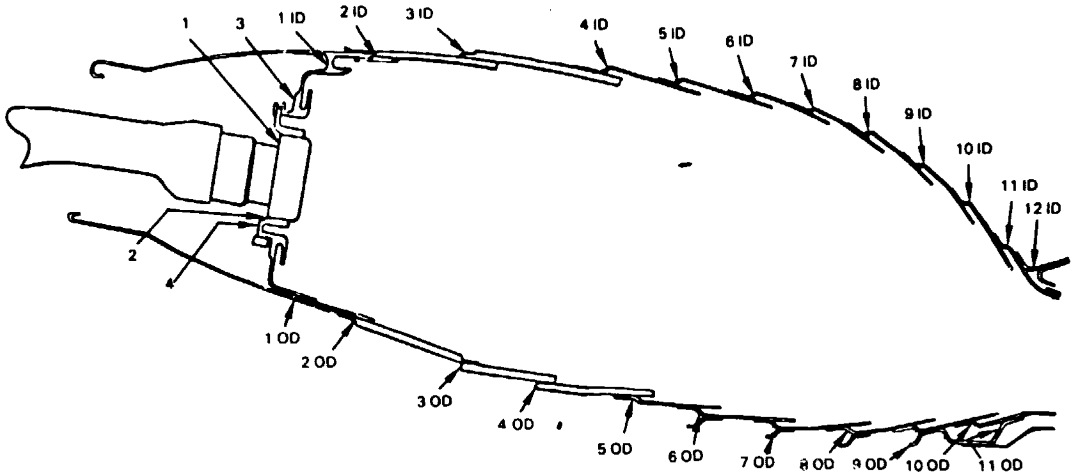

	BULKHEAD HOOD	AREA CM²	AREA IN²
1	FUEL NOZZLE	8.00*	1.240*
2	INSERT	7.48*	1.160*
3	BULKHEAD COOLING	6.23	0.965
4	INSERT COOLING	6.45	0.999

*Acd

BYPASS AIR	AREA CM²	AREA IN²
OD TURBINE COOLING AIR	31.06	4.814
ID TURBINE COOLING AIR	30.89	4.787
ENDWALL COOLING AIR	17.42	2.700

LINER COOLING					
INNER LINER			OUTER LINER		
LOUVER	AREA CM²	AREA IN²	LOUVER	AREA CM²	AREA IN²
1 ID	2.465	.3820	1 OD	5.523	.8560
2 ID	2.089	.3237	2 OD	3.843	.5957
3 ID	1.947	.3017	3 OD	2.752	.4265
4 ID	5.165	.8006	4 OD	2.181	.3380
5 ID	4.768	.7390	5 OD	6.497	1.0070
6 ID	3.754	.5818	6 OD	5.007	.7760
7 ID	2.608	.4042	7 OD	4.418	.6848
8 ID	2.336	.3620	8 OD	2.878	.4460
9 ID	3.121	.4838	9 OD	2.905	.4502
10 ID	1.696	.2628	10 OD	4.558	.7064
11 ID	2.128	.3298	11 OD	3.352	.5196
12 ID	4.728	.7328			

LOUVER NUMBER	AIR TYPE	PENETRATIONS				
		NUMBER	TYPE	DIAMETER CM	DIAMETER IN	SPACING
5 OD	DILUTION	7	SHARP EDGE HOLE	2.459	.968	INLINE
6 OD	DILUTION	7	SHARP EDGE HOLE	2.459	.968	INLINE
4 ID	DILUTION	7	SHARP HOLE HOLE	2.459	.968	INLINE
5 ID	DILUTION	7	SHARP HOLE HOLE	2.459	.968	INLINE

Figure A-8 Combustor Hole Pattern in JT9D-7 Bulkhead Burner; Configuration VG-7

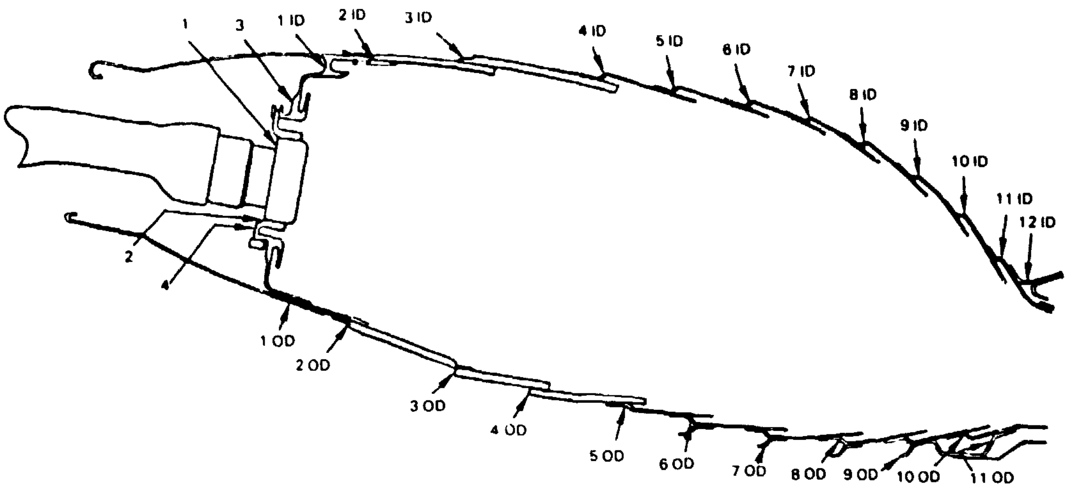

	BULKHEAD HOOD	AREA CM²	AREA IN²
1	FUEL NOZZLE	8.00*	1.240*
2	INSERT	7.48*	1.160*
3	BULKHEAD COOLING	6.23	0.965
4	INSERT COOLING	6.45	0.999

*Acd

BYPASS AIR	AREA CM²	AREA IN²
OD TURBINE COOLING AIR	31.06	4.814
ID TURBINE COOLING AIR	30.89	4.737
ENDWALL COOLING AIR	17.42	2.700

LINER COOLING					
INNER LINER			OUTER LINER		
LOUVER	AREA CM²	AREA IN²	LOUVER	AREA CM²	AREA IN²
1 ID	2.465	.3820	1 OD	5.523	.8560
2 ID	2.089	.3237	2 OD	3.843	.5957
3 ID	1.947	3017	3 OD	2.752	.4265
4 ID	5.165	.8006	4 OD	2.181	.3380
5 ID	4.768	.7390	5 OD	6.497	1.0070
6 ID	3.754	.5818	6 OD	5.007	.7760
7 ID	2.608	.4042	7 OD	4.418	.6848
8 ID	2.336	.3620	8 OD	2.878	.4460
9 ID	3.121	.4838	9 OD	2.905	.4502
10 ID	1.696	.2628	10 OD	4.558	.7064
11 ID	2.128	.3298	11 OD	3.352	.5196
12 ID	4.728	.7328			

LOUVER NUMBER	AIR TYPE	PENETRATIONS				
		NUMBER	TYPE	DIAMETER		SPACING
				CM	IN	
2 OD	COMBUSTION	8	GROMMET HOLE	2.223	.875	BETWEEN
3 OD	COMBUSTION	7	GROMMET HOLE	1.588	.625	INLINE
2 ID	COMBUSTION	8	GROMMET HOLE	2.062	.812	BETWEEN
3 ID	COMBUSTION	8	GROMMET HOLE	2.062	.812	INLINE

Figure A-9 Combustor Hole Pattern in JT9D-7 Bulkhead Burner; Configuration VG-8

APPENDIX B
FUEL INJECTOR SPRAY EVALUATION

APPENDIX B

FUEL INJECTOR SPRAY EVALUATION

Fuel atomization and spray characterization tests were conducted on the injectors that were used in the configurations of the single stage and variable geometry combustors that were evaluated during this program. Figure B-1 is a schematic diagram of the air and fuel supply systems in the test facility. The test injector was installed in a plenum box and ambient temperature air was supplied to the plenum to provide airflow through either the nozzle nut passages or the aerating air passages of the injector. The supply pressure in the plenum was adjusted to match the air velocity occurring in these passages at the appropriate engine operating condition. For injection evaluations at the cold start condition the fuel was cooled using a fuel conditioning system. The test fuel was contained in a piston accumulator which is surrounded with acetone cooled by liquid nitrogen and refrigeration systems. Once the test fuel reached the desired temperature, it was pushed out by injecting JP-7 behind the piston. The test fuel flow rate was determined by measuring the flow rate of the room temperature JP-7 fuel.

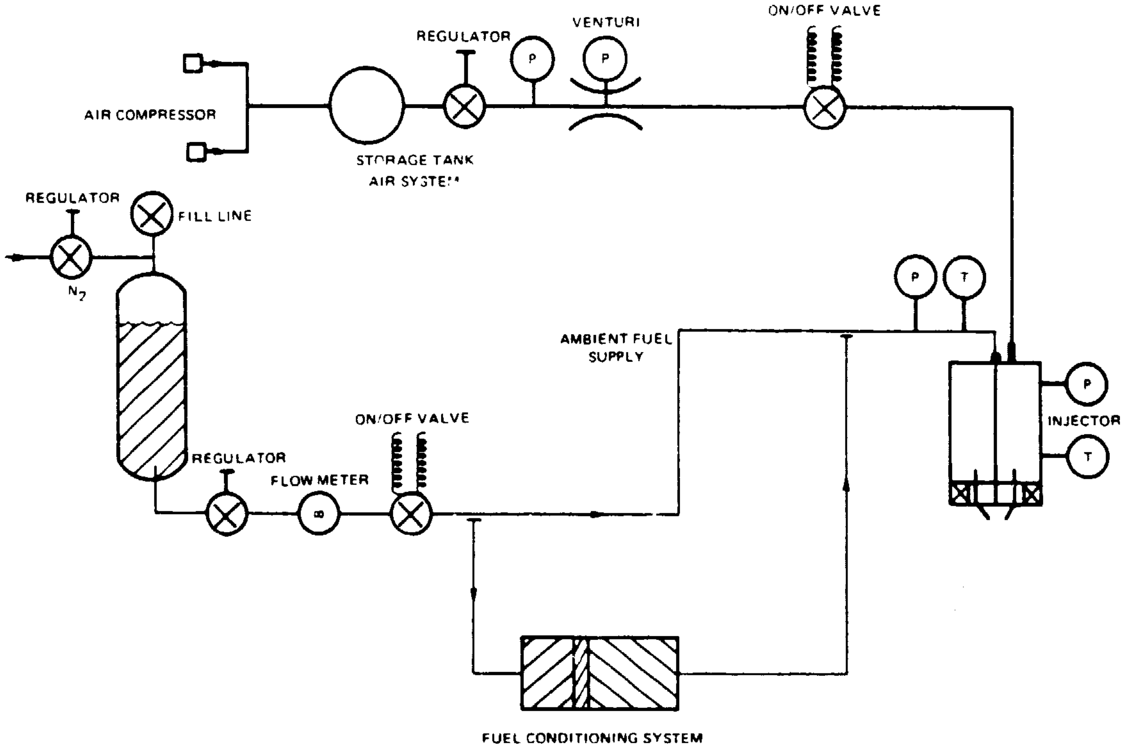

Figure B-1 Schematic Diagram of Air and Fuel Supply to Fuel Injector Test Facility

Each injector was tested on three fuels: Jet A, Experimental Referee Broad Specification Fuel (ERBS) and Marine Diesel fuel. The properties of these fuels, as determined by laboratory analysis, are listed in Table B-1.

While not used in the remainder of the program, the Marine Diesel fuel had been selected as the third test fuel because it had a viscosity level considerably above ERBS which would provide a reasonably wide range of atomization properties.

Table B-1

Properties of Test Fuels for Fuel Injector Evaluation

	Fuel		
	Jet A	ERBS	Marine Diesel
Specific Gravity 289/289°K (60/60°F)	0.8076	0.8388	0.8576
Viscosity - centistokes			
at 297°K (75°F)	1.73	2.2	3.65
at 250°K (-10°F)	5.2	7.7	18.6
Surface Tension - dynes/cm at 297°K (75°F)	27.6	30.6	31.6
Aromatic Content - % volume	19.7	31.9	39.4

The tests were conducted at simulated idle, cruise, takeoff and cold starting conditions of the JT9D-7F engine, the latter with 250°K (-10°F) fuel temperature. Data were obtained on the droplet size distribution, spray angle and spray quality. Spray angle data was obtained with a twenty tube patternator rake positioned 10.16 cm (4 inches) downstream of the injector face. Fifteen tubes on the rake were positioned in a close density on a radial line across the spray while the other five tubes were located in diametrically opposite but wider spaced positions to check on spray symmetry. Two parameters of interest were defined from the patternator rake data:

Mean Spray Angle - the angle including 50 percent of the total volume flow of the spray as measured from the injector centerline.

Spray Band Width - the double angle between rays subtending 25 percent and 75 percent of the total volume flow of the spray.

Droplet size distribution in the spray was obtained with a Malvern particle size analyzer with the laser beam intersecting the spray at a plane 7.62 cm (3 inches) from the injector face. Two characteristic drop sizes are of interest:

Sauter Mean Diameter - the single droplet size with the same surface area to volume ratio as the entire spray.

Peak Density Diameter - the droplet size with the greatest mass fraction of the spray.

These four spray angle and atomization parameters are tabulated in Table B-2 for each combination of injector type, fuel and simulated engine operating condition tested.

Table B-2

Fuel Injector Spray and Atomization Characteristics

Injector	Production: Duplex Pressure Atomized			Baseline Duplex Injector: Duplex Fuel Schedule			Baseline Duplex Injector: Aerated Single Pipe Mode		
Used in Configuration	SS-1			SS-2, SS-3, SS-5, SS-6			VG-1, VG-5, VG-6		
Fuel	Jet A	ERBS	Diesel	Jet A	ERBS	Diesel	Jet A	ERBS	Diesel
CONE ANGLE (1)									
Cold Start	58.58	63.91	53.10	65.88	66.95	66.77	65.88	66.95	65.77
Idle	44.88	47.82	45.38	55.80	57.53	56.51	55.80	57.53	56.51
Cruise	41.00	46.40	42.91	50.06	51.93	48.78	50.06	51.93	48.78
Takeoff	53.35	57.41	59.02	66.02	66.60	65.40	66.02	66.60	65.40
CONE WIDTH (2)									
Cold Start	23.23	16.90	25.98	23.56	22.34	23.94	23.56	22.34	23.94
Idle	27.97	22.42	23.23	19.32	22.44	21.35	19.32	22.44	21.35
Cruise	12.13	13.68	13.38	18.72	18.97	22.88	18.72	18.97	22.88
Takeoff	8.70	9.38	10.03	18.69	18.46	18.08	18.69	18.46	18.08
SAUTER MEAN DIAMETER - MICRONS									
Cold Start	33	36	65	121	130	115	121	130	115
Idle	74	77	103	38	38	42	38	38	42
Cruise	81	86	103	26	32	46	26	32	46
Takeoff	69	63	95	12	29	51	12	29	51
PEAK DENSITY DROPLET SIZE - MICRONS (3)									
Cold Start	70	79	114	180	183	181	180	183	181
Idle	132	137	182	82	82	88	82	82	88
Cruise	162	171	182	104	93	109	104	93	109
Takeoff	164	169	178	128	114	159	128	114	159

Injector	Modified Injector: Duplex Fuel Schedule			Modified Injector: Aerated Single Pipe Mode		
Used in Configuration	SS-4, SS-7			VG-2		
Fuel	Jet A	ERBS	Diesel	Jet A	ERBS	Diesel
CONE ANGLE (1)						
Cold Start	67.17	56.11	48.30	67.50	67.39	67.36
Idle	51.40	52.97	45.45	54.04	55.84	53.82
Cruise	52.06	50.57	49.03	56.26	58.16	54.83
Takeoff	65.63	62.51	64.37	68.24	70.66	68.19
CONE WIDTH (2)						
Cold Start	28.43	23.03	25.52	22.02	22.15	22.22
Idle	21.67	23.73	21.69	20.54	19.94	18.53
Cruise	17.24	17.78	18.67	17.06	16.85	15.96
Takeoff	20.33	19.53	21.75	17.08	15.89	17.35
SAUTER MEAN DIAMETER - MICRONS						
Cold Start	43	51	78	105	125	99
Idle	25	15	23	27	20	31
Cruise	17	13	16	20	13	33
Takeoff	15	-	-		-	46
PEAK DENSITY DROPLET SIZE - MICRONS (3)						
Cold Start	77	90	139	165	191	148
Idle	55	60	72	71	79	78
Cruise	67	37	88	77	71	108
Takeoff	59	-	92		-	144

Injector	Variable Single Pipe Aerating Injector: Closed Position			Variable Single Pipe Aerating Injector: Open Position		
Used in Configuration	VG-4, VG-7, VG-8			VG-3		
Fuel	Jet A	ERBS	Diesel	Jet A	ERBS	Diesel
CONE ANGLE (1)						
Cold Start	66.28	65.88	68.04	61.37	59.27	63.02
Idle	59.23	54.31	54.44	49.11	47.21	49.94
Cruise	60.68	56.67	58.90	52.51	47.67	49.97
Takeoff	76.57	71.59	71.83	69.52	67.73	67.60
CONE WIDTH (2)						
Cold Start	21.57	23.17	22.27	25.19	25.42	[illegible]
Idle	17.97	20.49	18.42	19.47	20.87	25.05
Cruise	15.10	17.05	16.99	15.20	16.82	20.52
Takeoff	14.85	15.50	14.66	18.32	19.01	[illegible]
SAUTER MEAN DIAMETER - MICRONS						
Cold Start	102	89	132	72	95	124
Idle	20	27	21	29	35	33
Cruise	24	30	17	18	24	32
Takeoff	26	38	13	15	32	47
PEAK DENSITY DROPLET SIZE - MICRONS (3)						
Cold Start	161	150	189	182	169	174
Idle	63	73	66	62	66	71
Cruise	63	81	94	71	77	96
Takeoff	76	101	140	99	100	126

NOTES:
(1) Total included angle.
(2) 50 percent of droplets in this angle.
(3) Droplet size with greatest number of droplets.

APPENDIX C
TABULATED TEST DATA

APPENDIX C

TABULATED TEST DATA

Data are presented in three tables. Table C-1 lists emissions data including identification of combustor inlet and operating conditions. The emissions indices listed are after correction to standard combustor inlet conditions as defined in Section 6.3.

Table C-2 provides data on the liner metal temperature at all test points at the cruise and higher power level. Point numbers followed by an "N" indicate those at the design fuel air ratio for the particular nominal condition. Data are presented, where applicable, from thermocouples located in the primary and secondary or dilution zone of the liner and on the bulkhead. Temperatures are reported as the differential above combustor inlet total temperature. D-TM is the highest recorded temperature in that zone while D-TA is the average of the readings from the N thermocouples that were operational in that zone.

Table C-3 lists the lean blowout fuel air ratios of the combustor configurations at the idle inlet condition.

Table C-1
Combustor Emissions Data

CONFIGURATION SS-1 CURRENT PRODUCTION COMBUSTOR

PT NO	OPERATING CONDITION	INLET PRES MPA	INLET TEMP DEG-K	BURNER AIRFLOW KG/SEC	METERED F/A RATIO	FUEL TYPE	FUEL TEMP DEG-K	PRI FUEL %	SEC FUEL %	CARBON BAL F/A RATIO	CO2 %	SPECIF HUMID G/KG	CORR CO EI G/KG	CORR THC EI G/KG	CORR NOX EI G/KG	CORR COMB EFFIC	SAE SMOKE NUMBER
2	IDLE	0.372	450.3	4.077	0.0115	JET A	294.	50.	50.	0.0109	2.200	1.438	53.099	19.849	3.637	96.50	0.5
3	IDLE	0.365	450.6	4.113	0.0074	ERBS	292.	71.	29.	0.0073	1.367	0.312	119.837	73.608	2.873	88.37	5.2
4	IDLE	0.377	450.5	4.041	0.0139	ERBS	292.	42.	58.	0.0136	2.900	0.311	23.260	5.645	3.712	98.81	0.6
5	IDLE	0.372	450.3	4.032	0.0107	ERBS	292.	50.	50.	0.0104	2.133	0.280	64.005	25.043	3.704	95.58	3.7
6	IDLE	0.372	449.2	4.934	0.0109	ERBS	291.	51.	49.	0.0109	2.267	0.685	54.133	14.413	3.450	97.04	3.0
7	IDLE	0.373	447.2	4.122	0.0109	12.3%	292.	49.	51.	0.0111	2.300	0.603	55.935	18.679	4.169	96.49	5.9
8	IDLE	0.37[illegible]	447.5	4.109	0.0112	11.8%	292.	50.	50.	0.0111	2.333	0.606	53.639	16.349	4.557	96.79	7.0
9	IDLE	0.367	447.6	4.195	0.0084	11.8%	291.	67.	33.	0.0089	1.767	0.615	102.362	41.375	3.572	92.57	13.6
10	IDLE	0.378	447.9	4.036	0.0144	11.8%	291.	58.	42.	0.0141	3.033	0.613	27.790	6.726	4.465	98.57	5.2
11	APPROACH	0.903	581.2	8.277	0.0164	JET A	290.	19.	81.	0.0164	3.500	0.622	2.991	0.336	8.525	99.89	2.0
12	APPROACH	0.902	581.5	8.503	0.0158	ERBS	290.	21.	79.	0.0145	3.200	0.612	2.449	0.302	7.128	99.91	3.4
13	CRUISE	0.943	702.0	7.982	0.0229	JET A	285.	16.	84.	0.0226	4.833	0.544	2.259	0.100	18.862	99.94	6.1
14	CRUISE	0.944	703.3	6.014	0.0234	ERBS	284.	16.	84.	0.0225	4.833	0.541	2.429	0.200	13.246	99.92	11.8
15	CRUISE	0.937	702.3	8.014	0.0226	12.3%	282.	16.	84.	0.0216	4.700	0.546	1.948	0.132	17.806	99.94	8.0
16	CRUISE	0.939	703.2	8.041	0.0227	11.8%	281.	16.	84.	0.0217	4.767	0.541	1.952	0.099	18.626	99.94	5.1
17	CLIMB	1.962	728.4	16.644	0.0214	JET A	284.	8.	92.	0.0225	4.800	0.468	0.929	0.100	23.209	99.97	6.5
18	CLIMB	1.941	734.3	16.630	0.0200	ERBS	284.	9.	91.	0.0202	4.367	0.465	0.656	0.164	26.771	99.96	7.8
19	TAKEOFF	2.239	761.6	17.279	0.0207	JET A	288.	9.	91.	0.0223	4.800	0.428	0.562	0.198	37.395	99.96	3.3
20	TAKEOFF	2.268	760.6	17.370	0.0206	ERBS	287.	8.	92.	0.0220	4.767	0.426	0.536	0.100	37.331	99.98	3.5
21	TAKEOFF	2.232	760.7	17.338	0.0179	JET A	288.	10.	90.	0.0191	4.100	0.430	0.395	0.231	28.581	99.96	3.5
22	TAKEOFF	2.257	762.2	17.361	0.0180	ERBS	287.	10.	90.	0.0192	4.133	0.420	0.367	0.133	30.414	99.98	4.8
23	TAKEOFF	2.245	759.7	17.365	0.0179	11.8%	287.	10.	90.	0.0191	4.167	0.441	0.431	0.099	33.049	99.98	3.1
24	TAKEOFF	2.259	762.0	17.193	0.0207	11.8%	287.	8.	92.	0.0229	5.000	0.255	0.500	0.100	41.950	99.98	2.3
25	TAKEOFF	2.257	760.4	17.297	0.0206	12.3%	285.	9.	91.	0.0226	4.933	0.210	0.500	0.100	40.359	99.98	2.9
26	TAKEOFF	2.209	770.2	15.651	0.0202	ERBS	287.	9.	91.	0.0211	4.600	0.277	0.555	0.261	35.588	99.96	3.0

CONFIGURATION SS-2 REFERENCE BULKHEAD COMBUSTOR

PT NO	OPERATING CONDITION	INLET PRES MPA	INLET TEMP DEG-K	BURNER AIRFLOW KG/SEC	METERED F/A RATIO	FUEL TYPE	FUEL TEMP DEG-K	PRI FUEL %	SEC FUEL %	CARBON BAL F/A RATIO	CO2 %	SPECIF HUMID G/KG	CORR CO EI G/KG	CORR THC EI G/KG	CORR NOX EI G/KG	CORR COMB EFFIC	SAE SMOKE NUMBER
2	IDLE	0.371	452.7	4.132	0.0101	JET A	284.	59.	41.	0.0093	1.967	0.457	30.402	3.415	3.066	98.90	4.5
3	IDLE	0.364	454.7	4.100	0.0111	ERBS	281.	51.	49.	0.0100	2.100	0.359	26.493	1.841	3.659	99.14	2.3
4	APPROACH	0.899	579.9	8.190	0.0160	JET A	284.	21.	79.	0.0148	3.167	0.317	1.238	0.0	10.394	99.97	1.5
5	APPROACH	0.895	583.0	8.186	0.0159	ERBS	284.	22.	78.	0.0149	3.200	0.316	1.200	0.0	10.446	99.97	1.6
6	CRUISE	0.940	694.3	7.692	0.0194	JET A	284.	18.	82.	0.0175	3.733	0.314	1.126	0.0	21.493	99.97	2.6
7	CRUISE	0.942	699.4	7.714	0.0193	ERBS	283.	20.	80.	0.0174	3.733	0.314	1.129	0.0	21.139	99.97	2.0
8	CLIMB	1.967	734.9	16.086	0.0[illegible]93	JET A	284.	[illegible]	91.	0.0180	3.867	0.263	0.532	0.033	32.742	99.98	2.0
9	CLIMB	1.973	739.4	16.159	0.0191	ERBS	283.	9.	91.	0.0175	3.733	0.272	0.534	0.033	31.774	99.98	2.3
10	TAKEOFF	2.269	767.4	17.796	0.0193	JET A	288.	9.	91.	0.0174	3.733	0.435	0.570	0.101	41.373	99.98	3.2
11	TAKEOFF	2.258	765.2	17.846	0.0191	ERBS	286.	9.	91.	0.0166	3.600	0.433	0.467	0.100	41.895	99.98	4.5
14	IDLE	0.375	452.7	4.109	0.0124	JET A	284.	46.	54.	0.0113	2.400	0.441	9.582	0.440	3.936	99.73	0.0

ORIGINAL PAGE IS
OF POOR QUALITY

Table C-1 (Cont'd)
Combustor Emissions Data

CONFIGURATION SS-2 REFERENCE BULKHEAD COMBUSTOR*

PT NO	OPERATING CONDITION	INLET PRES MPA	INLET TEMP DEG-K	BURNER AIRFLOW KG/SEC	METERED F/A RATIO	FUEL TYPE	FUEL TEMP DEG-K	PRI FUEL %	SEC FUEL %	CARBON BAL F/A RATIO	CO2 %	SPECIF HUMID G/KG	CORR CO EI G/KG	CORR THC EI G/KG	CORR NOX EI G/KG	CORR COMB EFFIC	SAE SMOKE NUMBER
****	*********	*****	*****	*******	*******	*****	*****	****	****	******	*****	******	******	******	******	*****	******
2	IDLE	0.371	452.7	4.132	0.0101	JET A	284.	59.	41.	0.0093	1.967	0.457	28.058	3.114	2.828	98.99	4.5
3	IDLE	0.364	454.7	4.100	0.0111	ERBS	281.	51.	49.	0.0100	2.100	0.359	23.633	1.611	3.299	99.24	2.3
4	APPROACH	0.899	579.9	8.190	0.0160	JET A	284.	21.	79.	0.0148	3.167	0.317	1.138	0.0	9.651	99.97	1.5
5	APPROACH	0.895	583.0	8.186	0.0159	ERBS	284.	22.	78.	0.0149	3.200	0.316	1.133	0.0	9.791	99.97	1.6
6	CRUISE	0.940	694.3	7.692	0.0194	JET A	284.	18.	82.	0.0175	3.733	0.314	1.027	0.0	19.344	99.98	2.6
7	CRUISE	0.942	699.4	7.714	0.0193	ERBS	283.	20.	80.	0.0174	3.733	0.314	1.029	0.0	19.171	99.98	2.0
8	CLIMB	1.967	734.9	16.086	0.0193	JET A	284.	9.	91.	0.0180	3.867	0.263	0.532	0.0	30.777	99.99	2.0
9	CLIMB	1.973	739.4	16.159	0.0191	ERBS	283.	9.	91.	0.0175	3.733	0.272	0.500	0.0	29.010	99.99	2.3
10	TAKEOFF	2.269	767.4	17.796	0.0193	JET A	288.	9.	91.	0.0174	3.733	0.435	0.503	0.101	37.298	99.98	3.2
11	TAKEOFF	2.258	765.2	17.846	0.0191	ERBS	286.	9.	91.	0.0166	3.600	0.433	0.400	0.100	36.230	99.98	4.5
14	IDLE	0.375	452.7	4.109	0.0124	JET A	284.	46.	54.	0.0113	2.400	0.441	8.600	0.372	3.640	99.76	0.0

CONFIGURATION SS-3 INCREASED PRIMARY ZONE RESIDENCE TIME

PT NO	OPERATING CONDITION	INLET PRES MPA	INLET TEMP DEG-K	BURNER AIRFLOW KG/SEC	METERED F/A RATIO	FUEL TYPE	FUEL TEMP DEG-K	PRI FUEL %	SEC FUEL %	CARBON BAL F/A RATIO	CO2 %	SPECIF HUMID G/KG	CORR CO EI G/KG	CORR THC EI G/KG	CORR NOX EI G/KG	CORR COMB EFFIC	SAE SMOKE NUMBER
2	IDLE	0.371	442.4	4.118	0.0104	ERBS	279.	53.	47.	0.0100	2.133	0.542	26.450	2.377	2.982	99.10	2.3
3	IDLE	0.357	446.7	4.195	0.0083	ERBS	278.	78.	22.	0.0085	1.733	0.514	79.426	15.337	1.063	96.19	1.6
4	IDLE	0.378	445.0	4.086	0.0142	ERBS	279.	53.	47.	0.0132	2.833	0.500	5.524	0.239	3.690	99.84	2.1
5	IDLE	0.362	447.7	5.025	0.0108	ERBS	279.	53.	47.	0.0107	2.267	0.510	28.100	1.500	2.265	99.14	1.5
6	APPROACH	0.890	577.9	8.290	0.0159	ERBS	282.	19.	81.	0.0137	2.933	0.449	0.960	0.232	8.950	99.95	2.5
7	CRUISE	0.950	695.0	7.769	0.0233	ERBS	281.	15.	85.	0.0193	4.200	0.465	2.411	0.167	21.342	99.92	2.1
8	CLIMB	1.960	735.9	16.131	0.0215	ERBS	281.	9.	91.	0.0135	4.033	0.370	1.027	0.099	36.150	99.96	2.5
9	TAKEOFF	2.274	768.3	18.050	0.0179	ERBS	281.	9.	91.	0.0165	3.567	0.393	0.537	0.134	38.688	99.97	2.0
10	TAKEOFF	2.259	769.0	17.878	0.0204	ERBS	282.	8.	92.	0.0183	3.967	0.382	0.801	0.100	45.450	99.97	2.2
11	TAKEOFF	2.252	771.5	18.091	0.0158	ERBS	282.	11.	89.	0.0148	3.200	0.376	0.333	0.200	37.251	99.97	2.5

CONFIGURATION SS-4 ALTERNATE FUEL INJECTOR

PT NO	OPERATING CONDITION	INLET PRES MPA	INLET TEMP DEG-K	BURNER AIRFLOW KG/SEC	METERED F/A RATIO	FUEL TYPE	FUEL TEMP DEG-K	PRI FUEL %	SEC FUEL %	CARBON BAL F/A RATIO	CO2 %	SPECIF HUMID G/KG	CORR CO EI G/KG	CORR THC EI G/KG	CORR NOX EI G/KG	CORR COMB EFFIC	SAE SMOKE NUMBER
2	IDLE	0.366	444.7	3.991	0.0117	ERBS	283.	49.	51.	0.0096	2.033	0.592	23.399	1.320	3.096	99.28	2.8
3	IDLE	0.365	444.2	4.009	0.0098	ERBS	283.	57.	43.	0.0087	1.800	0.846	54.711	9.705	2.935	9[illegible]3	3.2
4	IDLE	0.368	444.7	4.009	0.0145	ERBS	282.	39.	61.	0.0124	2.667	0.546	6.206	0.033	4.133	99.[illegible]	2.6
5	IDLE	0.364	446.9	4.871	0.0111	ERBS	285.	50.	50.	0.0094	2.000	1.016	34.713	2.268	2.672	98.90	2.0
6	APPROACH	0.894	581.2	8.190	0.0150	ERBS	285.	20.	80.	0.0228	4.900	0.792	0.865	0.100	7.455	99.97	12.3
7	CRUISE	0.942	695.3	7.556	0.0240	ERBS	284.	15.	85.	0.0195	4.233	0.803	0.930	0.033	16.639	99.97	3.0
8	CLIMB	1.964	735.4	15.832	0.0231	ERBS	283.	8.	92.	0.0195	4.233	0.393	0.631	0.066	30.637	99.98	5.0
9	TAKEOFF	2.252	775.2	17.710	0.0183	ERBS	284.	9.	91.	0.0163	3.500	0.436	0.266	0.100	31.260	99.98	2.1
10	TAKEOFF	2.246	767.9	17.669	0.0204	ERBS	284.	8.	92.	0.0180	3.900	0.447	0.365	0.0	33.882	99.99	3.3
11	TAKEOFF	2.249	765.2	17.565	0.0225	ERBS	283.	8.	92.	0.0192	4.133	0.469	0.399	0.0	37.667	99.99	3.1

*EMISSION EI BASED ON METERED FUEL-AIR RATIO

Table C-1 (Cont'd)
Combustor Emissions Data

CONFIGURATION SS-5 RICH PRIMARY ZONE

PT NO	OPERATING CONDITION	INLET PRES MPA	INLET TEMP DEG-K	BURNER AIRFLOW KG/SEC	METERED F/A RATIO	FUEL TYPE	FUEL TEMP DEG-K	PRI FUEL %	SEC FUEL %	CARBON BAL F/A RATIO	CO2 %	SPECIF HUMID G/KG	CORR CO EI G/KG	CORR THC EI G/KG	CORR NOX EI G/KG	CORR COMB EFFIC	SAE SMOKE NUMBER
****	*********	*****	*****	*******	*******	*****	*****	****	****	******	*****	******	******	******	******	*****	******
2	IDLE	0.367	447.0	4.013	0.0115	JET A	289.	49.	51.	0.0119	2.529	1.248	9.502	0.245	4.886	99.75	0.1
3	IDLE	0.367	445.5	4.010	0.0099	JET A	288.	58.	42.	0.0105	2.215	1.232	13.402	1.582	4.216	99.50	0.0
4	IDLE	0.368	445.8	3.994	0.0147	JET A	288.	39.	61.	0.0150	3.160	1.247	11.141	0.0	5.826	99.74	0.0
5	IDLE	0.367	445.3	3.993	0.0115	ERBS	288.	50.	50.	0.0113	2.433	1.239	9.642	0.525	4.641	99.71	0.2
6	IDLE	0.367	445.0	3.989	0.0101	ERBS	287.	57.	43.	0.0105	2.240	1.261	13.044	1.684	4.078	99.49	0.0
7	IDLE	0.368	444.8	3.997	0.0145	ERBS	287.	39.	61.	0.0145	3.117	1.291	10.865	0.062	5.889	99.73	0.0
8	APPROACH	0.894	581.0	8.114	0.0160	ERBS	288.	21.	79.	0.0160	3.447	1.189	2.265	0.0	13.855	99.95	1.3
9	CRUISE	0.943	692.9	7.676	0.0237	ERBS	286.	15.	85.	0.0254	5.498	1.248	7.455	0.0	14.984	99.82	13.2
10	CLIMB	1.967	734.1	15.854	0.0231	ERBS	285.	8.	92.	0.0249	5.381	1.196	2.522	0.0	23.146	99.94	6.4
11	TAKEOFF	2.252	768.2	17.608	0.0204	ERBS	285.	8.	92.	0.0226	4.885	1.140	1.241	0.002	33.981	99.97	2.8
14	IDLE	0.369	459.3	3.981	0.0117	JET A	289.	50.	50.	0.0120	2.558	1.244	8.480	0.093	5.651	99.79	0.0
15	IDLE	0.368	459.0	4.011	0.0101	JET A	289.	57.	43.	0.0106	2.256	1.270	10.820	0.707	4.763	99.67	0.0
16	IDLE	0.369	457.6	4.001	0.0146	JET A	289.	39.	61.	0.0149	3.170	1.248	10.610	0.0	6.286	99.75	0.0

CONFIGURATION SS-6 MODERATELY LEAN PRIMARY ZONE

PT NO	OPERATING CONDITION	INLET PRES MPA	INLET TEMP DEG-K	BURNER AIRFLOW KG/SEC	METERED F/A RATIO	FUEL TYPE	FUEL TEMP DEG-K	PRI FUEL %	SEC FUEL %	CARBON BAL F/A RATIO	CO2 %	SPECIF HUMID G/KG	CORR CO EI G/KG	CORR THC EI G/KG	CORR NOX EI G/KG	CORR COMB EFFIC	SAE SMOKE NUMBER
2	IDLE	0.364	444.6	4.063	0.0115	JET A	285.	50.	50.	0.0113	2.228	0.803	70.545	54.779	3.368	91.93	0.1
3	IDLE	0.363	443.2	4.085	0.0111	ERBS	284.	51.	49.	0.0109	2.149	0.826	78.203	64.309	3.312	90.48	0.3
4	IDLE	0.364	443.1	4.109	0.0094	ERBS	284.	59.	41.	0.0093	1.687	0.812	96.725	138.377	2.998	81.19	0.4
5	IDLE	0.364	443.0	4.090	0.0132	ERBS	284.	43.	57.	0.0130	2.732	0.806	43.029	8.931	3.892	97.90	0.4
6	IDLE	0.363	446.0	4.914	0.0111	ERBS	282.	50.	50.	0.0111	2.080	0.831	83.253	114.771	2.352	84.27	0.1
7	IDLE	0.365	444.9	4.070	0.0113	12.3%	283.	50.	50.	0.0109	2.156	0.856	81.370	67.014	2.627	90.00	0.6
8	IDLE	0.365	444.9	4.079	0.0113	11.8%	283.	51.	49.	0.0107	2.106	0.811	80.856	73.825	2.360	89.12	0.1
9	IDLE	0.363	444.8	4.092	0.0098	11.8%	283.	58.	42.	0.0096	1.784	1.186	95.739	125.967	2.006	82.40	0.1
10	IDLE	0.365	445.1	4.077	0.0133	11.8%	283.	42.	58.	0.0133	2.731	0.845	45.287	13.371	3.180	97.21	1.0
11	APPROACH	0.889	587.6	8.283	0.0157	JET A	283.	21.	79.	0.0156	3.347	0.798	1.051	0.224	10.402	99.95	0.1
12	APPROACH	0.869	584.7	8.272	0.0158	ERBS	283.	21.	79.	0.0151	3.255	0.794	1.111	0.676	10.520	99.89	0.5
13	CRUISE	0.938	699.5	7.787	0.0182	JET A	284.	20.	80.	0.0173	3.707	0.828	0.686	0.012	17.555	99.98	0.4
14	CRUISE	0.941	695.4	7.801	0.0181	ERBS	283.	0.	100.	0.0171	3.682	0.864	0.703	0.158	17.686	99.96	0.1
15	CRUISE	0.940	701.8	7.811	0.0181	12.3%	281.	19.	81.	0.0170	3.680	0.826	0.683	0.004	18.987	99.98	0.1
16	CRUISE	0.939	707.4	7.791	0.0181	11.8%	281.	20.	80.	0.0169	3.683	0.790	0.692	0.116	19.597	99.97	0.1
17	CLIMB	1.961	737.9	16.155	0.0181	JET A	284.	10.	90.	0.0177	3.799	0.724	0.341	0.014	26.745	99.99	0.4
18	CLIMB	1.963	742.7	16.088	0.0182	ERBS	283.	10.	90.	0.0178	3.841	0.722	0.353	0.019	28.977	99.99	0.3
19	TAKEOFF	2.184	768.3	17.924	0.0180	JET A	285.	9.	91.	0.0183	3.912	0.701	0.349	0.029	32.720	99.99	1.3
20	TAKEOFF	2.163	769.1	17.980	0.0160	JET A	285.	9.	91.	0.0164	3.505	0.725	0.288	0.049	32.703	99.99	1.0
21	TAKEOFF	2.249	768.9	17.924	0.0183	ERBS	283.	9.	91.	0.0179	3.864	0.728	0.364	0.025	34.406	99.99	1.7
22	TAKFOFF	2.247	769.9	17.952	0.0162	ERBS	283.	10.	90.	0.0162	3.485	0.730	0.276	0.025	35.029	99.99	0.5
23	TAKEOFF	2.246	769.3	17.883	0.0181	11.8%	283.	9.	91.	0.0179	3.919	2.039	0.335	0.031	37.547	99.99	1.3
24	TAKEOFF	2.252	771.7	17.834	0.0183	12.3%	281.	9.	91.	0.0181	3.923	0.755	0.334	0.015	35.539	99.99	1.6
29	IDLE	0.366	463.9	4.075	0.0114	JET A	284.	50.	50.	0.0114	2.257	0.769	63.615	51.963	3.557	92.46	0.0
30	IDLE	0.367	464.3	4.055	0.0112	ERBS	282.	50.	50.	0.0111	2.198	0.804	70.243	57.943	3.731	91.47	0.0
31	IDLE	0.367	464.6	4.086	0.0097	ERBS	283.	58.	42.	0.0096	1.810	0.814	92.737	113.497	3.378	84.37	0.0
32	IDLE	0.365	465.4	4.072	0.0132	ERBS	283.	44.	56.	0.0129	2.719	0.808	38.621	5.923	4.371	98.37	0.0

Table C-1 (Cont'd)
Combustor Emissions Data

CONFIGURATION SS-7 FINAL SINGLE STAGE

PT NO	OPERATING CONDITION	INLET PRES MPA	INLET TEMP DEG-K	BURNER AIRFLOW KG/SEC	METERED F/A RATIO	FUEL TYPE	FUEL TEMP DEG-K	PRI FUEL %	SEC FUEL %	CARBON BAL F/A RATIO	CO2 %	SPECIF HUMID G/KG	CORR CO EI G/KG	CORR THC EI G/KG	CORR NOX EI G/KG	CORR COMB EFFIC	SAE SMOKE NUMBER
****	*********	*****	*****	*******	*******	*****	*****	****	****	******	*****	******	******	******	******	*****	******
2	IDLE	0.367	448.0	3.991	0.0113	JET A	293.	51.	49.	0.0134	2.812	1.226	24.463	5.025	3.498	98.84	0.0
3	IDLE	0.367	442.4	3.959	0.0115	ERBS	292.	52.	48.	0.0136	2.862	1.220	27.134	6.672	3.481	98.57	0.0
4	IDLE	0.367	442.7	3.976	0.0106	ERBS	292.	56.	44.	0.0116	2.401	1.215	46.644	17.381	2.807	96.83	0.0
5	IDLE	0.367	445.4	3.964	0.0137	ERBS	293.	43.	57.	0.0163	3.476	1.216	14.237	1.281	4.248	99.51	0.0
6	IDLE	0.367	448.2	3.987	0.0117	12.3%	291.	50.	50.	0.0138	2.936	1.181	25.380	5.857	3.627	98.69	0.0
7	IDLE	0.367	449.4	3.978	0.0115	11.6%	291.	51.	49.	0.0134	2.861	1.197	30.078	7.656	3.668	98.35	0.0
8	IDLE	0.356	449.3	3.996	0.0098	11.8%	291.	59.	41.	0.0113	2.355	1.164	57.761	21.378	2.833	96.03	0.0
9	IDLE	0.366	449.3	3.975	0.0144	11.8%	291.	41.	59.	0.0170	3.675	1.211	11.487	0.823	4.600	99.62	0.0
10	APPROACH	0.892	578.7	8.215	0.0155	JET A	293.	22.	78.	0.0197	4.227	1.182	0.995	0.003	11.007	99.98	0.1
11	APPROACH	0.892	578.9	8.244	0.0155	ERBS	292.	21.	79.	0.0192	4.142	1.176	1.301	0.011	11.090	99.97	0.1
12	CRUISE	0.938	697.0	7.686	0.0232	JET A	293.	16.	84.	0.0305	6.593	1.161	2.212	0.011	25.061	99.95	0.9
13	CRUISE	0.940	697.9	7.743	0.0230	ERBS	292.	15.	85.	0.0300	6.537	1.175	2.021	0.0	24.748	99.95	1.1
14	CRUISE	0.941	698.3	7.624	0.0234	12.3%	291.	15.	85.	0.0302	6.605	1.160	2.002	0.0	26.114	99.95	3.8
15	CRUISE	0.938	698.6	7.672	0.0232	11.8%	291.	15.	85.	0.0298	6.560	1.168	1.794	0.0	26.258	99.96	0.9
16	CLIMB	1.960	738.8	15.892	0.0203	JET A	291.	9.	91.	0.0256	5.510	2.203	0.417	0.030	40.140	99.99	0.8
17	CLIMB	1.962	738.0	15.906	0.0202	ERBS	291.	9.	91.	0.0254	5.497	0.967	0.404	0.023	39.678	99.99	1.1
18	TAKEOFF	2.248	766.0	17.508	0.0202	JET A	291.	9.	91.	0.0250	5.383	0.980	0.333	0.015	47.394	99.99	2.0
19	TAKEOFF	2.250	765.7	17.604	0.0180	JET A	292.	10.	90.	0.0228	4.893	0.872	0.255	0.027	47.028	99.99	0.6
20	TAKEOFF	2.247	766.4	17.642	0.0199	ERBS	290.	9.	91.	0.0253	5.481	0.914	0.326	0.013	47.931	99.99	1.7
21	TAKEOFF	2.250	765.7	17.607	0.0180	ERBS	291.	10.	90.	0.0223	4.825	0.916	0.241	0.010	46.889	99.99	0.5
22	TAKEOFF	2.252	766.6	17.555	0.0201	12.3%	286.	9.	91.	0.0254	5.517	0.889	0.333	0.022	49.150	99.99	0.7
23	TAKEOFF	2.251	767.1	17.630	0.0200	11.8%	288.	9.	91.	0.0254	5.573	0.877	0.321	0.011	51.569	99.99	0.4

C-3

Table C-1 (Cont'd)
Combustor Emissions Data

CONFIGURATION VG-1 REFERENCE VARIABLE GEOMETRY

PT NO	OPERATING CONDITION	INLET PRES MPA	INLET TEMP DEG-K	BURNER AIRFLOW KG/SEC	METERED F/A RATIO	FUEL TYPE	FUEL TEMP DEG-K	PPI FUEL %	SEC FUEL %	CARBON BAL F/A RATIO	CO2 %	SPECIF HUMID G/KG	CORR CO EI G/KG	CORR THC EI G/KG	CORR NOX EI G/KG	CORR COMB EFFIC	SAE SMOKE NUMBER
****	*********	*****	*****	*******	*******	*****	*****	****	****	******	*****	******	******	******	******	*****	******
2	IDLE	0.372	453.3	4.122	0.0111	JET A	284.	0.	100.	0.0102	2.167	0.476	16.119	1.139	4.138	99.50	2.3
3	IDLE	0.364	454.6	4.136	0.0096	EPBS	281.	0.	100.	0.0089	1.900	0.363	55.694	8.954	2.552	97.59	2.9
4	IDLE	0.366	454.7	4.082	0.0144	EPBS	282.	0.	100.	0.0.27	2.700	0.364	10.441	0.991	4.248	99.63	1.5
5	IDLE	0.365	454.8	4.122	0.0111	EPBS	281.	0.	100.	0.0101	2.133	0.320	28.060	2.338	3.233	99.05	1.7
6	IDLE	0.365	441.3	4.889	0.0111	EPBS	283.	0.	100.	0.0100	2.067	0.583	57.752	9.938	2.529	97.43	1.8
7	IDLE	0.365	446.9	4.091	0.0112	12.3%	287.	0.	100.	0.0096	2.067	0.427	38.463	3.389	3.422	98.66	6.8
8	IDLE	0.369	445.9	4.073	0.0111	11.8%	286.	0.	100.	0.0100	2.133	0.432	42.544	4.391	3.373	98.45	2.9
9	IDLE	0.366	442.6	4.109	0.0096	11.8%	285.	0.	100.	0.0086	1.700	0.901	101.575	44.753	1.966	92.15	2.5
10	IDLE	0.368	442.4	4.054	0.0144	11.8%	285.	0.	100.	0.0125	2.733	1.355	11.861	1.296	4.348	99.56	2.7
11	APPROACH	0.898	582.8	8.181	0.0159	JET A	284.	0.	100.	0.0151	3.233	0.319	1.136	0.0	11.174	99.97	1.7
12	APPROACH	0.895	582.2	8.195	0.0159	EPBS	284.	0.	100.	0.0148	3.200	0.314	1.100	0.0	11.488	99.97	1.7
13	CRUISE	0.940	695.2	7.705	0.0194	JET A	285.	0.	100.	0.0177	3.833	0.374	1.093	0.0	20.231	99.97	3.5
14	CRUISE	0.933	698.8	7.787	0.0192	EPBS	284.	0.	100.	0.0169	3.667	0.385	0.987	0.0	20.877	99.98	3.1
15	CRUISE	0.938	697.6	7.773	0.0192	12.3%	285.	0.	100.	0.0169	3.667	0.351	1.025	0.0	21.141	99.98	3.3
16	CRUISE	0.937	695.0	7.755	0.0192	11.8%	285.	0.	100.	0.0171	3.733	0.364	1.056	0.0	21.487	99.97	2.4
17	CLIMB	1.964	731.6	16.054	0.0193	JET A	286.	0.	100.	0.0173	3.733	0.244	0.498	0.0	31.678	99.99	2.1
18	CLIMB	1.957	732.0	16.045	0.0192	ERBS	285.	0.	100.	0.0171	3.733	0.242	0.529	0.0	31.799	99.99	2.2
19	TAKEOFF	2.263	767.6	17.773	0.0193	JET A	288.	0.	100.	0.0175	3.767	0.408	0.535	0.0	38.675	99.99	3.8
20	TAKEOFF	2.256	768.7	17.868	0.0172	JET A	288.	0.	100.	0.0159	3.400	0.263	0.466	0.0	37.466	99.99	1.8
21	TAKEOFF	2.255	772.3	17.896	0.0171	EPBS	287.	0.	100.	0.0153	3.300	0.237	0.300	0.067	39.201	99.99	2.9
22	TAKEOFF	2.257	766.6	17.891	0.0192	EPBS	286.	0.	100.	0.0169	3.667	0.260	0.433	0.0	39.389	99.99	4.3
23	TAKEOFF	2.257	764.3	17.819	0.0173	11.8%	286.	0.	100.	0.0151	3.300	0.263	0.300	0.0	40.577	99.99	2.1
24	TAKEOFF	2.262	763.3	17.791	0.0193	11.8%	285.	0.	100.	0.0168	3.667	0.258	0.434	0.0	42.011	99.99	2.2
25	TAKEOFF	2.261	765.3	17.791	0.0194	12.3%	285.	0.	100.	0.0170	3.700	0.253	0.434	0.0	41.155	99.99	2.9
26	TAKEOFF	2.259	768.2	15.927	0.0194	EPBS	285.	0.	100.	0.0165	3.567	0.246	0.367	0.0	43.751	99.99	2.3

Table C-1 (Cont'd)
Combustor Emissions Data

CONFIGURATION VS-1 REFERENCE VARIABLE GEOMETRY*

PT NO	OPERATING CONDITION	INLET PRES MPA	INLET TEMP DEG-K	BURNER AIRFLOW KG/SEC	METERED F/A RATIO	FUEL TYPE	FUEL TEMP DEG-K	PRI FUEL %	SEC FUEL %	CARBON BAL F/A RATIO	CO2 %	SPECIF HUMID G/KG	CORR CO EI G/KG	CORR THC EI G/KG	CORR NOX EI G/KG	CORR COMB EFFIC	SAE SMOKE NUMBER
2	IDLE	0.372	453.3	4.122	0.0111	JET A	284.	0.	100.	0.0102	2.167	0.476	14.678	1.005	3.780	99.54	2.3
3	IDLE	0.364	454.6	4.136	0.0096	EPBS	281.	0.	100.	0.0089	1.900	0.363	51.430	8.233	2.372	97.78	2.9
4	IDLE	0.366	454.7	4.082	0.0144	EPBS	282.	0.	100.	0.0127	2.700	0.364	9.020	0.859	3.769	99.68	1.5
5	IDLE	0.365	454.8	4.122	0.0111	EPBS	281.	0.	100.	0.0101	2.133	0.319	25.326	2.075	2.934	99.15	1.7
6	IDLE	0.365	441.3	4.889	0.0111	EPBS	283.	0.	100.	0.0100	2.067	0.588	52.092	8.984	2.228	97.68	1.8
7	IDLE	0.365	446.9	4.091	0.0112	12.3%	287.	0.	100.	0.0096	2.067	0.427	33.231	2.695	2.971	98.85	6.8
8	IDLE	0.369	445.9	4.073	0.0111	11.8%	286.	0.	100.	0.0100	2.133	0.432	37.588	3.825	3.045	98.64	2.9
9	IDLE	0.366	442.6	4.109	0.0096	11.8%	285.	0.	100.	0.0086	1.700	0.901	89.934	39.278	1.785	93.09	2.5
10	IDLE	0.368	442.4	4.084	0.0144	11.8%	285.	0.	100.	0.0125	2.733	1.365	10.333	1.063	3.831	99.62	2.7
11	APPROACH	0.898	582.8	8.181	0.0159	JET A	284.	0.	100.	0.0151	3.233	0.319	1.070	0.0	10.609	99.98	1.7
12	APPROACH	0.895	582.2	8.195	0.0159	EPBS	284.	0.	100.	0.0148	3.200	0.314	1.000	0.0	10.685	99.98	1.7
13	CRUISE	0.940	695.2	7.705	0.0194	JET A	285.	0.	100.	0.0177	3.833	0.374	1.027	0.0	18.468	99.98	3.5
14	CRUISE	0.933	693.8	7.787	0.0192	EPBS	284.	0.	100.	0.0169	3.667	0.335	0.921	0.0	18.388	99.98	3.1
15	CRUISE	0.938	697.6	7.773	0.0192	12.3%	285.	0.	100.	0.0169	3.667	0.351	0.892	0.0	18.569	99.98	3.3
16	CRUISE	0.937	695.0	7.755	0.0192	11.8%	285.	0.	100.	0.0171	3.733	0.364	0.924	0.0	19.093	99.98	2.4
17	CLIMB	1.964	731.6	16.054	0.0193	JET A	286.	0.	100.	0.0173	3.733	0.144	0.465	0.0	28.403	99.99	2.1
18	CLIMB	1.957	732.0	16.045	0.0192	EPBS	285.	0.	100.	0.0171	3.733	0.242	0.430	0.0	28.249	99.99	2.2
19	TAKEOFF	2.263	767.6	17.773	0.0193	JET A	288.	0.	100.	0.0175	3.767	0.403	0.468	0.0	35.162	99.99	3.8
20	TAKEOFF	2.256	768.7	17.868	0.0172	JET A	288.	0.	100.	0.0159	3.400	0.263	0.400	0.0	34.671	99.99	1.8
21	TAKEOFF	2.255	772.3	17.896	0.0171	EPBS	287.	0.	100.	0.0153	3.300	0.237	0.300	0.067	34.247	99.99	2.9
22	TAKEOFF	2.257	766.6	17.891	0.0192	EPBS	286.	0.	100.	0.0169	3.667	0.260	0.400	0.0	34.662	99.99	4.3
23	TAKEOFF	2.257	764.3	17.819	0.0173	11.8%	286.	0.	100.	0.0151	3.300	0.263	0.300	0.0	35.405	99.99	2.1
24	TAKEOFF	2.262	763.3	17.791	0.0193	11.8%	285	0.	100.	0.0163	3.667	0.258	0.363	0.0	36.429	99.99	2.2
25	TAKEOFF	2.261	765.3	17.791	0.0194	12.3%	285.	0.	100.	0.0170	3.700	0.253	0.367	0.0	36.256	99.99	2.9
26	TAKEOFF	2.259	768.2	15.927	0.0194	EPBS	285.	0.	100.	0.0165	3.567	0.246	0.267	0.0	37.247	99.99	2.3

ORIGINAL PAGE IS OF POOR QUALITY

CONFIGURATION VS-2 ALTERNATE FUEL INJECTOR SINGLE PIPE MODE*

PT NO	OPERATING CONDITION	INLET PRES MPA	INLET TEMP DEG-K	BURNER AIRFLOW KG/SEC	METERED F/A RATIO	FUEL TYPE	FUEL TEMP DEG-K	PRI FUEL %	SEC FUEL %	CARBON BAL F/A RATIO	CO2 %	SPECIF HUMID G/KG	CORR CO EI G/KG	CORR THC EI G/KG	CORR NOX EI G/KG	CORR COMB EFFIC	SAE SMOKE NUMBER
2	IDLE	0.369	447.9	3.995	0.0113	EPBS	286.	0.	100.	0.0095	2.033	1.010	32.393	3.126	1.781	98.86	3.0
3	IDLE	0.368	449.2	4.045	0.0097	EPBS	286.	0.	100.	0.0073	1.567	1.042	54.447	18.735	1.996	96.49	1.8
4	IDLE	0.368	450.5	4.036	0.0144	EPBS	285.	0.	100.	0.0106	2.300	0.914	8.499	0.100	3.136	99.79	2.5
5	IDLE	0.366	453.9	4.875	0.0112	EPBS	285.	0.	100.	0.0086	1.867	1.010	43.408	7.784	2.728	98.04	2.3
6	APPROACH	0.892	583.4	8.172	0.0160	EPBS	284.	0.	100.	0.0230	4.900	0.761	0.796	0.0	7.519	99.98	3.5
7	CRUISE	0.963	704.5	7.619	0.0239	EPBS	285.	0.	100.	0.0188	4.133	0.540	0.985	0.0	13.117	99.98	4.4
8	CLIMB	1.962	737.0	15.891	0.0231	EPBS	284.	0.	100.	0.0199	4.333	0.454	0.630	0.0	26.707	99.98	4.1
9	TAKEOFF	2.254	772.7	17.692	0.0184	EPBS	284.	0.	100.	0.0159	3.467	0.470	0.266	0.0	27.327	99.99	2.8
10	TAKEOFF	2.247	773.5	17.615	0.0205	EPBS	284.	0.	100.	0.0171	3.700	0.419	0.332	0.232	30.838	99.96	2.0
11	TAKEOFF	2.240	774.5	17.642	0.0225	EPBS	284.	0.	100.	0.0195	4.233	0.420	0.496	0.0	34.123	99.99	3.1

*EMISSION EI BASED ON METERED FUEL-AIR RATIO

ORIGINAL PAGE IS
OF POOR QUALITY

Table C-1 (Cont'd)
Combustor Emissions Data

CONFIGURATION VS-3 VARIABLE FUEL INJECTOR OPEN POSITION*

PT NO	OPERATING CONDITION	INLET PRES MPA	INLET TEMP DEG-K	BURNER AIRFLOW KG/SEC	METERED F/A RATIO	FUEL TYPE	FUEL TEMP DEG-K	PRI FUEL %	SEC FUEL %	CARBON BAL F/A RATIO	CO2 %	SPECIF HUMID G/KG	CORR CO EI G/KG	CORR THC EI G/KG	CORR NOX EI G/KG	CORR COMB EFFIC	SAE SMOKE NUMBER
2	IDLE	0.366	448.0	4.016	0.0112	ERBS	282.	100.	0.	0.0101	2.133	0.524	29.347	3.541	2.741	98.87	5.0
3	APPROACH	0.855	551.9	8.132	0.0161	ERBS	281.	0.	100.	0.0140	3.000	0.510	0.725	0.297	8.201	99.95	4.9
4	CRUISE	0.964	695.0	7.624	0.0239	JET A	286.	0.	100.	0.0221	4.767	0.340	1.563	0.0	21.997	99.96	3.6
5	CRUISE	0.956	694.0	7.687	0.0240	ERBS	285.	0.	100.	0.0207	4.567	0.353	1.314	0.0	21.298	99.97	3.4
6	CRUISE	0.929	694.1	7.719	0.0203	ERBS	285.	0.	100.	0.0190	4.133	0.346	0.851	0.0	19.690	99.98	2.0
7	CLIMB	1.999	734.2	15.814	0.0233	ERBS	284.	0.	100.	0.0208	4.533	0.309	0.574	0.0	35.134	99.99	3.4
8	TAKEOFF	2.305	765.7	17.955	0.0216	JET A	286.	0.	100.	0.0203	4.467	0.316	0.545	0.0	43.577	99.99	2.6
9	TAKEOFF	2.304	767.9	17.678	0.0195	JET A	287.	0.	100.	0.0190	4.033	0.312	0.408	0.0	41.823	99.99	4.8
10	TAKEOFF	2.307	764.8	17.664	0.0195	ERBS	285.	0.	100.	0.0185	4.033	0.307	0.375	0.0	40.255	99.99	2.6
11	TAKEOFF	2.298	765.2	17.678	0.0216	ERBS	285.	0.	100.	0.0204	4.400	0.307	0.467	0.0	44.143	99.99	2.8

CONFIGURATION VS-4 VARIABLE FUEL INJECTOR CLOSED POSITION*

PT NO	OPERATING CONDITION	INLET PRES MPA	INLET TEMP DEG-K	BURNER AIRFLOW KG/SEC	METERED F/A RATIO	FUEL TYPE	FUEL TEMP DEG-K	PRI FUEL %	SEC FUEL %	CARBON BAL F/A RATIO	CO2 %	SPECIF HUMID G/KG	CORR CO EI G/KG	CORR THC EI G/KG	CORR NOX EI G/KG	CORR COMB EFFIC	SAE SMOKE NUMBER
2	IDLE	0.367	452.1	3.878	0.0117	JET A	286.	0.	100.	0.0093	1.933	0.446	26.324	2.714	2.366	99.34	0.4
3	IDLE	0.367	452.1	3.932	0.0097	JET A	286.	0.	100.	0.0080	1.633	0.447	44.913	8.247	1.647	97.99	0.1
4	IDLE	0.368	452.1	3.873	0.0150	JET A	286.	0.	100.	0.0116	2.467	0.446	9.926	0.432	2.482	99.72	1.1
7	IDLE	0.367	452.0	3.841	0.0151	ERBS	285.	0.	100.	0.0114	2.467	0.447	11.209	0.562	2.157	99.67	0.1
8	APPROACH	0.894	584.3	8.063	0.0162	ERBS	285.	0.	100.	0.0134	2.833	0.467	1.897	0.166	13.841	99.94	0.4
9	CRUISE	0.937	700.1	7.687	0.0237	ERBS	282.	0.	100.	0.0173	3.833	0.486	1.156	0.0	17.725	99.97	2.4
10	CLIMB	1.964	736.5	15.810	0.0231	ERBS	281.	0.	100.	0.0175	3.867	0.434	0.631	0.0	29.726	99.98	3.1
11	TAKEOFF	2.266	771.1	17.587	0.0254	ERBS	280.	0.	100.	0.0177	3.933	0.393	0.502	0.0	37.474	99.99	3.0

*EMISSION EI BASED ON METERED FUEL-AIR RATIO

Table C-1 (Cont'd)
Combustor Emissions Data

CONFIGURATION VG-5 LEAN PRIMARY ZONE

PT NO	OPERATING CONDITION	INLET PRES MPA	INLET TEMP DEG-K	BURNER AIRFLOW KG/SEC	METERED F/A RATIO	FUEL TYPE	FUEL TEMP DEG-K	PRI FUEL %	SEC FUEL %	CARBON BAL F/A RATIO	CO2 %	SPECIF HUMID G/KG	CORR CO EI G/KG	CORR THC EI G/KG	CORR NOX EI G/KG	CORR COMB EFFIC	SAE SMOKE NUMBER
****	*********	*****	*****	*******	*******	*****	*****	****	****	******	*****	******	******	******	******	*****	******
2	IDLE	0.366	449.8	4.120	0.0109	ERBS	282.	0.	100.	0.0125	2.282	0.820	108.724	118.361	1.757	83.38	1.2
3	APPROACH	0.895	583.2	8.263	0.0157	ERBS	282.	0.	100.	0.0181	3.893	0.796	0.862	0.500	8.287	99.92	0.7
4	CRUISE	0.944	705.5	7.793	0.0201	JET A	283.	0.	100.	0.0234	5.013	0.773	1.021	0.282	14.581	99.94	0.7
5	CRUISE	0.942	706.9	7.822	0.0180	ERBS	281.	0.	100.	0.0205	4.420	0.743	0.577	0.184	14.122	99.96	0.7
6	CRUISE	0.941	707.2	7.778	0.0202	ERBS	280.	0.	100.	0.0230	4.961	0.720	0.873	0.095	14.693	99.97	1.3
7	CLIMB	1.964	734.2	15.984	0.0190	ERBS	284.	0.	100.	0.0224	4.851	0.715	0.444	0.017	21.891	99.99	1.0
8	TAKEOFF	2.253	776.2	17.809	0.0190	JET A	285.	0.	100.	0.0222	4.762	0.709	0.491	0.057	27.437	99.98	1.5
9	TAKEOFF	2.253	771.1	17.702	0.0170	JET A	285.	0.	100.	0.0201	4.325	6.071	0.312	0.017	28.386	99.99	1.3
10	TAKEOFF	2.253	767.2	17.755	0.0191	ERBS	283.	0.	100.	0.0224	4.840	0.758	0.423	0.016	27.500	99.99	1.7
11	TAKEOFF	2.252	767.6	17.824	0.0170	ERBS	283.	0.	100.	0.0202	4.373	0.716	0.292	0.021	25.940	99.99	1.2

CONFIGURATION VG-6 RICH PRIMARY ZONE

PT NO	OPERATING CONDITION	INLET PRES MPA	INLET TEMP DEG-K	BURNER AIRFLOW KG/SEC	METERED F/A RATIO	FUEL TYPE	FUEL TEMP DEG-K	PRI FUEL %	SEC FUEL %	CARBON BAL F/A RATIO	CO2 %	SPECIF HUMID G/KG	CORR CO EI G/KG	CORR THC EI G/KG	CORR NOX EI G/KG	CORR COMB EFFIC	SAE SMOKE NUMBER
2	IDLE	0.369	448.5	4.027	0.0112	JET A	290.	0.	100.	0.0117	2.495	1.479	9.031	0.681	4.373	99.71	0.3
3	IDLE	0.367	449.7	4.060	0.0111	ERBS	290.	0.	100.	0.0115	2.453	1.328	10.178	1.018	4.493	99.64	0.6
4	IDLE	0.349	450.1	4.098	0.0096	ERBS	290.	0.	100.	0.0103	2.152	1.507	30.527	16.375	3.601	97.20	0.0
5	IDLE	0.368	450.4	4.026	0.0145	ERBS	290.	0.	100.	0.0149	3.183	1.515	13.012	1.904	5.714	99.47	0.0
6	IDLE	0.368	450.8	4.007	0.0113	12.3%	290.	0.	100.	0.0116	2.503	1.533	10.112	1.375	4.635	99.59	0.6
7	IDLE	0.369	450.8	4.023	0.0113	11.8%	291.	0.	100.	0.0114	2.484	1.513	10.878	1.247	4.602	99.59	0.4
8	IDLE	0.368	451.3	4.050	0.0098	11.8%	291.	0.	100.	0.0105	2.211	1.533	29.428	16.170	3.841	97.35	0.0
9	IDLE	0.358	451.3	4.018	0.0145	11.8%	292.	0.	100.	0.0149	3.227	1.543	13.026	0.849	5.681	99.58	0.0
10	APPROACH	0.895	583.1	8.198	0.0161	JET A	289.	0.	100.	0.0167	3.572	1.284	2.739	0.043	13.807	99.93	1.5
11	APPROACH	0.893	583.9	8.196	0.0161	ERBS	289.	0.	100.	0.0166	3.565	1.287	2.617	0.0	14.591	99.94	2.3
12	CRUISE	0.946	697.7	7.528	0.0211	JET A	290.	0.	100.	0.0216	4.638	1.293	4.406	0.0	18.645	99.90	2.5
13	CRUISE	0.947	694.4	7.576	0.0208	ERBS	289.	0.	100.	0.0215	4.627	1.304	4.142	0.005	19.836	99.90	3.7
14	CRUISE	0.946	694.7	7.596	0.0208	12.3%	291.	0.	100.	0.0214	4.642	1.286	3.628	0.0	20.400	99.91	3.9
15	CRUISE	0.945	696.1	7.598	0.0208	11.8%	291.	0.	100.	0.0212	4.621	1.284	3.4[illegible]	0.0	21.249	99.92	4.2
16	CLIMB	1.968	747.2	15.813	0.0207	JET A	291.	0.	100.	0.0221	4.735	1.110	2.062	0.018	28.947	99.95	2.1
17	CLIMB	1.971	744.3	15.793	0.0208	ERBS	289.	0.	100.	0.0220	4.765	1.138	1.900	0.020	30.735	99.95	1.8
18	TAKEOFF	2.252	768.5	17.586	0.0185	JET A	290.	0.	100.	0.0200	4.278	1.059	0.924	0.025	40.023	99.98	0.8
19	TAKEOFF	2.255	767.2	17.566	0.0207	JET A	290.	0.	100.	0.0223	4.770	1.050	1.659	0.021	32.074	99.96	2.0
20	TAKEOFF	2.256	771.6	17.599	0.0185	ERBS	290.	0.	100.	0.0198	4.269	1.067	1.013	0.015	42.903	99.97	0.4
21	TAKEOFF	2.253	769.2	17.603	0.0206	ERBS	289.	0.	100.	0.0221	4.778	0.924	1.559	0.008	34.514	99.96	1.8
22	TAKEOFF	2.256	770.5	17.604	0.0206	12.3%	293.	0.	100.	0.0220	4.788	1.062	1.538	0.008	35.822	99.96	2.5
23	TAKEOFF	2.254	749.6	17.635	0.0206	11.8%	293.	0.	100.	0.0220	4.798	1.099	1.681	0.007	37.359	99.96	2.4
27	IDLE	0.368	465.2	4.010	0.0113	JET A	291.	0.	100.	0.0120	2.551	1.525	7.748	0.125	4.360	99.80	0.0
28	IDLE	0.368	468.1	4.025	0.0113	ERBS	291.	0.	100.	0.0116	2.493	1.550	7.786	0.095	4.220	99.80	0.0
29	IDLE	0.369	468.7	4.033	0.0099	ERBS	291.	0.	100.	0.0103	2.197	1.538	15.092	2.709	3.497	99.32	0.0
30	IDLE	0.368	469.3	4.044	0.0145	ERBS	291.	0.	100.	0.0148	3.178	1.533	11.393	0.338	6.178	99.69	0.0

Table C-1 (Cont'd)
Combustor Emissions Data

CONFIGURATION VG-7 FINAL VARIABLE GEOMETRY LOW POWER AIR SCHEDULE

PT NO	OPERATING CONDITION	INLET PRES MPA	INLET TEMP DEG-K	BURNER AIRFLOW KG/SEC	METERED F/A RATIO	FUEL TYPE	FUEL TEMP DEG-K	PRI FUEL %	SEC FUEL %	CARBON BAL F/A RATIO	CO2 %	SPECIF HUMID G/KG	CORR CO EI G/KG	CORR THC EI G/KG	CORR NOX EI G/KG	CORR COMB EFFIC	SAE SMOKE NUMBER
2	IDLE	0.365	445.9	3.976	0.0109	JET A	292.	0.	100.	0.0134	2.809	1.317	20.875	4.138	4.315	99.02	0.0
3	IDLE	0.364	446.8	3.985	0.0110	ERBS	[illegible]	0.	100.	0.0134	2.844	1.312	23.256	5.336	4.589	98.81	0.0
4	IDLE	0.364	446.2	3.988	0.0097	ERBS	291.	0.	100.	0.0117	2.437	1.314	33.602	12.371	3.607	97.72	0.0
5	IDLE	0.364	446.9	3.981	0.0140	ERBS	291.	0.	100.	0.0176	3.771	1.318	13.169	0.492	5.277	99.62	0.0
6	IDLE	0.364	447.9	3.980	0.0110	12.3%	291.	0.	100.	0.0131	2.788	1.320	23.981	5.610	4.618	98.75	0.0
7	IDLE	0.363	445.2	3.980	0.0111	11.8%	290.	0.	100.	0.0132	2.845	1.162	24.651	6.995	4.845	98.55	0.0
9	IDLE	0.363	445.7	3.979	0.0141	11.8%	291.	0.	100.	0.0170	3.686	1.339	12.826	0.717	5.118	99.60	0.0
10	APPROACH	0.892	571.8	8.039	0.0157	JET A	292.	0.	100.	0.0194	4.158	1.289	1.318	0.002	15.114	99.97	1.3
11	APPROACH	0.892	582.0	8.042	0.0157	ERBS	292.	0.	100.	0.0194	4.182	1.279	1.259	0.049	16.113	99.96	1.0
12	CRUISE	0.940	701.6	7.575	0.0231	JET A	292.	0.	100.	0.0290	6.251	1.288	4.702	0.0	20.972	99.89	24.2
13	CRUISE	0.941	703.8	7.585	0.0233	ERBS	292.	0.	100.	0.0292	6.346	1.308	4.380	0.005	22.712	99.90	34.9
14	CLIMB	1.971	731.8	15.648	0.0192	JET A	292.	0.	100.	0.0230	4.946	1.023	0.472	0.0	38.397	99.99	7.8
15	CLIMB	1.980	734.9	15.654	0.0192	ERBS	292.	0.	100.	0.0227	4.922	1.024	0.459	0.005	42.026	99.99	11.1
16	TAKEOFF	2.269	763.8	17.339	0.0191	JET A	292.	0.	100.	0.0233	5.011	1.044	0.140	0.0	45.361	100.00	30.8
17	TAKEOFF	2.269	764.0	17.341	0.0191	ERBS	291.	0.	100.	0.0229	4.962	1.038	0.395	0.0	49.832	99.99	18.7

CONFIGURATION VG-8 FINAL VARIABLE GEOMETRY HIGH POWER AIR SCHEDULE

PT NO	OPERATING CONDITION	INLET PRES MPA	INLET TEMP DEG-K	BURNER AIRFLOW KG/SEC	METERED F/A RATIO	FUEL TYPE	FUEL TEMP DEG-K	PRI FUEL %	SEC FUEL %	CARBON BAL F/A RATIO	CO2 %	SPECIF HUMID G/KG	CORR CO EI G/KG	CORR THC EI G/KG	CORR NOX EI G/KG	CORR COMB EFFIC	SAE SMOKE NUMBER
2	IDLE	0.365	449.8	4.073	0.0107	JET A	287.	0.	100.	0.0121	2.464	1.047	46.377	23.985	2.856	96.11	0.0
3	IDLE	0.365	450.5	4.062	0.0109	ERBS	286.	0.	100.	0.0122	2.501	1.040	49.493	24.338	3.033	95.92	0.0
4	APPROACH	0.889	583.7	7.997	0.0157	JET A	287.	0.	100.	0.0135	3.069	1.057	0.269	0.0	9.548	99.99	1.0
5	APPROACH	0.890	580.3	8.054	0.0157	ERBS	286.	0.	100.	0.0133	3.033	1.043	0.345	0.0	9.945	99.99	1.7
6	CRUISE	0.938	705.5	7.613	0.0230	JET A	286.	0.	100.	0.0199	4.519	1.040	0.711	0.0	17.867	99.98	1.7
7	CRUISE	0.938	700.5	7.607	0.0231	ERBS	286.	0.	100.	0.0203	4.636	1.051	0.613	0.0	17.642	99.99	3.7
8	CRUISE	0.937	700.0	7.648	0.0231	12.3%	281.	0.	100.	0.0195	4.521	1.053	0.688	0.0	18.299	99.98	4.2
9	CRUISE	0.939	700.2	7.633	0.0231	11.8%	282.	0.	100.	0.0199	4.622	1.034	0.615	0.003	18.396	99.98	3.9
10	CLIMB	1.960	735.8	15.902	0.0208	JET A	288.	0.	100.	0.0250	5.385	0.706	0.277	0.082	26.385	99.98	1.0
11	CLIMB	1.961	736.8	15.851	0.0208	ERBS	285.	0.	100.	0.0250	5.418	0.849	0.279	0.012	27.294	99.99	1.0
12	TAKEOFF	2.245	770.9	17.531	0.0209	JET A	289.	0.	100.	0.0250	5.363	0.835	0.272	0.003	32.903	99.99	1.0
13	TAKEOFF	2.243	772.1	17.496	0.0189	JET A	289.	0.	100.	0.0225	4.818	1.219	0.215	0.0	33.478	99.99	1.0
14	TAKEOFF	2.246	772.6	17.489	0.0209	ERBS	286.	0.	100.	0.0247	5.355	0.748	0.260	0.0	35.813	99.99	1.3
15	TAKEOFF	2.243	772.7	17.506	0.0188	ERBS	288.	0.	100.	0.0222	4.800	0.758	0.198	0.0	35.275	100.00	1.0
16	TAKEOFF	2.245	773.6	17.569	0.0209	12.3%	284.	0.	100.	0.0247	5.379	0.789	0.260	0.0	36.848	99.99	1.9
17	TAKEOFF	2.242	773.0	17.592	0.0209	11.8%	287.	0.	100.	0.0245	5.369	0.773	0.262	0.0	37.449	99.99	1.3

OF POOR QUALITY

Table C-1 (Cont'd)
Combustor Emissions Data

CONFIGURATION AV-1 ADVANCED VORBIX COMBUSTOR

PT NO	OPERATING CONDITION	INLET PRES MPA	INLET TEMP DEG-K	FUEL TYPE	METERED F/A RATIO	PILOT FUEL %	CARBON BAL F/A RATIO	CO2 %	CORR CO EI G/KG	CORR THC EI G/KG	CORR NOX EI G/KG	CORR COMB EFFIC	SAE SMOKE NUMBER
2	IDLE	0.425	473.8	JET A	0.0067	100.00	-	0.06	0.0	16.97	2.19	98.04	
3	IDLE	0.407	476.3	ERBS	0.0080	100.00	-	0.08	3.33	5.92	0.0	99.23	
4	IDLE	0.431	477.5	11.8%	0.0071	100.00	-	0.32	10.33	2.93	8.59	99.40	
5	IDLE	0.438	474.4	JET A	0.0081	100.00	0.0102	2.15	10.49	6.34	3.87	99.02	
6	IDLE	0.447	475.3	JET A	0.0096	100.00	0.0116	2.47	9.39	1.96	5.42	99.56	0.2
7	IDLE	0.450	476.7	JET A	0.0120	100.00	0.0147	3.10	10.71	0.09	6.26	99.74	
8	IDLE	0.443	475.3	ERBS	0.0086	100.00	0.0098	2.09	10.80	4.72	3.94	99.19	
9	IDLE	0.437	475.3	ERBS	0.0097	100.00	0.0112	2.40	10.43	2.18	5.70	99.50	0.1
10	IDLE	0.450	474.7	ERBS	0.0118	100.00	0.0141	2.99	12.53	0.26	6.85	99.67	
11	IDLE	0.438	476.9	11.8%	0.0084	100.00	0.0108	2.27	10.29	3.87	4.09	99.29	
12	IDLE	0.435	476.4	11.8%	0.0098	100.00	0.0127	2.67	10.12	1.51	5.57	99.58	0.9
13	IDLE	0.430	476.8	11.3%	0.0118	100.00	0.0151	3.18	13.10	0.12	6.79	99.67	
14	APPROACH	1.159	621.4	JET A	0.0146	86.80	0.0180	3.80	8.58	2.40	14.35	99.52	0.4
15	APPROACH	1.156	619.0	JET A	0.0140	89.42	0.0172	3.63	8.73	2.63	14.71	99.49	
16	APPROACH	1.175	618.7	JET A	0.0157	80.95	0.0185	3.91	14.55	4.13	14.12	99.19	
17	APPROACH	1.156	622.5	ERBS	0.0145	85.13	0.0179	3.77	17.18	4.65	15.60	99.05	0.4
18	CRUISE	1.362	756.6	JET A	0.0201	21.72	0.0237	5.07	1.19	0.08	12.45	99.96	0.1
19	CRUISE	1.362	753.0	ERBS	0.0206	21.58	0.0244	5.25	1.34	0.06	13.98	99.96	0.1
20		2.060	777.3	JET A	0.0182	30.11	0.0205	4.37	1.35	0.05	15.21	99.96	
21		2.051	765.8	JET A	0.0180	20.75	0.0201	4.29	4.78	0.47	13.43	99.83	
22		2.047	767.0	JET A	0.0183	14.89	0.0206	4.37	11.60	2.34	12.96	99.46	
23		2.066	767.5	JET A	0.0247	15.35	0.0279	6.03	1.82	0.06	19.74	99.95	
24	CLIMB	2.545	773.8	JET A	0.0204	20.77	0.0227	4.85	1.34	0.05	17.41	99.96	0.5
25	CLIMB	2.540	773.8	ERBS	0.0212	19.75	0.0251	5.40	1.24	0.04	20.70	99.97	0.4
26	CLIMB	2.579	777.4	JET A	0.0224	17.15	0.0254	5.46	0.89	0.03	20.29	99.98	
27	TAKEOFF	2.762	818.1	JET A	0.0184	20.96	0.0215	4.61	1.61	0.09	21.25	99.95	
28	TAKEOFF	2.770	810.2	JET A	0.0213	19.18	0.0243	5.22	0.90	0.08	24.59	99.97	
29	TAKEOFF	2.790	817.8	JET A	0.0222	17.34	0.0261	5.62	0.67	0.07	26.81	99.98	4.4
30	TAKEOFF	2.752	814.7	JET A	0.0206	29.31	0.0234	5.00	0.34	0.04	24.39	99.99	
31	TAKEOFF	2.773	816.0	JET A	0.0197	38.78	0.0225	4.83	0.30	0.04	33.24	99.99	
32	TAKEOFF	2.773	819.7	ERBS	0.0196	20.68	0.0231	4.96	0.53	0.04	24.60	99.98	0.1
33	TAKEOFF	2.788	812.2	ERBS	0.0195	31.28	0.0228	4.90	0.36	0.04	27.39	99.99	0.2
34	TAKEOFF	2.774	821.3	ERBS	0.0207	39.42	0.0220	4.73	0.35	0.04	33.38	99.99	1.9
35	TAKEOFF	2.773	817.5	11.8%	0.0207	20.78	0.0234	5.00	0.61	0.03	26.14	99.98	0.1
36	TAKEOFF	2.769	816.5	11.8%	0.0203	30.19	0.0233	4.99	0.37	0.03	28.53	99.99	
37	TAKEOFF	2.785	820.4	11.8%	0.0187	38.10	0.0269	4.99	0.29	0.03	35.62	99.99	

Table C-2
Combustor Liner Temperature Data

CONFIGURATION SS-1 CURRENT PRODUCTION COMBUSTOR

PT NO	ENGINE COND	FUEL TYPE	PT4 MPA	TT4 DEG-K	F/A	<** PRIMARY **> D-TM DEG-K	D-TA DEG K	N	<* SECONDARY *> D-TM DEG-K	D-TA DEG-K	N	<** BULKHEAD **> D-TM DEG-K	D-TA DEG-K	N
****	******	****	******	*****	******	*****	*****	**	*****	*****	**	*****	*****	**
13	CRUISE	JETA	0.9425	699.	0.0229	234	151	14	172	107	13	0	0	0
14	CRUISE	ERBS	0.9438	702.	0.0236	256	170	14	179	112	13	0	0	0
15	CRUISE	12.3	0.9418	704.	0.0232	277	191	14	186	116	13	0	0	0
16	CRUISE	11.8	0.9404	702.	0.0233	289	200	14	190	119	13	0	0	0
17N	CLIMB	JETA	1.9732	729.	0.0223	273	146	14	153	94	13	0	0	0
17	CLIMB	JETA	1.9663	746.	0.0222	261	144	14	148	91	13	0	0	0
18N	CLIMB	ERBS	1.9663	746.	0.0222	263	148	14	148	92	13	0	0	0
18	CLIMB	ERBS	1.9490	732.	0.0205	239	139	14	139	83	13	0	0	0
19N	TAKEOFF	JETA	2.2717	762.	0.0258	331	169	14	187	112	13	0	0	0
19	TAKEOFF	JETA	2.2427	762.	0.0206	259	146	14	126	81	13	0	0	0
20	TAKEOFF	ERBS	2.2379	762.	0.0207	262	151	14	154	85	13	0	0	0
21	TAKEOFF	JETA	2.2345	761.	0.0179	223	127	14	136	74	13	0	0	0
22N	TAKEOFF	ERBS	2.2427	762.	0.0258	322	167	14	181	107	13	0	0	0
22	TAKEOFF	ERBS	2.2621	762.	0.0179	224	130	14	136	73	13	0	0	0
23	TAKEOFF	11.8	2.2421	759.	0.0180	229	132	14	134	72	13	0	0	0
24N	TAKEOFF	11.8	2.2338	761.	0.0257	321	168	14	187	108	13	0	0	0
24	TAKEOFF	11.8	2.2552	757.	0.0208	276	164	14	156	89	13	0	0	0
25N	TAKEOFF	12.3	2.2331	758.	0.0258	326	168	14	189	111	13	0	0	0
25	TAKEOFF	12.3	2.2600	760.	0.0207	271	159	14	160	87	13	0	0	0
26N	TAKEOFF	ERBS	2.2490	773.	0.0244	316	176	14	167	104	13	0	0	0
26	TAKEOFF	ERBS	2.2324	771.	0.0201	269	159	14	146	83	13	0	0	0

CONFIGURATION SS-2 REFERENCE BULKHEAD COMBUSTOR

PT NO	ENGINE COND	FUEL TYPE	PT4 MPA	TT4 DEG-K	F/A	<** PRIMARY **> D-TM DEG-K	D-TA DEG-K	N	<* SECONDARY *> D-TM DEG-K	D-TA DEG-K	N	<** BULKHEAD **> D-TM DEG-K	D-TA DEG-K	N
****	******	****	******	*****	******	*****	*****	**	*****	*****	**	*****	*****	**
6N	CRUISE	JETA	0.9425	702.	0.0237	279	133	15	141	70	8	0	0	0
6	CRUISE	JETA	0.9356	696.	0.0195	212	97	15	107	49	8	0	0	0
7N	CRUISE	ERBS	0.9328	692.	0.0235	303	153	15	147	73	8	0	0	0
7	CRUISE	ERBS	0.9349	700.	0.0193	231	115	15	112	52	8	0	0	0
8N	CLIMB	JETA	1.9435	734.	0.0229	334	154	15	174	74	8	0	0	0
8	CLIMB	JETA	1.9559	734.	0.0192	258	119	15	140	54	8	0	0	0
9N	CLIMB	ERBS	1.8291	734.	0.0214	374	174	15	178	77	8	0	0	0
9	CLIMB	ERBS	1.9359	737.	0.0191	280	134	15	142	56	8	0	0	0
10N	TAKEOFF	JETA	2.2579	758.	0.0253	376	168	15	218	92	8	0	0	0
10	TAKEOFF	JETA	2.2558	759.	0.0193	293	121	15	149	54	8	0	0	0
11N	TAKEOFF	ERBS	2.2455	766.	0.0252	391	172	15	210	88	8	0	0	0
11	TAKEOFF	ERBS	2.2558	764.	0.0192	310	131	15	154	57	8	0	0	0

Table C-2 (Cont'd)
Combustor Liner Temperature Data

CONFIGURATION SS-3 INCREASED PRIMARY ZONE RESIDENCE TIME

PT NO	ENGINE COND	FUEL TYPE	PT4 MPA	TT4 DEG-K	F/A	<** PRIMARY **> D-TM DEG-K	D-TA DEG-K	N	<* SECONDARY *> D-TM DEG-K	D-TA DEG-K	N	<** BULKHEAD **> D-TM DEG-K	D-TA DEG-K	N
****	******	****	******	*****	******	*****	*****	**	*****	*****	**	*****	*****	**
7	CRUISE	EPBS	0.9466	695.	0.0234	273	159	17	182	76	8	0	0	0
8N	CLIMB	ERBS	1.9739	746.	0.0223	261	157	17	192	73	8	0	0	0
8	CLIMB	EPBS	1.9442	735.	0.0214	259	154	17	192	71	8	0	0	0
9N	TAKEOFF	ERBS	2.2434	773.	0.0248	309	184	17	233	95	8	0	0	0
9	TAKEOFF	EPBS	2.2538	768.	0.0179	231	138	17	177	61	8	0	0	0
10	TAKEOFF	ERBS	2.2538	770.	0.0202	263	161	17	198	73	8	0	0	0
11	TAKEOFF	ERBS	2.2393	770.	0.0157	193	116	17	156	51	8	0	0	0

CONFIGURATION SS-4 ALTERNATE FUEL INJECTOR

PT NO	ENGINE COND	FUEL TYPE	PT4 MPA	TT4 DEG-K	F/A	<** PRIMARY **> D-TM DEG-K	D-TA DEG-K	N	<* SECONDARY *> D-TM DEG-K	D-TA DEG-K	N	<** BULKHEAD **> D-TM DEG-K	D-TA DEG-K	N
****	******	****	******	*****	******	*****	*****	**	*****	*****	**	*****	*****	**
7	CRUISE	EPBS	0.9376	692.	0.0241	232	161	17	143	71	8	0	0	0
8	CLIMB	ERBS	1.9594	757.	0.0231	204	129	17	126	39	8	0	0	0
9	TAKEOFF	ERBS	2.2414	768.	0.0183	181	104	17	121	44	8	0	0	0
10	TAKEOFF	EPBS	2.2441	761.	0.0204	202	126	17	137	53	8	0	0	0
11N	TAKEOFF	EPBS	2.2469	768.	0.0252	259	171	17	174	76	8	0	0	0
11	TAKEOFF	ERBS	2.2469	766.	0.0225	226	148	17	151	61	8	0	0	0

CONFIGURATION SS-5 RICH PRIMARY ZONE

PT NO	ENGINE COND	FUEL TYPE	PT4 MPA	TT4 DEG-K	F/A	<** PRIMARY **> D-TM DEG-K	D-TA DEG-K	N	<* SECONDARY *> D-TM DEG-K	D-TA DEG-K	N	<** BULKHEAD **> D-TM DEG-K	D-TA DEG-K	N
****	******	****	******	*****	******	*****	*****	**	*****	*****	**	*****	*****	**
9	CRUISE	EPBS	0.9438	690.	0.0238	312	203	9	200	143	5	569	391	5
10	CLIMB	EPBS	1.9690	723.	0.0232	287	181	9	177	123	5	529	352	5
11N	TAKEOFF	ERBS	2.2510	769.	0.0256	280	176	9	192	130	5	383	267	5
11	TAKEOFF	ERBS	2.2531	736.	0.0204	254	177	9	165	117	5	511	336	5

ORIGINAL PAGE IS OF POOR QUALITY

Table C-2 (Cont'd)
Combustor Liner Temperature Data

CONFIGURATION SS-6 MODERATELY LEAN PRIMARY ZONE

PT NO	ENGINE COND	FUEL TYPE	PT4 MPA	TT4 DEG-K	F/A	<** PRIMARY **> D-TM DEG-K	D-TA DEG-K	N	<* SECONDARY *> D-TM DEG-K	D-TA DEG-K	N	<** BULKHEAD **> D-TM DEG-K	D-TA DEG-K	N
****	******	****	******	*****	******	*****	*****	**	*****	*****	**	*****	*****	**
13N	CRUISE	JETA	0.9363	704.	0.0233	356	159	14	122	92	4	393	203	5
13	CRUISE	JETA	0.9390	698.	0.0182	279	117	14	81	59	4	399	175	5
14N	CRUISE	ERBS	0.9390	697.	0.0233	348	155	14	117	88	4	404	202	5
14	CRUISE	ERBS	0.9383	693.	0.0181	265	139	14	90	66	4	381	187	5
15N	CRUISE	12.3	0.9383	696.	0.0236	374	210	14	148	114	4	380	233	5
15	CRUISE	12.3	0.9383	706.	0.0181	288	146	14	91	67	4	373	191	5
16N	CRUISE	11.8	0.9376	707.	0.0235	368	211	14	147	113	4	386	233	5
16	CRUISE	11.8	0.9383	707.	0.0182	291	151	14	92	68	4	388	197	5
17N	CLIMB	JETA	1.9621	730.	0.0230	319	181	14	142	103	4	327	193	5
17	CLIMB	JETA	1.9628	734.	0.0182	242	135	14	99	68	4	332	164	5
18N	CLIMB	ERBS	1.9628	734.	0.0229	290	181	14	148	103	4	338	190	5
18	CLIMB	ERBS	1.9594	729.	0.0181	242	149	14	106	72	4	349	177	5
19N	TAKEOFF	JETA	2.2483	764.	0.0251	462	232	14	191	137	4	334	207	5
19	TAKEOFF	JETA	2.2517	775.	0.0182	348	154	14	103	67	4	275	151	5
20	TAKEOFF	JETA	2.2159	778.	0.0159	289	123	14	78	47	4	253	130	5
21N	TAKEOFF	ERBS	2.2455	768.	0.0253	465	232	14	199	139	4	257	195	5
21	TAKEOFF	ERBS	2.2490	800.	0.0183	339	143	14	82	45	4	217	127	5
22	TAKEOFF	ERBS	2.2476	769.	0.0162	314	149	14	96	63	4	252	148	5
23N	TAKEOFF	11.8	2.2296	769.	0.0250	479	242	14	178	128	4	261	200	5
23	TAKEOFF	11.8	2.2483	768.	0.0182	383	182	14	116	78	4	266	168	5
24N	TAKEOFF	12.3	2.2469	767.	0.0253	338	221	14	187	134	4	272	206	5
24	TAKEOFF	12.3	2.2483	772.	0.0183	243	161	14	116	78	4	273	168	5

CONFIGURATION SS-7 FINAL SINGLE STAGE

PT NO	ENGINE COND	FUEL TYPE	PT4 MPA	TT4 DEG-K	F/A	<** PRIMARY **> D-TM DEG-K	D-TA DEG-K	N	<* SECONDARY *> D-TM DEG-K	D-TA DEG-K	N	<** BULKHEAD **> D-TM DEG-K	D-TA DEG-K	N
****	******	****	******	*****	******	*****	*****	**	*****	*****	**	*****	*****	**
12	CRUISE	JETA	0.9390	681.	0.0232	0	0	0	179	107	13	293	262	6
13	CRUISE	ERBS	0.9404	684.	0.0230	0	0	0	189	114	13	323	292	6
14	CRUISE	12.3	0.9397	684.	0.0234	0	0	0	197	119	13	340	307	6
15	CRUISE	11.8	0.9369	684.	0.0232	0	0	0	199	122	13	348	317	6
16N	CLIMB	JETA	1.9553	718.	0.0227	0	0	0	209	114	13	334	282	6
16	CLIMB	JETA	1.9573	714.	0.0203	0	0	0	174	95	13	290	252	6
17N	CLIMB	ERBS	1.9518	719.	0.0228	0	0	0	213	118	13	339	293	6
17	CLIMB	ERBS	1.9621	717.	0.0203	0	0	0	179	100	13	294	261	6
18N	TAKEOFF	JETA	2.24[illegible]	743.	0.0251	0	0	0	238	131	13	359	292	6
18	TAKEOFF	JETA	2.2469	742.	0.0201	0	0	0	174	96	13	286	247	6
19	TAKEOFF	JETA	2.2531	742.	0.0180	0	0	0	149	82	13	241	212	6
20N	TAKEOFF	ERBS	2.2552	742.	0.0251	0	0	0	245	137	13	367	303	6
20	TAKEOFF	ERBS	2.2552	742.	0.0202	0	0	0	178	98	13	278	248	6
21	TAKEOFF	ERBS	2.2490	742.	0.0180	0	0	0	151	84	13	237	216	6
22N	TAKEOFF	12.3	2.2503	743.	0.0249	0	0	0	246	139	13	372	307	6
22	TAKEOFF	12.3	2.2483	743.	0.0200	0	0	0	179	101	13	278	250	6
23N	TAKEOFF	11.8	2.2372	743.	0.0247	0	0	0	242	138	13	363	307	6
23	TAKEOFF	11.8	2.2483	741.	0.0201	0	0	0	179	100	13	278	253	6

Table C-2 (Cont'd)
Combustor Liner Temperature Data

CONFIGURATION VG-1 REFERENCE VARIABLE GEOMETRY

PT NO	ENGINE COND	FUEL TYPE	PT4 MPA	TT4 DEG-K	F/A	<** PRIMARY **> D-TM DEG-K	D-TA DEG-K	N	<* SECONDARY *> D-TM DEG-K	D-TA DEG-K	N	<** BULKHEAD **> D-TM DEG-K	D-TA DEG-K	N
****	******	****	******	*****	******	*****	*****	**	*****	*****	**	*****	*****	**
13N	CRUISE	JETA	0.9383	697.	0.0238	338	142	15	173	84	7	0	0	0
13	CRUISE	JETA	0.9376	697.	0.0195	237	102	15	131	58	7	0	0	0
14N	CRUISE	ERBS	0.9359	697.	0.0237	385	180	15	187	93	7	0	0	0
14	CRUISE	ERBS	0.9266	698.	0.0191	269	127	15	138	63	7	0	0	0
15N	CRUISE	12.3	0.9369	698.	0.0235	404	157	15	196	99	7	0	0	0
15	CRUISE	12.3	0.9363	698.	0.0192	284	141	15	143	66	7	0	0	0
16N	CRUISE	11.8	0.9349	696.	0.0234	322	141	15	163	78	7	0	0	0
16	CRUISE	11.8	0.9356	696.	0.0192	291	148	15	143	67	7	0	0	0
17N	CLIMB	JETA	1.9766	734.	0.0231	410	173	15	215	96	7	0	0	0
17	CLIMB	JETA	1.9635	733.	0.0192	304	116	15	159	62	7	0	0	0
18N	CLIMB	ERBS	1.9608	728.	0.0230	398	160	15	202	88	7	0	0	0
18	CLIMB	ERBS	1.9511	728.	0.0193	320	132	15	161	63	7	0	0	0
19N	TAKEOFF	JETA	2.2882	765.	0.0253	403	171	15	232	105	7	0	0	0
19	TAKEOFF	JETA	2.2407	764.	0.0192	327	123	15	160	63	7	0	0	0
20	TAKEOFF	JETA	2.2531	768.	0.0172	291	107	15	138	52	7	0	0	0
21	TAKEOFF	ERBS	2.2462	767.	0.0171	297	117	15	140	53	7	0	0	0
22N	TAKEOFF	ERBS	2.2565	763.	0.0254	450	184	15	235	106	7	0	0	0
22	TAKEOFF	ERBS	2.2524	764.	0.0193	346	135	15	161	63	7	0	0	0
23	TAKEOFF	11.8	2.2538	764.	0.0172	300	127	15	146	55	7	0	0	0
24N	TAKEOFF	11.8	2.2448	763.	0.0259	453	193	15	241	110	7	0	0	0
24	TAKEOFF	11.8	2.2517	763.	0.0194	351	145	15	164	66	7	0	0	0
25N	TAKEOFF	12.3	2.2386	764.	0.0254	442	186	15	236	106	7	0	0	0
25	TAKEOFF	12.3	2.2510	764.	0.0194	347	142	15	164	65	7	0	0	0
26N	TAKEOFF	ERBS	2.2283	759.	0.0253	473	196	15	246	113	7	0	0	0
26	TAKEOFF	ERBS	2.2359	763.	0.0192	351	143	15	168	69	7	0	0	0

CONFIGURATION VG-2 ALTERNATE FUEL INJECTOR SINGLE PIPE MODE

PT NO	ENGINE COND	FUEL TYPE	PT4 MPA	TT4 DEG-K	F/A	<** PRIMARY **> D-TM DEG-K	D-TA DEG-K	N	<* SECONDARY *> D-TM DEG-K	D-TA DEG-K	N	<** BULKHEAD **> D-TM DEG-K	D-TA DEG-K	N
****	******	****	******	*****	******	*****	*****	**	*****	*****	**	*****	*****	**
7	CRUISE	ERBS	0.9528	699.	0.0238	232	154	17	163	77	8	0	0	0
8	CLIMB	ERBS	1.9615	735.	0.0232	209	145	17	164	70	8	0	0	0
9	TAKEOFF	ERBS	2.2407	769.	0.0184	179	103	17	125	45	8	0	0	0
10	TAKEOFF	ERBS	2.2400	769.	0.0205	194	119	17	143	54	8	0	0	0
11N	TAKEOFF	ERBS	2.2455	769.	0.0255	255	165	17	187	81	8	0	0	0
11	TAKEOFF	ERBS	2.2434	769.	0.0226	206	139	17	160	63	8	0	0	0

Table C-2 (Cont'd)
Combustor Liner Temperature Data

CONFIGURATION VG-3   VARIABLE FUEL INJECTOR OPEN POSITION

PT NO	ENGINE COND	FUEL TYPE	PT4 MPA	TT4 DEG-K	F/A	<** PRIMARY **> D-TM DEG-K	D-TA DEG-K	N	<* SECONDARY *> D-TM DEG-K	D-TA DEG-K	N	<** BULKHEAD **> D-TM DEG-K	D-TA DEG-K	N
****	******	****	******	*****	******	*****	*****	**	*****	*****	**	*****	*****	**
4	CRUISE	JETA	0.9625	695.	0.0242	299	186	15	173	80	8	0	0	0
5	CRUISE	ERBS	0.9521	694.	0.0239	307	215	15	181	87	8	0	0	0
6	CRUISE	ERBS	0.9273	694.	0.0203	242	174	15	151	67	8	0	0	0
7	CLIMB	ERBS	2.0021	732.	0.0234	290	195	15	182	76	8	0	0	0
8N	TAKEOFF	JETA	2.2641	764.	0.0264	272	194	15	218	96	8	0	0	0
8	TAKEOFF	JETA	2.2607	764.	0.0216	269	175	15	175	68	8	0	0	0
9	TAKEOFF	JETA	2.2731	765.	0.0196	227	155	15	156	57	8	0	0	0
10	TAKEOFF	ERBS	2.2710	763.	0.0196	231	162	15	157	58	9	0	0	0
11	TAKEOFF	ERBS	2.2648	763.	0.0216	264	181	15	172	67	8	0	0	0

CONFIGURATION VG-4   VARIABLE FUEL INJECTOR CLOSED POSITION

PT NO	ENGINE COND	FUEL TYPE	PT4 MPA	TT4 DEG-K	F/A	<** PRIMARY **> D-TM DEG-K	D-TA DEG-K	N	<* SECONDARY *> D-TM DEG-K	D-TA DEG-K	N	<** BULKHEAD **> D-TM DEG-K	D-TA DEG-K	N
****	******	****	******	*****	******	*****	*****	**	*****	*****	**	*****	*****	**
9	CRUISE	ERBS	0.9369	697.	0.0237	247	168	16	141	71	8	0	0	0
10	CLIMB	ERBS	1.9490	736.	0.0230	252	158	16	148	67	8	0	0	0
11	TAKEOFF	ERBS	2.2710	766.	0.0255	267	174	16	163	77	8	0	0	0

CONFIGURATION VG-5   LEAN PRIMARY ZONE

PT NO	ENGINE COND	FUEL TYPE	PT4 MPA	TT4 DEG-K	F/A	<** PRIMARY **> D-TM DEG-K	D-TA DEG-K	N	<* SECONDARY *> D-TM DEG-K	D-TA DEG-K	N	<** BULKHEAD **> D-TM DEG-K	D-TA DEG-K	N
****	******	****	******	*****	******	*****	*****	**	*****	*****	**	*****	*****	**
4N	CRUISE	JETA	0.9418	698.	0.0234	302	153	15	112	63	8	186	81	3
4	CRUISE	JETA	0.9390	706.	0.0201	237	121	15	91	44	8	158	69	3
5N	CRUISE	ERBS	0.9369	705.	0.0234	277	137	15	106	57	8	181	79	3
5	CRUISE	ERBS	0.9411	707.	0.0181	232	125	15	93	41	8	166	73	3
6	CRUISE	ERBS	0.9425	707.	0.0202	270	147	15	95	51	8	188	83	3
7N	CLIMB	ERBS	1.9663	738.	0.0227	381	163	15	116	63	8	164	91	3
7	CLIMB	ERBS	1.9635	736.	0.0190	343	146	15	96	49	8	151	82	3
8N	TAKEOFF	JETA	2.2448	774.	0.0249	426	174	15	141	82	8	177	101	3
8	TAKEOFF	JETA	2.2469	773.	0.0190	344	137	15	96	47	8	144	77	3
9	TAKEOFF	JETA	2.2[illegible]17	765.	0.0169	300	120	15	82	38	8	129	61	3
10N	TAKEOFF	ERBS	2.2331	766.	0.0253	446	196	15	153	89	8	197	108	3
10	TAKEOFF	ERBS	2.2483	766.	0.0189	356	149	15	98	49	8	154	83	3
11	TAKEOFF	ERBS	2.2517	766.	0.0169	315	132	15	84	41	8	141	77	3

Table C-2 (Cont'd)
Combustor Liner Temperature Data

CONFIGURATION VG-6 RICH PRIMARY ZONE

PT NO	ENGINE COND	FUEL TYPE	PT4 MPA	TT4 DEG-K	F/A	<** PRIMARY **> D-TM DEG-K	D-TA DEG-K	N	<* SECONDARY *> D-TM DEG-K	D-TA DEG-K	N	<** BULKHEAD **> D-TM DEG-K	D-TA DEG-K	N
****	******	****	******	*****	******	*****	*****	**	*****	*****	**	*****	*****	**
12N	CRUISE	JETA	0.9404	700.	0.0243	227	161	8	166	114	5	395	286	5
12	CRUISE	JETA	0.9445	696.	0.0210	196	129	8	123	82	5	443	288	5
13N	CRUISE	ERBS	0.9397	697.	0.0240	223	154	8	154	107	5	443	302	5
13	CRUISE	ERBS	0.9438	693.	0.0208	213	163	8	139	96	5	428	301	5
14N	CRUISE	12.3	0.9432	700.	0.0243	221	172	8	165	116	5	427	305	5
14	CRUISE	12.3	0.9445	693.	0.0208	227	176	8	145	102	5	476	324	5
15N	CRUISE	11.8	0.9438	695.	0.0240	273	211	8	196	142	5	477	346	5
15	CRUISE	11.8	0.9445	696.	0.0208	237	183	8	148	104	5	455	320	5
16N	CLIMB	JETA	1.9621	731.	0.0258	278	179	8	192	134	5	324	257	5
16N	CLIMB	JETA	1.9684	724.	0.0236	263	167	8	162	111	5	332	254	5
16	CLIMB	JETA	1.9649	746.	0.0208	221	143	8	127	83	5	361	252	5
17N	CLIMB	ERBS	1.9594	746.	0.0233	256	183	8	167	116	5	362	269	5
17	CLIMB	ERBS	1.9677	735.	0.0208	232	164	8	134	90	5	359	262	5
18N	TAKEOFF	JETA	2.2469	784.	0.0257	222	161	8	184	118	5	216	153	5
18	TAKEOFF	JETA	2.2545	735.	0.0185	159	115	8	92	53	5	171	127	5
19	TAKEOFF	JETA	2.2531	777.	0.0207	186	138	8	119	78	5	188	156	5
20N	TAKEOFF	ERBS	2.2517	787.	0.0257	238	173	8	191	123	5	223	172	5
20	TAKEOFF	ERBS	2.2490	769.	0.0185	179	139	8	107	69	5	197	160	5
21	TAKEOFF	ERBS	2.2552	770.	0.0206	216	161	8	131	89	5	211	175	5
22N	TAKEOFF	12.3	2.2503	771.	0.0256	259	189	8	203	137	5	229	189	5
22	TAKEOFF	12.3	2.2579	771.	0.0206	247	168	8	130	87	5	271	225	5
23N	TAKEOFF	11.8	2.2538	775.	0.0256	285	200	8	207	141	5	262	235	5
23	TAKEOFF	11.8	2.2600	762.	0.0207	237	173	8	134	90	5	315	244	5

CONFIGURATION VG-7 FINAL VARIABLE GEOMETRY LOW POWER AIR SCHEDULE

PT NO	ENGINE COND	FUEL TYPE	PT4 MPA	TT4 DEG-K	F/A	<** PRIMARY **> D-TM DEG-K	D-TA DEG-K	N	<* SECONDARY *> D-TM DEG-K	D-TA DEG-K	N	<** BULKHEAD **> D-TM DEG-K	D-TA DEG-K	N
****	******	****	******	*****	******	*****	*****	**	*****	*****	**	*****	*****	**
12	CRUISE	JETA	0.9363	696.	0.0231	0	0	0	227	122	11	289	266	6
13	CRUISE	ERBS	0.9397	703.	0.0233	0	0	0	234	126	11	304	279	6
14N	CLIMB	JETA	1.9856	729.	0.0228	0	0	0	242	117	11	297	268	6
14	CLIMB	JETA	1.9814	730.	0.0192	0	0	0	182	79	11	264	240	6
15N	CLIMB	ERBS	1.9587	730.	0.0228	0	0	0	241	117	11	310	277	6
15	CLIMB	ERBS	1.9828	732.	0.0192	0	0	0	184	83	11	279	251	6
16N	TAKEOFF	JETA	2.2572	759.	0.0251	0	0	0	294	146	11	294	277	6
16	TAKEOFF	JETA	2.2614	762.	0.0191	0	0	0	186	82	11	259	245	6
17N	TAKEOFF	ERBS	2.2290	761.	0.0251	0	0	0	288	141	11	313	283	6
17	TAKEOFF	ERBS	2.2648	764.	0.0192	0	0	0	137	79	11	273	252	6

Table C-2 (Cont'd)
Combustor Liner Temperature Data

CONFIGURATION VG-8 FINAL VARIABLE GEOMETRY HIGH POWER AIR SCHEDULE

PT NO	ENGINE COND	FUEL TYPE	PT4 MPA	TT4 DEG-K	F/A	<** PRIMARY **> D-TM DEG-K	D-TA DEG-K	N	<* SECONDARY *> D-TM DEG-K	D-TA DEG-K	N	<** BULKHEAD **> D-TM DEG-K	D-TA DEG-K	N
****	******	****	******	*****	******	*****	*****	**	*****	*****	**	*****	*****	**
[illegible]	CRUISE	JETA	0.9390	704.	0.0232	0	0	0	100	64	14	299	247	4
[illegible]	CRUISE	ERBS	0.9383	704.	0.0231	0	0	0	108	70	14	325	264	4
8	CRUISE	12.3	0.9383	700.	0.0231	0	0	0	117	74	14	337	291	4
9	CRUISE	11.8	0.9369	700.	0.0232	0	0	0	120	76	14	346	295	4
10N	CLIMB	JETA	1.9601	753.	0.0227	0	0	0	93	48	14	269	237	4
10	CLIMB	JETA	1.9587	731.	0.0208	0	0	0	101	59	14	285	247	4
11N	CLIMB	ERBS	1.9580	731.	0.0224	0	0	0	121	74	14	309	272	4
11	CLIMB	ERBS	1.9635	741.	0.0208	0	0	0	97	56	14	288	246	4
12N	TAKEOFF	JETA	2.2434	772.	0.0248	0	0	0	131	77	14	301	271	4
12	TAKEOFF	JETA	2.2441	771.	0.0210	0	0	0	99	56	14	286	246	4
13	TAKEOFF	JETA	2.2407	772.	0.0188	0	0	0	83	47	14	275	224	4
14N	TAKEOFF	ERBS	2.2386	773.	0.0245	0	0	0	134	78	14	317	279	4
14	TAKEOFF	ERBS	2.2427	773.	0.0208	0	0	0	103	58	14	300	257	4
15	TAKEOFF	ERBS	2.2434	773.	0.0189	0	0	0	87	49	14	291	241	4
16N	TAKEOFF	12.3	2.2441	774.	0.0249	0	0	0	137	80	14	326	296	4
16	TAKEOFF	12.3	2.2421	774.	0.0210	0	0	0	107	61	14	309	269	4
17N	TAKEOFF	11.8	2.2441	774.	0.0248	0	0	0	137	79	14	323	293	4
17	TAKEOFF	11.8	2.2414	773.	0.0210	0	0	0	102	58	14	307	264	4

Table C-3
Combustor Lean Stability Data

LEAN BLOWOUT SUMMARY

CONFIGURATION	FUEL TYPE	PT M-PA	TT DEG-K	WAB KG/SEC	FUEL/AIR RATIO AT BLOWOUT
SS-1	JET-A	0.3781	456	4.25	0.0042
	ERBS	0.3764	444	4.26	0.0042
	11.8	0.3733	454	4.19	0.0043
SS-2	JET-A	0.3585	453	4.12	0.0044
	ERBS	0.3593	451	4.15	0.0046
SS-3	ERBS	0.3595	447	4.17	0.0049
SS-4	ERBS	0.3680	445	4.01	0.0049
SS-5	JET-A	0.3662	446	4.03	0.0037
	ERBS	0.3636	444	4.03	0.0047
SS-6	JET-A	0.3375	452	4.15	0.0023
	ERBS	0.3579	444	4.12	0.0025
	11.8	0.3636	445	4.15	0.0027
VG-1	JET-A	0.3683	453	4.19	0.0061
	ERBS	0.3623	441	4.11	0.0063
	11.8	0.3646	441	4.13	0.0060
VG-2	ERBS	0.3716	446	4.04	0.0058
VG-3	ERBS	0.3640	448	4.14	0.0041
VG-4	JET-A	0.3672	451	3.93	0.0047
	ERBS	0.3604	451	3.97	0.0052
VG-5	ERBS	0.3671	446	4.02	0.0076
VG-6	JET-A	0.3673	449	4.09	0.0040
	ERBS	0.3671	451	4.06	0.0052
	11.8	0.3673	452	4.04	0.0060
VG-8	JET-A	0.3666	445	4.04	0.0045
	ERBS	0.3656	451	4.08	0.0050
	11.8	0.3633	450	4.10	0.0049
AV-1	JET-A	0.456	472	2.90	0.0057
	ERBS	0.452	472	2.88	0.0066
	11.8	0.455	473	2.88	0.0053